Thèse de doctorat

# Genetic adaptation of methylotrophic bacteria for industrial production of chemical compounds

Thèse de doctorat de l'Université Paris-Saclay préparée dans l'UMR Génomique Métabolique du Genoscope, Commissariat à l'Énergie Atomique et aux Énergies Alternatives et à l'université d'Evry

NNT: 2019SACLE004
École doctorale n°577 : Structure et Dynamique des Systèmes Vivants (SDSV)
Spécialité : Science de la vie et de la santé

Thèse présentée et soutenue à Évry, le 12 mars 2019, par

**Sophia Belkhelfa**

**Composition du Jury :**

| | |
|---|---|
| Matthieu Jules<br>Professeur, AgroParis Tech (SyBER) | Président |
| Françoise Bringel<br>Directrice de recherche, CNRS (GMGM) | Rapporteur |
| Olivier Tenaillon<br>Directeur de recherche, Inserm Paris 6 (IAME) | Rapporteur |
| Denis Thibaut<br>Directeur du département Fermentation, Global Bioenergies | Examinateur |
| Rodrigo Ledesma Amaro<br>Directeur de recherche, Imperial College London | Examinateur |
| Marcel Salanoubat<br>Directeur de recherche, CNRS (UMR8030) | Directeur de thèse |
| Volker Döring<br>Ingénieur-Chercheur, CEA (UMR8030) | Co-Encadrant de thèse |

# ACKNOWLEDGMENT

**“If you want to go fast, go alone. If you want to go far, go together.”**

Mes premiers remerciements sont destinés à Patrick Wincker et Jean Weissenbach, directeurs du Genoscope, qui m'ont permis de pouvoir passer ces trois années de thèse au sein de cet institut.

Je témoigne toute ma gratitude à l'égard des membres de mon jury, Françoise Bringel, Olivier Tenaillon, Denis Thibaut, Matthieu Jules ainsi que Rodrigo Ledesma Amaro pour avoir accepté de faire partie des membres de mon jury et pour avoir dédié du temps à l'étude de mon travail.

Un grand merci à Marcel Salanoubat, directeur de l'unité mixte de recherche 8030, mais surtout mon directeur de thèse, pour m'avoir soutenue et supportée ces 3 dernières années. Chacune de mes requêtes a toujours été suivie d'un grand « NON », pour généralement se poursuivre par un second essai de ma part enrichi d'un argumentaire. Celui débouchant souvent sur un ultime entretien, régulièrement conclu par une réponse favorable à ma requête initiale. Si j'ai bien appris une chose de sa part, c'est qu'il faut toujours persévérer. J'ai été ravie de pouvoir travailler et apprendre à ses côtés.

Je remercie également Madeleine Bouzon, responsable du Laboratoire des Applications (LA) sans qui ce projet n'aurait pas été possible. Je suis reconnaissant pour sa disponibilité, nos discussions scientifiques mais surtout pour son excellent sens critique quant à la mise en forme des figures. Je suis également reconnaissante du temps passé ces derniers mois à me soutenir dans la rédaction de ma thèse et de mon article.

Un grand merci à mon encadrant de thèse Volker Döring. Je le remercie pour la confiance qu'il m'a accordée en revenant me chercher pour ce contrat doctoral. Nous avons travaillé en tout et pour tout trois ans et 10 mois. Je tiens donc à le remercier pour son écoute, ses conseils et ses discussions scientifiques très enrichissantes. Il a su me donner sa confiance en me laissant l'autonomie dont j'avais besoin pour pouvoir m'épanouir dans ce projet. Même si nous n'avons pas toujours été d'accord, il a toujours été ouvert à la discussion. Finalement nous avons su entretenir cette relation malgré nos caractères opposés qui ont su se compléter. Je tiens aussi à le remercier pour ces derniers mois à me soutenir dans la rédaction de ma thèse et de mon article. J'espère avoir acquis plus de rigueur en travaillant à ses côtés et lui avoir transmis un peu de mon optimisme infaillible.
Merci à tous les membres de mon équipe :

Laurence Cattolico, pour ces conseils avisés, notamment concernant la manipulation des méthylotrophes qu'elle avait essayé de dompter auparavant. Ils m'ont été d'une aide précieuse.
Isabelle Bocaut, pour tous ses petits déjeunés préparés : qu'il neige, qu'il pleuve où qu'il vente. Elle a toujours été là pour m'aider, même quand il s'agissait de nettoyer des tâches sur mes vêtements. C'est une vraie maman.
Nathalie Vega, pour avoir été à l'écoute et m'avoir supportée dans mes projets parfois un peu trop ambitieux concernant l'utilisation du FACS. Mais surtout pour son sourire manifeste à la lecture des résultats négatifs…
Valérie Delmas, maman numéro 2 de ce laboratoire, a su secourir toutes mes plantes laissées pour mortes que je lui ai volontiers léguée. Mais elle a surtout été d'une grande aide pour ce projet dans lequel elle s'est grandement investie. Je tiens donc à la remercier pour tout ce qu'elle a fait pour moi et pour mon projet.
Anne Berger, j'espère que tous les laboratoires du monde ont la chance de compter parmi eux une Anne. Elle a mis toute la volonté possible à la réalisation de projets dont elle savait pourtant qu'ils avaient peu de chance d'aboutir. Pour cela il faut beaucoup de courage et de patience. Sa rigueur a été un atout incontesté durant ces 3 années et j'espère qu'elle prendra conscience de sa valeur au sein de ce laboratoire.
Ivan Dubois, le patriarche, l'homme le plus gentil du monde. Il a été mon mentor pour la machine d'évolution, le GM3, il m'a montré tous les rouages quotidiens à l'entretien de cette machine et a suivi avec moi ces évolutions. Mais il a surtout été un très bon ami et un soutien quotidien. Il a toujours été présent pour me ramener jusqu'au « noctilien » et patienter avec moi.
Julien Patrouix et Laurent Gaillon, qui ont toujours été disponibles et pédagogues pour répondre à mes questions concernant le GM3.
Parvathi Chandra, Hela Benaissa et Yassine Ajilil qui ont été mes stagiaires. J'ai eu la chance de pouvoir encadrer ces 3 personnes pour mener à bien mon projet. Je tiens à les remercier car ils ont su être patients avec moi et leurs dynamismes m'ont été d'un grand secours.

Je tiens aussi à remercier tous mes collaborateurs :
Véronique de Berardini, pour m'avoir toujours ouvert la porte et avoir pris autant de plaisir à partager ses connaissances, sa bonne humeur quotidienne avec moi. Merci aussi pour son soutien quotidien et de s'être soucié du fait que mes soirées au laboratoire soient au moins remplies de sucreries qui m'ont aidée à tenir.

Alain Perret, pour tous ces vifs échanges durant lesquels il a pu me montrer que j'avais tort (parfois…). Ce fut un réel plaisir pour moi de travailler avec lui.
Karine Labadie, Corinne Cruaud et Aude Perdereau avec qui j'ai pu discuter des projets de séquençages, qui ont été à l'écoute de mes besoins et ont su me donner de très bons conseils.
Jean-Marc Aury, qui m'a volontiers aidée dans l'assemblage de mon génome et qui a pris le temps de vulgariser son travail pour moi.
Zoe Rouy et Shahinaz Gas pour m'avoir aidée dans les procédures de déclaration de mes données génomiques et de transcriptomiques et d'avoir fait le lien entre l'institut, EBI et moi.
Christophe Lechapelais, pour toutes ces discussions devant des graphiques toutes droites sorties de la masse ou encore ces débats sur « quel test statistique était le plus adéquat ? ». Mais surtout pour tous ces moments plaisants où j'ai pu relever notre différence d'âge. Parce qu'il est le plus jeune (mentalement) des plus âgés.
Ekatherina Dariy, pour avoir mis au point tous les protocoles de détection de mes échantillons en masse, même si cela n'a pas été le plus simple. Merci de ne pas avoir lâché prise et d'avoir persévéré, c'est grâce à cela qu'on y est arrivé.
Emilie Pateau, notre collaboration fut courte mais intense… C'est toujours agréable de la voir se plaindre avec le sourire, surtout après avoir vu son travail remarquable.
Adrien et Virginie pour leur aide dans le projet MCR, la production des protéines et la mise au point des protocoles.
Gabor Gyapay, pour avoir pris le temps de partager tant de chose avec moi, ses connaissances du FACS, ses années d'expériences, ses souvenirs de vacances, son énergie inépuisable.
Emmanuelle Petit, mon mentor ARN. Elle a su me guider dans l'obtention de mes ARN et a pris le temps de me transmettre tous son savoir. Mais ce que je vais surtout déplorer sont ses accueils chaleureux et son soutien qui m'ont fait chaud au cœur.
David Roche, mon bio-informaticien souffre-douleur. Je suis probablement venue le voir un millier de fois pour qu'il m'explique ce qu'il avait fait avec mes données… Comment devrais-je analyser mes données ? Quelles options extraordinaires de MicroScope pouvaient m'être utiles ? Il a toujours été à l'écoute de mes problèmes et nous avons toujours réussi à trouver une solution à deux. Parfois, mes projets pouvaient lui prendre plus de 50% de son temps de travail, et pourtant, il ne m'a jamais mise à la porte de son bureau. Il a su être patient avec moi et, si j'ai pris conscience de l'importance d'avoir un bio-informaticien dans une équipe de recherche, c'est grâce au plaisir que j'ai prise à travailler et à apprendre à ces côtés.

Jean-Louis Petit…, ingénieur au CEA, mais pour moi, c'est comme s'il avait déjà passé 10 thèses. Ma thèse n'aurait jamais abouti sans lui. Je lui dois beaucoup : des protocoles ; des conseils avisés ; mais aussi un soutien quotidien, même quand il fallait déplacer des congélateurs il a été là pour m'aider. Ces râlements quotidiens vont énormément me manquer.

Un merci chaleureux à tous ceux qui ont été là au quotidien, durant ces pauses café, ces repas, ces réunions, ces sorties piscines, cinéma, bowling, escape game, weekend etc… Mais aussi pour tous ces petits conseils partagés avec moi par: Magali Boutard, Pascal Bazir, Christine Pelle, Sebastien Chaussonnerie, Nadia Perrache, Peggy Sirvain, Agnès Barbance, Karine Vaxelaire, Aurélie Jouenne, Mathieu Dubois, Amine Madoui, David Vallenet, Benjamin Istace.

Catherine Contrepois, Régis Brillant, Véronique Tancray, Jean-Marc Barbance, Thibaut Audouy et Frack Anière qui ont toujours été présent quand j'avais un papier à signer, une commande à réaliser, un infors à réparer … Merci à eux, car même s'ils sont dans l'ombre ils jouent chaque jour un rôle crucial.

Un merci particulier aux thésards et post-docs, aux stagiaires du Genoscope. Pour tous ces moments de bonne humeur et pour leur soutien. Vivre cette thèse à leurs côtés fut thérapeutique pour moi et je tiens à les en remercier : Ombeline Mayol, Thomas Bessonnet, Marion Thomas, Chloé Lelièvre, Oriane Dellanegra, Wiliam Rostain, Adam Carpaco, Kevin Sugier, Romuald Lasojadart, Steff Horeman et Nazim Sarica.

Un mot particulier Tristan Cerisy, qui m'a toujours soutenu et poussé dans mes choix. Un autre pour Tiffany Souterre, pour avoir su me guider et me montrer la voie, sans qui je ne serais peut-être pas arrivée jusque-là. Mais surtout pour avoir été mon amie, avec notre petite équipe qui compte aussi Cécile Jacry et Audam Chhun. Nous avons tous eu la chance d'être réunis par un homme exceptionnel : Andrew Tolonen. Personnellement, il a été mon superviseur à iGEM, mon professeur, mon collègue, mais aussi un ami. Il m'a donné de précieux conseils que j'ai toujours essayé de suivre. Je lui serai toujours reconnaissante et il sera pour toujours mon modèle scientifique.

# Table of content

ACKNOWLEDGMENT ..... 2
LIST OF FIGURES ..... 10
LIST OF TABLES ..... 13
LIST OF SUPPLEMENTARY DATA ..... 15
LIST OF ABBREVIATIONS ..... 16
I. INTRODUCTION ..... 20
I.1. The transition from fossil to renewable energy sources – a global challenge ..... 21
I.2. Reduced one-carbon compounds as energy carriers ..... 22
I.3. Bioproduction as promising production process of fuels and chemicals ..... 23
I.4. Natural methylotrophy ..... 24
I.5. Synthetic methylotrophy ..... 27
I.6. Natural methylotrophic organisms as biotechnological platform strains ..... 30
I.7. *Methylobacterium extorquens* as biotechnological platform organism ..... 31
I.8. Strain toxicity of solvents to biofuel production and the adaptation to higher tolerance ..... 34
I.8.1. Toxicity of solvents to microorganisms ..... 34
I.8.2. Toxicity of methanol to microorganisms ..... 36
I.9. Enhanced growth under limited oxygen conditions ..... 38
I.10. Directed evolution of microbial strains ..... 40
I.11. Long term propagation of cell populations ..... 42
I.11.1. Serial transfer ..... 42
I.11.2. Continuous culture ..... 42
I.11.3. The GM3 device of automated continuous culture ..... 43
I.11.4. Strain evolution in the GM3: turbidostat and medium swap regimes ..... 45
I.11.5. Evolved *M. extorquens* strains as production chassis ..... 49
I.12. Objectives of the present work ..... 51
II. MATERIALS & METHODS ..... 54
II.1. Microbiologic protocols ..... 55
II.1.1. Bacterial strains and growth conditions ..... 55
II.1.2 Tests of sensitivity to antibiotics ..... 58
II.1.3 Electroporation ..... 59
II.1.4. Directed evolution in continuous culture using GM3 device ..... 60
II.2. Molecular biology protocols ..... 63
II.2.1. PCR Amplification ..... 63

II.2.2. Nucleic acid purification ..... 64
II.2.3. Directed mutagenesis protocol ..... 64
II.2.4. Gene cloning using restriction enzymes ..... 65
II.2.5. Gene cloning by using ligation independante clonoing (LIC) protocol ..... 66
II.2.6. Genomic DNA extraction and sequencing ..... 68
II.2.7. Transcriptomics analysis ..... 69
II.3. Metabolomic protocols ..... 70
II.3.1. Protocol A: on filter ..... 70
II.3.2. Protocol B: in 5 mL liquid culture ..... 71
II.3.3. Protocol C: in 2.5 mL liquid culture in 24 wells-plates ..... 72
II.3.4. Lactate quantification ..... 72
II.3.5. 3-Hydroxypropionic acid quantification ..... 73
II.4. Biochemistry ..... 74
II.4.1. Production and purification of proteins ..... 74
II.4.2. MetY characterization ..... 75
II.4.3. NMCR and CMCR enzymatic assay ..... 76
II.5. FAME analysis ..... 76
II.6. Cell sorting ..... 77
II.6.1. Size of the cells ..... 77
III. RESULTS ..... 78
III.1. Characterization of methylotrophic bacteria with serine cycle metabolisms ..... 79
III.1.1. Characterization of strain *Methylobacterium extorquens* TK 0001 ..... 80
III.1.2. Characteristics of growth and biomass yield ..... 80
III.1.3. Test of pH-dependence of growth ..... 83
III.1.4. Test of antibiotic resistance ..... 84
III.1.5. Introduction of plasmids into TK 0001 cells ..... 85
III.1.6. Genomic sequencing of *M. extorquens* TK 0001 ..... 86
III.2. Directed strain evolution to growth on high methanol concentrations ..... 88
III.2.1. Directed evolution of strain *Methylobacterium extorquens* TK 0001 to growth with 10% methanol ..... 89
III.2.2. Directed evolution of strain *Methylobacterium extorquens* AM1 to growth with 10% methanol _chamber 1 ..... 101
III.2.3. Directed evolution of strain *Methylobacterium extorquens* AM1 to growth with 10% methanol _chamber 2 ..... 108
III.2.4. Enzymatic characterization of wildtype and mutated O-acetyl-L-homoserine sulfhydrylase (MetY) ..... 111

II.2.5. Effects of *metY* overexpression on methanol toxicity ..... 114
II.2.6. Genome-wide mRNA expression responses during methanol stress ..... 115
III.3. Directed evolution of *Methylobacterium extorquens* AM1 to growth under oxygen shortage ..... 122
III.4. Dosage of D-lactate production from D-lactate dehydrogenase overexpressing cells ..... 126
III.5. Production of 3-hydroxypropionic acid ..... 129
III.5.1. Enzymatic pathway ..... 129
III.5.2. Cloning and *in vitro* tests of MCR inserts ..... 130
III.5.3. Screening of new reductases ..... 132
IV. PUBLICATIONS ..... 136
V. DISCUSSION ..... 148
SUPPLEMENTARY DATA ..... 158
REFERENCES ..... 175
RESUME ..... 195

# LIST OF FIGURES

Figure 1: Resulting product from methanol by ADI Analytics energy insight and consulting …..
Figure 2: Closed C-cycle, from carbon dioxide to bulk/fine chemicals ……..……
Figure 3: Conversion routes of methane to its four oxidized C1 derivatives ……..……
Figure 4: Methanol conversion of different types of methylotrophic bacteria in a simplified version ……..……..……..…….
Figur 5: Overview of the general respiratory chain for eukaryotic and prokaryotic cells ……....
Figure 6: Chemostat and turbidostat principle ……..……..……..
Figure 7: GM3 device with double vessels system/wash systems ……..…….……
Figure 8: Production tree from 3-Hydroxypropionic acid ……..…….…
Figure 9: Experimental protocol of growth assays using the Bioscreen C reader …….
Figure 10: Protocol of measurement of dried bacteria weight ……..……...
Figure 11: Protocol of disc diffusion tests to check antibiotic sensitivity ……..……..…
Figure 12: Methanol quantification by a fluorometric test ……..……..…
Figure 13: Plasmid map of pET22 and pTE102 generate from APE ……..……..…
Figure 14: Protocol for preparing samples from solid culture on filter ……..……..
Figure 15: Principle of the Acetic acid assay test from Megazyme ……..……...
Figure 16: Physiological aspects of *M. extorquens* TK 0001 grown on mineral medium plates and in liquid culture supplemented with 1% methanol ……..……..……
Figure 17: Growth curves of strains TK 0001, PA1 and AM1 on different succinate concentrations recorded with a Bioscreen plate reader ……..……..
Figure 18: Determination of OD600nm and dry cell mass of strains TK 0001, PA1 and AM1 after 48 hours of growth in mineral medium supplemented with 100 mM succinate …….…
Figure 19: Dry cell mass production of *M. extorquens* TK 0001 on methanol and succinate after 48 hours of growth at 30°C in Erlenmeyer flasks ……..……..
Figure 20: Circular representation of *Methylobacterium extorquens* TK 0001 chromosome…...
Figure 21: Growth profile of strains *M. extorquens* TK 0001 and AM1 on mineral medium supplemented with different methanol concentrations ……..……
Figure 22: Adaptation of *M. extorquens* TK 0001 bacteria to increasing methanol concentrations in GM3-driven continuous culture ……..…….
Figure 23: Growth phenotype of *M. extorquens* TK 0001 wildtype strain and methanol evolved isolates G4105 and G4521 ……..……..……

Figure 24: Growth of *M. extorquens* TK 0001 wildtype strain and evolved isolates from the GM3 population on minimum media supplemented with: 1%, 5%; 7%; 8%, 10% methanol (v/v) ……..……..……..…….
Figure 25: Growth profile of *Methylobacterium extorquens* TK 0001 and G4105 with different carbon sources at different concentrations ……..……...……..
Figure 26: FAME analysis of the fatty acid composition of membrane samples obtained from strain *M. extorquens* TK 0001 and the evolved derivatives G4105 and G4521 ……..……
Figure 27: Adaptation of *M. extorquens* AM1 bacteria to increasing methanol concentrations in GM3-driven continuous culture ……..…….……
Figure 28: Growth aspect of cultures of *Methylobacterium extorquens* AM1 and the evolved isolates on methanol ……..…….……..……
Figure 29: Growth profile of isolates from evolved AMM1 population in smm supplemented with 1% MeOH: the population AMM5, AMM7 and AMM8 ……..……..….
Figure 30: Growth phenotype of *M. extorquens* AM1 wildtype strain and methanol evolved isolates from AMM5 (G4609) ……..…….…….……..……
Figure 31: Growth profile in smm supplemented with different formate concentrations of AM1 WT and G4609 ……..……..…….……..……..
Figure 32: FAME analysis of the fatty acid composition of membrane samples obtained from strain *M. extorquens* AM1 and the evolved derivatives G4609 and G4706 ……..…….…….
Figure 33: Evolution AMM10 chamber 2. Adaptation of *M. extorquens* AM1 bacteria to increasing methanol concentrations in GM3-driven continuous culture ……..……..……..
Figure 34: Sequence alignment of O-acetyl-L-homoserine sulfhydrylase (MetY) from *Methylobacterium extorquens* TK 0001/AM1 with MetY from *Wolinella succinogene*s ……..
Figure 35: Methionine biosynthesis pathways of *Methylobacterium extorquens* TK 0001 and AM1 from L-homoserine as deduced from genomic annotation...……..……
Figure 36: Growth of *M. extorquens* methanol adapted strain G4105 transformed with the empty vector pTE102 or the plasmid pTE102*_metY*……..……...….
Figure 37: Functional categorization of differentially expressed genes (DEGs) in *M. extorquens* TK 0001 wildtype strain and G4105 evolved strain upon exposure to methanol …..…….
Figure 38: Adaptation profile of *M. extorquens* AM1 to growth with reduced oxygen supply in the GM3 ……..…….……..……..
Figure 39: Growth phenotype of *M. extorquens* TK 0001 wildtype strain and methanol evolved isolates from MEM5 (G4105) with and without pTE102 ldhA ……..…….……...

Figure 40: Lactate amount formed by G4605, G4836, G4891 and G4892 ……..……..……..
Figure 41: Overview of the 3-HP production from acetyl-CoA using MCR from *C. aurantiacus* or CMCR/NMC. ……..……
Figure 42: 3-HP detection with NMCR and CMCR *in vitro* activity from *Chloroflexus aurantiacus* ……..……..……..…….
Figure 43: Schema of the inserts constructed for 3-HP production ……..……..
Figure 44: NMCR and CMCR screening steps……..…….…….....
Figure 45: Results of the screened proteins ……..…….…..
Figure 46: Sequence comparison between all CDS annoted as *metY* in *Methylobacterium extorquens* TK 0001 and AM1 ……..……..……..

# LIST OF TABLES

Table 1: Attempts of synthetic methylotrophy …….
Table 2: Examples of the production of industrial compounds by methylotrophic strains from various carbon sources…….
Table 3: *Methylobacterium extorquens* as biotechnological platform organism…….
Table 4: Examples of potential biofuel producer strains adapted to solvent tolerance…….
Table 5: Examples of potential biofuel producer strains adapted to methanol tolerance……..
Table 6: Top value-added chemicals from biomass. ……
Table 7: Composition of standard mineral medium ……....
Table 8: SL-4 composition ……...
Table 9: SL-6 composition……
Table 10: Protocol for thermocycler program using Pfx……..
Table 11: Protocol for thermocycler program for touchdown using Pfx……..
Table 12: Table of primers designed for directed mutagenesis of *cmcr* gene……..
Table 13: List of plasmids…….
Table 14: Lysed and washed buffer …….
Table 15: Elution buffer……
Table 16: Composition of reaction mix for the screening…….
Table 17: Growth of *M. extorquens* strains AM1, PA1 and TK 0001 on mineral medium plates supplemented with different carbon compounds. ……..….
Table 18: Growth yield after 48h growth in liquid mineral medium supplemented with different glycine and pyruvate concentrations……
Table 19: Cell density of *M. extorquens* TK 0001 cultures after 72 hours of growth on mineral medium buffered at neutral and various acidic pH values. ……...……..……...
Table 20: Filter patch antibiotic resistance test of strain TK 0001 on mineral methanol plates.....
Table 21: Antibiotic resistance test of strain TK 0001 on mineral methanol plates. ……..
Table 22: Plasmids used to transform *M. extorquens* TK 0001 cells by electroporation or conjugation. ……..
Table 23: Genome size and organization of *Methylobacterium extorquens* strains ……
Table 24: Genetic differences in isolates sampled at various time points of the adaptation of *M. extorquens* TK 0001 to high methanol concentrations. Isolates were obtained from samples of

the evolving bacterial population adapted to growth on minimal medium supplemented with 5% (MEM5), 7% (MEM7), 8% (MEM8) and 10 % (MEM10) methanol. ……..….
Table 25: Genetic differences in population sampled at various time points of the adaptation of *M. extorquens* TK 0001 to high methanol concentrations. ……..…….
Table 26: Genetic differences in isolates sampled at various time points of the adaptation of *M. extorquens* AM1 to high methanol concentrations……..……..
Table 27: SNPs in the isolates from the population AMM10 chamber 2…….…….
Table 28: Mutated genes common to six, five or four isolates obtained from AMM10_chamber 2 culture…….
Table 29: Mutations in MetY identified in the isolates analyzed at each step of the adaptation to increasing concentrations of methanol of both *M. extorquens* strains TK 0001 and AM1 and Kinetic parameters *metY*-encoded wildtype O-acetyl-L-homoserine sulfhydrylase of *M. extorquens* TK 0001……..……...…….
Table 30: List of transcripts specifically regulated during growth for 5 minutes and 3 hours at 5% methanol, and for 3 hours at 1% methanol…….
Table 31: List of mutations in the evolved strains to oxygen deficiency. AMM1 to AMM3 corresponding to isolates from the population before the pulse and from AMM4 to AMM6 corresponds to isolates after the pulses……..……...
Table 32: Generation time between each step of population for *Methylobacterium extorquens* TK 0001 and AM1 . ……...……..

# LIST OF SUPPLEMENTARY DATA

Table S1: Library of promoters tested in *Methylobacterium extorquens*. ……..

Figure S1: Summary of Nanopore data, Illumina data and Assemblage data. ……

Figure S2: Pan-core genome analysis of the *Methylobacterium extorquens* genome: AM1, CM4, DM4, PA1 and TK 0001. ……..

Table S2: DNA sequence for each selected isolate from the evolved population MEM and AMM. ……...

Figure S3: Growth profile of *M. extorquens* TK 0001 and MEM5 population in smm supplemented with methanol between 1% to 5%. ……...

Figure S4: Growth profile of 3 isolates from MEM5 population in smm supplemented with 5%, 6% or 7% MeOH. ……..……..

Figure S6: Growth profile of isolates from MEM8 population in smm supplemented with 1%, 8% and 9% ……..……..……..……..……..……..……

Table S3: Mutations identified in the evolved derivatives of *M. extorquens* TK 0001 isolated at each step of progressive adaptation to higher concentrations of methanol, 5%, 7%, 8% and 10% (v/v). ……..……..……..……..……..……..……..

Figure S5: Growth profile of isolates from MEM7 population in smm supplemented with 1%, 5%, 7% and 8% MeOH. ……..……..……..……..……..……

Figure S10: Kinetic curves of METY *M. extorquens* TK 0001 with the different substrats: O-acetyl-L-homoserine, sulfide and methanol using SigmaPlot. ……..……..……..…..

Table S6: RNA sequence and accession number. ……..……..……..……..……

Table S7: eggNOG class repartition for the CDS from *M. extorquens* TK 0001. ……...

Table S8: Codon usage table for *Methylobacterium extorquens*. ….. …….

Figure S11: Codon optimization of N-terminal part of MCR from *C. auriantacus* using the codon usage for *M. extorquens*. ……...

Figure S12: Clustering of the 27 candidates of interest ……...

Figure S13: SDS Gel of the NMCR and CMCR protein. ……..……..

# LIST OF ABBREVIATIONS

| Abbreviations | Full name |
|---|---|
| 3-HP | 3-hydroxypropionic acid |
| ADP | adenosine di-Phosphate |
| a-KAO | alpha-ketoglutarate dependent dioxygenases |
| AMM | *Methylobacterium extorquens* AM1 evolution on methanol |
| Amp | ampicillin |
| ARTP | atmospheric and room-temperature plasma |
| ATP | adenosine Tri-Phosphate |
| BET | ethidium bromide |
| BLAST | basic local alignment search tool |
| bp | base pair |
| $^{13}C$ | carbon 13 |
| C1 | one carbon |
| CDS | coding sequences |
| CLU | 5-chlorouracil |
| CMCR | C-terminal part malonyl-CoA reductase |
| $CO_2$ | carbon dioxide |
| CoA | coenzyme A |
| coxA | cytochrome c oxidase subunit I |
| DNA | deoxyribonucleic acid |
| dxs | 1-deoxyxylulose-5-phosphate synthase |
| EU | European Union |
| F6P | D-fructose-6-phosphate |
| FACS | fluorescence-activated cell sorter |
| FAME | fatty acid methyl esters |
| FC | foldchange |
| Fld | formaldehyde |
| $FPH_2$ | reduced flavoprotein |
| GckA | glycerate-2-kinase |
| Gly-Gly | dipeptide glycine |
| GM3 | Genemat – directed evolution automaton |
| $H_2O$ | water |
| $H_4MPT$ | tetrahydro- methanopterine |
| $H_4T$ | tetrahydrofolate |
| HPLC | high performance liquid chromatography |
| HprA | hydroxypyruvate reductase |
| HPS | 3-hexulose-6-phosphate synthase |
| indel | insertion/deletion |
| Kan | kanamycin |
| $k_{cat}$ | turnover number |

| | |
|---|---|
| $K_M$ | Michaelis constant |
| LB | Luria-Bertani medium |
| ldhA | D-lactate dehydrogenase |
| Mdh | malate deshydrogenase |
| MCC | methanol condensation cycle |
| MEM | *Methylobacterium extorquens* TK 0001 evolution on methanol |
| MeOH | methanol |
| metY | O-acetyl-L-homoserine dulfhydrylase |
| MCR | malonyl-CoA reductase |
| MIC | minimal inhibitory concentration |
| MTK | malate reacts to malate thiokinase |
| mutS | DNA mismatch repair |
| NAD+/NADH | nicotinamide adenine dinucleotide (oxidized/reduced form) |
| NADP/NADPH | nicotinamide adenine dinucleotide phosphate (oxidized/reduced form) |
| NaOH | sodium hydroxide |
| NMCR | N-terminbal part malonyl-CoA reductase |
| OD | optical density |
| OECD | organisation for economic co-operation and development |
| ORF | open reading fram |
| ori | origine of replication |
| PCR | polymerase chain reaction |
| pH | potential of hydrogen |
| PHA | polyhydroxyalkanoates |
| PHB | polyhydroxybutyrate |
| PHI | 6-phospho-3-hexulose isomerase |
| RES | renewable energy sources |
| Ros | transcriptional regulatory protein |
| RNA | ribonucleic acid |
| RNA-Seq | RNA sequencing |
| rpsL | 30s ribosomal protein s12 |
| rRNA | ribosomal RNA |
| Ru5P | D-ribulose-5-phosphate |
| RuMP | ribulose monophosphate |
| SD | standard deviation |
| SDS-PAGE | sodium dodecyl sulfate polyacrylamide gel electrophoresis |
| SgA | serine-glyoxylate aminotransferase |
| sHsp | small heat shock proteins |
| smm | standard mineral medium |
| SNP | single-nucleotide polymorphism |
| SpeedVac | speed vacuum evaporator |
| Succ | succinate |
| T | thymine |
| TBE | tris, borate, EDTA |

| | |
|---|---|
| Tet | tetracyclin |
| TRIS | tris(hydroxymethyl)aminomethane |
| tRNA | transfert RNA |
| UV | ultraviolet |
| WT | wildtype |

**Organisms**

| | |
|---|---|
| *B. methanolicus* | *Bacillus methanolicus* |
| *B. stearothermophilus* | *Bacillus stearothermophilus* |
| *C. glutamicum* | *Corynebacterium glutamicum* |
| *C. necator* | *Cupravidus necator* |
| *C. phytofermentans* | *Clostridium phytofermentans* |
| *E. coli* | *Escherichia coli* |
| *M. extorquens* | *Methylobacterium extorquens* |
| *M. gastri* | *Mycobacterium gastri* |
| *M. organophilum* | *Methylobacterium organophilum* |
| *P. pastoris* | *Pishi Pastoris* |
| *S. cerevisiae* | *Saccharomyces cerevisiae* |

# I. INTRODUCTION

## I.1. The transition from fossil to renewable energy sources – a global challenge

In 2015, fossil energy accounts for over 80% of total energy consumption worldwide (statistics from Energy Information Agency, 2014). This dependence has an economic, but also an ecological impact. Fossil fuels like oil, coal and natural gas liberate carbon, stored over millions of years in the earth crust, as $CO_2$ when used for household heating, transportation or in industrial processes. The greenhouse gas $CO_2$ is for a large part directly responsible for the global warming recorded since the onset of the industrial revolution. In this context, the European Commission presented a new version of the directive for the promotion of renewable energy sources (RES), as part of the broader 'Clean Energy for all Europeans' package. The main purpose of the recast RES directive is to increase the share of RES in the European Union (EU) energy mix to at 27 % by 2030 (from European Council in October 2014), to ensure that the EU becomes the world leader in renewable energy (RED II, 2016).

During the last decades, technologies aiming at the utilization of renewable energy sources have been developed. These include solar energy, wind power, geothermal energy, ocean mechanical energy and biomass. However, these energy sources are not available everywhere and some depend on weather conditions. Also, they cannot directly aliment transportation engines. Technologies for efficient energy storage, in the form of electricity, are not yet available. For a global use of alternative energy sources, suitable carrier molecules have to be employed which are produced via the conversion of electricity into chemical energy.

The most prominent carrier molecule already used today is molecular hydrogen. $H_2$ can be produced directly through electrolysis of water and can aliment fuel cells installed in transport vehicles (Lipman, 2011). However, other compounds than hydrogen are gaining interest as chemical energy carriers. Among them are the reduced one-carbon compounds formic acid and methanol. The usefulness of formic acid and methanol as molecules linking renewable energy production and consumption is twice: they can be produced from $CO_2$ through reduction driven by electricity, and they can serve as feedstocks for fermentations.

## I.2. Reduced one-carbon compounds as energy carriers

In the present work, we focused on the use of methanol as fermentation feedstock. Worldwide methanol production is growing constantly, with a total volume of 49 million metric tons produced in 2010, 75 million metric tons in 2015 and estimated 95 million metric tons in 2021 (IHS Markit, 2017). This increment of annual production capacity will continue to lead to a decrease of its price thus rendering its use even more attractive.

Methanol has a wide variety of applications as precursor for numerous industrial products like formaldehyde, acetic acid or dimethyl ether etc. (Figure 1). These derivatives are for the majority essential building block chemicals (Komaba Shinichi et al., 2018; Leopold Eugen, 2018; Montes Martin et al., 2018). In addition, around 200,000 tons of methanol are utilized as chemical feedstock. Methanol is a clean-burning and biodegradable substance (Boudemagh et al., 2006; Dhamwichukorn et al., 2001; Kaszycki and Kołoczek, 2000).

Methanol can be produced from syngas (Abubackar et al., 2011), a gas composed primarily of carbon monoxide (30-60%), hydrogen (25-30%), methane (0-5%), and carbon dioxide (5-15%) (Source: The National Energy Technology Laboratory). Also, methanol can be produced with a competitive price from carbon dioxide and hydrogen as energy donor (Ghasemzadeh et al., 2018; Methanol, Process Economics Program Report 43C, 2000). Hydrogen is in turn obtained using renewable energy sources like wind and solar energy (Anicic et al., 2014; Pérez-Fortes et al., 2016). To reduce the production costs, one of the challenge is to reduce the cost of renewable hydrogen, which constitutes the major part of total methanol price (Lyubovsky, 2017). The other challenge is the $CO_2$ supply, which can be provided from agricultural and agroforestal wastes treatments. The seasonality and regionalist agricultural production tends to add complexity to this supply chain (Gontard et al., 2018). Besides from agriculture, $CO_2$ can also be captured from industrial sites like steel plants or cement factories.

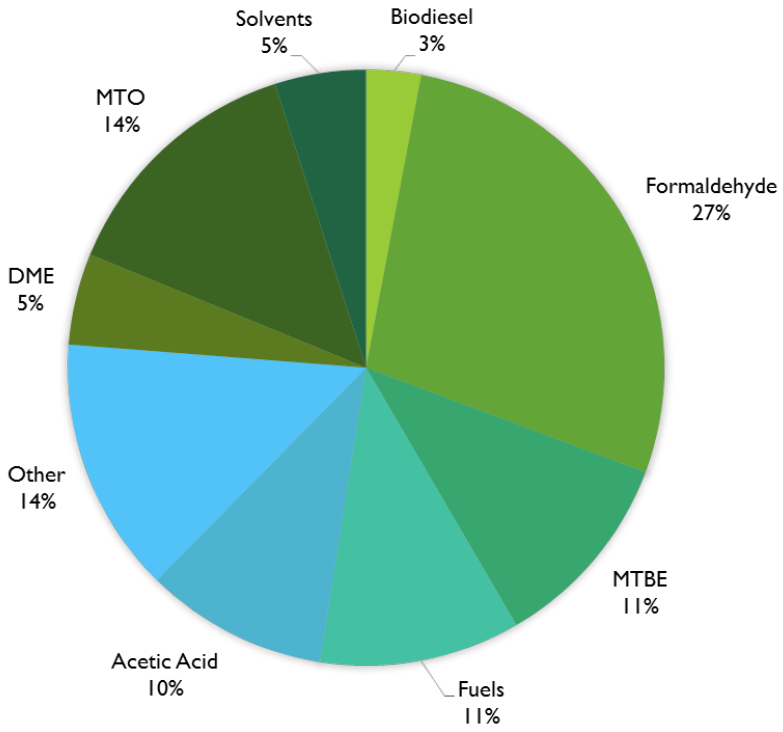


**Figure 1: Resulting product from methanol (2016) by ADI Analytics energy insight and consulting. DME for dimethyl ether MTO for methanol and MTBE for methyl tert-butyl ether.**

## I.3. Bioproduction as promising production process of fuels and chemicals

Today, the majority of the large-scale fermentation processes use carbohydrates as the carbon and energy source for the producer microorganisms. The carbohydrates are obtained from agricultural crops growing on arable land, thus entailing a competition with the feed and food sector (Muffler and Ulber, 2008). It is imperative to save food supplies and be prepared when the world's population will reach 8.3 billion for 2030 (Organisation for Economic Co-operation and Development (OECD), the bioeconomy to 2030 – designing a policy agenda, OECD Publishing 13 (2009) ; (Kircher, 2012).

Using feedstock derived from non-food sources such as ligno-cellulose is an alternative that has been developed these last years (Tian et al., 2018; Zeng, 2019). However, an efficient exploitation is still hampered by technical difficulties (Ochsner et al., 2015). Another possibility to avoid competition with the alimentation sector is to employ photoautotrophic microorganisms like cyanobacteria and microalgae which convert atmospheric $CO_2$ to complex carbon compounds using the sunlight as energy source (Vasco2 project, Jupiter 1000 project). Difficulties related to $CO_2$ capture, high surface need and costly separations of produced

chemicals from low density cultures have to be overcome to render this approach economically viable (Singh and Geuzebroek, 2018).

A biotechnology based on the fermentation of methanol synthesized from $CO_2$ and $H_2$ produced using renewable energy could limit the dependence on carbohydrates in industrial biotechnology (Pfeifenschneider et al., 2017; Schrader et al., 2009) and enable the setup of a closed production cycle avoiding fossil carbon and energy sources (Goeppert et al., 2014; Hwang et al., 2015) (Figure 2).

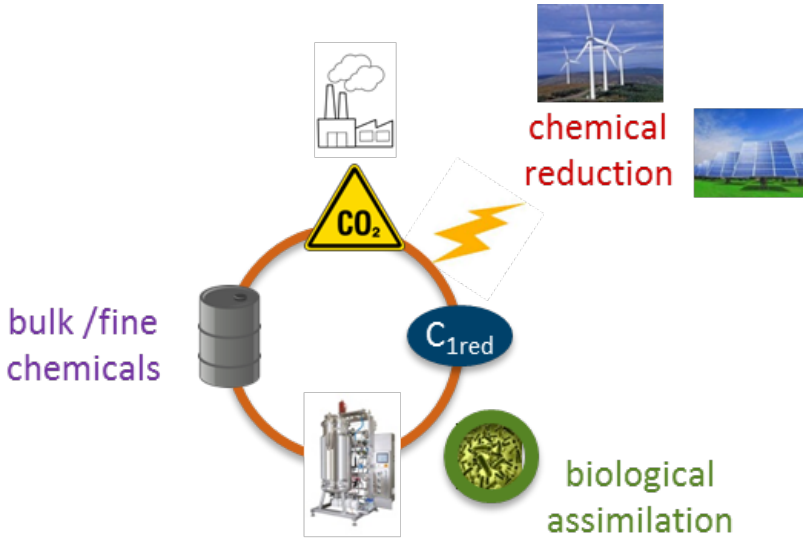


**Figure 2: Closed C-cycle, from carbon dioxide to bulk/fine chemicals.**

## I.4. Natural methylotrophy

A variety of methylotrophic microorganisms are found in almost all kinds of natural habitats (Butterfield et al., 2016; Chistoserdova et al., 2009; Faria and Bharathi, 2006; Meena et al., 2015; Thulasi et al., 2018). Methylotrophs are part of different branches of the tree of life such as yeast, archaea and bacteria (Chistoserdova et al., 2009). Some rely completely on one carbon (C1) compounds (obligate methylotrophs) while others can also grow on multi-carbon sources (as facultative methylotrophs). The C1 substrates used can vary between strains; methanol is the common compound assimilated, other bacteria have the ability to use methane ($CH_4$), formate (HCOOH), carbon dioxide ($CO_2$), carbon monoxide (CO), methane sulfonate, amino methane, chloromethane etc. (Chistoserdova, 2018; Dürre and Eikmanns, 2015) (Figure 3).

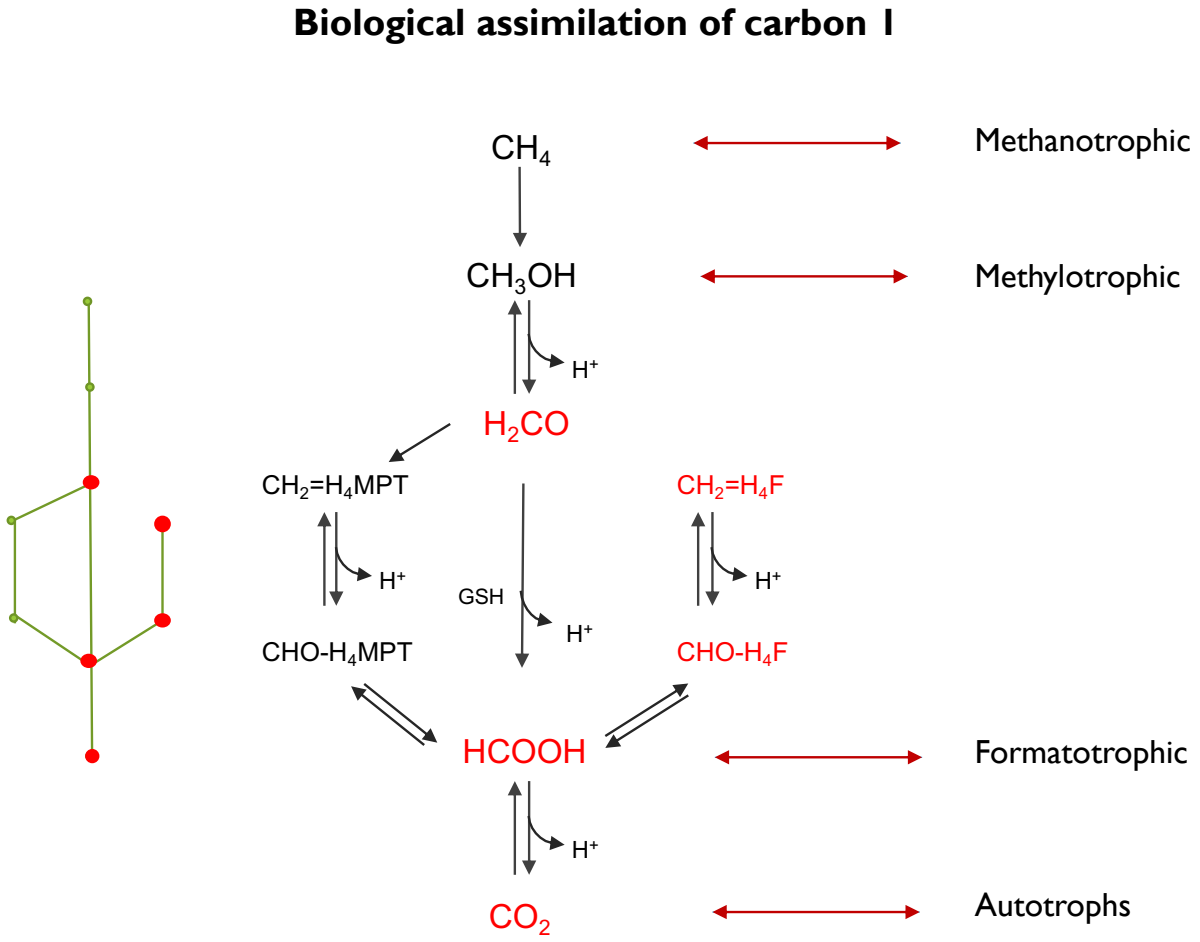


**Figure 3: Conversion routes of methane to its four oxidized C1 derivatives. In red the entry points in the central carbon metabolism of methylotrophic or autotrophic organisms.**

There are two principal metabolic routes of methanol assimilation among the methylotrophic strains: the serine cycle and the ribulose monophosphate (RuMP) cycle (Figure 4).

Organisms like *Bacillus methanolicus* relying on the RuMP cycle for the assimilation of reduced C1-compounds fix formaldehyde to D-ribulose-5-phosphate (Ru5P) to form a hexulose-6-phosphate which is isomerized to D-fructose-6-phosphate (F6P). These conversions are catalyzed by 3-hexulose-6-phosphate synthase (HPS) and 6-phospho-3-hexulose isomerase (PHI), the key enzymes of the pathway. F6P is phosphorylated to fructose 1,6-bisphosphate which aliments "classical" heterotrophic routes like the pentose phosphate, the Entner-Doudoroff and the Embden-Meyerhof pathways. The formaldehyde acceptor Ru5P is regenerated from F6P and glyceraldehyde-3-phosphate through a series of carbon transfer and isomerization reactions (Yurimoto et al., 2009).

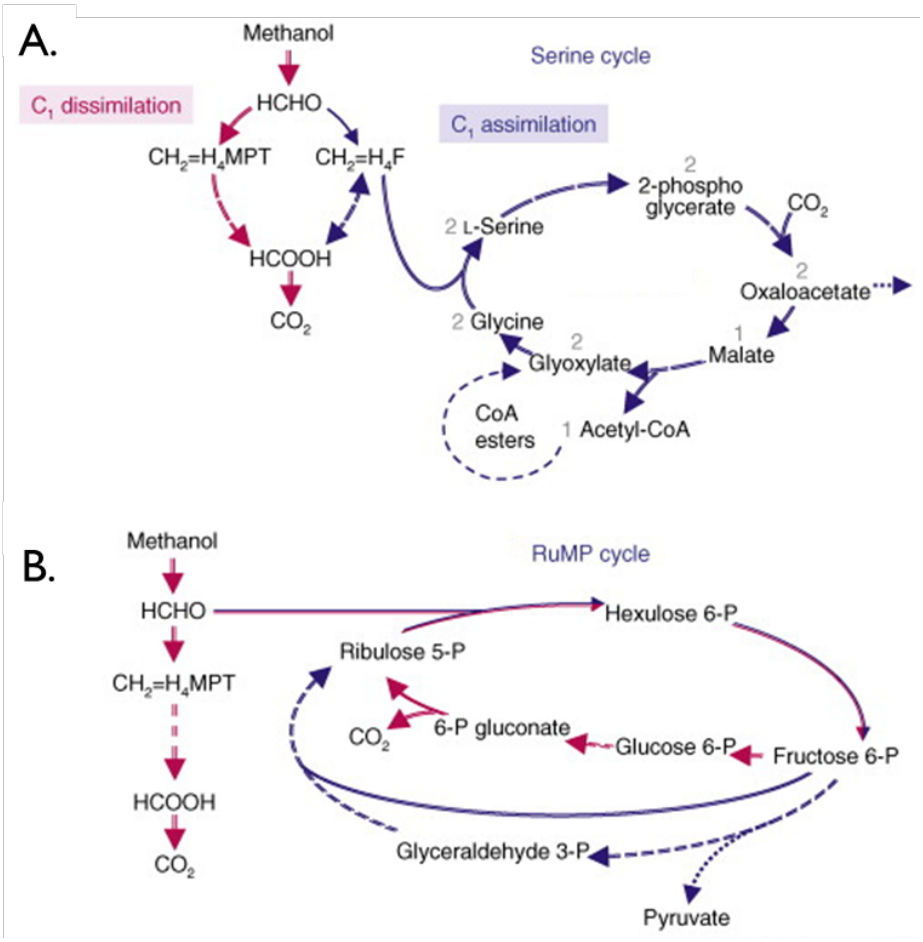


**Figure 4: Methanol conversion of different types of methylotrophic bacteria in an adapted version from** Schrader et al., 2009. **(A) Methanol conversion in a serine-cycle methylotroph, such as *Methylobacterium extorquens* AM1. (B) Molecular pathways for methanol conversion in a ribulose monophosphate (RuMP)-cycle methylotroph, such as *Bacillus methanolicus*. In both panels, dissimilatory pathways are depicted in red and assimilatory pathways in blue. Dotted arrows represent exemplary possible exit points of metabolites for biosynthetic reactions.**

The formaldehyde assimilation pathway is exergonic and presents the following stoichiometry:

$$3HCHO + NAD^+ + ADP = pyruvate + NADH + ATP$$

Other organisms like *Methylobacterium extorquens* relying on the serine cycle for the assimilation of reduced C1-compounds, fix formaldehyde on the carrier molecule tetrahydro-methanopterine ($H_4MPT$) through the action of the formaldehyde activating enzyme Fae. The C1 moiety is oxidized to formate and released. Formate can then be further oxidized to $CO_2$ or fixed on tetrahydrofolate ($H_4T$) with concomitant consumption of an ATP. The C1 moiety is reduced and enters the carbon metabolism via fixation to glycine to form serine, which is transformed to 2-phospho-D-glycerate by the action of 3 enzymes characterizing the cycle, i.e.

serine-glyoxylate aminotransferase (SgaA), hydroxypyruvate reductase (HprA) and glycerate-2-kinase (GckA). 2-phospho-D-glycerate is transformed to oxaloacetate, a metabolite of the TCA cycle. Oxaloacetate is reduced to malate by the malate dehydrogenase (Mdh). Malate reacts to malate thiokinase (MTK) to form malyl-CoA, which will be cleaved to form acetyl-CoA and glyoxylate. This key enzyme aliments the ethylmalonyl-CoA pathway, which is essential to regenerate the glyoxylate through a series of reactions involving thioesters (Anthony, 2011).

Due to the intricate interplay of different pathways, the stoichiometry of the serine cycle is complicated to establish. The following carbon and energy balance was proposed (Anthony, 1982) ($FPH_2$:reduced flavoprotein):

$$CO_2 + 2\ HCHO + 2\ NADH + 2\ ATP = pyruvate + 2\ NAD^+ + 2\ ADP + FPH_2$$

By comparing the energy balance of the two pathways, it becomes obvious that the RuMP cycle is more favorable than the serine cycle.

## I.5. Synthetic methylotrophy

With methanol becoming more available as renewable feedstock for bioconversions, efforts are made to implant methylotrophic pathways in non-methylotrophic platform organisms like *E. coli* (Bennett et al., 2018; Gonzalez et al., 2018; Whitaker et al., 2017; Zhang et al., 2017). Synthetic methylotrophs could circumvent some of the drawbacks of their natural counterparts, notably low growth, low production titers of small metabolites and limiting electron availability due to their strict dependence on oxygen as final electron acceptor (Pfeifenschneider et al., 2017). Also, protocols and tools for molecular genetics are still less available and elaborated as is the case for strains like *E. coli* (Whitaker et al., 2015).

Mostly, the strategies followed to construct synthetic methylotrophs were based on the introduction of the C1-assimilation module of RuMP cycle methylotrophs, which fixes formaldehyde with the pentose phosphate pathway intermediate Ru5P. Only two heterologous enzymes must be expressed in *E. coli* to fix formaldehyde (HPS) and convert the hexulose-6-phosphate condensation product to F6P (PHI), an intermediate of the central carbon

metabolism. Besides its energetic efficiency, the low charge of heterologous enzymes makes the RuMP cycle a natural choice for synthetic methanol assimilation.

To serve as carbon source, methanol has to be oxidized to formaldehyde. Three groups of methanol oxidoreductases are described, using PQQ, NAD or molecular oxygen as electron acceptor. Methanol dehydrogenases depending on the ubiquitous cofactor NAD are usually chosen for synthetic methylotrophy. However, this class of methanol dehydrogenases shows lower activity than the other two classes. Active research is ongoing to obtain high performing NAD-dependent enzyme variants via screening and mutagenesis (Wu et al., 2016).

An additional difficulty for synthetic methylotrophy comes from the cytotoxic effect of formaldehyde on the cell. *Escherichia coli* and most other organisms possess defense systems based on detoxifying molecules like glutathione which spontaneously bind free formaldehyde. However, binding and subsequent oxidation of bound formaldehyde to formate and $CO_2$ lower is the biomass yield of methanol. To counteract oxidative loss, the formaldehyde must rapidly react with its Ru5P acceptor. A gain in catalytic activity of this anabolic reaction could be obtained through expression of an HPS-PHI fusion protein (Orita et al., 2007).

Until today, no true synthetic methylotrophic organism has been described. $^{13}C$ labeling experiments proved the incorporation of methanol in cellular components, but the methanol turnover was insufficient to support growth. In some applications, methanol was used as a side substrate to enhance the yield of biomass production from carbohydrates (Witthoff et al., 2015). Table 1 gives an account on progress towards methanol assimilation by non-methylotrophic organisms.

**Table 1: Attempts of synthetic methylotrophy adapted from** Bennett et al., 2018**.**

| Organism | Strategy | Achievements | Reference |
|---|---|---|---|
| ***Escherichia coli* (*in vitro*)** | Developed a methanol condensation cycle (MCC) by combining RuMP and NOG pathways for carbon-conserved, redox-balanced and ATP-independent higher alcohol production from methanol and sugar phosphates in a cell-free system. | MCC produced 13.3 mM ethanol from 33.5 mM methanol at 80% carbon yield<br>MCC produced 2.3 mM 1-butanol from 21.1 mM methanol at 50% carbon yield. | (Bogorad et al., 2014) |
| ***Escherichia coli* (in vitro, *in vivo*)** | Identified an activator-independent NAD-dependent MDH from *C. necator* N-1, a Gram-negative, mesophilic, non-methylotrophic bacterium. Performed directed evolution to improve enzyme kinetics toward methanol. | Increased methanol affinity and catalytic efficiency. Decreased 1-butanol affinity and catalytic efficiency. | (Wu et al., 2016) |
| ***Escherichia coli* (*in vitro*, *in vivo*)** | Constructed a scaffold less enzyme complex of *B. methanolicus* Mdh3 and *M. gastri* HPS-PHI fusion using an SH3-ligand interaction pair to improve formaldehyde channeling<br>Incorporated *E. coli* lactate dehydrogenase as an 'NADH sink' to improve methanol oxidation kinetics and carbon flux to F6P. | Improved *in vitro* F6P production from methanol by 97-fold.<br>Increased *in vivo* methanol oxidation rate by 9-fold and total *in vivo* methanol consumption by 2.3-fold. | (Price et al., 2016) |
| ***Escherichia coli* (*in vivo*)** | Identified a superior NAD-dependent MDH from *B. stearothermophilus* to use with the *B. methanolicus* RuMP pathway in a DfrmA genetic background.<br>Supplied small amounts of yeast extract (1 g/L) as a co-substrate to stimulate growth on methanol<br>Incorporated heterologous pathway for naringenin production from methanol. | Methanol supplementation improved biomass titers by up to 50% during growth with a small amount of yeast extract.<br>Observed RuMP pathway cycling as indicated by higher-order mass isotopomers<br>Improved naringenin production by 650% over the empty vector control in methanol and yeast extract. | (Whitaker et al., 2017) |
| ***Escherichia coli* (*in vivo*)** | Incorporation of the glycine synthase complex. | Formate and $CO_2$ assimilation providing 10% of the cellular carbon. | (Yishai et al., 2018) |
| ***Corynebacterium glutamicum* (*in vivo*)** | Incorporated *B. methanolicus* MDH and *B. subtilis* RuMP pathway into *C. glutamicum*<br>Supplied methanol as a co-substrate in a glucose minimal medium. | Achieved a methanol consumption rate of 1.7 mM/h in a glucose minimal medium<br>Methanol supplementation improved biomass titers by up to 30% during growth in glucose minimal medium<br>Observed up to 25.7% $^{13}C$-labeling in M+1 mass isotopomers of intracellular metabolites, specifically S7P. | (Witthoff et al., 2015) |
| ***Saccharomyces cerevisiae* (*in vivo*)** | Incorporated the methanol assimilation pathway (AOX, CTA, DAS and DAK) from *P. pastoris* into *S. cerevisiae*<br>Supplied small amounts of yeast extract (1 g /L) as a co-substrate to stimulate growth on methanol. | Achieved 1.04 g /L methanol consumption,<br>0.26 g/ L pyruvate production and a 3.13% increase in biomass titer in methanol minimal medium. | (Dai et al., 2017) |

## I.6. Natural methylotrophic organisms as biotechnological platform strains

As outlined above, reduced C1 compounds like methanol can be produced from $CO_2$ and renewable energy. Methanol is low in cost, soluble and easy to handle. It is more reduced than commonly used sugars which are needed for nutritional demands of a growing world population. Furthermore, the majority of microbial strains known do not grow on methanol as sole carbon and energy source. Industrial fermentations are therefore less inclined by contaminations then are the case for carbohydrates. Methylotrophic organisms can serve as metabolic chassis into which heterologous pathways can be introduced to produce platform chemicals for industrial purposes (Jiang et al., 2010; Ochsner et al., 2015) (Table 2). Since the 1960s, methylotrophic bacteria have been used industrially for the production of amino-acids, proteins, biodegradable plastics, etc. (Zhu et al., 2016).

**Table 2: Examples of the production of industrial compounds by methylotrophic strains from various carbon sources.**

| Carbon source | Product | Strain | Reference |
|---|---|---|---|
| **Methane** | Acetate | *Methanosarcina acetivorans* | (Ferry James Gregory et al., 2015) |
| | Lactate (0.8 g/L) | *Methylomicrobium buryatense* | (Henard et al., 2016) |
| | Crotonic acid | *Methylomicrobium buryatense 5GB1C* | (Garg et al., 2018) |
| **Methanol** | Polyhydroxybutyrate (PHB) | *Methylobacterium organophilum* | (Zúñiga et al., 2011) (Groleau et al.) |
| | (R)-2-hydroxy-4-phenylbutyric acid | *Pichia pastoris* | (Wang et al., 2018) |
| | Recombinant proteins | *Methylobacterium extorquens* | (Miguez et al., 2003) |
| **Methylamine** | L-lactic acid | *Candida boidinii* | (Osawa et al., 2009) |
| | Phytase | | (Takeshi et al., 1999) |
| | 1,3-propanediol | *Citrobacter freundii* | (Lisa Anne et al., 1995) |
| **Trimethylamine** | L-Lysine | *Methylophilus methylotrophus* | (Davidson et al., 1986; Gunji and Yasueda, 2006) |
| **Trimethylamine N-Oxide** | Carotenoide | *Rhodobacter capsulatus* | (G A Armstrong et al., 1990; Pollich and Klug, 1995) |
| | Cobalamin (vitamin B12) | | |
| | Auxin | *Pseudomonas aminovorans.* | (Ivanova et al., 2001; Large, 1972) |
| **Formate** | Ethanol | *Saccharomyces cerevisiae* | (Wilkins et al., 2007) |
| | Isobutanol and 3-methyl-1-butanol | *Ralstonia eutropha H16* | (Li et al., 2012) |
| **Carbon monoxide** | Magnetic nanoparticles | *Rhodospirillum rubrum* | (Schuler Dirk and Kolinko Isabel, 2015) |
| **Dimethyl ether** | L-amino acid | *Methylococcus capsulatus* | (Ono Yukiko et al., 2001) |
| **Dimethyl sulfoxide** | Quinone Pyrroloquinolin | *Hyphomicrobium Sp* | (De Bont et al., 1981) (Gak Evgeniy Rodionovich et al.) |
| **Dimethylsulfide** | Hydrocarbon | *Thiobacillus thioparus* | (Cho et al., 1991; Kurashova Viktor Mikhailovich and Sakhno Tamara Vladimirovna, 2002) |
| **$CO_2$** | Formic acid | *Shewanella oneidensis* | (Kim Yong Hwan et al., 2017) |

## I.7. *Methylobacterium extorquens* as biotechnological platform organism

As shown in the previous paragraph, methylotrophic bacteria can assimilate reduced C1 compounds either via the serine cycle or the RuMP cycle. *Methylobacterium extorquens (M. extorquens)* is the reference strain for the serine cycle pathway while *Methylophilus methylotrophus* is one of the most studied obligate RuMP cycle strain.

Through a comparison of these two strains, which included some experimental works, serious disadvantages of strain *Methylophilus methylotrophus* as potential production chassis became apparent:

- the lack of tools for genetic modifications compared to *M. extorquens*
- the restricted metabolism as obligate methylotroph
- the viscosity of the strain, compromising the usual protocols of molecular biology, and impeding automated continuous culture applications.

For these reasons, parallel work on RuMP cycle organism during this project was finally not considered.

*M. extorquens* AM1 as reference strain is the most extensively studied serine cycle strain (Ochsner et al., 2015). The whole genome of this strain, comprising a chromosome of (6,8 MB) and four plasmids has been sequenced (Vuilleumier et al., 2009). Progress in understanding the physiology and genetics of this strain, established metabolic models (Marx et al., 2005; Peyraud et al., 2011) and the development of tools for molecular biology enabled the realization of engineering projects. Several vector systems are now available for *M. extorquens* AM1. They include plasmids for protein expression using a panel of inducible promoters, as for instance the promoter PmxaF of the methanol dehydrogenase operon (Table S1). Expression from replicative plasmids is possible, as well as from the chromosome through integrative systems (katA site, attTn7-site). Protocols for mutagenesis, random cassette insertion and homologous recombination were established (Choi et al., 2006; Marx, 2004; Marx and Lidstrom, 2002; Schada von Borzyskowski et al., 2015). The broadened molecular biology toolbox was used to construct platform strains for the optimal use in biotechnological applications and to answer fundamental questions of evolution. Thus, attempts have been made to optimize methanol assimilation through rewiring central steps of formaldehyde conversion (Carroll et al., 2015) or to broaden the set of C1 compounds used as substrates (Michener et al., 2014; Zhu et al., 2016).

*M. extorquens* AM1 has found applications as chassis organism for bio-productions (Table 3). Its capacity to grow on complex carbon sources such as succinate simplifies the implementation of modified C1 assimilation routes and points to a large panel of metabolic intermediates prone to become starting points of new synthetic pathways (Eggeling and Sahm, 1981; Gommers et

al., 1988). Also, the thioesters constituting the ethylmalonyl-CoA pathway of glyoxylate regeneration are used as precursors for the production of fine or bulk chemicals (Korotkova et al., 2002; Yang et al., 2018). Additionally, secondary metabolites such as carotenoids produced by AM1 are of industrial interest, as well as the natural polymer polyhydroxybutyrate (PHB) (Schrader et al., 2009).

An industrial strain should validate a list of characteristics. The following key points are part of it:

- Genetic stability
- Efficient production of product
- Simple nutritional needs
- Cheap carbon and energy source
- Easily genetically-modified
- Safety
- Readily harvested from medium
- Readily breakable if intracellular product of interest
- Limited byproducts in fermentation medium.

Based on these characteristics, which will be discussed in this report, one of the alternative approaches is to create industrial strains to improve the phenotype of the natural strain in a directed way. In general, strain improvements aim at higher production and lower costs. In this study, two limiting aspects of natural methylotrophic strains are targeted: the methanol toxicity and the oxygen need.

**Table 3: *Methylobacterium extorquens* as biotechnological platform organism.**

| Strains | Carbon source | Production | Reference |
|---|---|---|---|
| ***M. extorquens* ATCC 55366** | methanol | Poly-β-hydroxybutyrate (PHB) | (Bourque et al., 1992, 1995; Taidi et al., 1994) |
| ***M. extorquens* ATCC 55366** | co-feeding methanol and 5-hexenoic acid | Polyhydroxyalkanoates (PHA) | (Höfer et al., 2011) |
| ***M. extorquens* ATCC 55366** | methanol | | (Orita et al., 2014) |
| ***M. extorquens* IBT no. 6** | methanol | | (Valentin and Steinbüchel, 1993) |
| ***M. extorquens* ATCC 55366** | methanol | Enterocin P | (Gutiérrez et al., 2005) |
| ***M. extorquens* K** | methanol and n-amyl alcohol methanol, ethanol, succinate | Poly(3-hydroxybutyrate-co-3-hydroxyvalerate) | (SHUNSAKU UEDA et al., 1992) |
| ***M. extorquens* AM1** | Succinate, methanol or ethylamine | 1-butanol | (Hu and Lidstrom, 2014) |
| ***M. extorquens* AM1** | Methanol, succinate | Mesaconic, methylsuccinic acid | (Sonntag et al., 2014) |
| ***M. extorquens* AM1** | Succinate, pyruvate, methanol or ethylamine | PHB | (Korotkova et al., 2002b)<br>(Khosravi-Darani et al., 2013)<br>(Mothes et al., 1998)<br>(Rohde et al., 2017) |
| ***M. extorquens* DSMZ 1340** | Methanol | Polyhydroxybutyrate | (Mokhtari-Hosseini et al., 2009) |
| ***M. extorquens* AM1** | Methanol | Sesquiterpenoid α-humulene | (Sonntag et al., 2015) |
| ***M. extorquens* AM1** | Methanol | Cry1Aan insecticidal protein | (Choi et al., 2008) |
| ***M. extorquens* VKM B-2064T** | Methanol | Vitamin B12 | (Ivanova et al., 2006) |
| ***M. extorquens strain P14*** | | PHB | (Ostafin et al., 1999) |

## I.8. Strain toxicity of solvents to biofuel production and the adaptation to higher tolerance

### I.8.1. Toxicity of solvents to microorganisms

The toxic nature of solvents for bacteria is a major barrier for an economically viable production of chemicals or for use as carbon sources.

Numerous reports describe the inhibitory effects on cell proliferation of the common bulk biofuel ethanol (Ruffing and Trahan, 2014), but also of n-butanol and isobutanol, compounds which have gained interest as potential biofuels due to their favorable physicochemical properties (Tseng and Prather, 2012). Usually, these solvent stressors have pleiotropic effects on the chemical integrity of cellular components and perturb vital cellular mechanisms in a variety of ways (Stephanopoulos et al., 2004). Besides approaches of rational design, where detoxifying membrane transporters (García et al., 2009; Kell et al., 2015) or chaperones are overexpressed to lower the toxic load of solvent stressors (Okochi et al., 2008), directed strain evolution strategies are followed to select for enhanced tolerance.

Evolution in continuous culture setups was applied to obtain biotechnological platform strains like *Saccharomyces cerevisiae*, *Escherichia coli* and *Clostridium phytofermentans* with enhanced ethanol tolerance (Ma and Liu, 2010; Tolonen et al., 2015; Yomano et al., 1998). Resistant mutants to n-butanol and isobutanol were selected for divers organisms including *Clostridium* strains (Hermann et al., 1985), *Escherichia coli*, (Reyes et al., 2011, 2013; Rutherford et al., 2010; Atsumi et al., 2010) and *Cyanobacteria* (Wang et al., 2014). Phenotypic analysis of resistant cells, using genomic, transcriptomic and metabolomic studies, often revealed complex patterns of adaptations, which depended on the nature of the solvent (Mukhopadhyay, 2015).

Frequently found changes in cell physiology involve the lipid content of cell membranes. Their rigidity can be reinforced through fast isomerization of cis into trans unsaturated fatty acids (Heipieper et al., 2003). Also, enhanced hydrophobicity is entailed via detachment of lipid vesicles from the membranes and subsequent biofilm formation (Eberlein et al., 2018). In addition, enhanced synthesis of peptidoglycan precursors, overexpression of chaperones and oxidative stress responses are frequently observed. In some cases, stress resistance could be attributed to point mutations in particular genes. This was the case for *M. extorquens* AM1 mutants growing with increased n-butanol concentrations, where a potassium-proton antiporter was found to partially account for the adaptive phenotype (Hu et al., 2016).

**Table 4: Examples of potential biofuel producer strains adapted to solvent tolerance.**

| Strains | How | Alcohol/solvent tolerance | References |
|---|---|---|---|
| ***Methylobacterium extorquens AM1*** | A combination of serial cultures in liquid and on plates was performed to isolate 1-butanol-tolerant mutants of *M. extorquens* AM1. | The adapted strains were able to grow on 0.15 % 1-butanol with limited inhibitory effect on the growth rate. The growth rate of the wildtype (WT) strain was reduced by 36.5% while the growth rates of the adapted strains were only reduced by 7.5 and 16.9 %. The adapted strain could grow on 0.5 % 1-butanol. | (Hu et al., 2016) |
| ***Chlorella vulgaris*** | Selection of strains adapted to isopropanol by using a serial transfer method. Reinoculation cycles were carried out over a 2-month period from colonies to liquid culture. | The adapted strains were able to grow in the presence of 16g.$L^{-1}$ of isopropanol (IPA). Specific growth rates between 0.0017 and 0.0038 $h^{-1}$ were obtained in the presence of 2–16 g $l^{-1}$ IPA, and a value of 0.0047 $h^{-1}$ evident under IPA-free conditions. | (McEvoy et al., 2004) |
| ***Clostridium beijerinckii*** | Selection of the adapted strain by using liquid serial transfer method. Process optimization was realized in batch fermentation. | The adapted strains were able to grow on 25g.$L^{-1}$ n-butanol. | (Isar and Rangaswamy, 2012) |
| ***Salmonella enterica*** | Selection of adapted strains through exposure to elevated ethanol concentrations of 2.5–10%. | The adapted strains were able to grow on 15% ethanol. | (He et al., 2016) |

### I.8.2. Toxicity of methanol to microorganisms

Methanol, albeit its current use as fuel surrogate in some applications, does not have the potential to become a biofuel as is the case for ethanol or possibly n-butanol. In consequence, the effects of methanol as solvent on cell proliferation have not been studied in great detail.

Reports dealing with its activity on cell components, notably proteins and lipid bilayers have been published. They show that methanol can change the structure of proteins through the stabilization of non-native globular intermediates and the reinforcement of alpha-helical and beta-sheet secondary conformations (Hwang et al., 2011; Kamatari et al., 1996; Perham et al., 2006). It increases the concentration of free oxygen radicals, which in turn, induce protein oxidation (Skrzydlewska et al., 2000). It can perturb enzymatic activities or even protein synthesis ( Busby *et al.*, 1999). Altered fluidity of lipid bilayers induced by methanol was also observed, with possible consequences on the spatial conformation of membrane proteins (Joo et al., 2012).

Only a few tentative of strain adaptations to higher methanol tolerance were reported (Table 5). With the exception of *M. extorquens* AM1 and *M. organophilum*, the strains do not belong to

the *bona fide* methylotrophic bacteria. In some cases, like for *Corynebacterium glutamicum*, methanol resistance was enhanced to counteract growth inhibition by methanol contained in impure glycerol feedstocks from bio-diesel factories (Leßmeier and Wendisch, 2015).

In addition to direct effects of methanol as alcohol solvent, the molecule can exhibit indirect toxicity due to its metabolic conversion to formaldehyde and formate (Chen et al., 2016; Liesivuori and Savolainen, 1991; Oyama et al. 2002). Formaldehyde is a highly cytotoxic compound due to its reactivity with amino acids but also with nucleobases (Heck et al., 1990). It can form DNA-protein, DNA-DNA and protein-protein cross-links, which destabilize the central cellular machinery and induce irreversible damages (Chen et al., 2016).

For methylotrophic strains, formaldehyde is the entry point of all reduced C1 compounds into the central carbon metabolism. An efficient metabolic conversion of formaldehyde to the intermediates of the assimilatory cycle is crucial for the cells. Thus, resistance of *Bacillus methanolicus* towards high methanol was found to depend on the overexpression of the genes coding for the key enzymes of the RuMP cycle, (HPS) and (PHI), converting formaldehyde into biomass (Jakobsen et al., 2006). Besides direct assimilation, the cells possess dissimilatory reactions of dehydrogenases depending on thiol cofactors like glutathione and mycothiol (Vorholt, 2002). In general, formaldehyde is oxidized to form a thiol formate ester, which in turn is hydrolyzed to formate and thiol. Formate can then be further oxidized to $CO_2$, thus delivering reducing equivalents. Besides thiol-dependent systems, thiol independent dehydrogenases of formaldehyde have been described (Duine, 1999).

Formate, the oxidation product of formaldehyde, is also toxic for the cell above a certain threshold. Its inhibitory effect on cell growth (Ostling and Lindgren, 1993) has not yet been well explained. Besides toxicity via oxidation, for some strains experimental evidence pointed to the conversion of methanol at high concentrations to the toxic methionine analogue methoxine (Leßmeier and Wendisch, 2015; Schotte et al., 2016).

**Table 5: Examples of potential biofuel producer strains adapted to methanol tolerance.**

| Strains | How | Methanol tolerance | References |
|---|---|---|---|
| ***Methylobacterium extorquens* AM1** | Mutagenesis of a cell population (Atmospheric and room-temperature plasma (ARTP)) and serial transfer to isolate strains with higher methanol tolerance. | The adapted strain was able to grow at 5% methanol. The final cell density of this strain was reported to be 7 to 10 times higher than the WT in this condition. | (Cui et al., 2018) |
| ***Aspergillus niger*** | Selection from the sector of colony showing growth despite 5% methanol in solid medium and finally obtained through the adaptation process for 22 weeks by sequential transfer of the spores to fresh medium containing 5% methanol. | The adapted strain was able to grow at 5% methanol. | (Mai et al., 2016) |
| ***Sporomusa ovata*** | Selection of the adapted strain by serial transfer on minimal medium supplemented with 2% methanol. | The adapted strain was able to grow on 2% methanol with a growth rate 5-fold higher than non-adapted. | (Tremblay et al., 2015) |
| ***Corynebacterium glutamicum*** | Selection of the adapted strain by serial transfer on minimal medium supplemented with 120 mM methanol. | The adapted strain was able to grow in the presence of 1M methanol. In this condition the growth rate was significantly increased. | (Leßmeier and Wendisch, 2015) |
| ***Methylobacterium organophilum*** | Selection of the adapted strain by serial transfer on minimal medium supplemented with 0,5% methanol. | The adapted strain was able to grow on 0,5% methanol. | (Joon-H et al., 1989) |

## I.9. Enhanced growth under limited oxygen conditions

*M. extorquens* strains are obligate aerobic bacteria relying on a high oxygen supply for growth (Bélanger et al., 2004). Oxygen availability is an important factor for aerobic microbial production processes. The lack of homogenous and sustained oxygen input in bioreactors can lead to performance losses due to a low oxygen solubility in the culture together with a rapid oxygen consumption (Limberg et al., 2017). To achieve an enhanced oxygen transfer rate, reactors with increased broth agitation have been constructed. Also, the use of oxygen supplies with elevated partial pressure and the aeration with pure oxygen are employed (Bélanger et al., 2004; Zhou et al., 2017). However, these technical solutions increase the production costs. In addition, high rates of agitated aeration provoke turbulences and shearing forces in the reactor which can be harmful to the cells (Zhou et al., 2015).

As an alternative, strain engineering to obtain methylotrophic chassis organisms with lowered oxygen demand for biomass production could be envisioned. Inefficient energy transfer during methanol oxidation and the subsequent oxygen reduction through the respiratory chain has been

identified as one of the reasons for high oxygen consumption of *M. extorquens* strains (Strovas et al., 2006; Van Dien and Lidstrom, 2002).

The respiratory chain of *Methylobacterium* species has not been studied in detail. In general, eukaryotic as well as bacterial respiratory chains comprise a set of membrane-bound protein complexes (complexes I to IV) which transfer electrons from a variety of donor molecules to a terminal acceptor (Borisov and Verkhovsky, 2015; Wessels et al., 2016). The electrons are shifted along a chain of intermediate electron carriers such as quinones, NADH, ferredoxins or c-type cytochromes. During aerobic growth, molecular oxygen serves as terminal acceptor, which is reduced to $H_2O$ by the terminal oxidase (complex IV). The energy released during the electron transfers is used to establish a proton or sodium gradient across the cell membrane, which in turn drives ATP synthesis by membrane-bound ATP synthases (complex V).

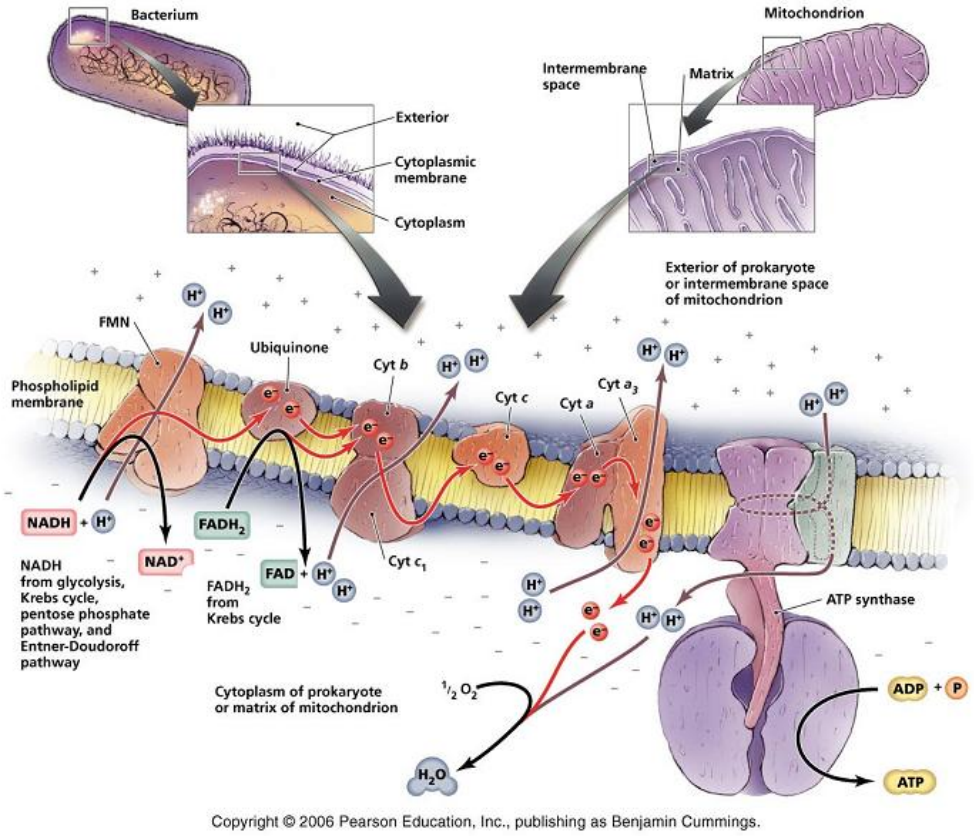


**Figure 5: Overview of the general respiratory chain for eukaryotic and prokaryotic cells.**

While the electron transfer system of mitochondria shows limited variation, the bacterial respiratory complexes are of diverse composition involving different types of oxidases and

electron carriers (Al-Attar and de Vries, 2013; Borisov et al., 2011). These variations reflect the necessary adaptation the cells have to undergo to cope with the changes in oxygen supply encountered in the environment. Automated gene annotation of the *M. extorquens* AM1 genome shows the presence of the respiratory complexes; the terminal electron carrier being a cytochrome c oxidase.

In this study, the GM3 continuous culture device was used to adapt *M. extorquens* AM1 to growth under oxygen-limited conditions. While the standard version of the GM3 uses compressed air to aerate the culture, new prototypes have been developed enabling variations in gas composition. Thus, the oxygen content can be lowered in a controlled way through a partial or total replacement of compressed air by nitrogen.

## I.10. Directed evolution of microbial strains

Growing cells are subject to spontaneous chromosomal mutations occurring at a certain rate. The rate depends on the organism; for *E. coli*, a rate of $2x10^{-10}$ mutations per base pair and generation was measured (Drake, 1991; Lee et al., 2012). Given the genome size to be around $4{,}6x10^{6}$ base pairs, there are $2x10^{-4}$ mutations per *E. coli* genome and generation. Statistically, in a 20 ml *E. coli* culture of $OD_{600}$=1 (around $1x10^{9}$ cells/ml), about every base pair of the *E. coli* genome is altered once in the cells.

The most frequent mutations occurring in a cell population are SNPs (single nucleotide polymorphisms), where a base pair is changed to another. If a SNP affects the gene coding region, the base pair change can lead to a replacement of an amino acid residue by another (missense mutation) or to the introduction of a stop codon (nonsense mutation). If the change does not alter the amino acid specified by the codon affected, the mutation is called synonymous. Small indels, deletions or insertions of two to a few base pairs, are also frequent. Larger chromosomal rearrangements, i.e. duplications, inversions or deletions of chromosomal fragments, are also found in growing cells.

Genomic mutations can have diverse origins. Mostly, they arise upon fidelity errors during the DNA replication process catalyzed by DNA polymerase III. Also, spontaneous chemical alterations of DNA bases like deamination of cytidine or oxidation of guanine, give rise to mismatched base pairs while read by the polymerase. Such modified bases can also be

contained in the nucleotide pool, causing errors upon incorporation in the newly synthesized DNA. Furthermore, DNA lesions like pyrimidine dimers are found (Pfeifer et al., 2005).

Often, mutations have deleterious effects on cellular viability. As consequence, cells possess a variety of sophisticated molecular systems assuring error prevention and correction. These include the proofreading activity of DNA polymerase subunit epsilon (DnaQ) acting as exonuclease. Error repair involves multi-protein complexes performing the detection of mispaired or chemically altered nucleotides, followed by the excision of a short DNA fragment containing the deviated bases and the synthesis of the excised DNA stretch from the template strand. In *E. coli*, the methyl mismatch repair (MME) is one of the best studied mechanisms of replication error correction (Kunkel and Erie, 2005). The template strand of replication is methylated at specific cytidine bases which are recognized by components of the MME complex. This guarantees the correct repair of errors introduced in the newly synthesized strand of the double helix.

Cells which are impaired in molecular systems of preventing and correcting chromosomal mutations often display a mutator phenotype characterized by an increased rate of spontaneous mutations (Horst et al., 1999; Miller, 1996). Depending on the repair system affected, certain types of mutations accumulate in the chromosome. For example, deficient activity of MutT, a nucleotide triphosphate phosphorylase eliminating 8-oxoguanine containing nucleotides from the DNA precursor pool, causes AT to CG transversions (Maki and Sekiguchi, 1992). Mutator strains can exhibit up to $10^3$ higher mutation rates than the wildtype (WT) strain (Horst et al., 1999).

Stress inducing conditions on bacterial growth have been shown to trigger a rise in the ratio of mutator strains in cellular populations (Bjedov, 2003; Foster, 2007; Swings et al., 2017). Different types of stresses including nutrient shortage, temperature shifts, exposition to antibiotics and chemical stressors can increase genetic variation and evolutionary adaptability. Another, more transient response of cells to stress conditions is the induction of the SOS regulon (Baharoglu and Mazel, 2014). Accumulation of single-strand DNA caused by double strand breaks entails a cascade of chromosomal events including the repair of DNA lesions by specialized enzymes like DNA polymerase IV and V. This translesion synthesis is error prone since most of the involved polymerases do not have a proofreading activity. Multiple factors

can provoke the SOS response, among them exposition to antibiotics and oxidative stress (Jena, 2012).

## I.11. Long term propagation of cell populations

Suspensions of microbial strains grown under defined conditions for long time periods enable the study of mutation accumulation and fixation in cell populations. It also opens the way to select descendants having acquired new phenotypes which might be of scientific interest and/or objects of industrial applications. Two types of evolution experiments with cell populations can be distinguished: serial cell transfer, and continuous culture (Barrick and Lenski, 2013).

### I.11.1. Serial transfer

The serial transfer, the simplest experimental setup of cell propagation, requires the daily dilution of the growing culture. In general, and depending on the generation time of the culture, the cells pass through all growth phases: lag, exponential, transition, and stationary phase. The longest evolution experiment of this kind has been performed by Lenski and coworkers to answer fundamental questions of mechanisms of evolution. In this experimentation, 12 independent *E. coli* populations were inoculated from the same ancestor. Daily serial transfer was realized during 66 000 generations (more than 18 years) in flasks containing minimal medium supplemented by glucose as carbon source (Barrick et al., 2009).

### I.11.2. Continuous culture

#### *I.11.2.1. Chemostat*

In the early fifties of the last century, Novick and Szilard and independently Jacques Monod theorized the chemostat concept of continuous culture (Novick and Szilard, 1950). A cell suspension of a given volume is grown under constant conditions. In regular intervals, a predefined fraction of the suspension is discarded as waste and replaced by the same volume of fresh growth medium (Figure 6). This medium contains all necessary nutrients in excess except one, which is provided in limited concentration. Mutants spontaneously arising in the population able to assimilate the limited nutrient more efficiently are selected and fixed in the population. The first chemostat devices constructed by Szilard and Monod automated the exchange of medium samples thus avoiding the need of the daily experimental intervention of

serial culture transfer. Furthermore, a culture grown in a chemostat is kept constantly in the exponential growth phase, which has consequences for the dynamics of mutation acquisition.

### *I.11.2.2. Turbidostat*

A slightly more complicated setup is required to realize a turbidostat selection. This continuous culture regime functions with an optical density threshold: each time the threshold is surpassed by the growing culture, a dilution pulse of fresh medium is provoked. The medium, as opposed to the chemostat, contains all nutriments in excess. Thus, the selection pressure imposed on the culture by the dilutions favors the fastest growing cells which are fixed in the population. The functioning of a turbidostat necessitates the recording of the optical density of the culture in real time and an activator device triggering the dilutions (Figure 6). As is the case for the chemostat, the cells grow exponentially during the entire culture period in the turbidostat.

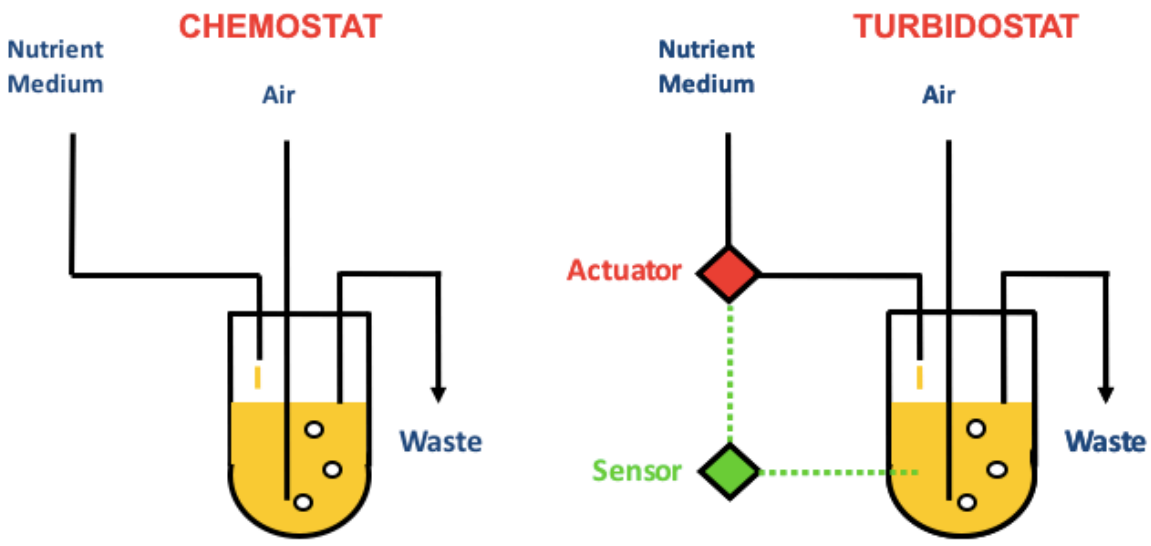


**Figure 6: Chemostat and turbidostat principle.**

## I.11.3. The GM3 device of automated continuous culture

Long term culturing of cell suspensions is hampered by the formation of biofilms on the inner vessel surface. In a population growing under a dilution regime, mutants capable of sticking to the vessel surface appear and are selected. By forming biofilms, these "sticky mutants" escape from the selection imposed on the culture through dilution pulses without acquiring the improved phenotype looked for.

To circumvent this obstacle, the GM3 self-cleaning device automating the operations of continuous culture was developed (Figure 7) (Mutzel et al., 2004; Mutzel and Marlière, 2001). The central idea of the GM3 setup is to install two identical cultivation vessels, connected by flexible tubings enabling the exchange of fluids between the vessels. In regular intervals fixed by the operator, the culture growing in vessel 1 is transferred into vessel 2, and vessel 1 is cleaned up by flow of a 5N NaOH solution followed by a step of rinsing with water. Subsequently, the culture moves from vessel 2 to 1, ending the cleaning cycle. In general, between two and four such cleaning cycles are programmed per 24 hours. The GM3 is a closed fluidic system kept under a low atmospheric pressure of 0.3 bar. All fluids (culture, NaOH, $H_2O$, growth media) move inside the device; their direction of flow is determined by the opening and closing of electro valves, which is programmed according to a storyboard (Figure 6 and 7).
The cell suspension (about 16 ml) growing in the vessel is constantly aerated by compressed air or other gas mixtures. Constant aeration counteracts cell sedimentation. The optical density of the culture is measured in real time enabling the fixation of thresholds necessary for the conduction of different continuous culture regimes.

Certain conditions must be met to realize a continuous culture experiment in the GM3. The cells cultivated need to exhibit an axenic, non-filamentous growth. Also, a residual growth rate of the culture is required, with at least one doubling per 24 hours. Without regular dilutions, the volume of the suspension will not stay constant due to evaporation. Furthermore, all ingredients of the growth media have to be totally soluble and must not chemically aggress the fluidic components.

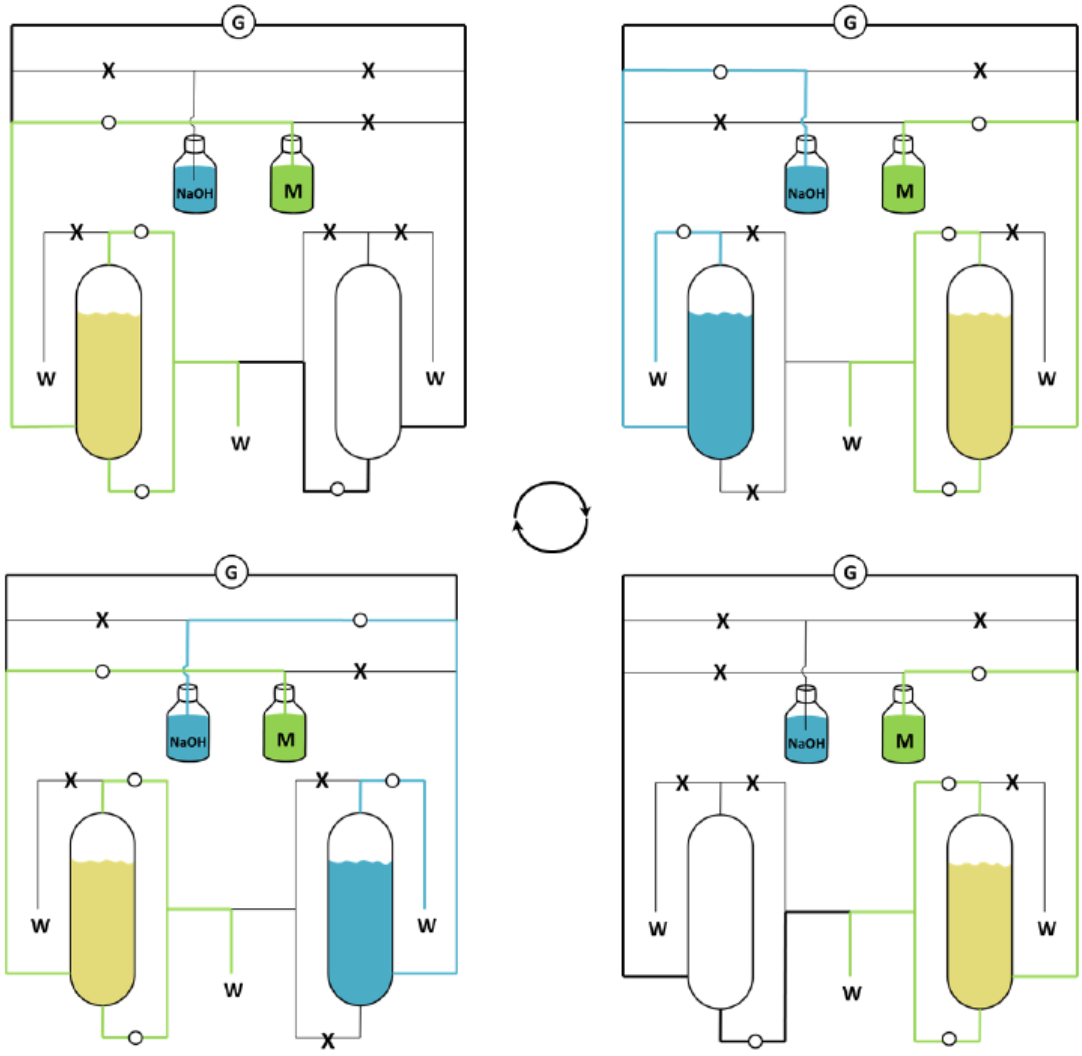


**Figure 7: GM3 device with double vessels system/wash systems (Souterre, 2017). Pressurized gas supply (G); medium source (M in green); sterilizing agent (NaOH 5 M in blue); waste (W); Bacterial cultures is shown in yellow. Valves are indicated by X and O for the closed and open states, respectively. Flows in the tubing are indicated by bold lines.**

### I.11.4. Strain evolution in the GM3: turbidostat and medium swap regimes

The turbidostat culture regime is very suitable for cell growth improvement and can easily be programmed in the GM3. However, the adaptation of strains to proliferate under conditions largely deviating from their native growth situation often requires more sophisticated culture setups. These adaptations can include growth on highly toxic compounds or the optimized functioning of new metabolic pathways in engineered cells. For such applications, an incremental change of the growth medium composition can be beneficial.

The conditional medium swap regime was developed for this purpose (Marlière et al., 2011). Two growth media are installed to dilute the culture. In general, medium 1, called relaxing medium, is permissive to growth of the cells to be evolved. Medium 2, called stressing medium, does not support growth of the cells at the beginning of the strain evolution. It marks the phenotypic objective of the experiment, i.e. the growth condition towards which the cells should evolve during adaptation. To realize a medium swap culture regime, an optical density (OD) threshold is fixed and dilution pulses programmed at regular intervals, as is the case for a chemostat. If the measured OD is below the threshold, the culture is diluted by the relaxing medium, otherwise by the stressing medium. This technique may be related to a morbidostat using a chemostat regime.

During a medium swap adaptation, the growth medium in the culture vessel is a mixture of relaxing and stressing medium. A mutant appearing in the population supporting faster growth at a given relaxing/stressing composition will trigger more dilution pulses from the stressing medium, thus changing the composition of the growth medium. Mutations will accumulate and shift the dilution ratio more and more towards the stressing medium. Finally, descendants of the original strain will appear capable of growing in the culture diluted exclusively by the stressing medium. The fixation of this descendant in the population marks the end of the adaptation experiment.

#### *I.11.4.1. Applications of the GM3 technology*

The methodology of continuous culture in the GM3 has been used to perform a number of strain adaptations with diverse objectives. These included the evolution of enzymes with new substrate specificities and the hardening of a cellulolytic bacterium towards a toxic degradation product of lignocellulose. Also, the implementation of new routes of the central carbon metabolism and the selection of bacteria with an altered DNA composition were achieved with this technology.

##### I.11.4.1.1. Evolution of an alpha-ketoglutarate dependent dioxygenase

The alpha-ketoglutarate dependent dioxygenases (a-KAO) catalyze the hydroxylation of non-activated C-H bonds in a stereospecific manner, reactions difficult to realize with the methods of classical organic chemistry. The co-substrate alpha-ketoglutarate is decarboxylated to succinate during the reaction, a precursor of essential C4 compounds of the metabolism.

A generic *in vivo* selection screen based on succinate-auxotrophy was constructed in *E. coli*. The auxotrophy could be complemented with different a-KAOs expressed in the cells. The substrate specificity of the isoleucine alpha-ketoglutarate dioxygenase from *Bacillus thuringensis* was enlarged towards the isoleucine analogue norvaline using a medium swap regime. Cultures adapted to growth on a succinate-free stressing medium with norvaline as specific dioxygenase substrate harbored missense mutants of the gene coding for the enzyme under selection. The specific activity of the mutated enzymes for norvaline was shown to be higher than the residual activity of the wildtype enzyme (Souterre, 2017).

#### I.11.4.1.2. Evolution of *Clostridium phytofermentans* to higher ferulate tolerance

Biofuel production from biomass using microorganisms able to metabolize plant polysaccharides is an alternative to fermentation processes depending on sugar feedstocks. The primary substrate, lignocellulose, is an intricate structure of polysaccharides and polyphenolic lignin. The enzymatic breakdown of lignocellulose by the anaerobic bacterium *Clostridium phytofermentans*, a cellulolytic model organism, releases phenolic growth inhibitors like ferulic acid.

A GM3 device constructed to enable cell adaptations under anoxic growth conditions was used to select descendants of *C. phytofermentans* with high tolerance towards ferulic acid. Medium swap adaptations were iterated by incrementing the ferulate concentration in the stressing medium by 0.5 $g.L^{-1}$. Five medium swap periods were conducted to obtain a culture growing with 3 $g.L^{-1}$ of ferulate. Between each medium swap, the GM3 was run in turbidostat mode until the growth rate of the culture was again lowered to the initial growth rate.

Ferulate-resistant isolates were obtained and analyzed. They grew robustly with 6 $g.L^{-1}$of ferulate, the solubility limit of this phenolic compound. DNA changes included SNPs, indels and DNA duplications involving IS elements. These mutational events were associated with fatty acid metabolism, gene regulation and the cell surface (Cerisy et al., 2017).

#### I.11.4.1.3. Implementation of a reductive route of formate assimilation in *E. coli*

Formate can be synthesized from $CO_2$ through electro reduction and function as carrier molecule linking renewable energy production with fermentation. As initial steps towards the

construction of a formatotrophic platform organism, a reductive route of formate assimilation was implemented in *E. coli* through consecutive growth adaptations of selection strains.

In a first step, a formate tetrahydrofolate ligase from *Clostridium kluyveri* was expressed in *E. coli* cells deleted for genes specifying serine hydroxymethyl transferase and the glycine cleavage complex. These cells, auxotrophic for tetrahydrofolate-attached C1 compounds, were adapted to growth on formate as sole C1 source via a medium swap continuous culture evolution conducted in the GM3.
Further selections for growth on formate and $CO_2$ as C1, glycine and serine source using medium swap adaptations established a reductive route of formate assimilation in *E. coli* accounting for about 11% of cellular carbon. $^{13}$C-formate labeling experiments confirmed the activity of the newly implemented pathway. During the continuous culture adaptations, mutations were fixed in genes of the reductive route resulting in changed enzymatic activity (FolD) or augmented expression level (FtfL) of pathway components (Döring et al., 2018).

#### I.11.4.1.4. Evolving a bacterium with an altered DNA composition

Descendants of *Escherichia coli* K12 were selected containing the non-canonical nucleobase, 5-chlorouracil (CLU), as constitutive component of their DNA. CLU replaced the canonical base thymine (T), of which it is a chemical homolog. An *E. coli* thymine auxotrophic strain was constructed depending on T supplementation in the medium to grow. The base CLU, when added to the medium, was converted into a deoxy-nucleoside by a heterologous nucleoside deoxyribosyltransferase and the nucleoside into a deoxy-nucleotide triphosphate by nucleoside and nucleotide kinases of the cells. In turn, the dCLU-triphosphate functioned as substrate for DNA polymerase III.

CLU could not replace T in the DNA of the unevolved selection strain. A medium swap was launched to perform the replacement by increment. The relaxing medium contained T, the stressing medium CLU in equal concentration. The optical density threshold was fixed at 0.6, corresponding to 80% transparency of the culture. After around six months of cultivation (around 1000 generations), the ratio stressing/relaxing dilution pulses reached 100%. HPLC analysis of the DNA of culture isolates showed a T replacement by CLU of 90%. The residual T molecules in the DNA came from chemical modifications of tRNA uracil bases. The deletion of some of the genes implicated lowered the T content further in the DNA of the isolates.

Genome sequencing of the evolved strains revealed a high number of mutations (>1000), reflecting the tendency of CLU to mispairing during DNA replication (Marlière et al., 2011).

### I.11.5. Evolved *M. extorquens* strains as production chassis

Evolving microbial producer strains with altered phenotypic traits like higher solvent resistance can impact metabolic fluxes and pools of intermediates in an unpredictable way. A biosynthetic pathway implemented in the cells commonly starts from a cellular metabolite belonging to the metabolic core. Given the double nature of methanol as toxic stressor and growth substrate for methylotrophic strains, derivatives adapted to higher methanol tolerance are susceptible to carry modified expression patterns of metabolic enzymes and regulators resulting in changes of the carbon and energy flow.

To assess the capacity of the evolved methanol tolerant strains to produce platform chemicals with high yield and to compare the performance with the wildtype cells, two compounds were chosen: D-lactic acid and 3-hydroxypropionic acid (3-HP).

D-lactic acid can be produced from the central metabolite pyruvate in a one-step reaction catalyzed by D-lactate dehydrogenase. In *M. extorquens* strains, a D-lactate dehydrogenase encoded by the gene *ldhA* is present. Overexpression of plasmid-borne *ldhA* from a constitutive promoter represents a easy metabolic setup for testing production capacities of wildtype and evolved strains grown on methanol.

The second compound, 3-hydroxypropionic acid, was chosen for the following reasons:

- 3-HP is one of the originally 12 chemicals listed by the American Department of Energy (DOE 2004) to have the highest potential for bio-based production (Table 6). The interest for these compounds comes from the fact that they can be converted to a number of high-value chemicals. Figure 8 shows the production tree of 3-hydroxypropionic acid comprising acrylic acid, a polymer precursor with a worldwide production volume of several million tons (Acrylic acid: World Market Outlook and Forecast up to 2018, Merchant Research and Consulting, 2014).

- 3-HP can be produced by a variety of synthetic routes parting starting from intermediates of the central carbon metabolism (Kumar et al., 2013). A reductive route from acetyl-CoA is particularly favorable since it necessitates the introduction of only two heterologous enzymatic activities in *M. extorquens* converting malonyl-CoA via two reductions into 3-HP (Liu et al., 2017):

  acetyl-CoA > malonyl-CoA > 3-oxopropanoate > 3-HP

  A bi-functional enzyme from *Chloroflexus aurantiacus* catalyzing both reduction reactions using NADPH as cofactor was described (Hügler et al., 2002).

- 3-HP production was reported from carbohydrates or other complex carbon sources by platform strains like *E. coli* (Song et al., 2016) and *S. cerevisiae* (Kildegaard et al., 2016), and from $CO_2$ by autotrophic organisms (Lan et al., 2015; Wang et al., 2016), but not from reduced C1 compounds. However, the publication during the course of the present work, of a *M. extorquens* AM1 derived producer strain finally added methanol to the list of feedstocks for 3-HP production (Yang et al., 2017a).

**Table 6: Top value-added chemicals from biomass. Department of energy, USA, 2004, modified 2010.**

| Compound | Production process |
|---|---|
| Succinic acid, malic acids | Fermentation |
| 2,5 furan dicarboxylic acid | Chemical from carbohydrates |
| 3-hydroxypropionic acid | Fermentation in preparation |
| Glycerol | From lipids (biodiesel) |
| Levulinic acid | Chemical from plant biomass |
| Sorbitol | Hydrogenation of glucose, fermentation |
| Xylitol | Hydrogenation of xylose, fermentation |
| Lactic acid | Fermentation |
| Isoprene | Fermentation (gas phase) |
| Biohydrocarbons | Fermentation |
| Hydroxymethylfurfural | Chemical from biomass |
| Furfural | Many process, chemical |
| Ethanol | Fermentation |

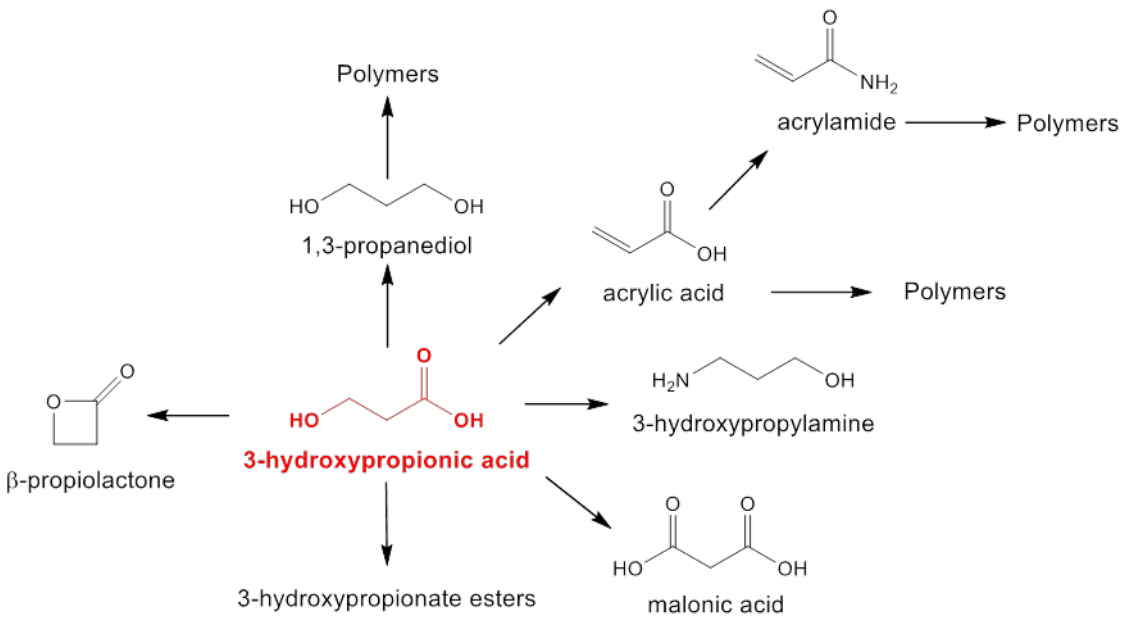


**Figure 8: Production tree of 3-hydroxypropionic acid.**

## I.12. Objectives of the present work

A wide range of biosynthetic pathways have been implemented in natural methylotrophic strains of the genus *Methylobacterium* enabling the production of various commodity chemicals from methanol, a renewable feedstock gaining interest for biotechnological processes. By contrast, less effort has been made to endow these strains with enhanced properties as production chassis. In this context, the following questions were asked:

- Can *M. extorquens* strains be evolved to stable growth on high methanol concentrations? Methanol as an alcohol solvent and as precursor of the oxidation intermediates formaldehyde and formate is toxic for cells. This toxicity limits production yields in fermentations.

- What would be the cellular processes taking place during such a methanol adaptation? Phenotypic, genomic, transcriptomic and biochemical analysis were to be conducted to identify mutated genes and changed regulatory networks and to test enzyme variants for new activity.

- Would the implementation of a synthetic route in a methanol tolerant cell enable the production of an industrial compound with higher yield than the same route implemented in the wildtype strain?

- Can *M. extorquens* strains be evolved to efficient growth under oxygen limiting concentrations? These obligate aerobic cells have a high oxygen demand causing difficulties for upscaling of fermentation processes and diminished product yield through the capture of high energy electrons by the respiratory chain.

# II. MATERIALS & METHODS

## II.1. Microbiologic protocols

### II.1.1. Bacterial strains and growth conditions

The strains *M. extorquens* AM1 (DSM n°1338) and TK 0001 (DSM n°1337) were grown at 30°C in standard mineral medium (smm) (modified medium DSMZ n°1629) supplemented with various carbon sources at different concentrations: methanol, succinate, formate, formaldehyde etc... (Table 7, 8 and 9). Growth media were solidified with 15 g/L agar for the preparation of Petri dishes.

**Table 7: Composition of standard mineral medium.**

| Component | Amount |
|---|---|
| $Na_2HPO_4.12H_2O$ | 7.03 g |
| $KH_2PO_4$ | 1.00 g |
| $(NH4)_2SO_4$ | 0.50 g |
| $MgCl_2.6H_2O$ | 0.10 g |
| $CaNO_3.4H_2O$ | 0.05 g |
| Solution SL-4 | 2 mL |
| NTA mix | 1 mL |
| Distilled water | q.s. 1L |

**Table 8: SL-4 composition.**

| Component | Amount |
|---|---|
| EDTA | 0.5 g |
| $FeSO_4.7H_2O$ | 0.2 g |
| Solution SL-6 | 800 mL |
| Distilled water | 200 mL |

**Table 9: SL-6 composition.**

| Component | Amount |
|---|---|
| $ZnSO_4.7H_2O$ | 0.1 g |
| $MnCl_2.4H_2O$ | 0.03 g |
| $H_3BO_3$ | 0.3 g |
| $CoCl_2.6H_2O$ | 0.2 g |
| $CuCl_2.6H_2O$ | 0.01g |
| $NiCl_2.6H_2O$ | 0.02 g |
| $Na_2MoO_4.2H_20$ | 0.03 g |
| $Na_2O_4W.2H_2O$ | 0.03 g |
| $H_4Na_2O_6W$ | 0.03 g |
| Distilled water | q.s. 1L |

### *II.1.1.1. Growth experiments in Erlenmeyer flasks*

The bacteria were grown in Erlenmeyer flasks in smm supplemented with a carbon source at 30°C with constant agitation during 5 days. The ratio of volume of culture / volume of the flask was of 1/5. The culture was sampled at regular intervals of time for cell density measurement. $OD_{600nm}$ was measured using an optical spectrophotometer (Beckmann) using 1 cm-wide optical cuvettes.

### *II.1.1.2. Growth experiments in Bioscreen C cell density reader*

For growth curve experiments a Microbiology Reader Bioscreen C apparatus (Thermo Fisher Scientific) was used. It consists of a thermostatic incubator and a culture growth-monitoring device (OD reader). Precultures in smm supplemented with 1 % methanol (v/v) were rinsed in smm and diluted in the growth medium to reach an $OD_{600nm}$ of 0.01; 200 µL aliquots of the cell suspensions were distributed into the multi-well plates. Temperature was set depending on the strain and all optical density measurements were carried out at 600 nm in six replicates over a period of at least 72h under continuous agitation. Each experiment was repeated twice (Figure 9).

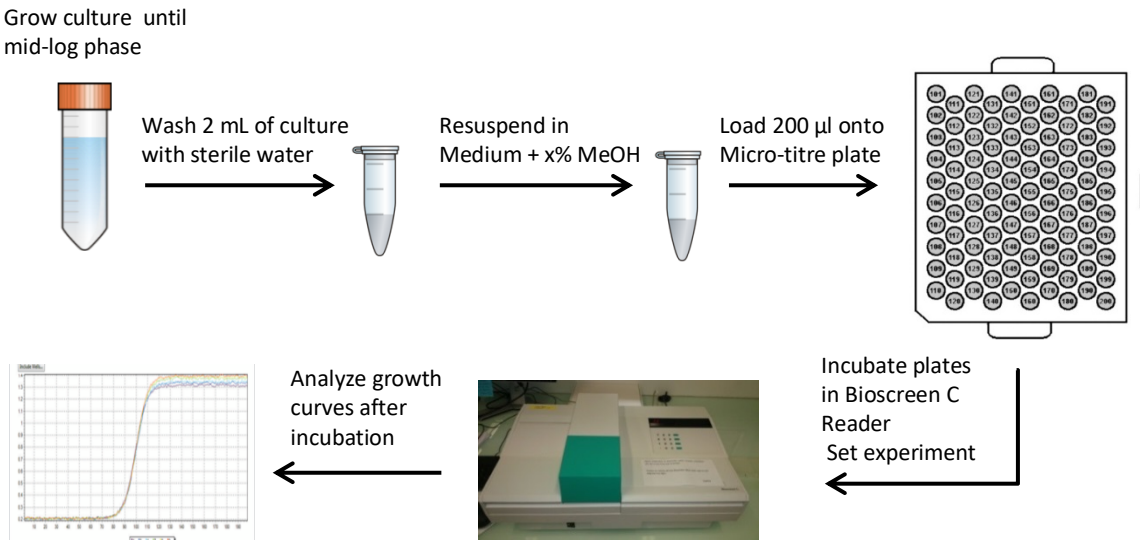


**Figure 9: Experimental protocol of growth assays using the Bioscreen C reader.**

### *II.1.1.3. Measurement of biomass production*

Biomass production on fixed methanol concentrations was determined as dried cell weight. For that bacterial cultures were grown until mid-log phase and 100 µl of a suspension of exponentially growing bacteria were diluted into 3mL of smm supplemented with 1% methanol. When the bacterial population entered the stationary phase (monitored by measuring the $OD_{600nm}$), 2 ml of the cell suspension were transferred to a pre-weighed 2 mL Eppendorf tube, centrifuged at 13000 rpm for 5 minutes. The supernatant was discarded. The cell pellet was dried for 15-20 minutes in a speed vacuum evaporator (SpeedVac). The tubes were weighed again and the weight of the dried cells determined. All measurements were performed in triplicates (Figure 10).

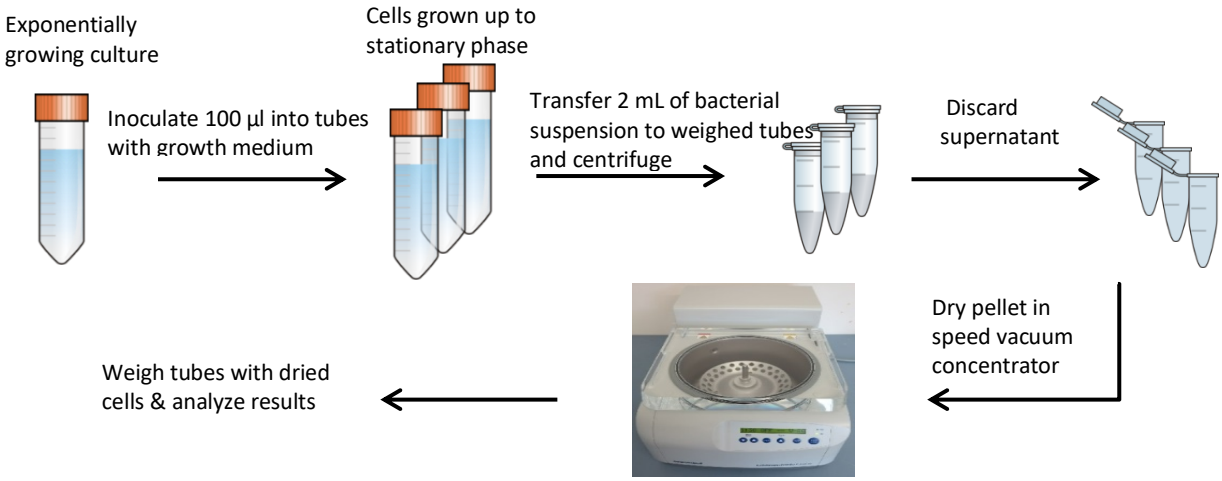


**Figure 10: Protocol of measurement of dried bacteria weight.**

### II.1.2 Tests of sensitivity to antibiotics

Disc diffusion tests were performed to determine the sensitivity of the bacterial strains to various antibiotics. 100 µl of a bacterial suspension were spread onto agar plates containing smm supplemented with 1% methanol. Sterile wafer discs of a diameter of 0.25-inch were placed onto the bacterial lawn and 10 µl of a solution of the antibiotic were poured onto the center of the disc. The plates were incubated at 30°C for 48h to 120 hours. Sensitivity or resistance to the antibiotic was determined by the diameter of the zone around the disc where no growth is visible (Figure 11). The minimal inhibitory concentration (MIC) of the various antibiotics was determined by plating 100 µl of a bacterial suspension on semi-solid smm supplemented with 1% methanol and a range of concentrations of antibiotic and incubating the plates for 48 hours at the temperature of optimal growth. The presence of colonies indicated resistance to the corresponding concentration and absence indicated sensitivity. MIC was defined as the lowest inhibitory antibiotic concentration. Along with assays on plate, antibiotic sensitivity was also monitored in liquid growth medium.

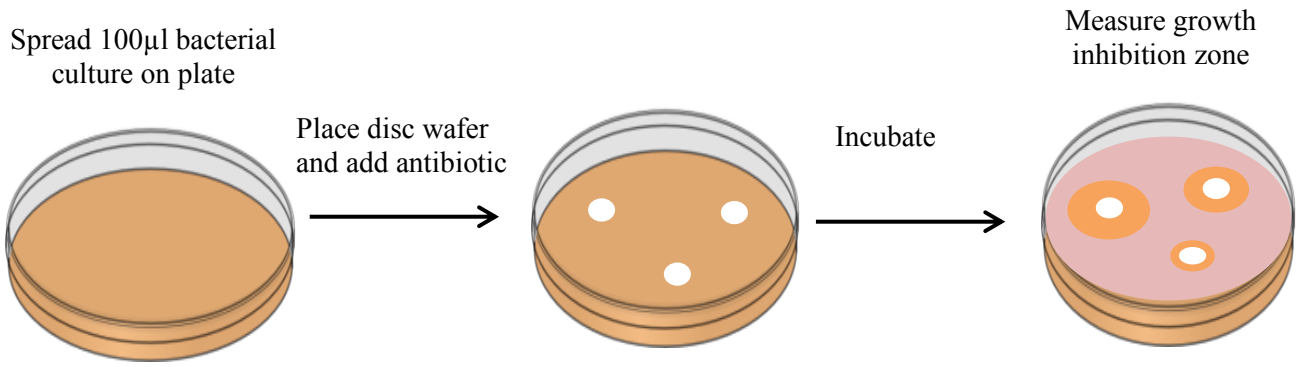


**Figure 11: Protocol of disc diffusion tests to check antibiotic sensitivity.**

### II.1.3 Electroporation

#### *II.1.3.1. Electrocompetent cells preparation of E. coli and M. extorquens strains*

An exponentially growing bacterial suspension was diluted 1/200 in smm supplemented with 1% methanol and incubated at a temperature corresponding to the bacterial strain optimum under continuous agitation. Once log phase was confirmed by measuring the optical density at 600nm, the culture was chilled on ice for 15 minutes. The culture was then centrifuged at 4000 rpm at 4 ºC for 30 minutes. The pellet was resuspended into 20 mL of an ice-cold sterile 10% glycerol solution. The washed cells were centrifuged at 4000 rpm at 4ºC for 30 minutes. The supernatant was discarded by gentle pipetting. The pellet was resuspended with 10 mL of an ice-cold sterile 10% glycerol solution. The washed cells were centrifuged again at 4000 rpm at 4ºC for 30 minutes. The supernatant was removed by gentle pipetting and the pellet was resuspended into 4 mL ice-cold sterile a 10% glycerol solution. The electrocompetent cells were stored at -80 ºC aliquoted in 100 µl in1 mL sterile Eppendorf tubes.

#### *II.1.3.2. Electroporation and chemical transformation of E. coli*

Each plasmid was introduced into electrocompetent cells by electroporation. 50 µL of competent cells were mixed on ice with 1 µL of ligation product and put in an ice-cold 1 mm wide electroporation cuvette. The cuvette was placed into the pulsing chamber and pulsed at set voltage of 1.8kV and resuspended in 1 ml of LB medium. The transformed strains were incubated at 37°C with agitation for 40 minutes before to be put on plate with selective medium.

#### *II.1.3.3. Electroporation of M. extorquens*

Electroporation was performed using a Bio-Rad Gene Pulser II. 500 ng of plasmid DNA was added to 100 µl of electrocompetent cells thawed on ice, gently mixed by pipetting and transferred to a sterile ice-cold Bio-Rad cuvette of 0.1cm gap. The cuvette was placed into the pulsing chamber and pulsed at set voltage of 1.25kV and resistance of 25Ω. Immediately after pulsing, 1 mL of smm supplemented with 1% methanol was added to the pulsed cells. The bacterial suspension was incubated under agitation at corresponding temperatures for 2 to 5h. The bacteria were then centrifuged at 13000 rpm for 3 minutes. 900 µl of the supernatant were discarded. The pelleted cells were resuspended in the remaining 100 µl of medium and spread onto agar plates containing smm supplemented with 1% methanol and the required antibiotic. The plates were incubated at the temperature corresponding to the bacterial strain optimal temperature for 48h.

### II.1.4. Directed evolution in continuous culture using GM3 device

Methanol resistant derivatives of *M. extorquens* AM1 and TK 0001 wildtype strains were selected using the GM3 automated self-cleaning cultivation devices. These devices enable long-term cultivation of growing bacteria by diluting automatically the cell suspension with pulses of fresh medium and discarding an equivalent volume of culture at the same time. A continuous flow of sterile air through the culture vessel ensures constant aeration and counteracts cell sedimentation. Different growth regimes can be programmed.

***Turbidostat***

This cultivation regime enables the selection of optimized growth in permissive conditions. Every 10 minutes, the optical density of the culture is automatically measured and compared to a fixed threshold ($OD_{600nm}$ value of 0.4). When the measured $OD_{600nm}$ exceeds the threshold, a pulse of fresh nutrient medium is injected into the culture and the same volume of used culture discarded. The dilutions ensure that the biomass in the vessel remains constant and that the bacteria grow at their maximal growth rate.

***Medium swap***

This regime enables gradual adaptation of a bacterial population to grow in a non-permissive or stressing medium. The growing culture can be diluted by either permissive or stressing

medium. The choice between the two dilutions media depends on the turbidity of the culture with respect to a set $OD_{600nm}$ threshold ($OD_{600nm}$ value of 0.4). When the $OD_{600nm}$ exceeds the threshold, a pulse of stressing medium is injected; otherwise a pulse of permissive medium is injected. Dilutions are triggered every 10 minutes with a fixed volume of medium, thus imposing a generation time on the cell population.

#### *II.1.4.1. Determination of the methanol concentration in liquid growth media*

The GM3 continuous culture automaton is a fluidic device. A pressure of 0,3 bar is constantly maintained in the system through the inflow of compressed air which assures the aeration of the cell culture and the programmed flow of liquids. The air is evacuated from the device entailing liquid evaporation.

To realize a long-term culture experiment, growth media – usually 5 liters - have to be prepared in the beginning of the evolution and must stay unchanged until their consumption through dilution pulses. Methanol being a volatile organic liquid (boiling point of 64,7°C at RT), we tested whether a culture regularly diluted by a growth medium containing 10% methanol in the GM3 fluctuated in its real time methanol content. A chemostat was programmed and the culture vessel filled with mineral medium supplemented with 10% methanol. Dilution pulses from the medium reservoir were programmed according to a generation time of 12 hours and the sterile culture medium kept under this regime for one month.

Samples were regularly taken and the methanol content dosed using a fluorometric method. Figure 12 shows that the methanol concentration did not lower with time. Some fluctuations were observed which, at least partially, can be attributed to the limited sensitivity of the dosing method.

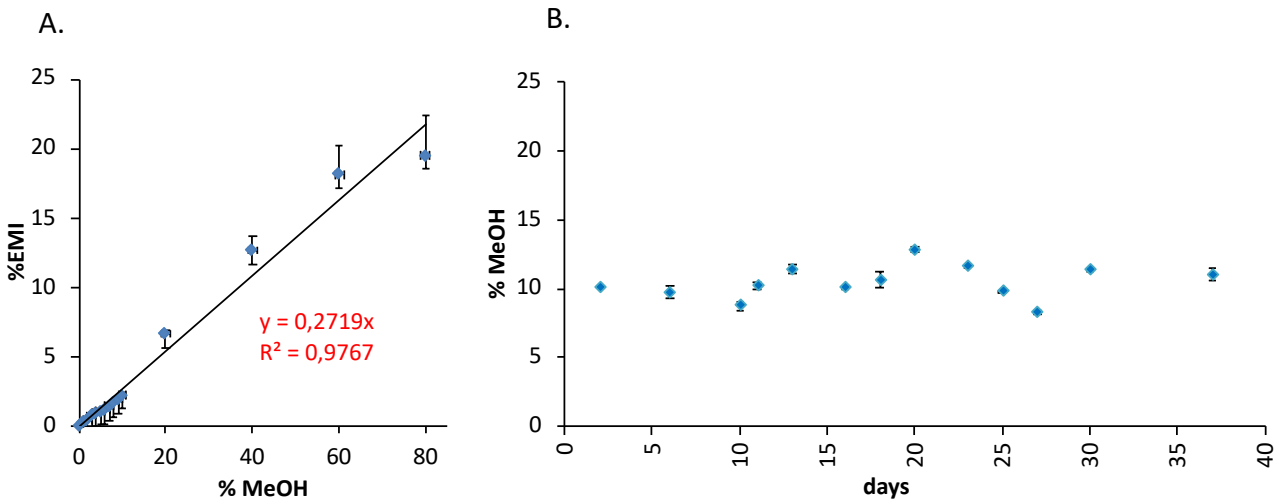


**Figure 12: Methanol quantification by a fluorometric test. The standard range with mean values of three replicates ± standard deviation (SD) (A). The methanol content in samples from a GM3 culture vessel containing sterile mineral medium supplemented with 10% methanol was determined for a period of 37 days ± SD (B).**

### *II.1.4.2. Evolution of M. extorquens TK 0001 and AM1 into GM3*

A population of growing cells of both strains *M. extorquens* TK 0001 and AM1 was injected into a GM3 cultivation device. The composition of the permissive and stressing media used during the evolution experiments; temperature and set generation time under medium swap regime were as follows:

- Selection of growth at 5% methanol: permissive medium: smm + 1 % methanol – stressing medium: smm + 5 % methanol – 30°C – generation time 8 hours for AM1 chamber 1, 10 hours for AM1 chamber 2 and 10h hours for TK 0001.
- Selection of growth at 7% methanol: permissive medium: smm + 5 % methanol – stressing medium: smm + 7 % methanol – 30°C – generation time 7h30 for AM1 chamber 1, 10 hours for AM1 chamber 2 and 13 hours for TK 0001.
- Growth adaptation at 8 % methanol: smm supplemented with 8 % methanol at 30°C.
- Growth adaptation at 9 % methanol: smm supplemented 9 % methanol at 30°C.
- Growth adaptation at 10 % methanol: smm supplemented 10 % methanol at 30°C.

## II.2. Molecular biology protocols

### II.2.1. PCR Amplification

The polymerase chain reaction (PCR) enables the amplification of DNA fragments identical to a template (chromosomal or plasmid DNA etc.). It requires the template DNA usually present in low amounts, specific single strand primers delineating the fragment to be amplified, a DNA polymerase active at high temperatures and a mix of the deoxynucleotides triphosphate in excess. The protocols consist of cycles of primer annealing; template-guided DNA synthesis and denaturation of the resulting double stranded DNA. Since each round amplifies the present templates, the overall amplification is exponential (Table 10).

All primers were designed by using APE software. PCR reactions were carried out in 50 µl with Platinum® Pfx DNA polymerase, Phusion polymerase (for high fidelity reactions) or DreamTaq™ DNA polymerase (for verification) according to the manufacturer's protocol.

**Table 10: Protocol for thermocycler program using Pfx.**

| Temperature | Time/ Cycles | |
|---|---|---|
| **95 °C** | For 5 minutes | |
| **95 °C** | 1 minute and 30 seconds | 25 cycles |
| **55 °C** | 30 seconds | |
| **72 °C** | 1 minute /kb | |
| **72 °C** | For 7 minutes | |
| **4 °C** | For storage | |

Elongation temperature varied for Pfx polymerase at 68 ºC. In case of high GC content, a touch-down protocol was performed. Touch-down protocols include cycles with varying temperatures for the annealing step starting with the highest temperature and decreasing by one degree for every cycle depending on the number of cycles set (Table 11). This approach increses the probability to operate at optimized conditions and to the initial number of templates for further amplification. An example of a touch-down PCR program is shown as follows:

**Table 11: Protocol for thermocycler program for touchdown using Pfx.**

| Temperature | | Time/ Cycles |
|---|---|---|
| **95 °C** | | For 10 minutes 1 cycle |
| | **95 °C** | 1 minute and 30 seconds |
| | **72* °C** | 30 seconds (decrease 1°C every cycle until 62°C) x 10 |
| | **68 °C** | 1 minute /kb |
| | **95 °C** | 1 minute and 30 seconds |
| | **55 °C** | 30 seconds x 25 |
| | **68 °C** | 1 minute /kb |
| **68 °C** | | For 7 minutes |
| **4 °C** | | For storage |

Yield and length of PCR products were verified using 1 % agarose gel electrophoresis in 1X Tris/Borate/EDTA (TBE) in the presence of ethidium bromide and visualization under ultraviolet (UV).

### II.2.2. Nucleic acid purification

For DNA purification, kits from QIAgen were used following manufacturer's instructions:

- QIAQuick PCR Purification kit was used to purify DNA fragments obtained after PCR amplification or plasmid digestion with restriction enzymes;
- QIAprep kit was used to extract plasmids from overnight bacterial cultures;
- MinElute kit was used to purify ligation products;
- Gel extraction kit was used to extract DNA fragments of determined length obtained after plasmid digestion with restriction enzymes and separation of the digestion products by electrophoretic migration in 1 % agarose gels.

### II.2.3. Directed mutagenesis protocol

Standard PCR protocol was used with specific primers containing the mutated site (Table 12). PCR product was treated with DpnI during 1h at 37°C. 1µL of the reaction was transformed into competent cells.

**Table 12: Table of primers designed for directed mutagenesis of C-terminal part of malonyl-CoA reductase *gene* (cmcr) .**

| Primers | Gene | Target mutation | Primer sequence (5' -> 3') |
|---|---|---|---|
| 5546 | *cmcr* | N940V-fw | CGCCGACCGC**GTT**GTCTCGGGCGAGACCTTCCACCCGTCGGGC |
| 5547 | *cmcr* | N940V-rv | CGCCCGAGAC**AAC**GCGGTCGGCGAGGTAGTAGA |
| 5548 | *cmcr* | K1106W-fw | GGTCGCGCGC**TGG**ATCGCCCTGTCGGATGGCGC |
| 5549 | *cmcr* | K1106W-rv | ACAGGGCGAT**CCA**GCGCGCGACCCGGAAGTGGT |
| 5550 | *cmcr* | S1114R-fw | GGATGGCGCC**AGA**CTCGCGCTGGTCACCCCCGAAACCACGG |
| 5551 | *cmcr* | S1114R-rv | CCAGCGCGAG**TCT**GGCGCCATCCGACAGGGCGA |

### II.2.4. Gene cloning using restriction enzymes

#### *II.2.4.1. Fast digestion*

Plasmid DNA was digested using fast digest restriction enzymes following the manufacturer recommendations (NEB). 1 µg of DNA was mixed with 1 µl of the desired fast digest enzymes and 2 µl of fast-digest buffer. The volume of the reaction mix was adjusted to 20 µl with nuclease-free sterile water. The reaction mix was incubated at 37ºC in a thermostatic heat-block for 5 minutes. To confirm the expected size of the digestion fragments, an aliquot of the digestion mix was analyzed by agarose gel electrophoresis and BET staining.

#### *II.2.4.2. Ligation*

1X ng of recipient vector and 5X ng of insert were mixed with 2 µl of ligation reaction buffer and 1 µl of T4 DNA Ligase (NEB). The volume of the reaction mix was adjusted to 10 µl with nuclease-free sterile water. The mixture was mixed thoroughly and incubated for 1 hour at 37ºC in a thermostatic bath. The ligation mix was chilled on ice, purified following the MinElute protocol and transformed into electrocompetent bacteria.

#### *II.2.4.3. E. coli transformation by electroporation*

β2033 competent cells were prepared according to the common protocol. 1µL of ligation product were mixed on ice with 50 µL of competent cells and introduced into an ice-cold 1 mm

wide electroporation cuvette. Cells were electroporated at 1.8 kV, resuspended in 1 ml of LB medium. The transformed strains were incubated at 37°C with agitation for 40 minutes before to be put on plate under selection pressure.

#### *II.2.4.2. Bacterial transformation using heat shock*

Competent cells were thawed on ice. 3 µl of the ligation mix were added to 100 µl of *E. coli*. The mixture was incubated for 20 minutes on ice. The cells were heat-shocked for 45 seconds at 42 ºC. The tube was removed and placed on ice for 2 minutes. 200 µl of LB medium was added and the tubes were incubated for 1 hour at 37 ºC. After incubation, aliquots were spread on LB agar plates and incubated at 37 ºC overnight.

### II.2.5. Gene cloning by using ligation independante clonoing (LIC) protocol

The wildtype and mutated forms of *metY* gene were PCR-amplified using the following primers: forward primer 5739 5'-AAAGAAGGAGATAGGATCATGCATCATCACCATCACCATTCGGACCAGACGCCC GCTTCAGTCTACG and reverse primer 5743 5'-GTGTAATGGATAGTGATCTTAGGCCGCCCGCGCCAGCGTT. The resulting fragments were inserted into a pET22b(+) vector (Novagen) modified for ligation independent cloning (Bastard et al., 2014). The sequence of all inserts was checked by Sanger sequencing. The resulting plasmids were introduced into *E. coli* BL21 (DE3) by transformation.

The list of the plasmid used in this thesis is shown in table 13.

**Table 13: List of plasmids. Amp for ampicillin, Tet for tetracyclin and Kan for kanamycin.**

| Plasmids | Details | Antibiotic |
|---|---|---|
| **pET22** | Figure 13_A | Amp |
| **pET22_metY** | metY from *M. extorquens* TK 0001 | Amp |
| **pET22_metY_T34M** | metY from G4105 | Amp |
| **pET22_metY_G113S** | metY from G4606 | Amp |
| **pET22_metY_D373G** | metY from G4607 | Amp |
| **pET22_metY_L389F** | metY from G4609 | Amp |
| **pET22_metY_G87F** | metY from G4597 | Amp |
| **pET22_ldhA** | ldhA from *M. extorquens* TK 0001 | Amp |
| **pET22_NMCR** | N-ter of MCR from *Chloroflexus aurantiacus* | Amp |
| **pET22_CMCR** | C-ter of MCR from *Chloroflexus aurantiacus* | Amp |
| **pET22_NMCR_ A0A074MHG1** | N-ter of MCR from *Erythrobacter litoralis* | Amp |
| **pET22_CMCR_ A0A074MHG1** | C-ter of MCR from *Erythrobacter litoralis* | Amp |
| **pET22_NMCR_ A0A117UU14** | N-ter of MCR from *Novosphingobium fuchskuhlens* | Amp |
| **pET22_NMCR_A7NN59** | N-ter of MCR from *Roseiflexus castenholzii* | Amp |
| **pET22_CMCR_ A7NN59** | C-ter of MCR from *Roseiflexus castenholzii* | Amp |
| **pRK2073** | addgene | Kan |
| **pTE100** | addgene | Tet |
| **pTE101** | addgene | Kan |
| **pTE102** | Figure 13_B | Tet |
| **pTE102_metY** | metY from *M. extorquens* TK 0001 | Tet |
| **pTE102_MCR** | MCR from *Chloroflexus aurantiacus* | Tet |
| **pTE102_MCR1** | NMCR and CMCR from *Chloroflexus aurantiacus* | Tet |
| **pTE102_MCR1*** | MCR1 with 3 muted sites on CMCR | Tet |
| **pTE102_MCR2** | NMCR from *Novosphingobium fuchskuhlens* and CMCR from *C. aurantiacus* | Tet |
| **pSEVA** | seva | |

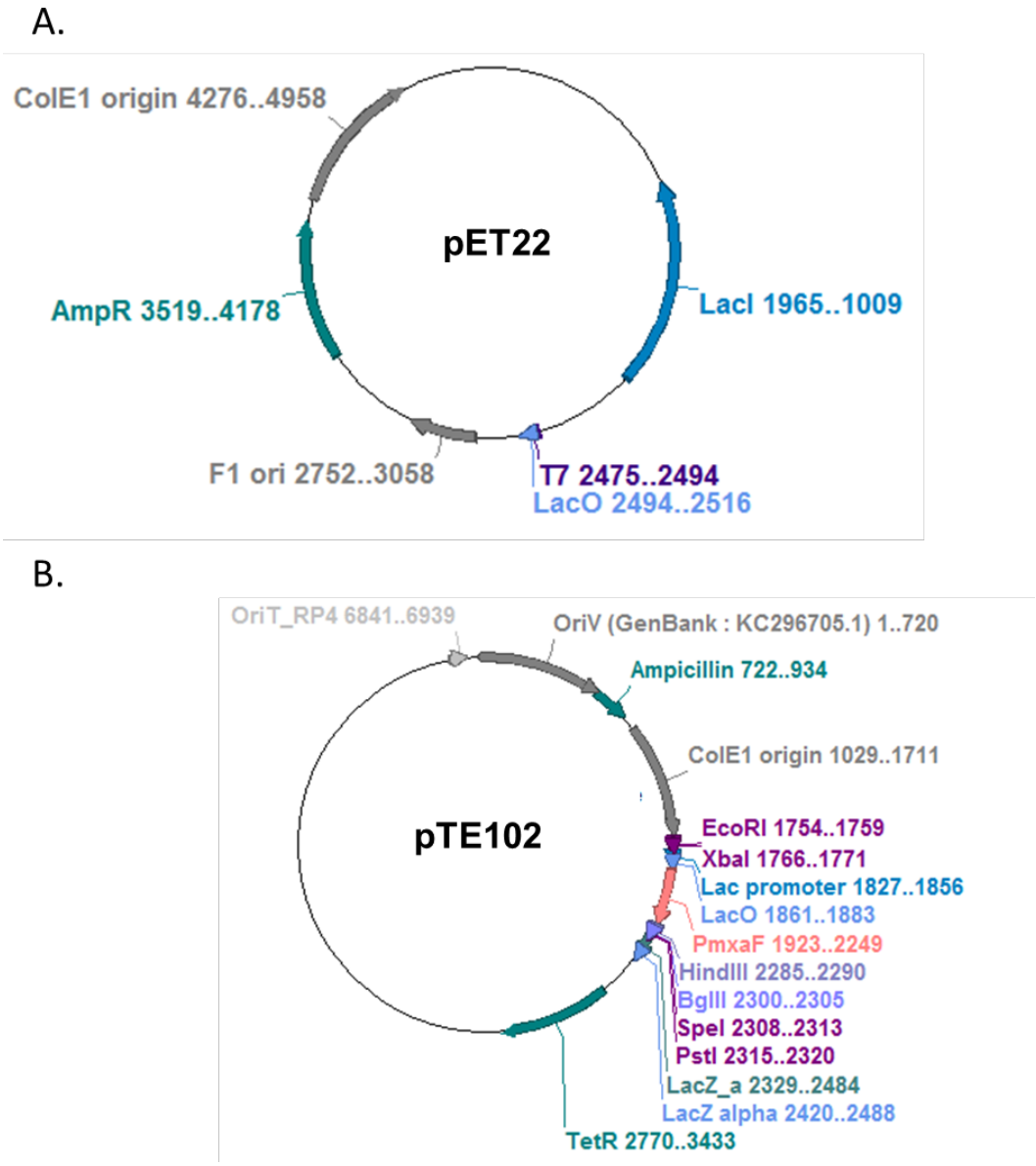


**Figure 13: Plasmid map of pET22 (A) and pTE102 (B) generate from APE software.**

### II.2.6. Genomic DNA extraction and sequencing

Genomic DNA (~200 ng) was extracted using the Sigma GenElute bacterial genomic DNA kit starting from 6 mL of overnight cultures. DNA was fragmented into fragments of 600-bp mean size by Covaris E220 (Covaris, Inc., Woburn, MA, USA). The DNA was end-repaired and ligated to Illumina compatible adapters using the NEBNext DNA sample prep master mix set 1 (New England BioLabs E6040). Ligation products were purified and amplified by 12 cycles of PCR using the Kapa Hifi HotStart NGS library amplification kit (Kapa Biosystems KK2611) with P5/P7 primers. PCR products were purified (0.8 volume SPRI beads) and run on a 2% agarose gel, and DNA (700 to 800 bp) was excised and purified using NucleoSpin extract II

DNA purification kit (Macherey-Nagel 740609). cDNA libraries were sequenced using 300-bp paired-end reads on an Illumina MiSeq instrument. The reads were compared to the *M. extorquens* TK 0001 genome reference (DDBJ/EMBL/GenBank accession number LT962688) or the *M. extorquens* AM1 genome reference (GenBank assembly: GCA_000022685.1) using the Microscope Platform (Vallenet et al., 2017).

### II.2.7. Transcriptomics analysis

#### *II.2.7.1. RNA extraction*

##### II.2.7.1.1. Test 1: using Trizol

RNeasy Mini Kit from QIAgen was first tested to extract total RNAs of *M. extorquens* strains. Despite repeated attempts, we did not obtain satisfactory yields. Consequently, the protocol for total RNA extraction described here was developed using the Trizol reagent (Sigma 93289). To 10 mL of bacterial culture grown up to log-phase, 1.25 mL of stabilization buffer was added (phenol). The mixture was chilled on ice, vortexed and transferred to a 15 mL tube. The supernatant was removed after centrifugation at 4000 rpm for 5 minutes at 4 °C. The pellet was resuspended in 1 mL TRI reagent and transferred to a 2 mL Eppendorf tube. After incubation for 5 minutes at room temperature, 200µl of chloroform were added. After vortexing for 15 seconds and incubating at room temperature for 15 minutes, the mixture was centrifuged at 12000 rpm for 15 minutes at 4°C. Three distinct phases were obtained: a transparent top phase, an intermediate white phase, and a pink bottom phase. The transparent top phase was transferred to a new Eppendorf tube, 500 µl of isopropanol were added. The mixture was vortexed and incubated at room temperature for 10 minutes. After centrifugation at 14000 rpm for 10 minutes at 4°C, the supernatant was carefully discarded without disturbing the pellet. Then, the pellet was resuspended into 1 mL of 75% ethanol after centrifugation at 14000 rpm for 5 minutes at 4°C, the supernatant was discarded. The pellet was air-dried for 10 minutes, and then resuspended in 94 µl of sterile water. The concentration of RNA was determined using a NanoDrop 2000 Spectrophotometer. An aliquot was run on 1% agarose gel to check for the presence of RNA.

##### II.2.7.1.2. Test 2: using MBER

Log-phase cultures ($OD_{600nm}$ around 0.5) of wildtype and evolved MEM5.35 *M. extorquens* TK 0001 strains in smm supplemented with 1% methanol was split into two parts. The first part

was maintained in the same growth conditions. Methanol was added to obtain 5% methanol. 50 mL from the culture were extracted 5 minutes and 3h after the split. Total RNA was extracted using MBER (Ambion 46_6036) and Trizol reagent (Sigma 93289). The sample yield was determined using a NanoDrop 2000 spectrophotometer. An aliquot was run on 1% agarose gel to check for the presence of RNA. The experiment was run in triplicates.

#### II.2.7.1.3. RNA preparation for sequencing (RNA seq)

RNA samples were treated using Turbo DNase I (Thermo Fisher Scientific) for 30 minutes at 37°C twice and then purified twice by Zymoclean (Zymo Research R1015) to remove RNA shorter than 200 bp. Five micrograms of total RNA were treated by Ribo-Zero (Illumina MRZMB126) for specific elimination of rRNA and purified by AMPure (total capture) into 10 µL of water. cDNA libraries were prepared from 100 ng of RNA using the Smarter stranded mRNA kit (Illumina 15031047) and sequenced on an Illumina HiSeq 2000 sequencer with paired-end 150-bp reads.

#### II.2.7.1.4. RNA-seq analysis

Transcriptome sequencing data were analyzed using the Tamara bioinformatics pipeline implemented in the Microscope platform (Médigue et al., 2017). In a first step, reads were mapped onto the *M. extorquens* TK 0001 genome reference (BWA-MEM v.0.7.4) (Li H., 2013). An alignment score equal to at least half of the read is required for a hit to be retained. To lower the false positive discovery rate, the SAMtools (v.0.1.8) (Li et al., 2009) were then used to extract reliable alignments from SAM formatted files. The number of reads matching each genomic object present on reference genome was subsequently computed with the toolset BEDTools (v.2.10.1) (Quinlan et al., 2010). Finally, the Bioconductor-DESeq package (v.1.4.1, Anders and Huber, 2010) were applied with default parameters to analyze raw counts data and test for differential expression between conditions.

## II.3. Metabolomic protocols

### II.3.1. Protocol A: on filter

5mL of bacteria culture with OD600 of 0.2 were filtrated on a filter PTFE 0.45 µM (from Merck Millipore) before to be put on plate containing 1.5% Agarose and smm supplemented with

specific methanol concentration. The plates were incubated at 30°C until log phase (around 0.8) before to be stopped by using quenching solution (80% acetonitrile, 20% methanol) in -30°C bath. For this the filter was placed in a cupule filled by 5mL of quenching solution and then sonicated at 4°C 5 minutes. The liquid solution with the cell is recovered and bacteria were lysed by 3 freeze/thaw cycles by freezing in liquid nitrogen + 65°C bath for 10 min. Samples were incubated 1h at 4°C, 150 RPM then centrifuged 3 min at 12000 rpm - 4°C. The supernatants were transferred into new tubes (Figure 14). Solvent was evaporated using a Speed Vacuum overnight. Lyophilizates were resuspended in 200 µL of mobile phase (80% acetonitrile and 20% methanol). The pellet is taken up in 200 µL of water (miliQ) and then subjected to ultrasound for 10 minutes, to promote extraction. Debris is removed after centrifugation (20 000g, 4°C and 10 minutes) and the supernatant and filtered (0.22 µm). 800 µL of mobile LC / MS phase are used to rinse the filter and added to the sample. The final sample is stored at 4°C for a week maximum.

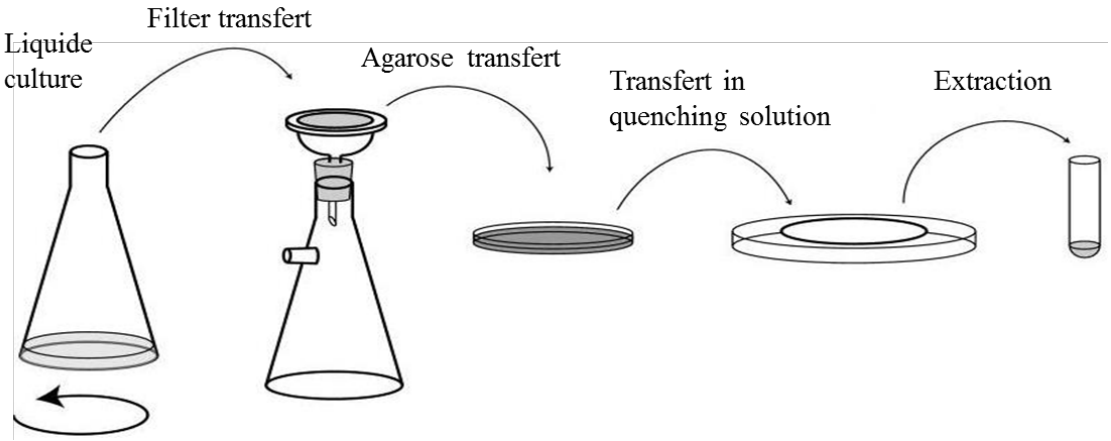


**Figure 14: Protocol for preparing samples from solid culture on filter. Adapted from (Stuani, 2014).**

### II.3.2. Protocol B: in 5 mL liquid culture

The cells were cultivated in 5 mL smm supplemented with 1% (v/v) methanol and sampled at early log phase or when entered into stationary phase. They were centrifuged at 4°C at 4000rpm for 10 minutes. The pelleted cells were suspended into 200µL of water/methanol/chloroform (1:3:1). Bacteria were lysed by 6 cycles of freeze (-30°C) – thawing (RT) during 1h. The lysates were centrifuged at 20 000g for10 minutes at 4°C and the supernatant was collected and evaporated in a speed vacuum evaporator (SpeedVac). The lyophilizate was resuspended in 200 µL of the mobile phase consisting in 80% acetonitrile and 20% 10mM ammonium acetate. The

solution was filtered on 0.22 µm filters. The filter was washed with 800µL of mobile phase. The total recovered solution (1 mL) was conserved at -80°C.

### II.3.3. Protocol C: in 2.5 mL liquid culture in 24 wells-plates

The metabolite extraction protocol was adapted from the Metabolomics Service Protocols from the University of Glasgow (http://www.polyomics.gla.ac.uk/assets/downloads/MSMetabolomicsPrepCells-Aug2013.pdf). A saturated overnight culture was diluted in fresh medium at an $OD_{600}$ = 0.05. 2.5 mL of the suspension were transferred into a well of a 24 wells-plate (Whatman; reference 7701-5110). The cells were grown until an $OD_{600nm}$ between 2.0 and 3.2 (mid-log phase) in a shaking incubator (Climo Shaker ISF1-X Kühner). The plate was then centrifuged at 2 700 g at 4°C for 10 minutes and the supernatant discarded. The cell pellet was suspended in 200 µl of water/methanol/acetonitrile (1:3:1) and placed in a cold bath (-80°C) composed of dry ice and ethanol. After cell freezing, the mixture was let at 25°C until complete thawing of the cells. This procedure was repeated twice to lyse the cells. The lysate was rocked on a shaker for one hour at 4°C, then centrifuged at 5 000 g at 4°C for 10 minutes. The supernatant was dried and stored at -80°C. Before LC/MS analysis, the metabolites were dissolved in 20 µl of water and 42 µl of an 80% acetonitrile - 20% 10 mM ammonium acetate mix, centrifuged at 5 000 g at 4°C for 10 minutes. Finally, the supernatant was filtered on a 0.22 µm filter (PTFE, Acroprep Advance, Pall).

### II.3.4. Lactate quantification

#### *II.3.4.1. HPLC*

Chromatographic separation was carried out on a Sequant ZICpHILIC columns 5 µm, 2.1x10 mm (Merck, Darmstadt, Germany) thermostated at 40°C with a mobile phase flow rate of 200 µL/minute. Aqueous solution of 10 mM ammonium acetate was used as phase A and acetonitrile as phase B. The following elution conditions were applied: 1 minute isocratic step at 80% of solvent B, 7 minutes linear gradient from 80% to 40% of solvent B, 2.5 minutes isocratic elution at 40% of solvent B, return to the initial composition (80% of solvent B) in 2 minutes, reconditioning step for 10 minutes.

#### *II.3.4.2. Mass spectrometry*

A mass spectrometer equipped with an electrospray ionization source (ESI) was operated in the negative ionization mode. Electrospray voltage was set at -4 kV. Sheath gas and auxiliary gas flow rates were set at 60 arbitrary units (a.u.) and 44 a.u., respectively, and the drying gas temperature was set at 275°C. The mass resolution power of the detector was 60,000. Raw data were analyzed using the Qual-browser module of Xcalibur version 2.2 (Thermo Fisher Scientific, France).

#### *II.3.4.3. Quantification*

A calibration curve for lactate was required to calculate its concentration. We prepared calibration solutions containing 0, 1, 2, 4, 5, 8, 10, 20, 25, 50 and 100 µM lactate. These solutions were prepared in an initial volume of 200 µl of water/methanol/acetonitrile (1:3:1 ratio) and were treated as the cell pellets (see above) before LC/MS injection. Samples were analyzed in the negative mode. The peak areas from Extracted Ion Chromatograms (EIC) of lactate were integrated. Metabolomes from 23 independent 2.5 mL cultures for each experimental condition were analyzed to estimate the metabolite concentration. The lyophilized metabolomes were suspended with 62 µl 80% acetonitrile - 20% 10 mM ammonium acetate. Samples were filtered on 0.22 µm filters prior to injection.

#### *II.3.4.4. Statistical analysis*

Statistical analyses were performed using XLSTAT (Addinsoft). Lactate amount in samples, expressed as chromatographic peak areas, were not normally distributed (Shapiro-Wilk test). Therefore, the non-parametric Kruskal-Wallis test ($p < 0.05$) was used to determine if lactate concentration was statistically different between the four strains ($p < 0.05$). A post-hoc non-parametric Mann-Whitney test was used for pairwise analyses ($p < 0.05$).

### II.3.5. 3-Hydroxypropionic acid quantification

The same protocol than for the Lactate was used for the 3-HP detection and quantification.

## II.4. Biochemistry

### II.4.1. Production and purification of proteins

The genes were cloned with an N-terminal 6xhistidine tag into a pET22b(+) (Novagen) modified for ligation independent cloning (Bastard et al. 2014). All primers used are listed in Table 1. The expression plasmids were transformed into *Escherichia coli* BL21-CodonPlus (DE3)-RIPL cells (Agilent Technologies). Overnight cultures of the plasmid-harbouring cells were diluted 1/50 into 50 mL of Terrific Broth and grown to an $OD_{600}$ of ~1.2 at 37°C. Gene expression was induced with 0.5 mM isopropyl-β-d-thiogalactopyranoside. The culture was incubated further for 16 h at 20°C. The cells were collected by centrifugation at 4000 rpm for 5 minutes at 4°C. The supernatant was removed and the cell pellets were freeze at -80°C (Vergne-Vaxelaire et al., 2018). The protein production was evaluated in an aliquot of the culture by sodium dodecyl sulfate polyacrylamide gel electrophoresis (SDS- PAGE) using the Invitrogen NuPAGE system. The cell pellets were thawed on ice and suspended in 4 mL Lysis Buffer (50 mM TRIS, pH 8.0, 50 mM NaCl, 10% glycerol, and 30 mM imidazole) containing 1 mM Pefabloc SC (Roche Applied Science) and 10 µL of LysonaseTM bioprocessing reagent. The cells were sonicated using an ultrasonic processor. The lysates were centrifuged at 4°C, 12000 rpm for 30 minutes. The supernatants were ultracentrifuged to remove the extracted membranes. The supernatants were loaded onto a Ni-nitrilotriacetic acid agarose column, washed with the purification buffer and buffer supplemented with 30 mM imidazole, and eluted with buffer supplemented with 250 mM imidazole (Table 14 and 15). The method of Bradford was applied to determine protein concentrations.

The protein overproduction was verified by sodium dodecyl sulfate polyacrylamide gel electrophoresis (SDS-PAGE). A 10 µL sample of each culture was mixed with 4 µL of loading buffer, 1 µL of SDS and heated 10 minutes at 90°C. The samples were then loaded on a 12% acrylamide gel in Nu PAGE MOPS Buffer and migrated for 1 h at 200 V. Gels were stained overnight in Coomassie blue (Simply Blue Safe Stain, Novex).

**Table 14: Lysed and washed buffer.**

| | Ci | Cf (mM) | 50 mL |
|---|---|---|---|
| **TRIS** | 1M | 50 | 2.5 |
| **NaCl** | 4M | 50 | 0.625 |
| **Glycerol** | 99.90% | 10 | 5 |
| **Imidazol** | 68.08 g/mol | 30 | 0.10212 |

**Table 15: Elution buffer.**

| | Ci | Cf (mM) | 50 mL |
|---|---|---|---|
| **TRIS** | 1M | 50 | 2.5 |
| **NaCl** | 4M | 50 | 0.625 |
| **Glycerol** | 99.90% | 10 | 5 |
| **Imidazol** | 68.08 g/mol | 250 | 0.851 |

### II.4.2. MetY characterization

The kinetic parameters of *metY*-encoded wildtype O-acetyl-L-homoserine sulfhydrylase of *M. extorquens* TK 0001were determined in a coupled enzymatic assay using an acetic acid assay kit (from Megazyme Figure 15). The oxidation of NADH concomitant with O-acetyl-L-homoserine (Toronto Research Chemicals) transhydrylation with either sodium sulfide (Sigma-Aldrich, 431648) or methanol (Sigma-Aldrich, 34860) was monitored at 340 nm in an optical spectrophotometer (SAFAS). Enzymatic reactions were performed at RT in 100µL total volume reaction at pH 7.4 containing NADH at 4 mM and initiated by the addition of 2 ng of the purified enzyme. For the wildtype protein assay, we varied the concentration of one substrate and set the other substrate at a saturating concentration (O-acetyl-L-homoserine with sulfide or methanol). The mutated proteins were tested with the saturating concentrations determined as described above.

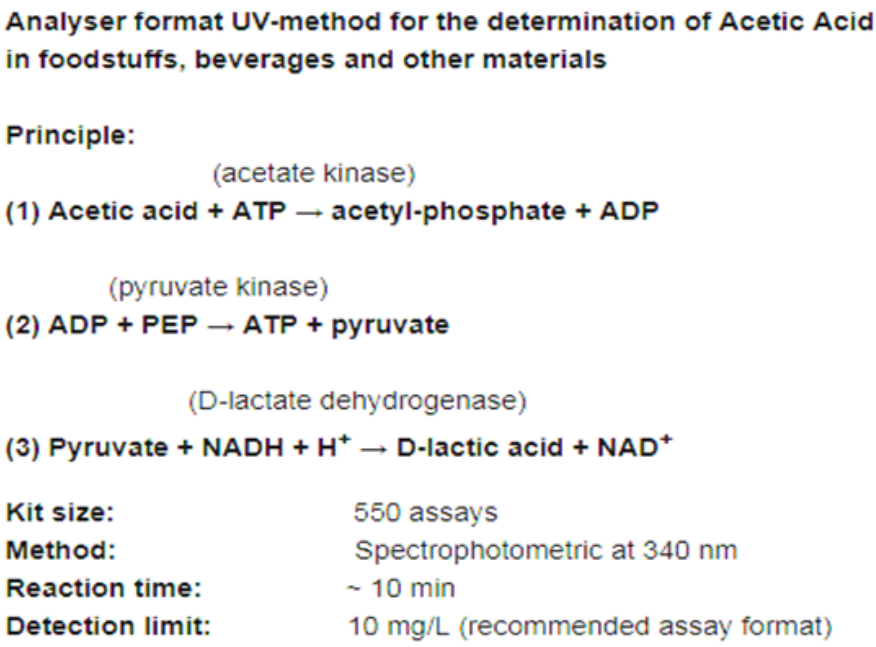


**Figure 15: Principle of the Acetic acid assay test from Megazyme.**

### II.4.3. NMCR and CMCR enzymatic assay

The catalytic activity was determined by mass spectrometry using the SpectraMax plus. Reaction mixture was prepared as shown on table 16. Enzymatic reactions were triggered by the addition of Malonyl-CoA at final concentration 0.15 mM. The consumption of the NADPH was following by the absorbance at 340nm.

**Table 16: Composition of reaction mix for the screening.**

| Compounds | Final concentration |
|---|---|
| Tris pH 7.2 | 100 mM |
| Malonyl CoA | 0.15 mM |
| MgCL2 | 2 mM |
| NADH | 0.2 mM |
| NADPH | 0.2 mM |
| NMCR | X |
| CMCR | X |

## II.5. FAME analysis

The fatty acid methyl esters (FAME) analyses were realized by the DSMZ identification service (Braunschweig, Germany), whole cell fatty acid contents were analyzed in wildtype and

evolved G4105. Cells were grown in smm supplemented with 1 % methanol until mid-log phase and collected by centrifugation, cooled on ice and sent to DSMZ.

## II.6. Cell sorting

### II.6.1. Size of the cells

The size of the cells was verified by using fluorescence-activated cell sorter (FACS) (MoFlo Astrios EQ de Beckman-Coulter). Bacterial cultures were prepared in smm medium supplemented with 1% methanol (MeOH) and washed with NaOH before injection. Using the filters forward and side scatter and the laser at 488nm the size of the cells was determined. 100 000 cells were analyzed by sample and compared to the size of the Sphero NanoFluorescents Particles Yellow (Spherotech NFPPS-52-4K) to the following size: 0.22µm – 0.45µm – 0.88µm – 1.35µm.

# III. RESULTS

## III.1. Characterization of methylotrophic bacteria with serine cycle metabolisms

Methylotrophic bacteria are principally divided into two groups according to their C1 assimilatory metabolism: The RuMP cycle and the serine cycle methylotrophs. The RuMP cycle has a more favorable energy balance than the serine cycle, i.e. for a given methanol input; more biomass is formed through the RuMP than the serine cycle (paragraph: I.4.).

In spite of their GC rich genome, we focused on the serine cycle methylotrophs of the *Methylobacterium* genus as starting point for industrial production strain evolution. This choice was guided by the following observations:

- *Methylobacterium* strains are used as production hosts for a variety of industrial chemicals, ranging from biofuels to carboxylic acids (chapter I table 3).

- Tools and protocols for molecular genetics are available for *Methylobacterium* strains.

- The strains, which are facultative methylotrophs, share a well-studied common metabolic core but differ in the range of C1 substrates assimilated.

- The strains possess a highly homologous genetic content but differ in genome organization.

- The main C1 assimilation route is not optimized in terms of energy preservation, and the pathway to replenish the C1 acceptor molecule glycine is complicated. This gives opportunities for strain ameliorations.

- The *Methylobacterium* strain repertoire contains non-characterized species of scientific interest with the potential to become biotechnological platform organisms. Their use in industrial processes can be an asset for patent issues.

### III.1.1. Characterization of strain *Methylobacterium extorquens* TK 0001

Among *M. extorquens* strains deposited in public strain collections but not studied in detail, we identified strain TK 0001, isolated from soil in Poland and available at the DSMZ (DSM n°1337), and proceeded to a physiological and genomic characterization. Figure 16 shows growth of this strain on mineral medium plates and in liquid cultures supplemented with 1% (v/v) methanol (MeOH). The cells form pink colored colonies and filaments typical for the *Methylobacterium* genus.

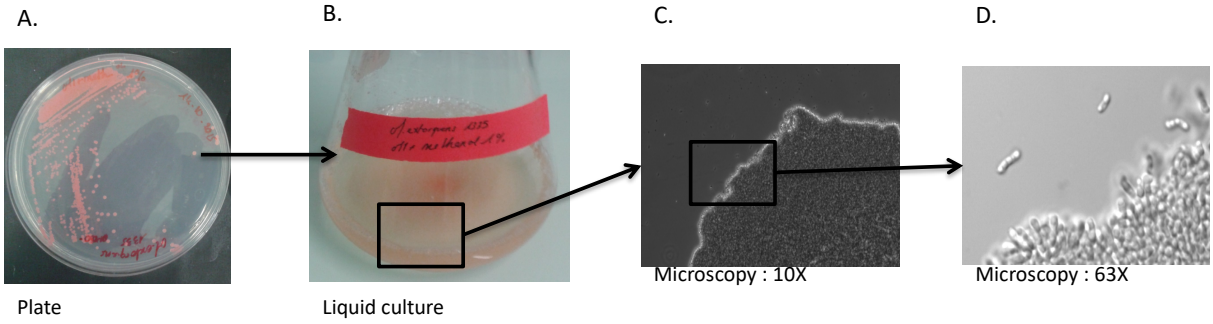


**Figure 16: Physiological aspects of *M. extorquens* TK 0001 grown on mineral medium plates (A) and in liquid culture (B) supplemented with 1% methanol. Cellular growth 10x (C) and 63x (D) magnified.**

### III.1.2. Characteristics of growth and biomass yield

Growth tests were performed on mineral medium plates supplemented with different complex carbon sources. To compare the growth capacities of TK 0001 with *M. extorquens* strains already characterized and used in biotechnological production setups, strains AM1 – the model strain of the genus – and PA1 were tested in parallel. As shown in Table 17, strain TK 0001, as the other two strains, could grow on the central carbon metabolites serine, pyruvate and succinate, showing it to also be a facultative methylotroph. Interestingly, glycine did not function as carbon source for either of the strains, pointing to a deficiency in uptake mechanisms for this amino acid. The dipeptide glycine (Gly-Gly) dipeptide could sustain proliferation of strains PA1 and TK 0001, but not of AM1. This observation can be of interest for the elaboration of selection screens aiming at the modification of the carbon metabolism and assimilation route of methanol.

The quantification of growth on pyruvate showed significantly lower growth yield of strain AM1 compared to the two other strains (Table 18).

**Table 17: Growth of *M. extorquens* strains AM1, PA1 and TK 0001 on mineral medium plates supplemented with different carbon compounds after 48 hours at 30°C. Gly-Gly is for the dipeptide glycine.**

| | Methanol | Glyoxylic acid | Gly-Gly | Glycine | Serine | Pyruvate | Succinate |
|---|---|---|---|---|---|---|---|
| | 1% (0,24M) | 20mM | 20mM | 20mM | 20mM | 20mM | 20mM |
| **AM1** | + | - | - | - | + | + | + |
| **PA1** | + | - | + | - | + | + | + |
| **TK 0001** | + | - | + | - | + | + | + |

**Table 18: Growth yield ($OD_{600mn}$) after 48h growth in liquid standard mineral medium supplemented with different glycine and pyruvate concentrations.**

| | Glycine | | Pyruvate | |
|---|---|---|---|---|
| | 20mM | 50mM | 20mM | 50mM |
| **AM1** | - | - | 0.363 | 0.249 |
| **PA1** | - | - | 1.215 | 1.857 |
| **TK 0001** | - | - | 1.536 | 1.484 |

Throughout this study, the quantification of bacterial growth was realized using two techniques: growth curve recording with a Bioscreen plate reader, and manual $OD_{600nm}$ measurement of cultures growing in Erlenmeyer flasks. The automated reading by the Bioscreen enables the parallel testing of a large array of growth media compositions, but has limited validity, notably concerning the maximum OD recorded. Due to the small growth volume (200 µL), evaporation of volatile ingredients must be taken into account. Also, cells can adhere differently on plastic surfaces influencing their growth behavior (Mceldowney and Fletcher, 1986).

A discrepancy between the two methods became apparent for growth on succinate. The strains AM1 and PA1 showed efficient growth in the plate reader with succinate as sole carbon and energy source (Figure 17). They reached an $OD_{600nm}$ of around 2 with 100 mM succinate after 48 hours, while strain TK 0001 did not grow above 0,5 OD (Figure 17A). However, a growth test conducted with the same medium in an Erlenmeyer flask (25 mL) gave an $OD_{600nm}$ after 48 hours between 4 and 5 for the three strains (Figure 18A).

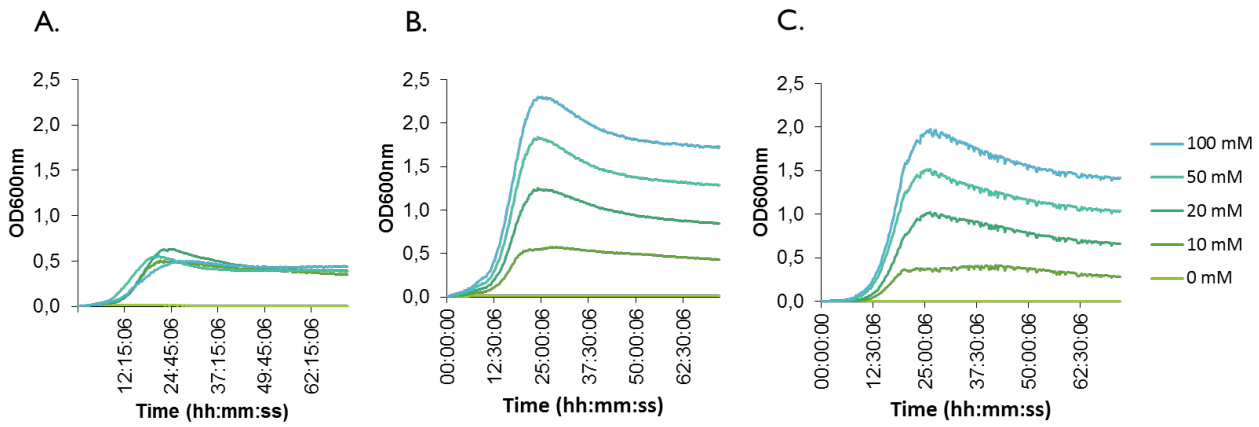


**Figure 17: Growth curves of strains TK 0001 (A), PA1 (B) and AM1 (C) on different succinate concentrations recorded with a Bioscreen plate reader.**

The parallel determination of cellular dry mass produced on 100 mM succinate after 48 hours also showed an approximately equal production for the three strains (Figure 18B).

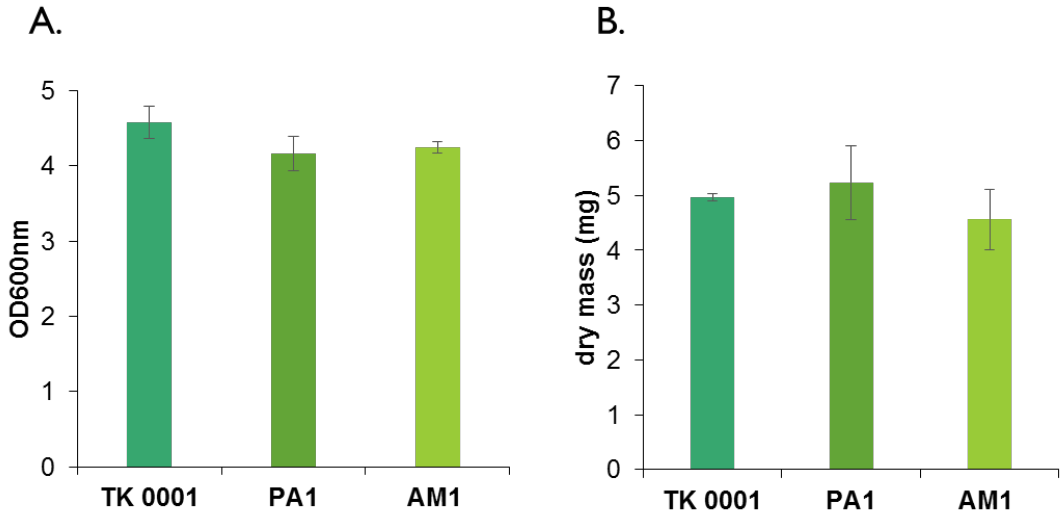


**Figure 18: Determination of OD600nm (A) and dry cell mass (B) of strains TK 0001, PA1 and AM1 after 48 hours of growth in mineral medium supplemented with 100 mM succinate.**

The growth yield after 48 hours of growth of strain TK 0001 with methanol was linear for a set of concentrations tested. By extrapolation, a yield of 2.8 x $10^{-5}$ mg.mL$^{-1}$.mM$^{-1}$ was calculated (1% MeOH equivalent to 0.24M) (Figure 19A). Linearity was also found for growth yield determination with succinate and by extrapolation a yield of 6.0 x $10^{-5}$ mg.mL$^{-1}$.mM$^{-1}$ succinate was calculated (Figure 19B). In terms of molarity, growth on succinate; which contains four carbon molecules; gives rise to more biomass production than growth on methanol. While

succinate contains four carbon atoms and methanol only one, the yield gap is not very high. However, the biomass yield by carbon is higher with methanol than succinate, methanol is more reduced and thus has higher energy content than succinate.

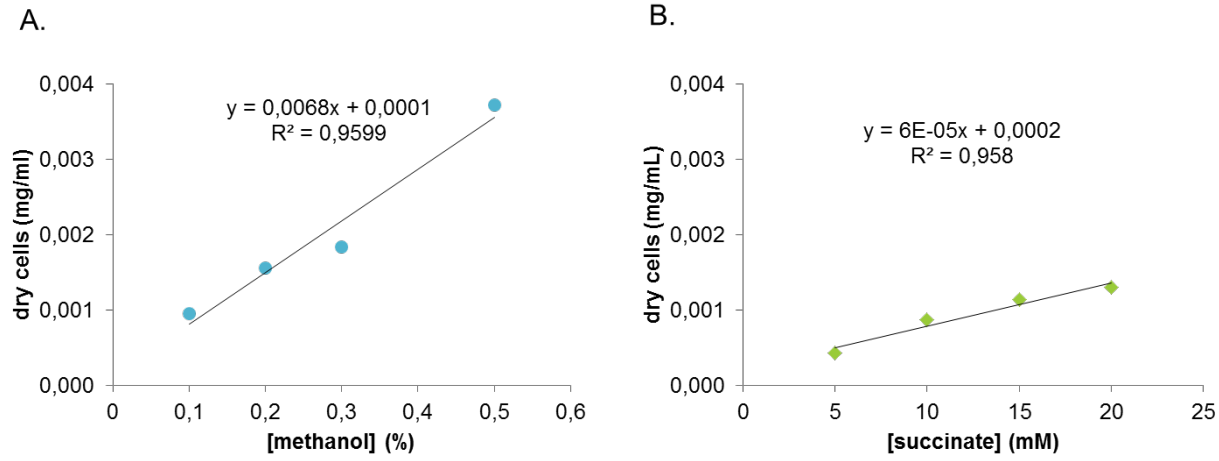


**Figure 19: Dry cell mass production of *M. extorquens* TK 0001 on methanol (blue points) (A) and succinate (green points) (B) after 48 hours of growth at 30°C in Erlenmeyer flasks. The linear equation deduced from the measured values is indicated.**

### III.1.3. Test of pH-dependence of growth

The resistance to acid conditions can be of interest for some biotechnological applications of a microbial platform strain, especially for the production of carboxylic acids (Kildegaard et al., 2014). Growth tests in mineral media buffered at different pH values (from pH 7 to pH 2) and supplemented with 1% methanol were performed. TK 0001 grows at an acid pH of 5.5 as well as at a neutral pH (Table 19). At pH 5.0, by contrast, growth is almost completely inhibited.

**Table 19: Cell density ($OD_{600nm}$) of *M. extorquens* TK 0001 cultures after 48 hours of growth on mineral medium buffered at neutral and various acidic pH values. Methanol at 1% was added as carbon source.**

| | $OD_{600nm}$ final | | |
|---|---|---|---|
| pH | R1 | R2 | Mean |
| 2.0 | 0,00 | 0,00 | 0,00 |
| 3.0 | 0,00 | 0,00 | 0,00 |
| 4.0 | 0,00 | 0,00 | 0,00 |
| 5.0 | 0,03 | 0,03 | 0,03 |
| 5.5 | 1,57 | 1,75 | 1,66 |
| 6.0 | 1,36 | 1,75 | 1,56 |
| 6.5 | 1,17 | 1,52 | 1,35 |
| 7.0 | 1,15 | 1,45 | 1,30 |

### III.1.4. Test of antibiotic resistance

A survey of resistance to diverse antibiotics commonly used for genetic manipulations was performed for strain TK 0001. A first evaluation was conducted using filter patches on solid mineral methanol medium to obtain a qualitative response (cf II.1.2). TK 0001 was found to be resistant to ampicillin and thiamphenicol, but sensible to tetracycline, kanamycin, rifampicin, chloramphenicol and streptomycin after 72 hours of incubation (Table 20). Erythromycin and chloramphenicol caused an initial halo of inhibition but residual growth upon longer incubation. Tests of a range of concentrations for each antibiotic revealed minimal inhibitory concentrations after 5 days of incubation on plates (Table 21).

**Table 20: Filter patch antibiotic resistance test of strain TK 0001 on mineral methanol plates. Growth (+) or inhibition zone formation (-) are indicated at 48 h and 72 h of incubation. Halo signifies residual growth around the filter. The experimentation was done in duplicate.**

| Erythromycin | | Tetracycline | | Kanamycin | | Rifampicin | | Ampicillin | | Chloramphenicol | | Streptomycin | | Thiamphenicol | | Eau | |
|---|---|---|---|---|---|---|---|---|---|---|---|---|---|---|---|---|---|
| 48h | 72h | 48h | 72h | 48h | 72h | 48h | 72h | 48h | 72h | 48h | 72h | 48h | 72h | 48h | 72h | 48h | 72h |
| + | Halo | - | - | - | - | - | - | + | + | - | Halo | - | - | Halo | + | + | + |

**Table 21: Antibiotic resistance test of strain TK 0001 on mineral methanol plates. Growth (+) or inhibition (-) on a given concentration of the antibiotics in the test plates are indicated.**

| | | Erythromycin | | Tetracycline | | Kanamycin | | Rifampicin | | Ampicillin | | Chloramphenicol | |
|---|---|---|---|---|---|---|---|---|---|---|---|---|---|
| | | 2d | 5d | 2d | 5d | 2d | 5d | 2d | 5d | 2d | 5d | 2d | 5d |
| Concentration (µg/mL) | 0 | + | + | + | + | + | + | + | + | + | + | + | + |
| | 5 | | | + | + | | | | | | | | |
| | 10 | + | + | - | - | | | | | | | | |
| | 20 | | | - | - | - | - | - | - | | | | |
| | 35 | - | + | - | - | | | | | | | + | + |
| | 50 | - | + | | | - | - | - | - | + | + | | |
| | 100 | | | | | | | | | + | + | | |

### III.1.5. Introduction of plasmids into TK 0001 cells

The introduction of genes into cells is an indispensable step in protocols of molecular genetics aiming at changing the cell phenotype. Thus, the overexpression of native or foreign proteins and the deletion of chromosomal loci through replacement by antibiotic resistance cassettes usually need to be performed in order to implement heterologous synthetic pathways into production strains. A number of plasmids are available for *M. extorquens* containing the broad host replication origin *oriV* (Lidstrom and Marx, 2001). In addition, some harbor the strong promoter PmxaF of the gene methanol dehydrogenase (*mdhA*) of *M. extorquens* AM1. Table 22 summarizes the plasmids used in this study.

Plasmids could be introduced into *M. extorquens* TK 0001 cells through electroporation. Transformed cells were selected on plates containing the appropriate concentration of antibiotic. An alternative method, based on the conjugational transfer of plasmids from *E. coli* to TK 0001 cells, was also successfully employed. Shuttle plasmids containing replication origins for both strains and an *oriT* mobilization module were used, together with a helper strain carrying plasmid pRK2073 (Bradley *et al.*, 2017, gift of F. Bringel, University of Strasbourg).

**Table 22: Plasmids used to transform *M. extorquens* TK 0001 cells by electroporation or conjugation.**

| Plasmid | Antibiotic | Characteristics | Ref |
|---|---|---|---|
| **pTE102** | tetracyclin | *oriV*, PmxaF | (Schada von Borzyskowski et al., 2015) |
| **pTE101** | kanamycin | *oriV* | Idem |
| **pTE100** | tetracyclin | *oriV* | Idem |
| **pSEVA227R** | kanamycin | *oriT*, mcherry | (Silva-Rocha et al., 2013) |
| **pRK2073** | kanamycin | *oriT* | (Bradley et al., 2017, provided by F. Bringel) |

### III.1.6. Genomic sequencing of *M. extorquens* TK 0001

Strains of the *Methylobacterium* genus differ in their genome organization. Some, like the reference strain AM1, harbor plasmids, while others contain only chromosomal DNA. No plasmids were found in *M. extorquens* strain TK 0001, using electrophoretic methods, data not shown. For this we examined the migration of agarose plug containing total DNA (as described by Maleszka et al., 1991).

The chromosomal DNA of TK0001 was extracted and sequenced at Genoscope using Illumina and Nanopore technologies, to reach 134 x coverage (Figure S1A and B). A single contig was obtained from the final assembly of 5.71 Mb with a G/C content of 68.2 % (Belkhelfa et al., 2018) (Figure S1C). Automatic functional annotation was performed using the microscope platform (Vallenet et al., 2017) (Figure 20). From the 6,251 genomic objects identified, 6,160 were coding sequences (CDSs), 17 miscellaneous RNAs, 59 tRNAs, and 15 rRNAs (5 5S, 5 16S, and 5 23S).

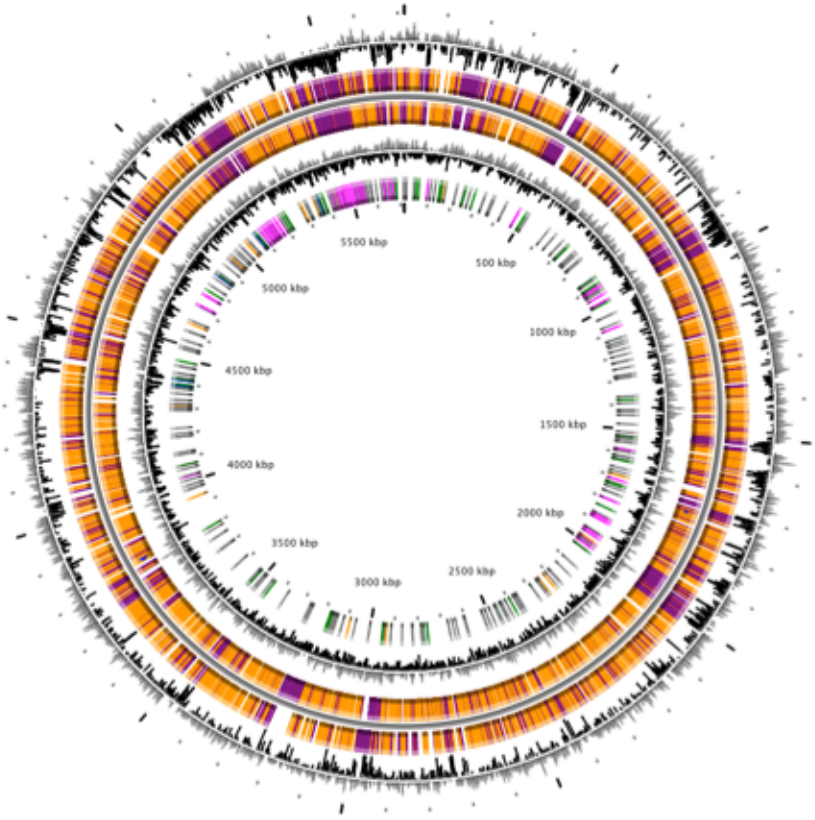


**Figure 20: Circular representation of *Methylobacterium extorquens* TK 0001 chromosome. Circles displays from the outside: (1) GC percent deviation in 1000 bp window, (2) predicted CDSs transcribed in the clockwise direction, (3) predicted CDSs transcribed in the counterclockwise direction, (4) GC skew (G+C/G-C) in a 1000 bp windows, (5) rRNA (blue), tRNA (green) misc_RNA (orange), transposable elements (pink), and pseudogenes (grey). (2) and (3) are color-coded according different categories: red and blue: MaGe validated annotations, orange: MicroScope automatic annotation with a reference genome, purple: primary/automatic annotations.**

The genome of TK 0001 was compared with the genomes of the *Methylobacterium extorquens* strains already sequenced (Table 23, Marx et al., 2012; Vuilleumier et al., 2009). All genomes are strongly related, TK 0001 and PA1 forming a subgroup in terms of genome size and absence of plasmids. A fraction of 24.3 % of the CDS of TK 0001 is specific to this strain, 62,0 % belong to the core genome of the genus (Figure S2).

In summary *M. extorquens* TK 0001 can grow in minimal medium supplemented with methanol, is genetically manipulable, and has a reduced size of its genome with regard to AM1. These promising results led us to evolve this strain in parallel with the AM1 model strain.

**Table 23: Genome size and organization of *Methylobacterium extorquens* strains.**

| Strain | Chromosome size | Plasmid number | GC% |
|---|---|---|---|
| TK 0001 | 5.6MB | 0 | 68 |
| PA1 | 5.5 MB | 0 | 68.2 |
| AM1 | 6.8 MB | 4 | 68.5 |
| CM4 | 6 MB | 2 | 68.2 |
| DM4 | 6.1MB | 2 | 68.2 |

## III.2. Directed strain evolution to growth on high methanol concentrations

Methanol serves as sole carbon and energy source for methylotrophic bacteria like *Methylobacterium extorquens*. As alcohol solvent, it interacts with cellular components altering their structure and chemical stability in a concentration dependent way. Its metabolic conversion to the cytotoxic compound formaldehyde is also a chemical threat to the cells. Growth tests in a plate reader demonstrated a growth maximum with 1% methanol for *M. extorquens* strains TK 0001 and AM1. At 2% methanol, growth was drastically inhibited (Figure 21). To use these strains as production chassis in biotechnological processes, higher methanol tolerance and biomass production would be of value. We used the GM3 technology of automated continuous culture to evolve the strains TK 0001 and AM1 to growth on methanol concentrations up to 10%.

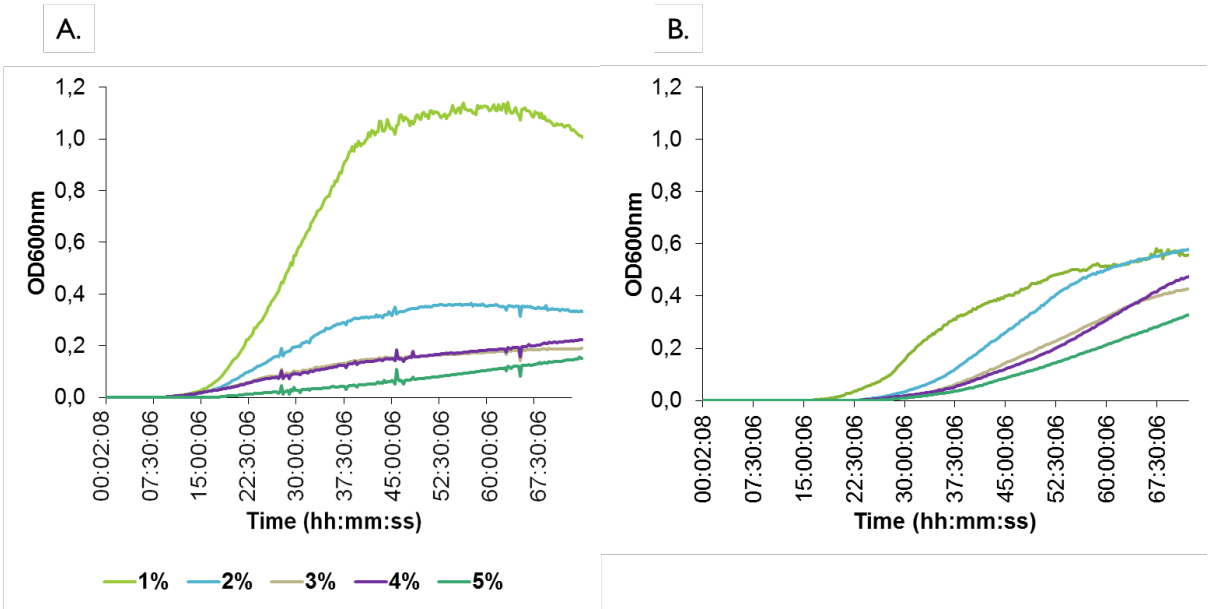


**Figure 21: Growth profile of strains *M. extorquens* TK 0001 (A) and AM1 (B) on mineral medium supplemented with different methanol concentrations. Mean values of six wells reader replicates were calculated.**

### III.2.1. Directed evolution of strain *Methylobacterium extorquens* TK 0001 to growth with 10% methanol

The adaptation of strain TK 0001 was initiated with a culture at 1% methanol growing in a turbidostat regime. As detailed above (paragraph I.11.2.2.), fastest growing cells are selected by diluting the culture with fresh medium each time a cell density threshold is passed. Throughout the adaptation experiment, the threshold fixed for turbidostat or medium swap growth periods corresponded to an $OD_{600nm}$ of 0.6.

Using the conditional medium swap regime, we adapted TK 0001 cells to growth on 5% methanol. This culture regime is characterized by regular dilution pulses at programmed intervals. The culture is diluted either by a relaxing or a stressing medium, depending whether the optical density measured is below (relaxing pulse) or above (stressing pulse) the threshold. The relaxing medium contained, as did the initial turbidostat culture, 1% methanol, while the stressing medium contained 5% methanol (Figure 22A). After an adaptation period of 11 days under this regime, the ratio of stressing to relaxing dilution pulses reached 100%, signifying that the cell population grew with 5% methanol (Figure 22B). After a short period (26 days) of growth with the 5% methanol medium in turbidostat to stabilize the cells and lower the generation time of the culture, MEM5 population shown methanol adaptation (Figure S3). Isolated colonies were obtained from the adapted cell population on solid medium containing 5% methanol. Six isolates were finally chosen from the best growing colonies for further analysis (Figure S4). One of the isolates, strain G4105, was used to inoculate a GM3 culture for further adaptation to 7% methanol. Again, a medium swap regime was employed, this time oscillating between 5% and 7% methanol for the relaxing and stressing medium, respectively. Growth of the culture with 7% methanol was obtained after 25 days (Figure 22C) and followed by a turbidostat growth period of 19 days to consolidate the culture. Colonies were obtained from the consolidated culture on 7% methanol plates and six isolates chosen from the best growers (Figure S5). Isolate G4201 was then adapted to growth at 8% methanol. Given the extremely high solvent concentration (1.7 M) in the cultures, adaptation was performed with an increment of 1% in turbidostat. After 65 days, six isolates were obtained showing growth with 8% methanol on plates and liquid (Figure S6). A culture from one of the isolates, strain G4363, was further adapted to growth with 9% and finally 10% methanol in turbidostat regimes. Again, six isolates were chosen from this final population of the evolution experiment for further analysis. All evolved isolates from TK 0001 were listed in Table S2A.

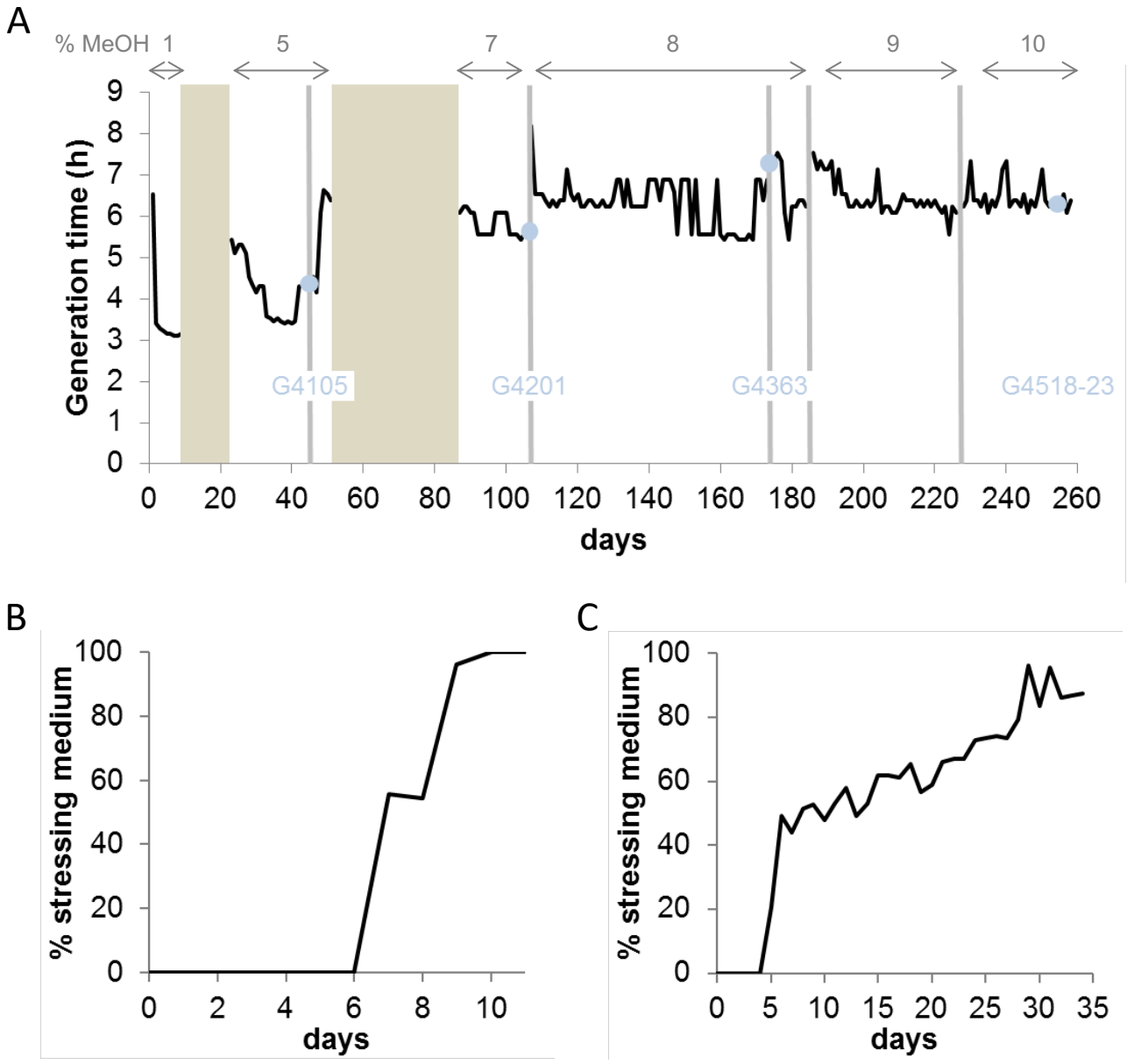


**Figure 22: Adaptation of *M. extorquens* TK 0001 to increasing methanol concentrations in GM3-driven continuous culture. (A). Growth rate over 260 days of a bacterial population cultivated on increasing methanol concentrations. Bronze areas correspond to periods of cultivation under medium-swap regime. Black lines show average daily generation time during cultivation periods under turbidostat regime. Methanol concentration of culture medium applied during each evolution step (delimited by vertical grey bars) is indicated in the above row. Blue points feature time points of sampling and isolation of adaptation intermediate strains. The name of the strain inoculated for next adaptation step is indicated. (B). Evolutionary kinetics of adaptive growth on minimal medium 5 % methanol of wildtype *M. extorquens* TK 0001 cultivated under medium-swap regime. A generation time of 10h was set by the volume of the medium pulses injected at regular time intervals. The daily ratio of stressing medium pulses is plotted is a function of time. (C) Evolutionary kinetics of adaptive growth on minimal medium 7 % methanol of the 5 % methanol-adapted strain G4105 cultivated under medium-swap regime. A generation time of 13 h was set by the volume of the medium pulses injected at regular time intervals. The daily ratio of stressing medium pulses is plotted is a function of time.**

### *III.2.1.1. Growth phenotypes of the adapted isolates*

We studied the growth phenotype of methanol-resistant TK 0001-derived strains. A first observation made for the adapted cells was a more homogenous growth in liquid culture characterized by the absence of filaments (Figure S7AB). This phenotype became obvious at an early stage of the evolution but was also apparent at later stages. Nevertheless, the size of the evolved strain G4105 from the fist evolved step population MEM5 is similar to the wildtype (Figure S7 CD).

The doubling time during exponential growth was determined for the strains G4105 (5% methanol adaptation) and G4521 (10% methanol adaptation) in Erlenmeyer flasks at permissive methanol concentrations and compared with the wildtype strain. Figure 23A shows a significant reduction of the doubling time at 0.25% methanol for both adapted strains as compared to the wildtype. The growth acceleration was much less pronounced at 1% methanol. In contrast, the determination of the maximal biomass yield revealed a considerable gain for the adapted strains at 1% methanol, but only a small effect at 0,25% (Figure 23B). No significant differences neither in growth rate nor yield was found for the two adapted strains tested.

We further examined whether the growth phenotypes of the resistant cells differ at high methanol concentrations using a plate reader. At 1 and 5% methanol, the adapted strains G4201 (adaptation to 7%), G4363 (adaptation to 8%) and G4521 (adaptation to 10%) showed overlapping growth curves (Figure 24A and B). Growth of strain G4105 (adaptation to 5%) was very similar but lagged for about 15 hours under these conditions. At 7% (Figure 24C) and 8% (Figure 24D) methanol, differences in growth behavior between the three strains adapted to higher methanol became apparent, with strain G4521 exhibiting fastest growth. These results show that the cell population continued to evolve until growth at 10% methanol in the turbidostat (Figure 24E).

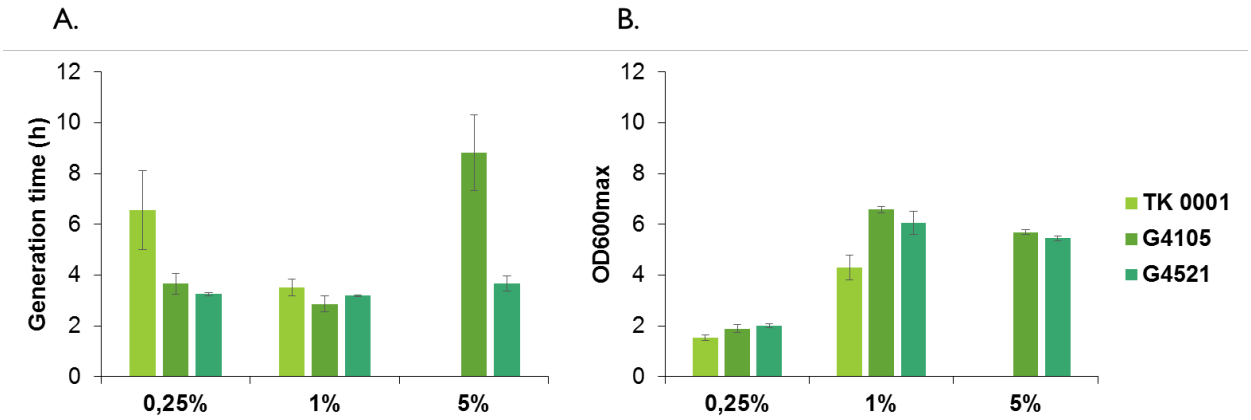


**Figure 23: Growth phenotype of *M. extorquens* TK 0001 wildtype strain and methanol evolved isolates G4105 and G4521. Generation time during exponential growth phase (A) and maximal $OD_{600nm}$ as an estimate of biomass yield (B) were determined after cultivation on minimal medium supplemented with 0.25%, 1% or 5% methanol (v/v). Each result is the mean of triplicates; ±standard deviation is indicated.**

Additionally, the growth phenotype of TK 0001 and G4105 (adapted to 5% MeOH) on different carbon sources using a plate reader were recorded (Figure 25). No significant difference between this two strains with succinate and formaldehyde. Contrariwise, an augmentation of the biomass production was observed for the evolved strain compared to the WT with formate.

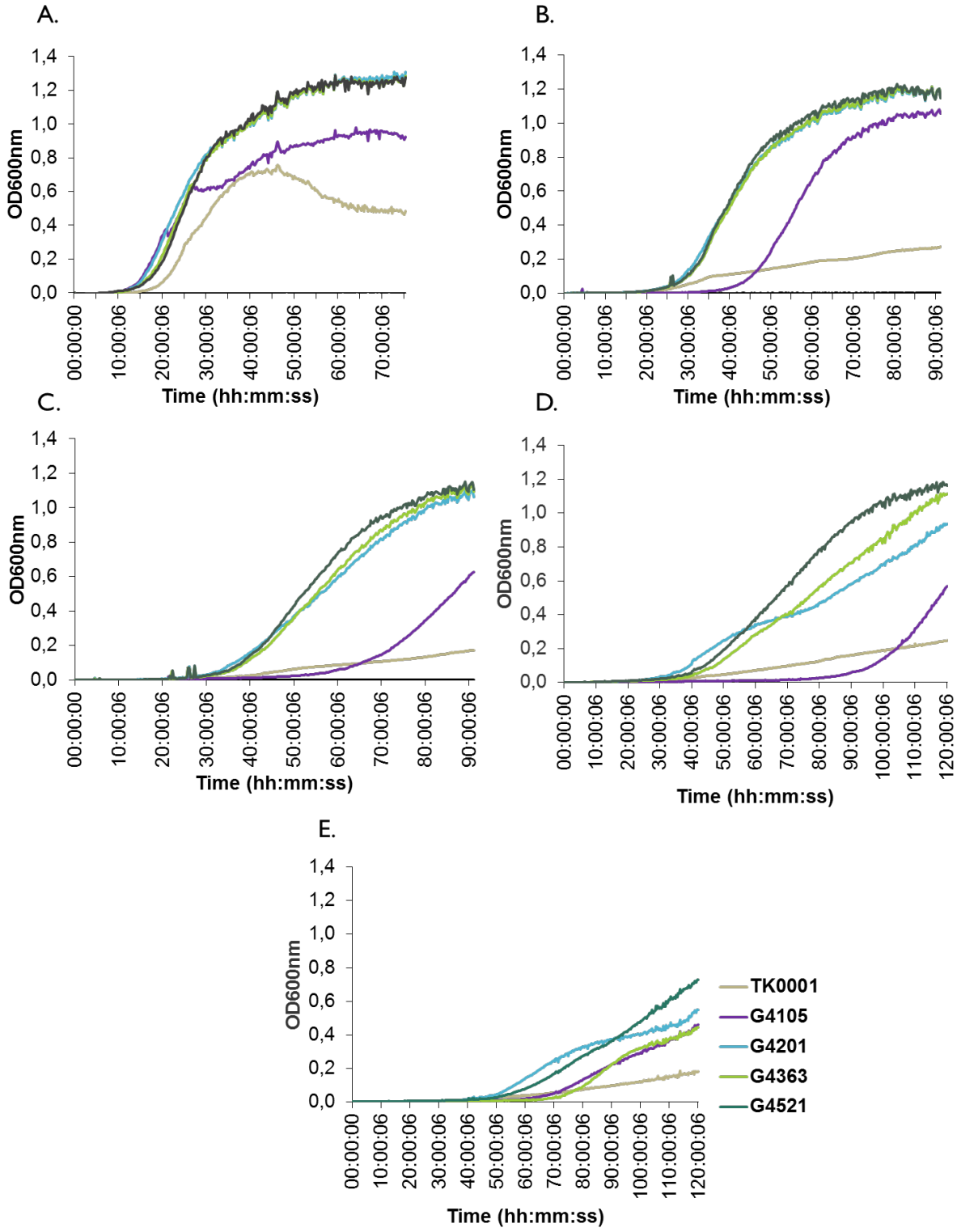


**Figure 24: Growth of *M. extorquens* TK 0001 wildtype strain and evolved isolates from the GM3 population on minimum media supplemented with: (A) 1%, (B) 5%, (C) 7%, (D) 8%, (E) 10% methanol (v/v). Growth experiments were performed in triplicates; measure deviations between samples were less than 5%.**

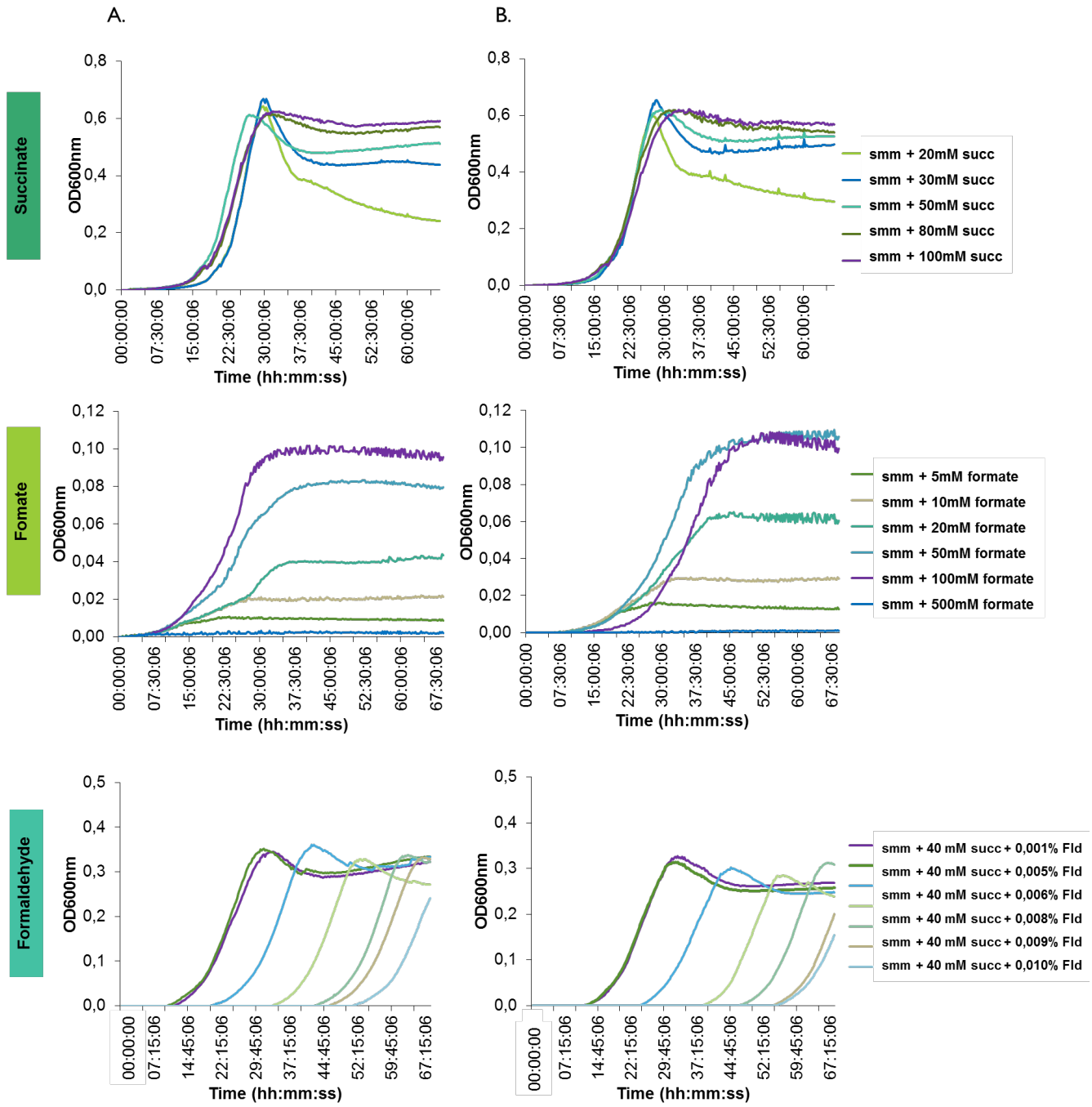


**Figure 25: Growth profile of *Methylobacterium extorquens* TK 0001 (A) and G4105 (B) with different carbon sources at different concentrations. Succ is for succinate and Fld for formaldehyde.**

### *III.2.1.2. Genomic analysis of adapted isolates*

To identify mutations which occurred during the adaptation of the cell populations to growth on high methanol, genomic sequencing was performed for the six isolates obtained from the cultures adapted to 5% (culture MEM5), 7% (culture MEM7), 8% (culture MEM8) and 10% (culture MEM10) methanol concentration, respectively, and compared with the wild type genome. Table S3 summarizes the mutations within each set of six isolates. Single nucleotide polymorphisms (SNP) and short deletions/insertions affected genes and intergenic regions. In addition, a chromosomal duplication was found in all isolates sequenced, containing 86 open reading frames (ORF) (Table S4).

Sequencing revealed only a small number of chromosomal mutations, which increased during the adaptation. This can be attributed to the fact that each subculture, which lasted between 200 and 300 generations, had a clonal origin, thus limiting the clonal variance of the overall adaptation. The mutations found in the intermediate strains used for subculture inoculation, i.e. G4105, G4201 and G4363, were all preserved during subsequent culturing (Table 24). Tree point mutations were shared among all isolates sequenced. While no direct link between the deletion in gene *dxs* coding for 1-deoxyxylulose-5-phosphate synthase and the missense mutation in a gene coding for an ATPase like protein can easily be found, the point mutation in gene *metY* coding for O-acetyl-L-homoserine sulfhydrylase affected a locus already shown to be involved in methanol resistance (Leßmeier and Wendisch, 2015; Schotte et al., 2016).

Besides the three mutations found in all isolates additional mutations were shared among isolates obtained from subcultures grown on higher methanol. The number augmented to eight for the isolates of subculture MEM10, among them missense mutations in two ribosomal genes, which might be of importance for the adaptation of these cells to the very high methanol concentration of 10% (Table 25). In addition, a 50 kbp chromosomal region (bp 444 548 to bp 500 229) containing 86 open reading frames was found duplicated in all isolates sequenced. Only a few of these ORFs could be functionally annotated, including the transcriptional regulatory protein Ros and two subunits of DNA polymerase V.

**Table 24: Genetic differences in isolates sampled at various time points of the adaptation of *M. extorquens* TK 0001 to high methanol concentrations. Isolates were obtained from samples of the evolving bacterial population adapted to growth on minimal medium supplemented with 5% (MEM5), 7% (MEM7), 8% (MEM8) and 10 % (MEM10) methanol. The genome of six isolates issued from each time point were sequenced and the divergences with respect to wildtype *M. extorquens* TK 0001 identified. Light orange: mutation identified at one unique time point. Medium orange: mutation identified at several time points. Dark orange: mutation found at all time points. x/6: ratio of isolates harboring the mutation. •: mutation present in all isolates at a time point. For each time point, the total number of mutations identified is indicated as well as the number of mutations common to all 6 isolates.**

| Mutation position on chromosome | Description of the mutated gene/locus | Mutation location | Mutation type | Distribution of the identified adaptive mutations | | | |
|---|---|---|---|---|---|---|---|
| | | | | Isolate G4105 5 % methanol | Isolate G4201 7 % methanol | Isolate G4363 8 % methanol | 6 isolates 10 % methanol |
| 61901 | glycosyl transferase | genic | ins -/C | | | | 1/6 |
| 1592421 | putative membrane protein (fragment) | genic | del C/- | • | | | • |
| 2811931 | putative type I secretion system ATPase | intergenic | snp | | | | • |
| 3075219 | metY, O-acetylhomoserine sulfhydrylase | genic | snp | • | • | • | • |
| 3382459 | ybhL putative inner membrane protein | genic | snp | | | | 1/6 |
| 3450711 | ATP-binding region, ATPase-like | genic | snp | • | • | • | • |
| 3495847 | rpsG, 30S ribosomal subunit S7 | genic | snp | | | | 1/6 |
| 3496069 | rpsG, 30S ribosomal subunit S7 | genic | snp | | | | 5/6 |
| 3496506 | rpsL, 30S ribosomal subunit S12 | genic | snp | | | • | • |
| 3815109 | shc, squalene-hopene cyclase | genic | snp | | | | 1/6 |
| 3821930 | dxs, 1-deoxyxylulose-5-phosphate synthase | genic | del T/- | • | • | • | • |
| 4425495 | putative CelB-like protein | genic | snp | | • | | • |
| 4453892 | conserved exported protein | genic | snp | | | • | • |
| 5486609 | protein of unknown function/protein of unknown function | intergenic | del G/- | | | | • |
| | | **Common mutations** | | **3** | **4** | **5** | **9** |

**Table 25: Genetic differences in population sampled at various time points of the adaptation of *M. extorquens* TK 0001 to high methanol concentrations. Isolates were obtained from samples of the evolving bacterial population adapted to growth on minimal medium supplemented with 5% (G4105), 7% (G4201), 8% (G4363) and 10 % (MEM10) methanol. The genome of six isolates issued from each time point were sequenced and the divergences with respect to wildtype *M. extorquens* TK 0001 identified. Light orange: mutation identified at one unique time point. Medium orange: mutation identified at several time points. Dark orange: mutation found at all time points. x/6: ratio of isolates harboring the mutation. •: mutation present in all isolates at a time point. For each time point, the total number of mutations identified is indicated as well as the number of mutations common to all 6 isolates.**

| GO label | GO Description | location | mutation type | Distribution of the identified adaptive mutations | | | |
|---|---|---|---|---|---|---|---|
| | | | | 5 % | 7 % | 8 % | 10 % |
| TK0001_v2_0071 | glycosyl transferase | genic | ins -/C | | | | 1/6 |
| TK0001_v2_1635 | transposase | genic | snp | | 1/6 | | |
| TK0001_v2_3055/ TK0001_v2_3056 | putative type I secretion system ATPase / pufC, photosynthetic reaction center cytochrome c subunit-related | intergenic | snp | | | | 5/6 |
| TK0001_v2_3284 | cckA, sensor hybrid histidine kinase with multiple PAS and response regulator receiver domains | genic | snp | | | 1/6 | |
| TK0001_v2_3284 | cckA, sensor hybrid histidine kinase with multiple PAS and response regulator receiver domains | genic | snp | | | 3/6 | |
| TK0001_v2_3350 | metY, O-acetylhomoserine sulfhydrylase | genic | snp | • | • | • | • |
| TK0001_v2_3504/ TK0001_v2_3505 | gapA, glyceraldehyde-3-phosphate dehydrogenase/ conserved protein of unknown function | intergenic | snp | | 4/6 | 4/6 | • |
| TK0001_v2_3606 | ybhL, conserved protein of unknown function; putative inner membrane protein | genic | snp | | | | 1/6 |
| TK0001_v2_3681 | ATP-binding region, ATPase-like | genic | snp | • | • | • | • |
| TK0001_v2_3750 | rpsG, 30S ribosomal protein S7 | genic | snp | | | | 1/6 |
| TK0001_v2_3750 | rpsG, 30S ribosomal protein S7 | genic | snp | | | | • |
| TK0001_v2_3751 | rpsL, 30S ribosomal protein S12 | genic | snp | | | 2/6 | • |
| TK0001_v2_4081 | shc, squalene-hopene cyclase | genic | snp | | | | 1/6 |
| TK0001_v2_4086 | dxs, 1-deoxyxylulose-5-phosphate synthase | genic | del T/- | • | • | • | • |
| TK0001_v2_4115 | glycosyl transferase | genic | del T/- | | 1/6 | | |
| TK0001_v2_4181/ TK0001_v2_4182 | sga, serine-glyoxylate aminotransferase/ conserved protein of unknown function | intergenic | snp | | 1/6 | | |
| TK0001_v2_4394 | putative glycoside hydrolase/deacetylase | genic | snp | | 1/6 | | |
| TK0001_v2_4698 | putative CelB-like protein (fragment) | genic | snp | | | 5/6 | • |
| TK0001_v2_4727 | conserved exported protein of unknown function | genic | snp | | | 1/6 | • |
| TK0001_v2_5755/ TK0001_v2_5756 | conserved protein of unknown function / protein of unknown function | intergenic | snp | 3/6 | | | |
| | | | **Total mutations** | **4** | **8** | **9** | **13** |
| | | | **Common mutations** | **3** | **3** | **3** | **8** |

### *III.2.1.3. Membrane composition analysis*

The biophysical properties of biological membranes are of importance for adaptive responses of bacteria to external stressors. Solvents have been found to impact the fluidity of the cell membrane by triggering compositional changes of their fatty acid composition. (Kabelitz et al., 2003; Oh et al., 2018; Roy, 2009). A Fatty Acid Methyl Ester (FAME) analysis was conducted for the TK 0001 WT strain and for two evolved strains G4105 and G4521 (Figure 26). No significant differences were observed between the WT and the evolved cells, indicating the membrane composition to be stable throughout the evolution on high methanol concentrations. Effects of solvent stressors on membrane composition are complex and depend on the organism (Huffer et al., 2011).

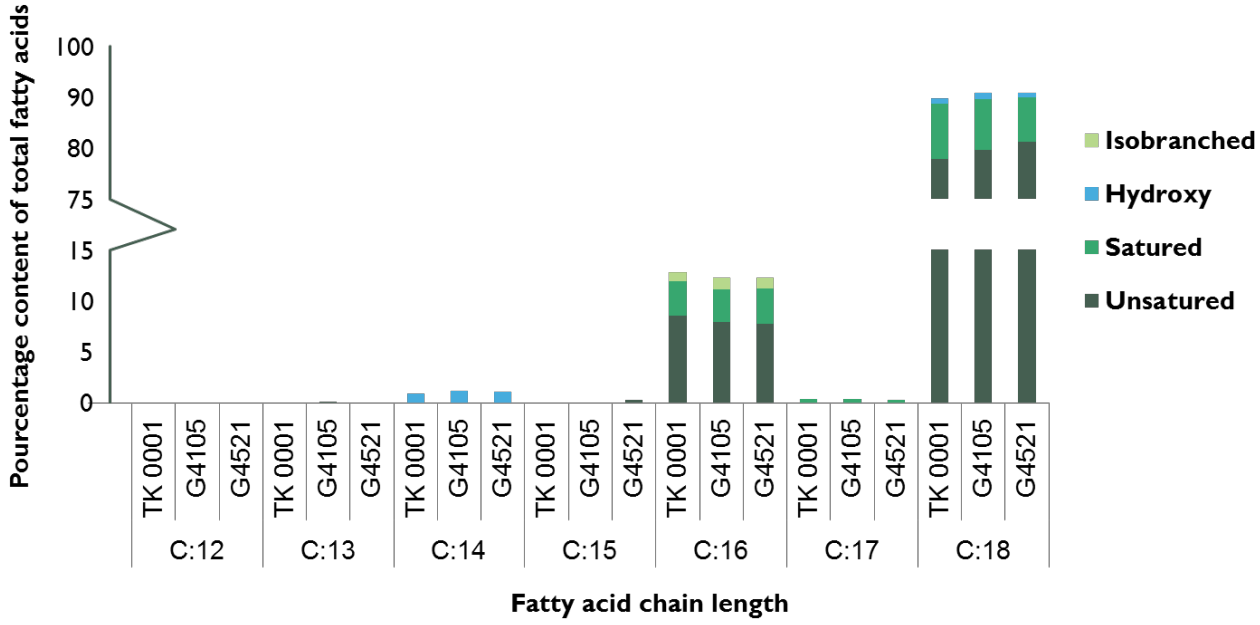


**Figure 26: FAME analysis of the fatty acid composition of membrane samples obtained from strain *M. extorquens* TK 0001 and the evolved derivatives G4105 (adapted to 5% MeOH) and G4521 (adapted to 10% MeOH) grown in smm supplemented with 1% methanol.**

### III.2.2. Directed evolution of strain *Methylobacterium extorquens* AM1 to growth with 10% methanol _chamber 1

In a parallel experiment, the *M. extorquens* reference strain AM1 was evolved to growth on 10% methanol in the GM3 automaton. Culture regimes, isolates selection and sequencing were performed as for the TK 0001 strain (Figure S8). The AM1 cells, however, were evolved to high methanol resistances from a single inoculate of the wild type strain. All evolved isolates from AM1 were listed in Table S2B.

Figure 27A shows the evolutionary path of the AM1 cell population to growth on 10% methanol. Like the TK 0001 cells, the AM1 cell population was subjected to conditional medium swap and turbidostat adaptations. The first medium swap period (1% to 5% methanol) took twice as long as the corresponding period for the TK 0001 adaptation (24 versus 11 days) (Figure 27B). For the second swap period (5% to 7% methanol), the ratio was 34 days for TK 0001 to 59 days for AM1 (Figure 27C). Strain AM1 was more resistant to the adaptation protocol than strain TK 0001.

#### *III.2.2.1. Growth phenotypes of the adapted isolates*

As for TK 0001 evolution, a homogenous growth of the adapted cells in liquid culture characterized by the absence of filaments was observed at early stage (Figure S9). This phenotype is also observed at later stages.

We further examined whether the growth phenotypes of the resistant cells differ at high methanol concentrations using a plate reader. All the adapted strains G4609 (adapted to 5%), 4638 (adaptation to 7%), G4600 (adaptation to 8%) and G706 (adaptation to 10%) showed a singular growth profiles in all methanol concentration tested (Figure 28) contrary to what was observed for TK 0001 adaptation. However, at high methanol concentration, 7%, 8% and 10% the isolate G4706 showed the shorter lag phase. These results show that the cell population continued to evolve until growth at 10% methanol in the turbidostat, even if at 1% MeOH the contrary observation is noted (Figure 29).

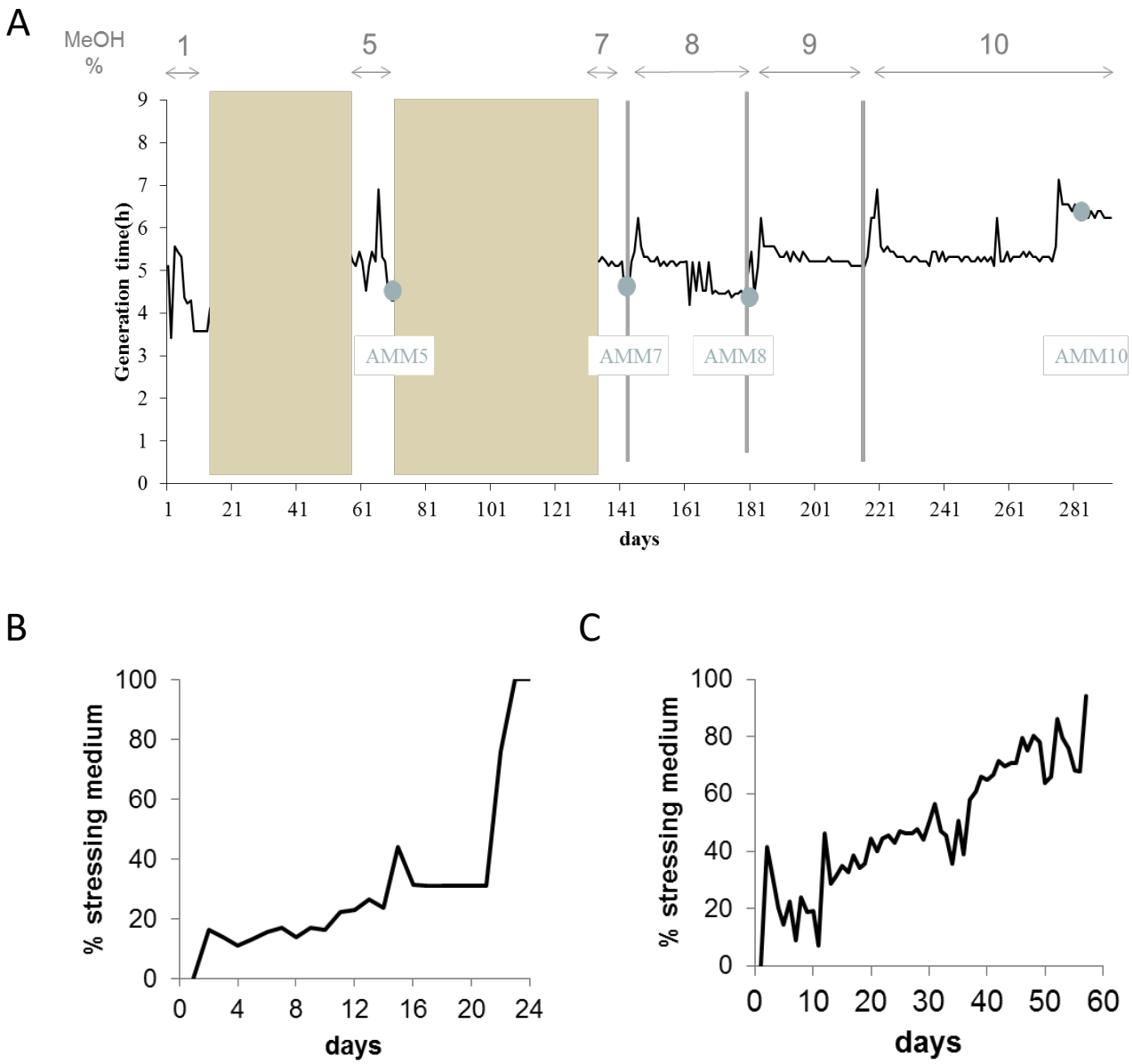


**Figure 27. Adaptation of *M. extorquens* AM1 bacteria to increasing methanol concentrations in GM3-driven continuous culture (A). Growth rate over 290 days of a bacterial population cultivated on augmenting methanol concentrations. Bronze areas correspond to periods of cultivation under medium-swap regime. Black lines show average daily generation time during cultivation periods under turbidostat regime. Methanol concentration of culture medium used during each evolution step (delimited by vertical grey bars) is indicated in the above row. Blue points feature time points of sampling and isolation of adaptation intermediate strains for physiology and genomic analysis. (B) Evolutionary kinetics of adaptive growth on minimal medium supplemented with 5 % methanol of *M. extorquens* AM1 wildtype bacteria cultivated under medium-swap regime. A generation time of 8h was set by the volume of the medium pulses injected at regular time intervals. The daily ratio of 5% methanol-containing stressing medium pulses is plotted is a function of time. (C) Evolutionary kinetics of adaptive growth on minimal medium supplemented with 7% methanol of the 5 % methanol-adapted AM1 cell population cultivated under medium-swap regime. A generation time of 7h30 was set by the volume of the medium pulses injected at regular time intervals. The daily ratio of the 7% methanol-containing stressing medium pulses is plotted is a function of time.**

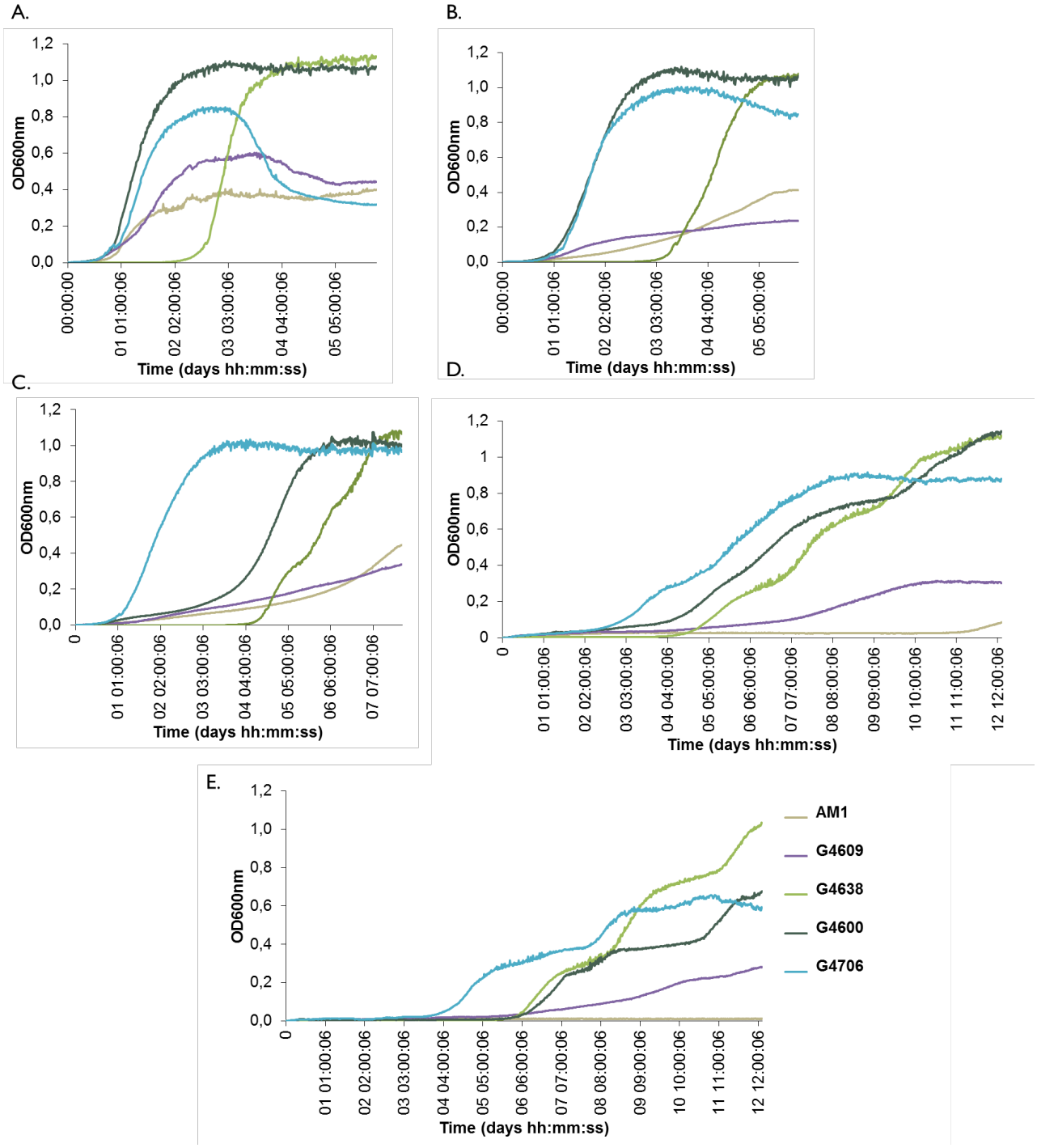


**Figure 28: Growth of *M. extorquens* AM1 wildtype strain and evolved isolates from the GM3 population on minimum media supplemented with: (A) 1%, (B) 5%; (C) 7%; (D) 8%, (EE) 10% methanol (v/v). Growth experiments were performed in triplicates; measure deviations between samples were less than 5%. WT *M. extorquens* AM1; 5% methanol-adapted strain G4609; 7% methanol-adapted strain G4638; 8 % methanol-adapted strain G4600; 10 % methanol-adapted strain G4706.**

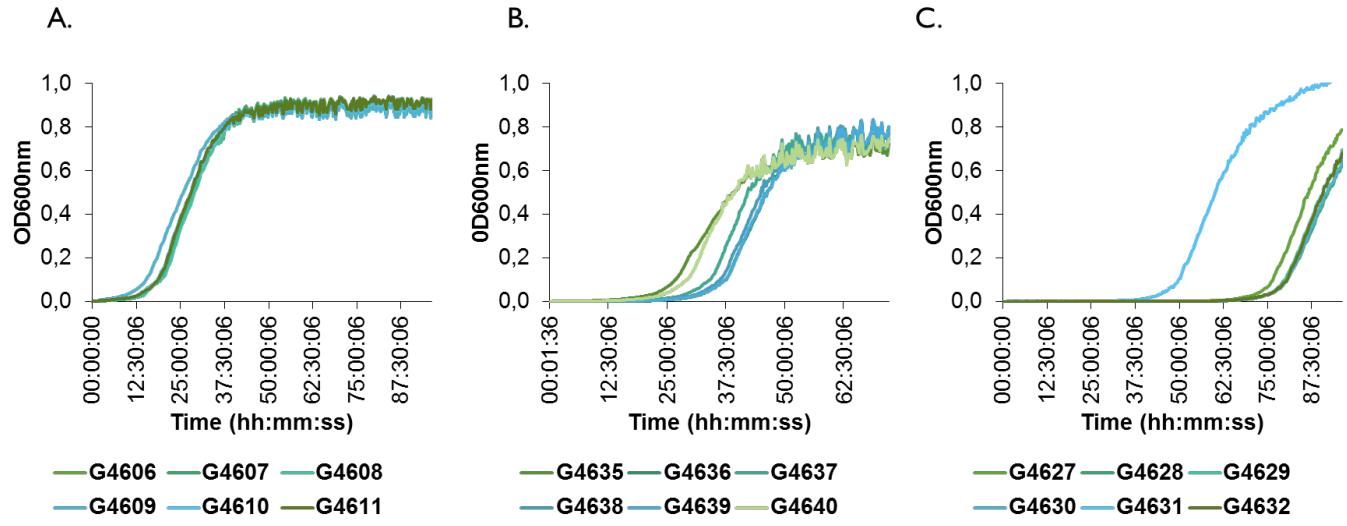


**Figure 29: Growth profile of isolates from evolved AMM1 population in smm supplemented with 1% MeOH: the population AMM5 (A), AMM7 (B) and AMM8 (C).**

The doubling time during exponential growth was determined for the strains AM1 wildtype and G4605 (5% methanol adaptation) in Erlenmeyer flasks at permissive methanol concentrations and compared with the wildtype strain. Figure 30A shows no significant reduction of the doubling time at 0.25% and 1% methanol for the adapted strain as compared to the wildtype. Likewise, the determination of the maximal biomass yield revealed no gain for the adapted strains at 0.25% and 1% methanol, (Figure 30B).

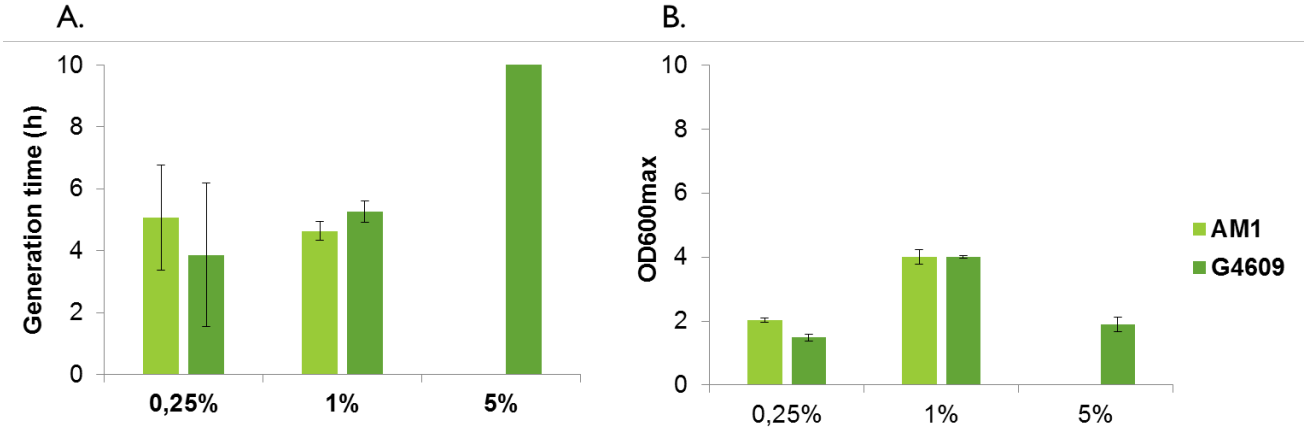


**Figure 30: Growth phenotype of *M. extorquens* AM1 wildtype strain and methanol evolved isolates from AMM5 (G4609). Generation time during exponential growth phase (A) and maximal $OD_{600nm}$ as an estimate of biomass yield (B) were determined after cultivation on minimal medium supplemented with 0.25%, 1% or 5% methanol (v/v). Each result is the mean of triplicates; ±standard deviation is indicated.**

Due to the observations done for growth of evolved TK 0001 strain on different carbon sources (Figure 25), the same experimentation was done for AM1 (Figure 31). The evolved strain at 5% MeOH G4609 produce more biomass than AM1 on the same formate concentration.

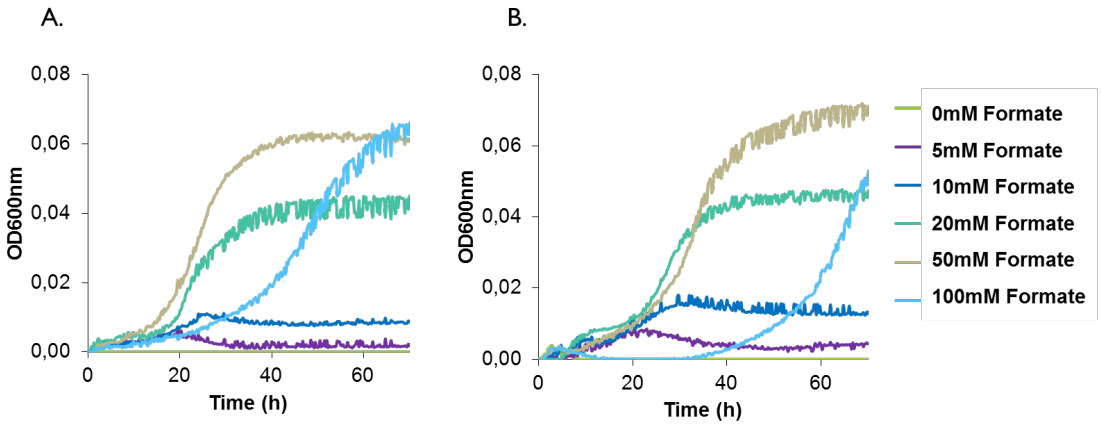


**Figure 31: Growth profile in smm supplemented with different formate concentrations of AM1 WT (A) and G4609 (B).**

### *II.2.2.2. Genomic analysis of adapted isolates*

Six isolates were obtained for each of four resistance points (5%, 7%, 8% and 10% methanol) along the continuous culture experiment and their genomic DNA sequenced as described for the TK 0001 evolution. The point mutations and short indels identified are listed in Table 26. The pattern of mutations shows a more even distribution compared to the pattern obtained for the TK 0001 isolates (Table 25), where mutations accumulated upon adaptation (Table S5). This difference can be attributed to the continuity of the AM1 evolution from a unique initial inoculation.

Five genes were found to be affected in all isolates obtained from the final 10% resistance culture, including gene *rpsL* coding for ribosomal protein S12. This locus was also affected in the TK 0001 cells adapted to very high methanol, albeit implicating a different residue (Table S3 and S5). As for the TK 0001 adaptation, the only gene mutated in all AM1 isolates sequenced was *metY* coding for O-acetyl-L-homoserine sulfhydrylase, showing this locus to be a hotspot of methanol-resistance. While a single mutation (T34M) was found in all TK 0001 methanol-resistant isolates, four different *metY* alleles were identified in the AM1 isolates, which were differentially distributed (Table 29A).

**Table 26: Genetic differences in isolates sampled at various time points of the adaptation of *M. extorquens* AM1 to high methanol concentrations. Isolates were obtained from samples of the evolving bacterial population adapted to growth on minimal medium supplemented with 5% (AMM5), 7% (AMM7), 8% (AMM8) and 10 % (AMM10) methanol. The genome of six isolates issued from each time point were sequenced and the divergences with respect to wildtype *M. extorquens* AM1 identified. Light orange: mutation identified at one unique time point. Medium orange: mutation identified at several time points. Dark orange: mutation common to all time points. x/6: ratio of isolates harboring the mutation at a time point. •: mutation present in all isolates at a time point. For each time point, the total number of mutations identified is indicated as well as the number of mutations common to all 6 isolates.**

| Gene label | Description of the mutated gene / locus | Location | Mutation type | Presence/absence of the identified adaptive mutations | | | |
|---|---|---|---|---|---|---|---|
| | | | | 6 isolates | 6 isolates | 6 isolates | 6 isolates |
| | | | | 5% | 7% | 8% | 10% |
| META1_0256 | glycosyl transferase | genic | snp | | • | • | • |
| META1_0742 | fragment of response regulator (N-terminal fragment) | genic | snp | 2/6 | | | |
| META1_0744 | fragment of response regulator (C-terminal fragment) | genic | snp | 1/6 | | | |
| META1_0767 | haloacid dehalogenase-like hydrolase | genic | ins | | 4/6 | • | • |
| META1_0809 | putative glycosyl transferase | genic | ins | | 1/6 | | |
| META1_0953 / META1_0954 | cysE, serine acetyltransferase / eshA | intergenic | snp | | 1/6 | | |
| META1_0984 | conserved protein of unknown function | genic | snp | 1/6 | | | |
| META1_1683 / META1_1684 | putative aminoglycoside phosphotransferase / putative O-acyltransferase | intergenic | snp | | | 1/6 | |
| META1_1766 / META1_1767 | fae, formaldehyde-activating enzyme / orf17 | intergenic | snp | | | 3/6 | |
| META1_1984 | putative catecholate siderophore receptor | genic | snp | | 1/6 | | |
| META1_2147 | protein of unknown function | genic | snp | | | | 1/6 |
| META1_2148 | rpsL, 30S ribosomal subunit protein S12 | genic | snp | | • | 3/6 | • |
| META1_2420 | clpX, ATP-dependent Clp protease ATP-binding subunit | genic | snp | | | 1/6 | • |
| META1_2508 | metY, O-acetylhomoserine sulfhydrylase | genic | snp | • | • | • | • |
| META1_2931 | pufB, light-harvesting complex 1 beta chain | genic | snp | | | | 1/6 |
| META1_3241 | ilvA, threonine deaminase | genic | snp | | 1/6 | | |
| META1_4035 | protein of unknown function | genic | snp | 2/6 | | | |
| META1_4041 / META1_4042 | rffG, dTDP-glucose dehydratase / rfbC, dTDP-4-dehydrorhamnose epimerase | intergenic | snp | | | | 1/6 |
| META1_4735 | MFS transporter membrane protein | genic | snp | | | | 1/6 |
| META1_5014 | mrp, antiporter inner membrane protein | genic | snp | • | | | |
| META1_5090 / META1_5091 | mraW, S-adenosyl-dependent methyltransferase / RNaseP | intergenic | snp | 2/6 | | | |
| META2 | grpE, protein GrpE, Hsp cofactor / fragment of transposase of ISMex11, IS3 | intergenic | snp | | 1/6 | | |
| p2META_0010 | conserved protein of unknown function | genic | snp | | 1/6 | | |
| | | **Total mutations** | | **7** | **10** | **7** | **9** |
| | | **Common mutations** | | **2** | **3** | **3** | **5** |

### *II.2.2.3. Membrane composition analysis*

As was done for the adapted cells of the TK 0001 evolution, Fatty Acid Methyl Ester (FAME) analysis was conducted for the AM1 WT strain and for two evolved strains G4609 and G4706 (Figure 32). Like for the TK 0001 isolates, no significant differences were observed between the AM1 WT and the evolved cells, showing that a stable membrane composition was preserved during the adaptation.

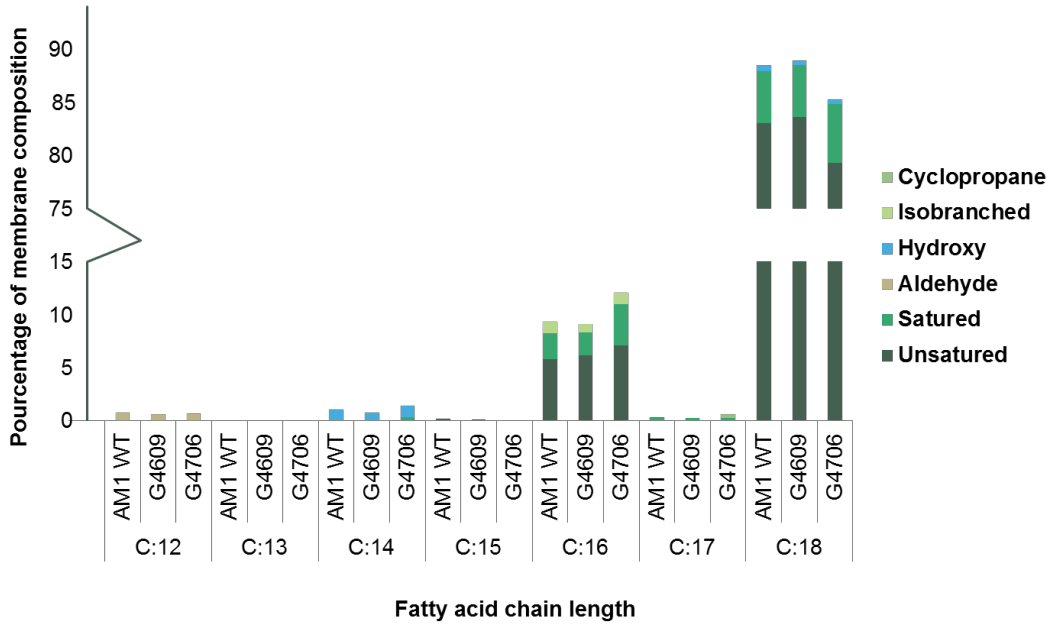


**Figure 32: FAME analysis of the fatty acid composition of membrane samples obtained from strain *M. extorquens* AM1 and the evolved derivatives G4609 (adapted to 5% MeOH) and G4706 (adapted to 10% MeOH) grown in smm supplemented with 1% methanol.**

## III.2.3. Directed evolution of strain *Methylobacterium extorquens* AM1 to growth with 10% methanol _chamber 2

The GM3 devices are conceived to enable strain adaptations in duplicate. While the TK 0001 evolution could not be duplicated for technical reasons, two AM1 cultures were adapted to high methanol in parallel. As shown in Figure 33, the "second chamber" adaptation proceeded through medium swap and turbidostat periods basically as did the first chamber culture described above.

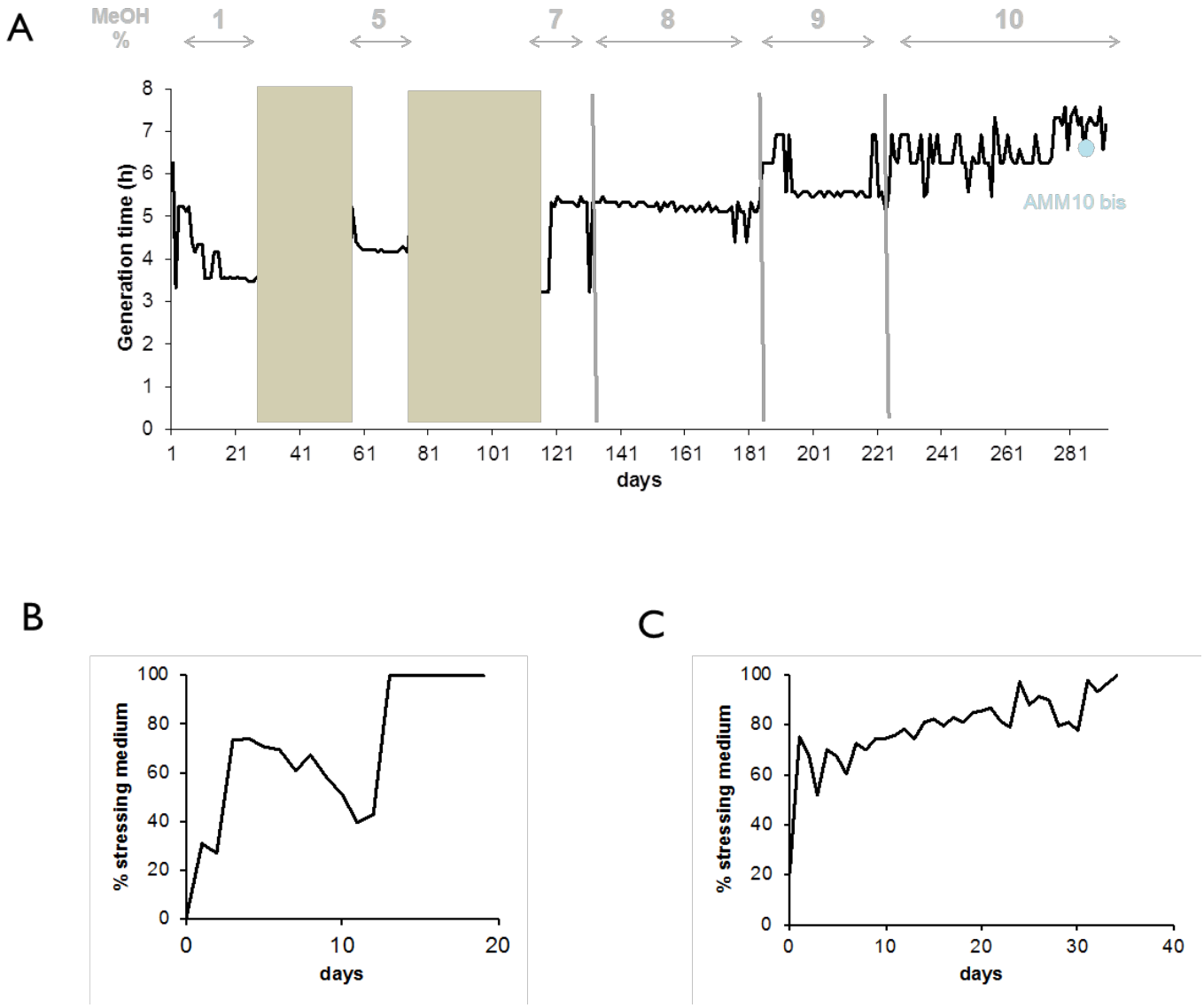


**Figure 33: Evolution AMM10 chamber 2. Adaptation of *M. extorquens* AM1 bacteria to increasing methanol concentrations in GM3-driven continuous culture. (A). Growth rate over 290 days of a bacterial population cultivated on augmenting methanol concentrations. Bronze areas correspond to periods of cultivation under medium-swap regime. Black lines show average daily generation time during cultivation periods under turbidostat regime. Methanol concentration of culture medium used during each evolution step (delimited by vertical grey bars) is indicated in the above row. Blue point feature time point of sampling and isolation of adaptation intermediate strains for physiology and genomic analysis. (B). Evolutionary kinetics of adaptive growth on minimal medium supplemented with 5 % methanol of *M. extorquens* AM1 wildtype bacteria cultivated under medium-swap regime. A generation time of 10h was set by the volume of the medium pulses injected at regular time intervals. The daily ratio of 5% methanol-containing stressing medium pulses is plotted is a function of time. (C) Evolutionary kinetics of adaptive growth on minimal medium supplemented with 7 % methanol of the 5 % methanol-adapted AM1 cell population cultivated under medium-swap regime. A generation time of 10h was set by the volume of the medium pulses injected at regular time intervals. The daily ratio of the 7% methanol-containing stressing medium pulses is plotted is a function of time.**

Mutational analysis was restricted to six final isolates growing with 10% methanol. As can be seen from Table 27, the number of SNPs found amounted to about 100 per isolate on average, approximately 10 times more than the final isolates of the chamber 1 culture. This result can be attributed to a probable mutator phenotype of the cells which all carried a base pair insertion in the *mutS* gene. Gene *mutS* specifies a protein implicated in the methyl-directed mismatch repair. Its inactivation in *E. coli* has been shown to raise the rate of spontaneous mutations by 10 (Sixma, 2001).

**Table 27: SNPs in the isolates from the population AMM10 chamber 2**

| Evolved strain | Total SNPs | genic | inter genic | Ts | A/G | G/A | C/T | T/C | Tv | A/C | A/T | G/C | G/T | C/A | C/G | T/A | T/G | Syn | Non syn | Non sense |
|---|---|---|---|---|---|---|---|---|---|---|---|---|---|---|---|---|---|---|---|---|
| **Total** | **561** | **492** | **69** | **456** | **185** | **49** | **18** | **204** | **36** | **2** | **0** | **1** | **8** | **7** | **6** | **0** | **12** | **63** | **429** | **0** |
| **G4709** | 44 | 40 | 4 | 37 | 15 | 6 | 0 | 16 | 3 | 0 | 0 | 0 | 0 | 1 | 1 | 0 | 1 | 5 | 35 | 0 |
| **G4710** | 106 | 93 | 13 | 87 | 36 | 8 | 1 | 42 | 6 | 0 | 0 | 0 | 2 | 1 | 1 | 0 | 2 | 8 | 85 | 0 |
| **G4711** | 117 | 102 | 15 | 93 | 37 | 8 | 2 | 46 | 9 | 0 | 0 | 1 | 2 | 2 | 2 | 0 | 2 | 12 | 90 | 0 |
| **G4712** | 126 | 113 | 13 | 106 | 44 | 11 | 7 | 44 | 7 | 1 | 0 | 0 | 2 | 1 | 1 | 0 | 2 | 14 | 99 | 0 |
| **G4713** | 79 | 70 | 9 | 66 | 27 | 9 | 6 | 24 | 4 | 0 | 0 | 0 | 0 | 1 | 1 | 0 | 2 | 13 | 57 | 0 |
| **G4714** | 89 | 74 | 15 | 67 | 26 | 7 | 2 | 32 | 7 | 1 | 0 | 0 | 2 | 1 | 0 | 0 | 3 | 11 | 63 | 0 |

Besides *mutS*, the missense mutation F119L in *metY* was found in all isolates, demonstrating again the role of this locus in methanol resistance. As shown in Table 28, six mutations were common to all sequenced isolates. Interestingly, the mutated putative CelB-like protein META1_1168 is fully homologous to the CelB-like protein TK0001_v2_4698 also impacted in all isolates adapted to 10 % methanol (Table 25). Furthermore, the gene META1_0767, which codes for a haloacid dehalogenase-like hydrolase, presents a missense mutation in five of the six isolates. In the late isolates from the duplicated evolution experiment performed in chamber 1, the insertion of 3 base pairs was identified in META1_0767 (Table 26). Also, one protein of the 30S ribosomal subunit, *rpsQ*-encoded, was mutated in five of the six isolates (Table 28).

**Table 28: Mutated genes common to six, five or four isolates obtained from AMM10_chamber 2 culture.**

| Gene Label | Description of the mutated gene / locus | Location | Mutation type | Presense/absence of the identified mutations | | | | | |
|---|---|---|---|---|---|---|---|---|---|
| | | | | G4709 | G4710 | G4711 | G4712 | G4713 | G4714 |
| META1_1168 | putative CelB-like protein | genic | snp | • | • | • | • | • | • |
| META1_1441 | otsA, osmoregulatory trehalose synthesis protein A | genic | snp | • | • | • | • | • | • |
| META1_1791 | putative succinoglycan biosynthesis transport protein exoP | genic | del | • | • | • | • | • | • |
| META1_2508 | metY, O-acetylhomoserine sulfhydrylase | genic | snp | • | • | • | • | • | • |
| META1_4678 | mutS, DNA mismatch repair protein | genic | ins | • | • | • | • | • | • |
| META1_4797 | conserved protein of unknown function | genic | snp | • | • | • | • | • | • |
| META1_0505 | protein of unknown function | genic | snp | | • | • | • | • | • |
| META1_0767 | haloacid dehalogenase-like hydrolase | genic | snp | | • | • | • | • | • |
| META1_0996 | protein of unknown function | genic | sns / snp | | • | • | • | • | • |
| META1_1200 | putative fused thiol:disulfide interchange protein precursor | genic | snp | | • | • | • | • | • |
| META1_2162 | rpsQ, 30S ribosomal subunit protein S17 | genic | snp | | • | • | • | • | • |
| META1_2276 | putative methyltransferase | genic | del | | • | • | • | • | • |
| META1_2648 | protein of unknown function | genic | snp | | • | • | • | • | • |
| META1_1861 | tkt, transketolase | genic | snp | • | | | • | • | • |
| META1_1932 | putative propionate-CoA ligase | genic | snp | | • | • | • | | • |
| META1_1949 | putative DNA topoisomerase I | genic | snp | | • | • | • | | • |
| META1_4005 | protein of unknown function | genic | snp | • | | | • | • | • |
| META1_4875 | putative histidine kinase | genic | snp | | • | • | • | | • |
| META1_5143 | valS, valine tRNA synthetase | genic | snp | • | • | • | • | | |

### III.2.4. Enzymatic characterization of wildtype and mutated O-acetyl-L-homoserine sulfhydrylase (MetY)

All intermediate and final isolates obtained from the high-methanol adaptations of *M. extorquens* strains TK 0001 and AM1 carried a missense mutation in the *metY* gene coding for O-acetyl-L-homoserine sulfhydrylase. This enzyme catalyzes the synthesis of homocysteine, a precursor of methionine, from O-acetyl-L-homoserine and hydrogen sulfide (Yamagata, 1989), but can also produce methionine directly from O-acetyl-L-homoserine and methanethiol (Bolten et al., 2010). Gene *metY* has been found to be implicated in methanol toxicity for *Corynebacterium glutamicum* (Leßmeier and Wendisch, 2015). In *Pichia pastoris* MetY was demonstrated to be related to the production of the toxic methionine analogue methoxine (O-methyl-L-homoserine) occurring during growth in high methanol. Methoxine can replace methionine during ribosomal protein synthesis leading to the accumulation of dysfunctional peptides (Schotte et al., 2016).

All *metY* genes sequenced from the TK 0001 isolates coded for the MetY variant T34M. By contrast, the AM1 isolates harbored four different *metY* alleles: G113S, D373G, L389F and G87S (Table 29). Through sequence comparison with MetY of *Wolinella succinogenes* (35% identity with the *M. extorquens* enzyme on 93% query cover, Figure 34), for which a crystal structure has been obtained, the mutant residues could be localized within the protein (Tran et al., 2011). Thus, residues T34 and L389 are part of the disordered N-terminal loop implicated in the monomer-monomer interface of the dimeric protein. Residues G87 and G113 seem to play a role in the active site, G87 most likely forming a hydrogen-bond with the pyridoxal-phosphate cofactor of the enzyme.

**Table 29: (A) Mutations in MetY identified in the isolates analyzed at each step of the adaptation to increasing concentrations of methanol of both *M. extorquens* strains TK 0001 and AM1 and (B) Kinetic parameters *metY*-encoded wildtype O-acetyl-L-homoserine sulfhydrylase of *M. extorquens* TK 0001.**

A

| *M. extorquens* strain | MetY mutation | Distribution of the mutations in MetY between isolates at each evolution step | | | |
|---|---|---|---|---|---|
| | | 5 % MeOH | 7% MeOH | 8 % MeOH | 10 % MeOH |
| TK 0001 | T34M | 6/6 | 6/6 | 6/6 | 6/6 |
| AM1 | G87S | - | 5/6 | 6/6 | 6/6 |
| | G113S | 2/6 | - | - | - |
| | D373G | 1/6 | - | - | - |
| | L389F | 3/6 | 1/6 | - | - |

B

| **Substrate** | $k_{cat}$ ($sec^{-1}$) | $K_M$ (mM) | $k_{cat}/K_M$ ($sec^{-1}.M^{-1}$) |
|---|---|---|---|
| O-acetyl-homoserine | 2.321 ± 0.119 | 1.30 ± 0.20 | 1847.508 |
| sulfide | 1.784 ± 0.115 | 0.80 ± 0.20 | 2146.811 |
| methanol | 0.498 ± 0.016 | 3150.0 ± 340.0 | 1.580 |


**Figure 34: Sequence alignment of O-acetyl-L-homoserine sulfhydrylase (MetY) from *Methylobacterium extorquens* TK 0001/AM1 with MetY from *Wolinella succinogenes* (PDB entry 3RI6, Tran et al., 2011). The conserved active-site residues are marked with asterisks; other less-conserved active-site residues of MetY are marked with a plus. The disordered loops of the adjacent monomers, which are predicted to bind to the PLP phosphate group, are marked with green circles. Residues which were changed during the TK 0001 and AM1 evolution are marked in red.**

We expressed the *metY* wildtype gene and all five mutants in *E. coli* and purified the proteins using standard methods. The kinetic parameters determined for the MetY wildtype enzyme are shown in Table 29B (Figure S10). Methanol was indeed found to be a substrate for the enzyme, corroborating earlier findings (see above). The $K_M$ for methanol was about 4000 times higher than the $K_M$ for sulfide. However, the $k_{cat}$ for methanol being only three times less than the $k_{cat}$ for sulfide, methoxine synthesis likely competes with the synthesis of homocysteine. Conversely, all five mutant MetY variants listed in Table 10A were found to be inactive. O-acetyl-L-homoserine did not measurably react with sulfide or with methanol in the *in vitro* tests. Thus, by abolishing the activity of the enzymes, the mutations also abolished the toxic side reaction with methanol.

Both *M. extorquens* strains harbor genes specifying enzymes of methionine biosynthesis via trans-sulfuration of O-acetyl-L-homoserine (Figure 35). Obviously, the sulfhydrylation pathway of methionine synthesis is dispensable for the cells.

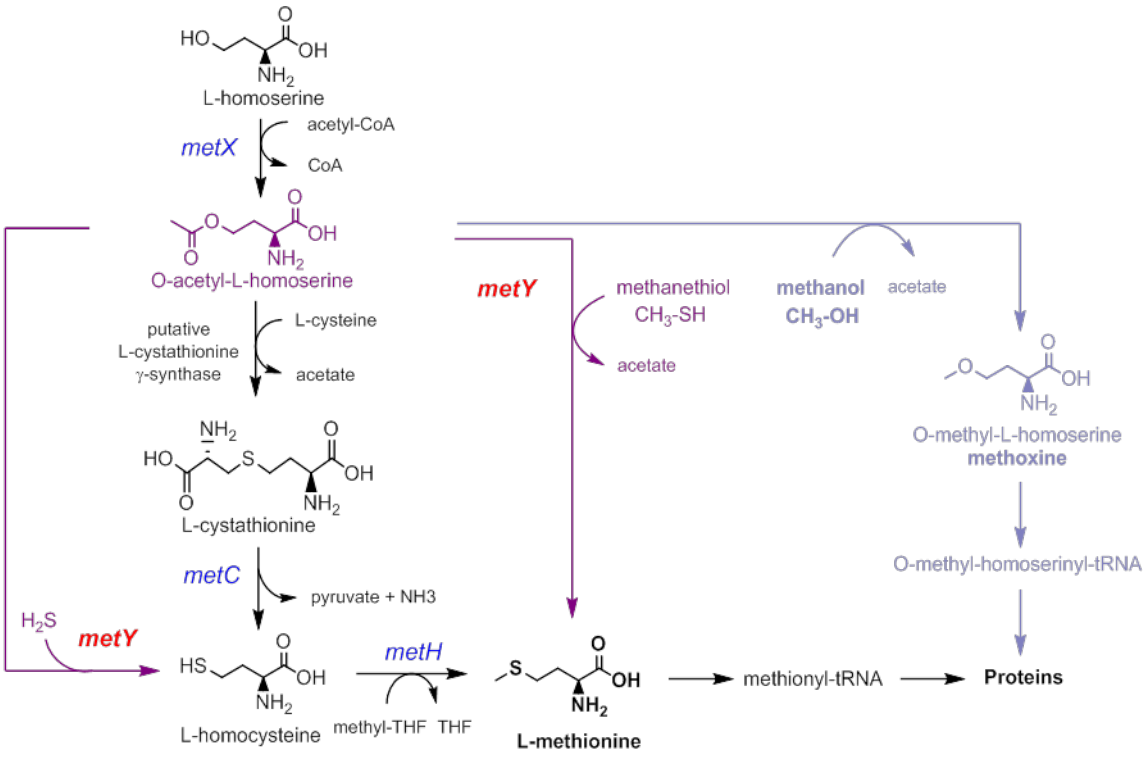


**Figure 35: Methionine biosynthesis pathways of *Methylobacterium extorquens* TK 0001 and AM1 from L-homoserine as deduced from genomic annotation. *metY*-encoded *O*-acetyl-L-homoserine sulfhydrylase catalyzes the conversion of *O*-acetyl-L-homoserine into L-homocysteine using sulfide as well as the direct conversion of *O*-acetyl-L-homoserine into L-methionine using methanethiol (reactions indicated in purple). Side-activity of MetY with methanol forms methoxine (reaction indicated in mauve). *metX* codes for L-homoserine *O*-acetyltransferase, *metC* for cystathionine beta-lyase, *metH* for methionine synthase.**

## II.2.5. Effects of *metY* overexpression on methanol toxicity

To further examine the possible role of the *metY* locus for methanol toxicity, we expressed the *metY* wildtype gene from plasmid pTE102 (Addgene, Figure13) in the methanol-tolerant strains G4105 and G4521 and tested for growth on different methanol concentrations. At a limiting concentration of methanol (0.25%) the G4105_pTE102 metY, conserved the same generation time than the cells containing an empty plasmid (Figure 36). As expected, at higher concentrations (1% and 5% (v/v) methanol the *metY* expressing cells grew more slowly, with a gain in doubling time of 28% at 5% methanol. Likewise, biomass production of G4105_pTE102 metY cells was lowered by about 26% at this high methanol concentration as compared with

the control cells. The same observations are done for G4521_pT102 metY compare to the cells containing an empty plasmid.

These results confirm the implication of O-acetyl-L-homoserine sulfhydrylase in methanol toxicity.

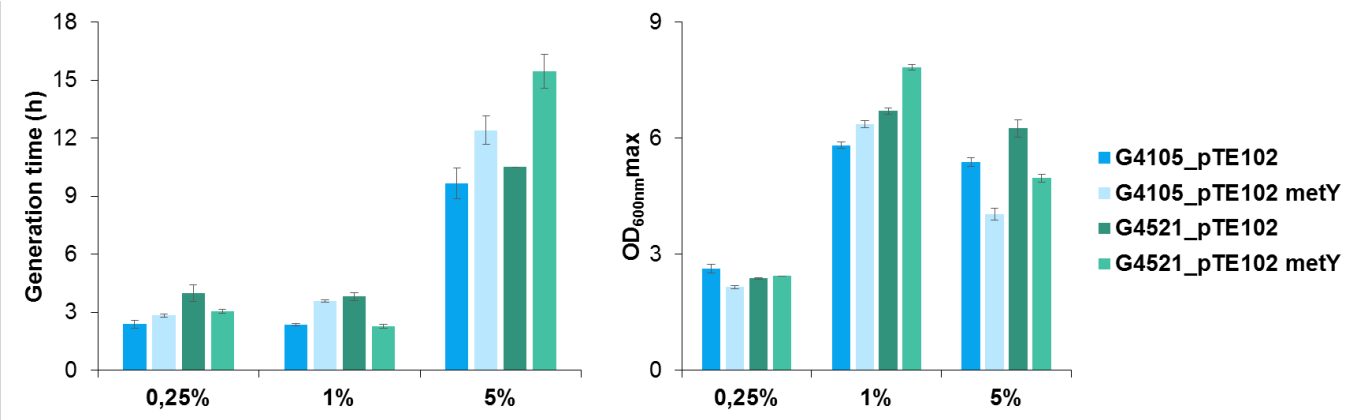


**Figure 36: Growth of *M. extorquens* methanol adapted strain G4105 and G4521 transformed with the empty vector pTE102 (dark green and blue bars) or the plasmid pTE102_*metY* (light green and blue bars). Generation time (A) and maximal $OD_{600nm}$ as an estimate of biomass yield (B) were determined after cultivation on minimal medium supplemented with 0.25, 1 % or 5 % methanol (v/v). Each result is the mean of triplicates; ±standard deviation is indicated.**

### II.2.6. Genome-wide mRNA expression responses during methanol stress

Besides chromosomal mutations, evolution of microorganisms to resist solvent stressors commonly provokes alterations of gene expression suggesting adaptive mechanisms at the level of transcription (Reyes et al., 2013). We performed a transcriptome analysis to study in a systematic way the gene expression response of the *M. extorquens* TK 0001 evolved strain G4105 to exposure to high methanol and compared with the response of the ancestor wild type strain (Table S6). We measured the variations of gene expression provoked by a short-term exposure (5 minutes) of mid-log phase cultures grown at 1% methanol to a stressing concentration of methanol (5%) and the modulation of gene expression in cells exposed to 1% or 5% methanol on the long run (after 3 hours of cultivation). RNA-Seq data were acquired, mapped, and normalized as described in the method section. RNA expression levels were compared between cells cultivated at 1% methanol and cells exposed to 5% methanol for 5 minutes or 3 hours. A threshold of $\log_2$ (FC) greater than 2 or less than -2 was chosen as minimal expression difference for the comparisons. The genes of *M. extorquens* TK 0001 were

automatically clustered into functional categories according to the orthologous framework eggNOG (Huerta-Cepas et al., 2018) operational at the MicroScope platform (Vallenet et al., 2017) (Table S7). The proportion of genes differentially expressed in each functional family was calculated (Figure 37).

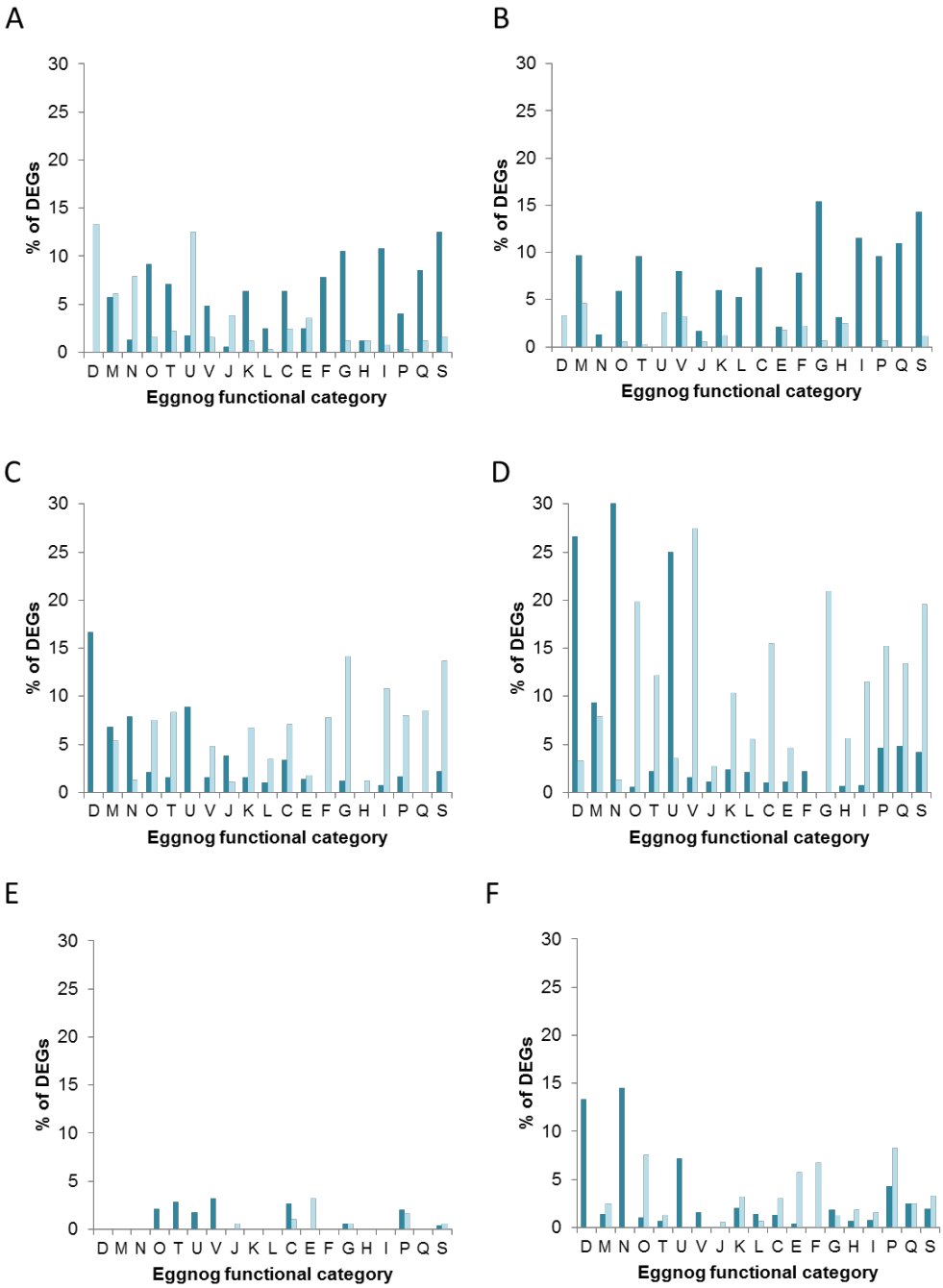


**Figure 37: Functional categorization of differentially expressed genes (DEGs) in *M. extorquens* TK 0001 wildtype strain (A, C, E) and G4105 evolved strain (B, D, F) upon exposure to methanol. Genes with $log_2$(fold change) ≥ 2 or $log_2$(fold change) ≤ 2 in response to 5 minutes methanol exposition (A, B) or after 3 hours cultivation on 5 % methanol (C, D) or on 1 % methanol (E, F) were categorized based on eggNOG functional classification. Bars represent the percentages of**

**overexpressed DEGs (deep blue) or repressed DEGs (light blue) in a given category. (A) Differential expression in strain TK 0001 exposed to 5 % or 1 % methanol for 5 min. (B) Differential expression in strain G4105 exposed to 5 % or 1 % methanol for 5 min. (C) Differential expression in strain TK 0001 exposed to 5 % methanol for 3 hours or 5 min. (D) Differential expression in strain G4105 exposed to 5 % methanol for 3 hours or 5 min. (E) Differential expression in strain TK 0001 exposed to 1 % methanol for 3 hours or 5 min. (F) Differential expression in strain G4105 exposed to 1 % methanol for 3 hours or 5 min.**

**Table 30: List of transcripts specifically regulated during growth for 5 minutes and 3 hours at 5% methanol, and for 3 hours at 1% methanol. $\log_2$ (FC) >2 are marked in red and <2 are in green.**

| LOCUS | FC | PRODUCT | TK0001 | | | G4105 | | |
|---|---|---|---|---|---|---|---|---|
| | | | 5' 5% | 3h 5% | 3h 1% | 5' 5% | 3h 5% | 3h 1% |
| TK0001_5382 | F | oxidoreductase, molybdopterin-binding SU | 5,29 | -4,44 | - | 3,39 | -6,18 | -3,45 |
| TK0001_5383 | F | molybdopterin oxidoreductase, FAD-binding SU | 6,04 | -5,15 | - | 5,89 | -7,85 | -2,46 |
| TK0001_5384 | F | oxidoreductase, molybdopterin-binding SU | 6,70 | -5,65 | - | 6,86 | -8,36 | -2,28 |
| TK0001_1878 | F | oxidoreductase, molybdopterin-binding SU | 3,80 | -3,94 | - | 4,20 | -6,39 | -2,74 |
| TK0001_3799 | F | oxidoreductase, molybdopterin binding | 2,86 | -2,12 | - | 3,15 | -2,90 | - |
| TK0001_2908 | G | Aldose-1-epimerase (Galactose mutarotase) | 2,64 | -2,75 | - | 3,87 | -3,24 | - |
| TK0001_4846 | G | putative glycoside hydrolase | 2,30 | -2,93 | - | 4,03 | -4,37 | - |
| TK0001_2604 | G | glycogen debranching enzyme | 5,68 | -4,62 | - | 4,91 | -6,34 | - |
| TK0001_1108 | G | putative glucoamylase or glycosyl hydrolase protein | 3,61 | -3,99 | - | 5,53 | -6,14 | - |
| TK0001_5727 | G | Gluconolactonase | 4,18 | -4,00 | - | 6,13 | -5,85 | - |
| TK0001_3368 | G | glucose-6-phosphate 1-dehydrogenase | 5,16 | -4,64 | - | 6,43 | -6,38 | - |
| TK0001_1646 | K | putative GreA/GreB family transcription | 3,80 | -3,23 | - | 4,15 | -4,17 | - |
| TK0001_4981 | K | RNA polymerase sigma factor | 3,77 | -3,76 | - | 4,32 | -4,11 | - |
| TK0001_1639 | K | RNA polymerase sigma-32 (sigma H) factor | 4,75 | -3,30 | - | 4,73 | -5,46 | - |
| TK0001_5451 | K | putative transcriptional regulator, XRE family | 5,00 | -4,29 | - | 4,99 | -4,92 | - |
| TK0001_3904 | K | putative Regulatory protein, Crp family | 5,16 | -3,48 | - | 5,21 | -4,29 | - |
| TK0001_4805 | L | DEAD/DEAH box helicase domain protein | 4,01 | -3,15 | - | 4,48 | -3,98 | - |
| TK0001_3360 | L | deoxyribodipyrimidine photolyase (DNA photolyase) | 4,45 | -3,72 | - | 5,33 | -4,86 | - |
| TK0001_4469 | L | putative UV damage endonuclease | 4,16 | -4,49 | - | 5,79 | -5,82 | - |
| TK0001_3960 | L | putative DNA topoisomerase I | 5,07 | -4,56 | - | 5,93 | -5,76 | - |
| TK0001_5627 | C | Cytochrome bd ubiquinol oxidase, subunit II | - | - | - | 3,46 | -2,36 | 1,27 |
| TK0001_0364 | C | putative cytochrome c, putative exported protein | 1,79 | -2,00 | - | 3,56 | -3,89 | - |
| TK0001_3348 | C | Ubiquinol-cytochrome c reductase complex, cytochrome b SU | -2,60 | -1,49 | - | 2,23 | - | - |
| TK0001_3349 | C | Ubiquinol-cytochrome c reductase complex, iron-sulfur | -2,35 | 2,10 | - | -1,31 | - | - |
| TK0001_2466 | C | oxidoreductase cytochrome c oxidase subunit II | - | -1,08 | - | 2,03 | - | - |
| TK0001_4539 | C | ATP synthase F1, alpha subunit | -2,04 | -1,04 | - | 2,15 | - | - |
| TK0001_4538 | C | ATP synthase F1, delta subunit | -1,93 | -1,13 | | 1,79 | 1,17 | |
| TK0001_4540 | C | ATP synthase F1, gamma subunit | -1,79 | - | | 1,90 | - | |
| TK0001_2319 | D | putative ATPase, putative partition protein (ParA) | -3,45 | 3,21 | - | -2,43 | 4,78 | 2,19 |
| TK0001_4852 | D | septum site-determining protein MinC | -2,38 | 2,80 | - | -1,08 | 3,20 | 1,67 |
| TK0001_4851 | D | septum site-determining protein MinD | -2,63 | 2,99 | - | - | 2,97 | 2,45 |
| TK0001_4850 | D | cell division topological specificity factor | -2,23 | 2,53 | - | - | 2,53 | 2,57 |
| TK0001_2829 | D | cell division protein | -1,65 | - | - | -1,85 | 2,16 | 1,38 |
| TK0001_2821 | D | cell division protein FtsA | -1,62 | 2,12 | - | - | 2,48 | 1,98 |
| TK0001_1437 | D | cell division protein | - | - | - | - | 2,04 | 2,01 |
| TK0001_3751 | J | 30S ribosomal protein S12 | -3,28 | 3,31 | - | -1,89 | - | -1,27 |
| TK0001_3750 | J | 30S ribosomal protein S7 | -3,10 | 3,14 | - | -1,62 | - | -1,26 |
| TK0001_2239 | J | 50S ribosomal protein L32 | -2,06 | 2,13 | - | -1,52 | - | - |
| TK0001_3749 | J | elongation factor G | -2,50 | 2,68 | - | -1,32 | - | -1,30 |
| TK0001_3716 | J | 50S ribosomal protein L24 | -2,01 | 1,95 | - | -1,05 | - | - |
| TK0001_0160 | J | 30S ribosomal protein S1 | - | 2,11 | - | -1,02 | 2,10 | - |
| TK0001_3715 | J | 50S ribosomal protein L14 | -2,01 | 1,95 | - | - | - | - |
| TK0001_3748 | J | fragment of protein chain elongation factor EF-Tu | -1,73 | 2,06 | - | - | - | - |
| TK0001_2706 | N | flagellar motor switch protein FliM | -2,31 | 2,32 | - | -1,66 | 3,74 | 1,81 |
| TK0001_3277 | N | flagellar basal-body rod protein FlgB | -2,25 | 2,22 | - | -1,49 | 2,95 | 1,29 |
| TK0001_2707 | N | flagellar fliL protein | -2,02 | 2,30 | - | -1,43 | 3,37 | 1,68 |
| TK0001_3278 | N | flagellar basal-body rod protein flgC | -2,34 | 2,46 | - | -1,22 | 2,75 | 1,32 |
| TK0001_3415 | N | pilus assembly protein cpaD | -1,88 | - | - | - | 3,17 | 3,07 |
| TK0001_5400 | N | flagellar biosynthesis protein | -1,85 | - | - | - | 2,34 | 1,80 |
| TK0001_2713 | N | fragment of Flagellar L-ring protein precursor (L-ring protein) | -1,70 | - | - | - | 2,84 | 2,93 |
| TK0001_1369 | N | flagellar motor switch protein | -1,66 | 1,32 | - | - | 2,58 | 2,20 |
| TK0001_2711 | N | flagellar protein FlgA | - | - | - | - | 2,41 | 2,90 |
| TK0001_3280 | N | flagellar biosynthesis | - | - | - | - | 2,26 | 1,99 |
| TK0001_4375 | O | ibpA, small heat shock protein | 3,57 | -2,95 | - | - | -3,43 | -3,20 |
| TK0001_3525 | O | clpB, protein disaggregation chaperone | 4,42 | -3,74 | - | - | -5,83 | -5,48 |
| TK0001_0752 | O | heat shock chaperone | 5,12 | -4,33 | - | - | -5,89 | -5,99 |
| TK0001_2810 | O | chaperone protein DnaK | - | - | - | - | -3,56 | -3,28 |
| TK0001_2381 | O | chaperonin Hsp60, large ATPase subunit of GroESL (part 1) | - | 2,36 | - | - | - | - |
| TK0001_2383 | O | chaperonin Hsp60, large ATPase subunit of GroESL (part 2) | - | 2,13 | - | - | - | - |
| TK0001_2610 | O | glutathione S-transferase | 2,86 | 1,37 | - | - | -2,99 | -2,49 |
| TK0001_1338 | P | putative TonB-dependent siderophore receptor | - | - | 1,33 | - | 3,86 | 3,86 |
| TK0001_2160 | P | TonB-dependent receptor | - | - | - | - | 3,18 | 3,17 |
| TK0001_3801 | P | TonB-dependent siderophore receptor (fragment) | - | - | - | - | 3,82 | 3,45 |
| TK0001_3802 | P | TonB-dependent siderophore receptor (fragment) | - | - | - | - | 2,84 | 2,37 |
| TK0001_3927 | P | putative TonB-dependent siderophore receptor | - | 2,94 | 2,70 | - | 6,69 | 6,48 |
| TK0001_3953 | P | Iron permease FTR1 | - | - | - | - | 2,32 | 2,17 |
| TK0001_5663 | P | putative TonB-dependent siderophore receptor | - | - | 1,41 | - | 4,88 | 5,23 |
| TK0001_1773 | Q | siderophore biosynthesis protein, IucA/IucC family | - | - | - | - | 3,25 | 4,07 |
| TK0001_5780 | P | ABC transporter, permease precursor, putative iron transporter | - | - | - | - | 4,08 | 3,62 |
| TK0001_4955 | P | ABC transporter, permease precursor, putative iron transporter | - | 4,49 | -1,68 | - | -4,52 | - |

The exposure of the adapted strain G4105 to 5% methanol for 5 minutes yielded comparable numbers of differentially expressed genes (663 genes overexpressed, 73 genes repressed). The

overall expression profile of the mutated strain was similar but not identical to that of the wildtype strain (Figure 39B) with categories G (15.4%) and I (lipid transport and metabolism, 11.5%) displaying the highest percentage of overexpressed genes. In addition, transcription was induced for genes belonging to the functional groups M (cell wall, membrane and envelope biogenesis, 9.7%), T (signal transduction mechanisms, 9.6%) and P (inorganic ion transport and metabolism, 9.6%). The percentage of downregulated genes was reduced within all of the functional categories with respect to the TK 0001 wildtype cells.

To study the effects of long-term exposure to high methanol on gene expression, transcriptome analysis was conducted on *M. extorquens* TK 0001 wild type and G4105 mutant cells grown for 3h in 5% methanol. The eggNOG profile of differentially expressed genes in TK 0001 wildtype cells (Figure 39C) shows that the overall expression pattern had reversed with respect to the short-term stress: functional groups dominated by either up- or downregulated genes changed the sign, with a total of 132 overexpressed and 596 repressed genes. Obviously, expression level changes induced by the methanol stress were mainly short-term responses not maintained during longer exposure to high methanol. In the case of evolved strain G4105, the RNA-Seq data collected after long-term methanol stress also revealed repression of genes, which were overexpressed as response to the 5 minutes methanol pulse. However, the overall picture differed from what was seen for the wildtype strain (Figure 39D). The number of differentially expressed genes was higher than after the short-term exposure (238 overexpressed, 894 repressed genes). Also, the percentage of overexpressed genes in categories N, D and U reached high values (32.9%; 26.7% and 25.0%, respectively) as was the case for the repressed genes in categories V (defense mechanisms), G, O (posttranslational modification, protein turnover, chaperons), and C (energy production and conversion) (27.4%; 21.0%; 19.9% and 15.5%, respectively).

Table 4 highlights some examples of short- and long-term methanol stress responses of the two strains at the expression level of particular genes. Transcripts coding for certain molybdenum-binding oxidoreductases, carbohydrate mobilization enzymes, regulators of transcription and proteins maintaining DNA topology and integrity are highly upregulated after 5 minutes but repressed to pre-stress levels after 3h of growth on high methanol. Since both strains showed comparable responses for these genes, the regulation of their expression was most likely not

altered during the continuous culture adaptation process. By contrast, expression differences between the two strains appeared for other functional gene families (Table 30), including:

**Genes coding for cytochrome-linked oxidoreductases and for ATP synthase (functional category C).** The transcription level of the enzymes is unchanged or lowered after the 5 minutes methanol stress for the TK 0001 wildtype cells, without a real recovery after 3 hours indicating a lowered energy production by the respiratory chain. By contrast, a strong upregulation is noted in the case of the adapted G4105 cells suggesting an enhanced metabolic activity triggered by the high methanol concentration in these cells.

**Genes coding for cell division proteins (functional category D).** Cell division activities seem to be lowered as a short-term stress response of the non-adapted cells. The cell division proteins of the adapted cells are less affected after 5 minutes, and strongly induced after 3 hours, reflecting their adaptation to growth at 5% methanol.

**Genes coding for ribosomal proteins (functional category J).** A number of proteins implicated in ribosomal translation are transcriptionally downregulated upon the short-term methanol stress in the wildtype and the adapted cells. However, the response is more pronounced in the wildtype strain, where the transcription levels were downregulated after 5 minutes of high methanol exposure but upregulated after 3 hours to reach pre-stress levels. The adapted cells reacted less violently after 5 minutes, but the expression level remained lowered after 3 hours of growth on 5% methanol. It is noteworthy that in isolates of both *M. extorquens* TK 0001 and AM1 adapted to very high methanol concentrations (8-10 %), some ribosomal genes were found to be mutated (Tables 1 & 2). The occurrence of translation errors upon treatment of ribosomes with solvent stressors have been described (Haft et al., 2014; So and Davie, 1964). Possibly, this downregulation limits the accumulation of wrongly translated proteins prone to impede cell proliferation (Mars et al., 2015).

**Genes coding for flagellar proteins (functional category N).** Transcripts coding for the biosynthesis, assembly and functioning of flagella assuring cell motility were downregulated after the 5 minutes stressing pulse. The repression of motility genes has been found to occur upon stress induction by a variety of chemicals including solvents (Rau et al., 2016). However, the genes were again upregulated after the long-term stress exposure. Both strains were affected

in this sense, but the respective genes of the adapted cells were less repressed after 5 minutes and higher expressed after 3 hours, suggesting a better maintenance of flagella functionality as a result of solvent stress adaptation.

**Heat shock proteins and chaperons (functional category O).** High overexpression of the ATP independent small heat shock proteins (sHsp) of the *ibpA* family was observed for the wild type cells as short-term stress response. Members of the sHsp were shown to be active on aggregation-prone proteins by keeping them in a native like conformation thus favoring their refolding by other ATP dependent cellular chaperones (Haslbeck et al., 2018; Mogk et al., 2002). *E. coli* cells overexpressed *ibpA* after exposure to the solvent stressor isopentenol (Foo et al., 2014). Interestingly, sHsp were found to be particularly active towards proteins involved in translation and transcription (Fu, 2014). On further incubation with 5% methanol, the wild type cells upregulated the Hsp60 chaperone group. Overexpression of the Hsp60 chaperonin GroESL also enhances cellular tolerance towards alcohols (Abdelaal et al., 2015; Zingaro and Terry Papoutsakis, 2013). The ATP-dependent GroESL complex differs in its activity mode and substrate range from the sHsps (Fu, 2014). No significant overexpression of chaperons was observed for the adapted cells.

**Iron uptake (functional category P).** Iron is a prosthetic component of proteins involved in numerous cellular processes (Andrews et al., 2003). In most microbes, complex machinery assures supply of iron from the environment. Cells secrete special chelating peptides, the siderophores, to capture the insoluble ferric-iron. Fe-charged siderophores are subsequently internalized via specific transport mechanisms. Genes implicated in iron homeostasis were not found to be differentially expressed upon short-term exposition of the two strains to high methanol. However, the adapted cells strongly upregulated a number of transcripts coding for Fe-siderophores and transporters during prolonged growth with high methanol.

Differences in gene expression patterns between non-adapted and adapted cells were also apparent upon growth with methanol at 1%, a concentration permissive for the wildtype cells. Significant transcript level variations were more frequent in the adapted cells (Figure 18E) (91 overexpressed and 150 repressed transcripts) than in the wildtype cells (Figure 18F) (46 overexpressed and 29 repressed transcripts). As was the case for the evolved cells grown in high methanol, genes associated with cell division, motility and intracellular trafficking

(categories D, N, and U) were upregulated. Conversely, genes involved in carbohydrate transport and metabolism (category G) were less down regulated after growth with 1% methanol for 3 hours.

In table 30 are listed the expression changes of representative genes occurring after three hours of incubation at 1% methanol compared with the changes determined after short- and long term 5% methanol stress. In the case of the adapted strain, genes associated with cell division, flagella biosynthesis and iron uptakes show a very similar response after 3 hours of growth under permissive and stressing growth conditions. By contrast, the expression level of these genes was found almost unaltered in the case of the wildtype cells grown under permissive conditions. Obviously, the cells evolved towards methanol tolerance exhibit an altered overall physiology, which is apparent also when proliferating under no-stress conditions.

## III.3. Directed evolution of *Methylobacterium extorquens* AM1 to growth under oxygen shortage

Evolving aerobic bacteria to efficient growth under conditions of low oxygen is of interest for biological applications. Strains with lowered oxygen transfer rates still exhibiting wild type biomass production yield and growth rate would be more robust towards fluctuations of oxygen and need less aeration during industrial production processes. In addition to issues related to technological applications, the adapted strains would be of interest for basic research. Bacterial respiratory chains are complex and highly regulated enabling the cells to adapt to changing oxygen supply in the environment. The adaptive responses could affect the respiratory chain as a whole through altered expression profiles of its components. Mutations in crucial parts of the system enhancing their performance under lowered availability of the terminal electron acceptor could also occur. The GM3 standard device was expanded for use with different gas mixtures. Nitrogen can replace compressed air to any chosen extent enabling growth under low oxygen pressure. Since the aeration of the device is stably maintained, the oxygen content can also be kept constant over time. *M. extorquens* AM1 was grown in mineral medium supplemented with 1% methanol in a turbidostat. The gas mixture aerating the GM3 device was changed from 100% compressed air to a final mixture of 20% compressed air/80% nitrogen. Figure 38 shows the intermediate air/nitrogen mixes employed. After a period of growth with 100% compressed air of around 20 days, a 50%/50% mix was adjusted and a generation time of about 7 hours recorded. The generation time lowered slightly over a 40%/60% and a

30%/70% mix period until a sudden drop of the generation time passing from 6h40 to 5h occurred and stayed constant for about 30 days. A switch to the final 20%/80% reestablished the generation time to around 6h.

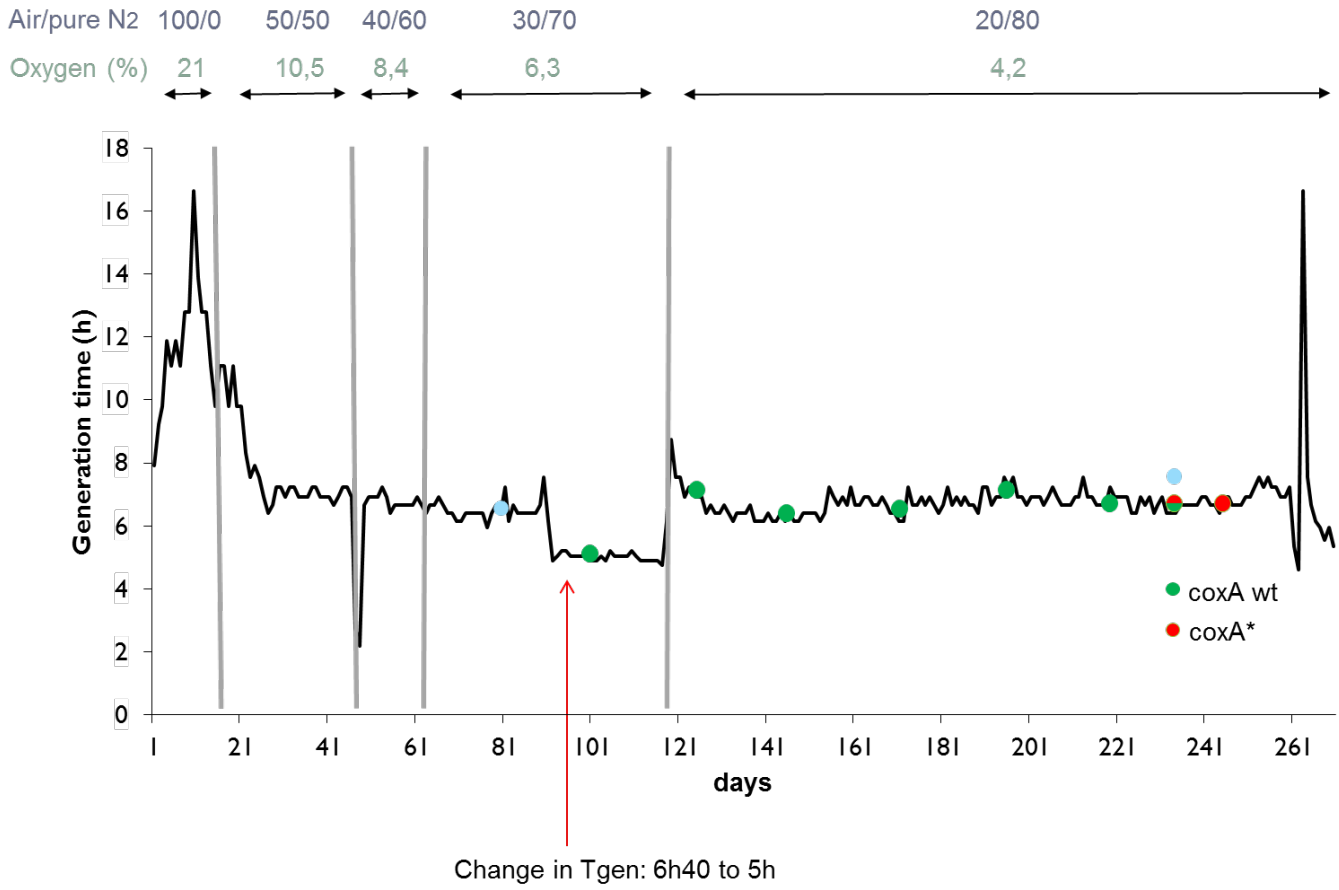


**Figure 38: Adaptation profile of *M. extorquens* AM1 to growth with reduced oxygen supply in the GM3. The compressed air/nitrogen mixes employed during the consecutive turbidostat culture phases and the corresponding oxygen content in the gas mixtures are indicated. Green and red bullets correspond to the results of coxA sequenced. Blue bullet corresponds to the isolates sequenced AMM1 to 3 for the first bullet and AMM4 to 6 for the second bullet.**

To detect mutations in the population possibly connected with the adaptation to tolerance for lowered oxygen supply, 3 isolates from the evolution at 6.3% oxygen (days 63) before the drop and 3 isolates from the evolution at 4.2% oxygen (days 150) were sequenced (Table 31).

**Table 31: List of mutations in the evolved strains to oxygen deficiency. AMM1 to AMM3 corresponding to isolates from the population before the pulse (red arrow Figure 40) and from AMM4 to AMM6 correspond to isolates after the pulses. Medium orange: mutation identified at several time points. Dark orange: mutation common to all time points. •: mutation present in the isolate.**

| chromosomal position | mutation type | mutation event | mutated gene | amino acid change | intergenic mutation (distance to the flanking gene) | AMM ox 1 | AMM ox 2 | AMM ox 3 | AMM ox 4 | AMM ox 5 | AMM ox 6 |
|---|---|---|---|---|---|---|---|---|---|---|---|
| 259121 | SNP | G/A | putative acyltransferase | E69E | | • | | | | | |
| 355589 | DEL | T/- | putative exported protein | | | | | • | | | |
| 355590 | DEL | C/- | putative exported protein | | | | | • | | | |
| 355592 | DEL | G/- | putative exported protein | | | | | • | | | |
| 355598 | DEL | C/- | putative exported protein | | | | | • | | | |
| 794119 | SNP | A/T | aloacid dehalogenase-like hydrolase | W37R | | | • | | | | |
| 889043 | SNP | C/T | putative SCP-like extracellular protein | A18V | | | | • | | | |
| 1221768 | SNP | T/G | Putative CelB-like protein | L464R | | • | • | • | • | • | • |
| 2243223 | SNP | G/A | rpsC | C64Y | | | | | | | • |
| 2249001 | SNP | C/T | rpoA | G289D | | | • | | | | |
| 2643058 | SNP | G/A | metY | L389F | | • | • | • | • | • | |
| 2643418 | DEL | G/- | metY | | | | | | | | • |
| 2643420 | DEL | C/- | metY | | | | | | | | • |
| 2643421 | DEL | T/- | metY | | | | | | | | • |
| 2643422 | DEL | C/- | metY | | | | | | | | • |
| 2777457 | SNP | T/G | protein of unknown function | P136P | | • | | • | • | | |
| 2794487 | INS | -/C | protein of unknown function | | | | | | • | • | |
| 2803789 | SNP | C/T | protein of unknown function | N21N | | • | | • | | | |
| 3532812 | INS | -/A | putative porin precursor | | | | | | • | • | |
| 3533009 | INS | -/G | putative porin precursor | | | | | | | | • |
| 3545189 | SNP | T/C | relA | T423A | | • | • | • | • | • | • |
| 3577429 | DEL | C/- | extracellular solute-binding protein family 3 | | | | | | • | • | |
| 3613829 | SNP | C/T | coxA | M270I | | | | | • | • | |
| 3719123 | SNP | T/C | putative membrane protein, diguanylate cyclase (GGDEF) domain | N126D | | | | | | | • |
| 4163559 | SNP | T/A | | | Site-specfic recombinase, phage integrase family/conserved protein of unknown function (204/301) | • | • | • | | | • |
| 4690858 | SNP | A/C | | | transposase of ISMex6, ISNCY family/putative lipolytic enzyme, putative esterase (85/207) | | | | | • | |
| 4690859 | SNP | T/G | | | transposase of ISMex6, ISNCY family/putative lipolytic enzyme, putative esterase (86/206) | | | | | • | |
| 4690860 | SNP | A/G | | | transposase of ISMex6, ISNCY family/putative lipolytic enzyme, putative esterase (87/205) | | | | • | • | |
| 4690862 | SNP | A/G | | | transposase of ISMex6, ISNCY family/putative lipolytic enzyme, putative esterase (89/203) | | | | • | • | |

We observed 2 missense mutations found in all evolved cells: mutation L464R in a putative CelB-like protein and mutation T423A in protein RelA. RelA produces guanosine 3',5'-bispyrophosphate (ppGpp) during the stringent response to amino acid starvation (Traxler et al., 2008). No link to the respiratory chain is apparent for these two proteins.

It must also be noted that the gene *metY* coding for O-acetyl-L-homoserine sulfhydrylase was mutated in all six isolates sequenced. The missense mutation L389F was found in five isolates, isolate 6 harbored a 4 base pair deletion.

In two of the three late isolates sequenced, an interesting missense mutation (M270I) in the gene *coxA* coding for the cytochrome c oxidase subunit I of the respiratory chain (EC:1.9.3.1) was found. This subunit is part of the complex IV catalyzing the reduction of oxygen to water. A direct link between this mutation and the adaptive low oxygen phenotype can be presumed. To investigate the apparition of this mutation, which was not present in the isolates taken from the culture before the adaptive switch, the *coxA* gene of isolates from different time points of the evolution was sequenced (Figure 40). Unexpectedly, the *coxA* mutation appeared late in the evolution and was not responsible for the drop-in generation time at 6.3% of oxygen (Table 31).

## III.4. Dosage of D-lactate production from D-lactate dehydrogenase overexpressing cells

The *M. extorquens* TK 0001 cells adapted to high methanol produced more biomass from methanol than the wildtype cells (Figure 23). This finding suggested that a compound synthesized by the adapted cells through a pathway branching from the central metabolism could be obtained in higher yield than synthesized by the wildtype cells. To verify this hypothesis, the one-step production of D-lactate from pyruvate, catalyzed by D-lactate dehydrogenase using $NADH_2$ as electron donor, was chosen as test system. Pyruvate is a metabolite of the central carbon metabolism. The pool sizes of pyruvate and $NADH_2$, both ultimately produced from methanol, are susceptible to be indicators of enhanced carbon flow in the cells.

Strain TK 0001 chromosome contains the D-lactate dehydrogenase gene *ldhA*. The expression profile of this gene during growth is not known. To obtain a strong and constitutive expression, the gene was cloned into plasmid pTE102 behind the strong promoter PmxaF and the plasmid construct introduced into the strains TK 0001 and G4105.

To assess the impact of *ldhA* overexpression on cell growth, the generation time and growth yield for strains TK 0001 and G4105 (from MEM5) and their plasmid were respectively determined. Figure 39 shows that the presence of the *ldhA* gene is a burden for the evolved cells, increasing the generation time and lowering the yield significantly at both 1% and 5% methanol, as compared with plasmid free cells for the evolved strain.. Also, and even more striking, the TK 0001 wildtype cells carrying the plasmid pTE102 *ldhA* grew on 5% methanol, with a generation time of around 8 hours. No obvious explanation can be found for these phenotypic effects of the overexpression of gene *ldhA*.

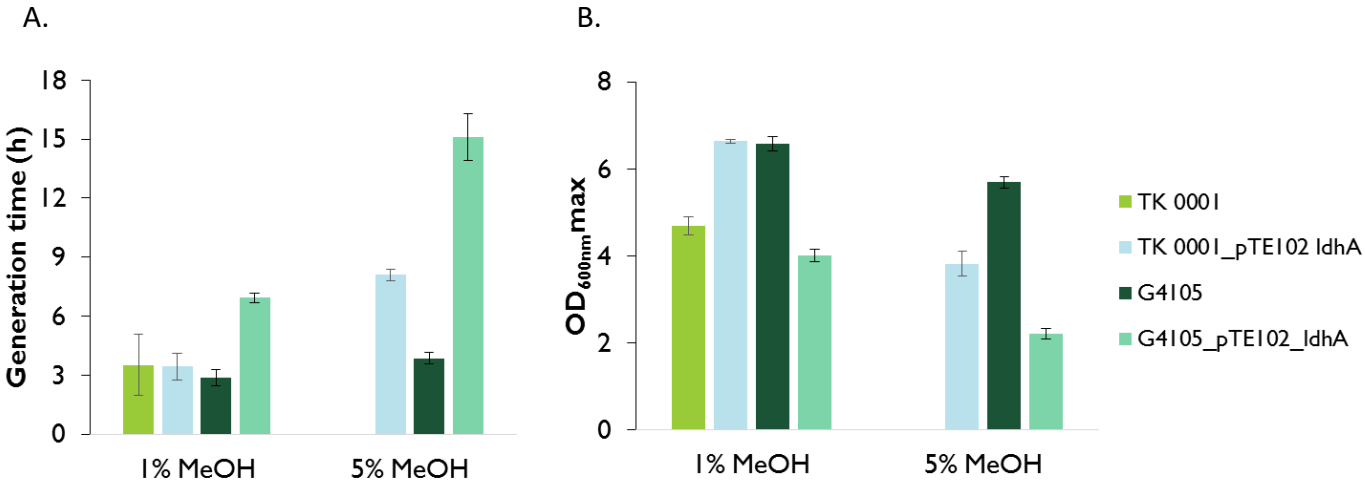


**Figure 39: Growth phenotype of *M. extorquens* TK 0001 wildtype strain and methanol evolved isolates from MEM5 (G4105) with and without pTE102 ldhA. Generation time during exponential growth phase (A) and maximal $OD_{600nm}$ as an estimate of biomass yield (B) were determined after cultivation on minimal medium supplemented with 1% and 5% methanol (v/v). Each result is the mean of triplicates; ±standard deviation is indicated.**

Quantification of lactate was conducted by LC-HRMS analysis, according to its EIC area in metabolomes and a calibration curve. From independent 2.5 ml cultures normalized at an $OD_{600nm} = 1$, we could estimate the amount of lactate produced in the different strains. Results are presented in Figure 40. The lactate amount was not different between samples TK 0001 empty plasmid and *pTE102 ldhA* and G4105 empty plasmid (group a) G4605 but was significantly higher in sample G4105 pTE102 *ldhA* ($p < 0.001$ between sample G4105 pTE102

*ldhA* and empty plasmid; $p < 0.001$ between G4105 pTE102 *ldhA* and TK 0001 with the same plasmid; and $p = 0.01$ between sample G4105 pTE102 *ldhA* and TK 0001 pTE102 *ldhA*).

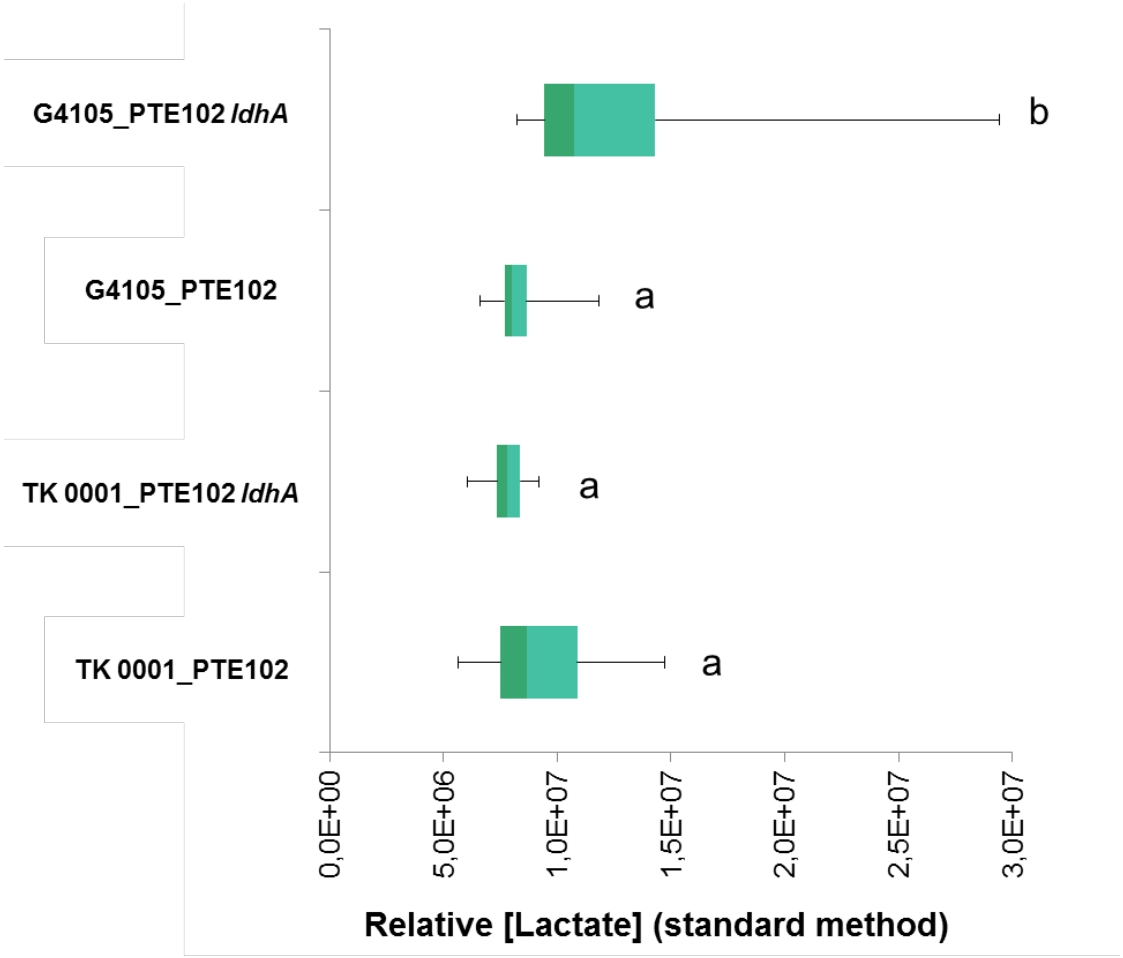


**Figure 40: Lactate amount (mean ± SEM) formed by G4605 (n = 23), G4836 (n = 23), G4891 (n = 23) and G4892 (n=23) and represented with quartile. Data were normalized for 2.5 ml cell cultures at an $OD_{600nm}$ = 1. A non-parametric Kruskal-Wallis test followed by a post-hoc Mann-Whitney test was used to determine difference between groups. TK 0001_pTE102, TK 0001_pTE102 *ldhA* and G4105_pTE102 are similar and G4105_pTE102 *ldhA* is statistically different ($p < 0.0083$).**

## III.5. Production of 3-hydroxypropionic acid

### III.5.1. Enzymatic pathway

Different production pathways of the platform chemical 3-hydroxypropionic acid (3-HP) from cellular metabolites have already been implemented in various industrial strains as *E. coli* or *S. cerevisiae* (de Fouchécour et al., 2018). To produce this compound by *M. extorquens* wildtype and adapted cells, a route starting from acetyl-CoA comprising three enzymatic steps was chosen (Yang et al., 2017). The first step, the carboxylation of acetyl-CoA to malonyl-CoA is catalyzed by the native acetyl-CoA carboxylase (Figure 41A). The reduction of malonyl-CoA to malonate semialdehyde and of malonate semialdehyde to 3-HP, which have not been described to occur in *Methylobacterium* strains, takes place in the thermophilic bacterium *Chloroflexus aurantiacus* (Holo, 1989). Malonyl-CoA reductase (MCR) from this organism possesses a bifunctional malonyl-CoA reductase (MCR; EC number 1.2.1.75) shown to convert malonyl-CoA to 3-HP with concomitant oxidation of two molecules of NADPH. Activity tests have revealed that MCR can be split into two parts, NMCR (amino acids 1 to 549) and CMCR (amino acids 550 to 1219) (Figure 41B). The CMCR polypeptide has activity as malonyl-CoA dehydrogenase, the NMCR polypeptide catalyzes the reduction of malonate semialdehyde to 3-HP (Figure 41A). Expressed separately, the two polypeptides are more active than the MCR holoenzyme (Liu et al., 2013).

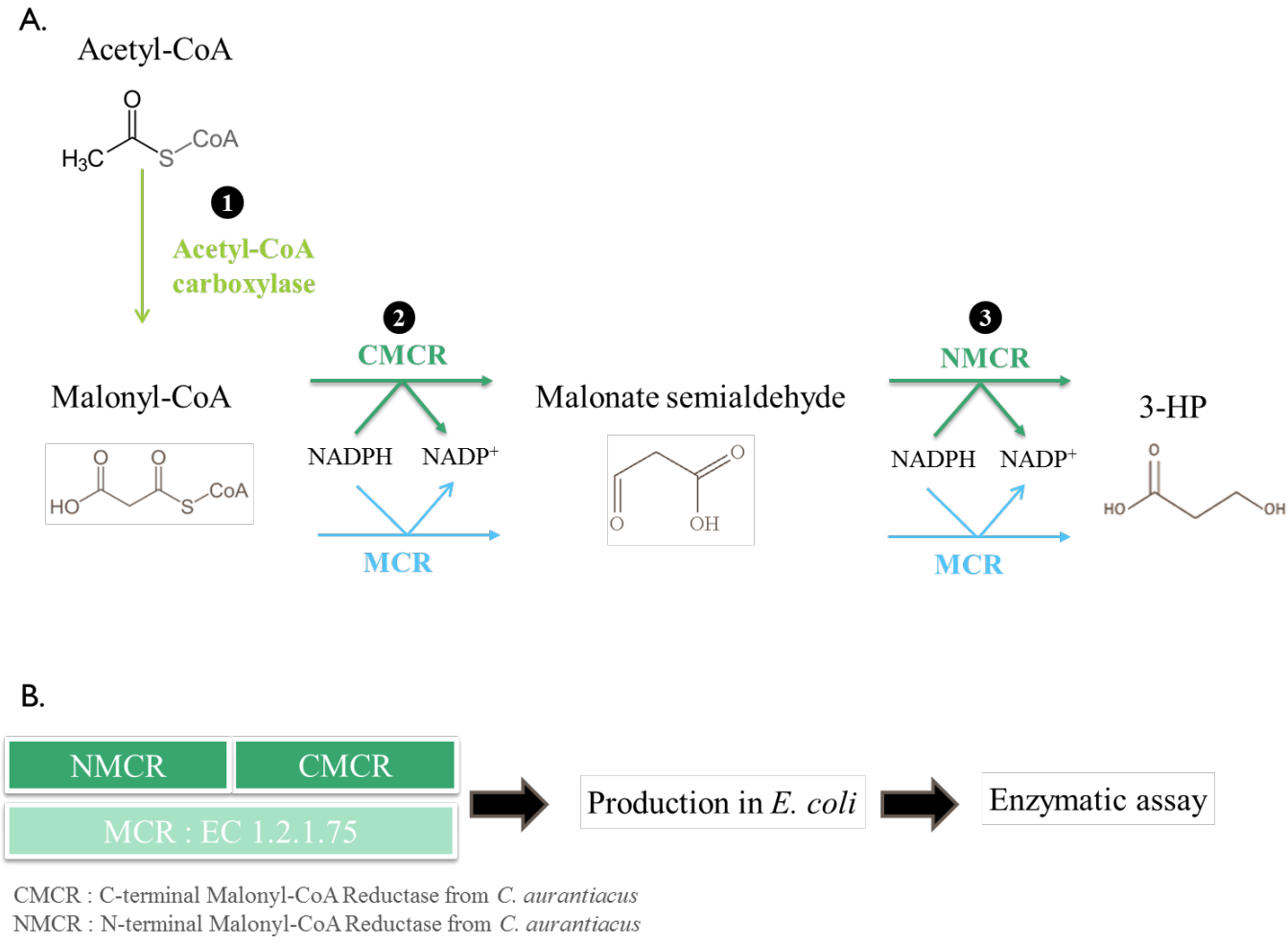


**Figure 41: Overview of the 3-HP (3-hydroxypropionic acid) production from acetyl-CoA using malonyl-CoA reductase from *C. aurantiacus* (MCR) or CMCR/NMC (A). *In vitro* test on MCR, NMCR and CMCR was realized using producing these 3 proteins independently produced in *E. coli* (B).**

### III.5.2. Cloning and *in vitro* tests of MCR inserts

The gene coding for MCR of *C. aurantiacus* was PCR amplified from genomic DNA and cloned into plasmid pET22 in order to introduce a His-tag at the N-terminus. In addition, NMCR and CMCR genes were also cloned separately in pET22. The activities of these 3 enzymes containing a His-tag were confirmed by detection of the 3-HP product in mass spectrometry (Figure 42).

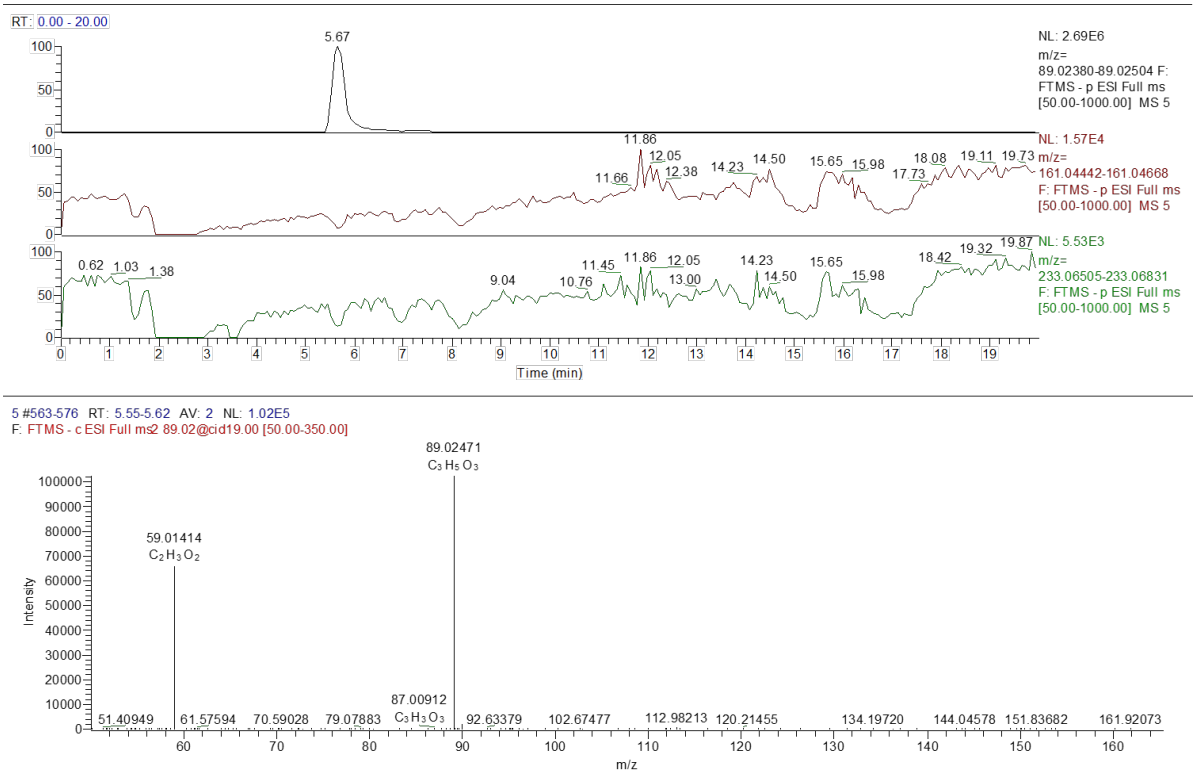


**Figure 42: 3-HP detection with NMCR and CMCR *in vitro* activity from *Chloroflexus aurantiacus*. The same result was observed for MCR activity.**

In the following, expression constructs optimizing the production of 3-HP were cloned into *M. extorquens* expression plasmid pTE102 (Figure 43).

Plasmid MCR: This plasmid contained the *mcr* gene sequence from *C. aurantiacus* under control of the PmxaF promoter (Figure 43A).

Plasmid MCRI: This plasmid contained the NMCR and CMCR sequences from *C. aurantiacus* in a version codon optimized for *M. extorquens*. Optimized codons were chosen from a codon usage table (Table S8) and atgme website (Figure S11). Also, an optimized independent ribosome binding site (RBS) was inserted 5' of each gene. The RBS were edited using an online RBS calculator tool (Salis, 2011); RBS 1 for NMCR and RBS 2 for CMCR (MCR1, Figure 43B).

To obtain enzymes with higher catalytic activity, two strategies were pursued: directed mutagenesis and screening of a protein library. Three mutations have been identified to increase the activity of CMCR: N940V, K1106W and S1114R (Liu et al., 2016). The CMCR wild type

was replaced by CMCR* containing the three mutated residues given the plasmid MCRI_mutated, (Figure 43C).

The second strategy used to increase the production was performed in collaboration with the LCAB laboratory at Genoscope and consisted in a gene library screening given the plasmid MCR2 (Figure 43D, see the explanation below).

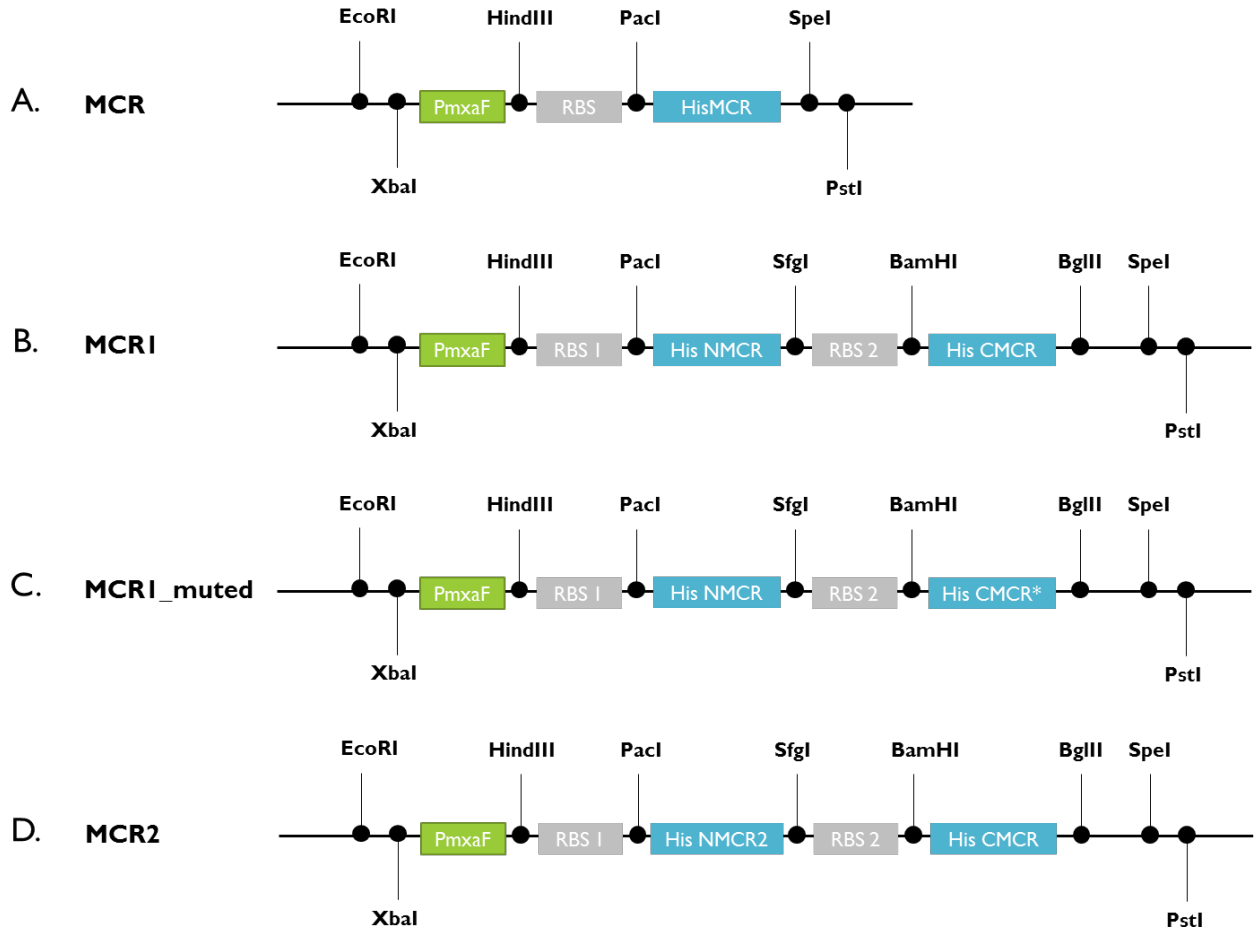


**Figure 43: Schema of the inserts constructed for 3-HP production. Promoters are labeled in green; RBS in grey, gene in blue and each spot correspond to restriction enzyme site. RBS 1 is the RBS optimized for NMCR, RBS 2 for CMCR and CMCR*designed the version of CMCR containing the mutated residues, N940V, K1106W and S1114R.**

### III.5.3. Screening of new reductases

The initial gene coding for MCR has been amplified from the genome of the thermophilic photosynthetic bacterium *C. aurantiacus*. The enzymes from thermophilic organisms are often found to be thermostable and to have their activity optimum at high temperatures. In

consequence, using enzymes from thermophiles for biosynthetic pathways in mesophilic producer hosts like *M. extorquens* can limit the production yields.

In order to identify new malonyl-CoA reductases from mesophilic organisms, a first *in silico* screen was performed based on sequence homologies between the *C. aurantiacus* MCR and protein sequences in public databases, focusing on genomes of sequenced bacteria and some metagenomes (Heuson et al., 2016). An identity threshold of at least 30% throughout 80% of the total peptide sequence of MCR from *C. aurantiacus* gave 27 candidate proteins (Figure 44A). The 27 protein sequences have been compared to each other and some clustering was apparent (Figure S12) reducing the number of proteins to be tested for malonyl-CoA reductase activity. The criterion of mesophilic growth temperature of the organisms hosting the proteins, reduced the number of candidates to 8 (Figure 44B). The 8 candidates have been again compared to each other and some clustering was apparent (Figure 44C). The selected proteins were split into a NMCR part and a CMCR part as was done for the *C. aurantiacus* MCR (Figure 44D). Only NMCR from the organism from *Novosphingobium fuchskuhlense* (DSM n°25065) and NMCR and CMCR from *Roseiflexus castenholzii* (DSM n°13941) and *Erythrobacter litoralis* (DSM n°8509) could be successfully cloned into expression vector pET22 and purified (Figure 45A, Figure S13).

The activity test consisted in monitoring the consumption of NADPH using malonyl-CoA as substrate. The malonate-semialdehyde, an unstable compound, is not commercially available. To test for NMCR activity, a CMCR enzyme must therefore be present. Several combinations were tested for activity (Figure 45B). Highest activity was seen with the combination of CMCR of *C. aurantiacus* and NMCR from *N. fuchskuhlense.* This combination was cloned into pTE102 yielding construct MCR2 (Figure 43D).

For a matter of time the different plasmids have not yet been tested *in vivo*.

**Figure 44: NMCR and CMCR screening steps. (A) 27 candidate proteins identified by blast sequence of NMCR and CMCR. (B) Selection of a mesophilic organism from each cluster group from the precedent comparison plus *C. aurantiacus*. (C) Clustering between the last 8 candidates (D) Split the 2 reductase activities as done for *C. aurantiacus* based on the same cutting region.**

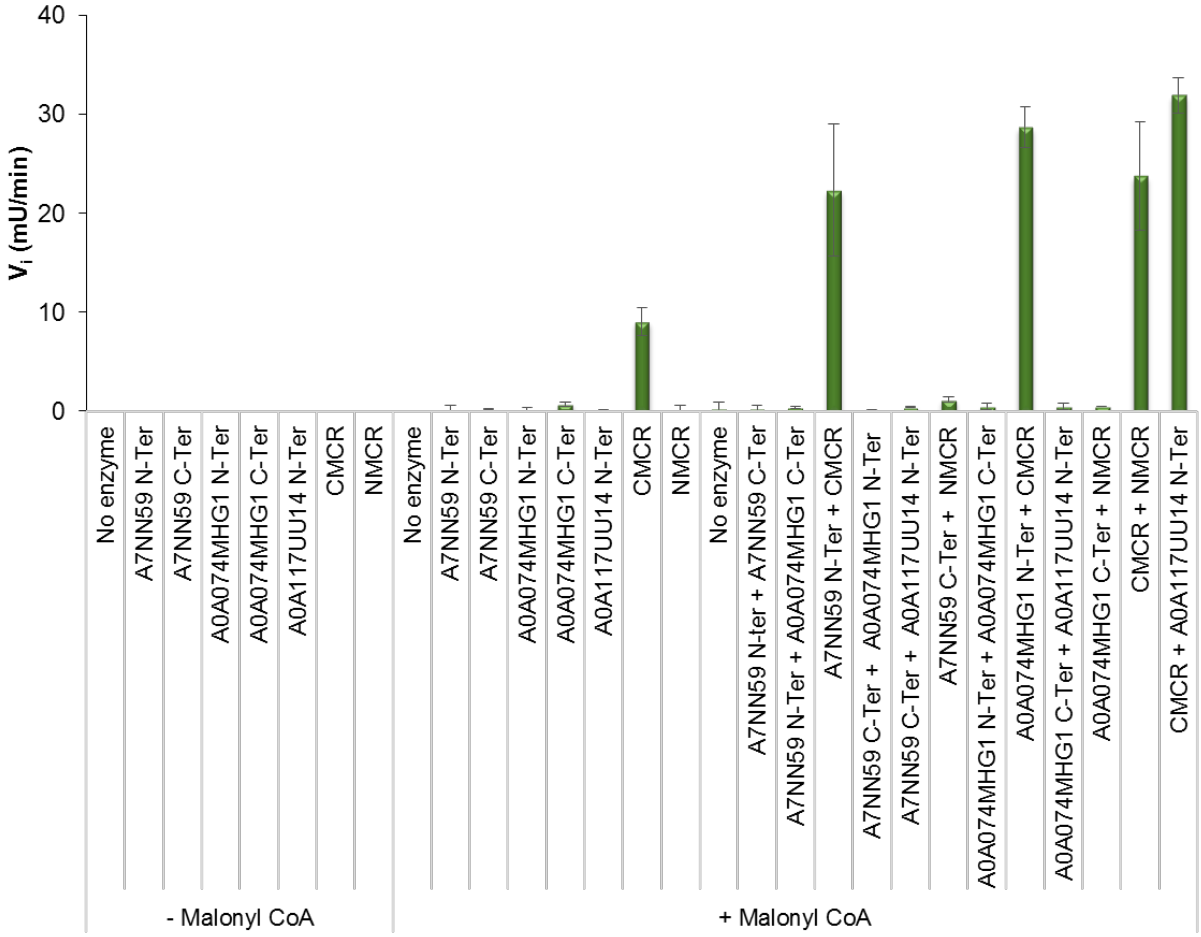


**Figure 45: Results of the screened proteins. Malonyl-CoA/malonate semialdehyde dehydrogenase activity of the enzymes determined by NADPH consumption at 340 nm.**

# IV. PUBLICATIONS

AMERICAN SOCIETY FOR MICROBIOLOGY | genomeAnnouncements™

PROKARYOTES

# Complete Genome Sequence of the Facultative Methylotroph *Methylobacterium extorquens* TK 0001 Isolated from Soil in Poland

**Sophia Belkhelfa,[a] Karine Labadie,[b] Corinne Cruaud,[b] Jean-Marc Aury,[b] David Roche,[a] Madeleine Bouzon,[a] Marcel Salanoubat,[a] Volker Döring[a]**

[a]Génomique Métabolique, Genoscope, Institut François Jacob, CEA, CNRS, Université d'Évry, Université Paris-Saclay, Evry, France

[b]Genoscope, Institut François Jacob, CEA, Evry, France

**ABSTRACT** *Methylobacterium extorquens* TK 0001 (DSM 1337, ATCC 43645) is an aerobic pink-pigmented facultative methylotrophic alphaproteobacterium isolated from soil in Poland. Here, we report the whole-genome sequence and annotation of this organism, which consists of a single 5.71-Mb chromosome.

The genus *Methylobacterium* contains rod-shaped Gram-negative bacteria and belongs to the family *Rhizobiales*. The members of this group of microorganisms are able to grow on reduced $C_1$ compounds such as methane, methanol, and methylamine as sole carbon and energy sources (1, 2). They have been isolated from diverse soil, air, and water environments (3). *Methylobacterium extorquens* TK 0001 was isolated from soil in Poland (4, 5).

*M. extorquens* TK 0001 was obtained from the DSMZ (Braunschweig, Germany) and was grown at 30°C in a minimal medium (DSMZ medium no. 1629) supplemented with 1% methanol. Genomic DNA was purified using the GenElute bacterial genomic DNA kit (Sigma). Genome sequencing was performed at Genoscope, using both Illumina and Nanopore technologies (6, 7). First, the long reads generated by the MinION device (Oxford Nanopore Technologies) were corrected using Canu software (8). The corrected reads were assembled using smartdenovo (https://github.com/ruanjue/smartdenovo), and the resulting assembly was then polished with the help of 2 × 150-bp paired-end reads generated by a MiSeq sequencer (Illumina) with a genome coverage of ~134×. The final assembly was composed of a single contig of 5.71 Mb with a GC content of 68.2%. Automatic functional annotation and comparative genome analysis were performed using the MicroScope platform (http://www.genoscope.cns.fr/agc/microscope) (9). In total, 6,251 genomic objects were identified comprising 6,160 coding sequences (CDSs), 17 miscellaneous RNAs, 59 tRNAs, and 15 rRNAs (5 5S, 5 16S, and 5 23S). The *M. extorquens* TK 0001 genome contains the *mxa* gene clusters (*mxaABCD* and *mxaFJGIR*) coding for methanol dehydrogenase and for enzymes involved in the synthesis of the periplasmic pyrroloquinoline quinone electron carrier. No methylamine dehydrogenase was found. The enzymes for the *N*-methylglutamate pathway, *mgsABC* and *gmaS*, are present, accounting for the growth on methylamine (10). Genes for the serine cycle and the ethylmalonyl-coenzyme A pathway implicated in $C_1$ assimilation are specified. *M. extorquens* TK 0001 is a facultative methylotroph growing also on complex carbon sources. Accordingly, the Entner-Doudoroff pathway and the pentose phosphate pathway are predicted, as well as the oxidative tricarboxylic acid cycle.

A comparative genome analysis was performed between TK 0001 and *M. extorquens* strains AM1, PA1, CM4, and DM4 showing that these strains are strongly related. A

**Received** 9 January 2018 **Accepted** 11 January 2018 **Published** 22 February 2018

**Citation** Belkhelfa S, Labadie K, Cruaud C, Aury J-M, Roche D, Bouzon M, Salanoubat M, Döring V. 2018. Complete genome sequence of the facultative methylotroph *Methylobacterium extorquens* TK 0001 isolated from soil in Poland. Genome Announc 6:e00018-18. https://doi.org/10.1128/genomeA.00018-18.



Address correspondence to Volker Döring, vdoring@genoscope.cns.fr.

fraction of 24.3% of the CDSs is specific to *M. extorquens* strain TK 0001, and 61.9% of the CDSs correspond to the core genome of this group of organisms.

**Accession number(s).** This whole-genome project has been deposited in DDBJ/EMBL/GenBank under the accession no. LT962688.

## ACKNOWLEDGMENTS

This work was financially supported by a CEA internal research project joining the Fundamental Research Division (DRF) and the Technological Research Division (DRT). The LABGeM (CEA/IG/Genoscope and CNRS UMR 8030) and the France Génomique national infrastructure (funded as part of Investissements d'Avenir program managed by the Agence Nationale pour la Recherche, contract ANR-10-INBS-09) are acknowledged for support within the MicroScope annotation platform and many other functionalities of the system.

## REFERENCES

1. Anthony C. 1982. The biochemistry of methylotrophs. Academic Press, New York, NY.
2. Schrader J, Schilling M, Holtmann D, Sell D, Filho MV, Marx A, Vorholt JA. 2009. Methanol-based industrial biotechnology: current status and future perspectives of methylotrophic bacteria. Trends Biotechnol 27:107–115. https://doi.org/10.1016/j.tibtech.2008.10.009.
3. Lidstrom ME. 2006. Aerobic methylotrophic prokaryotes. Springer, New York, NY.
4. Bousfield IJ, Green PN. 1985. Reclassification of bacteria of the genus *Protomonas* Urakami and Komagata 1984 in the genus *Methylobacterium* (Patt, Cole, and Hanson) emend. Green and Bousfield 1983. Int J Syst Bacteriol 35:209–209. https://doi.org/10.1099/00207713-35-2-209.
5. Urakami T, Komagata K. 1984. *Protomonas*, a new genus of facultatively methylotrophic bacteria. Int J Syst Bacteriol 34:188–201. https://doi.org/10.1099/00207713-34-2-188.
6. Magi A, Semeraro R, Mingrino A, Giusti B, D'Aurizio R. 2017. Nanopore sequencing data analysis: state of the art, applications and challenges. Brief Bioinform https://doi.org/10.1093/bib/bbx062.
7. Madoui MA, Engelen S, Cruaud C, Belser C, Bertrand L, Alberti A, Lemainque A, Wincker P, Aury JM. 2015. Genome assembly using nanopore-guided long and error-free DNA reads. BMC Genomics 16:327. https://doi.org/10.1186/s12864-015-1519-z.
8. Koren S, Walenz BP, Berlin K, Miller JR, Bergman NH, Phillippy AM. 2017. Canu: scalable and accurate long-read assembly via adaptive *k*-mer weighting and repeat separation. Genome Res 27:722–736. https://doi.org/10.1101/gr.215087.116.
9. Vallenet D, Calteau A, Cruveiller S, Gachet M, Lajus A, Josso A, Mercier J, Renaux A, Rollin J, Rouy Z, Roche D, Scarpelli C, Médigue C. 2017. MicroScope in 2017: an expanding and evolving integrated resource for community expertise of microbial genomes. Nucleic Acids Res 45:D517–D528. https://doi.org/10.1093/nar/gkw1101.
10. Nayak DD, Marx CJ. 2014. Methylamine utilization via the *N*-methylglutamate pathway in *Methylobacterium extorquens* PA1 involves a novel flow of carbon through $C_1$ assimilation and dissimilation pathways. J Bacteriol 196:4130–4139. https://doi.org/10.1128/JB.02026-14.

ACS Synthetic Biology
Letter
Cite This: ACS Synth. Biol. 2018, 7, 2742−2749
pubs.acs.org/synthbio

# NADPH-Auxotrophic *E. coli*: A Sensor Strain for Testing *in Vivo* Regeneration of NADPH

Steffen N. Lindner,*[,†] Liliana Calzadiaz Ramirez,[†] Jan L. Krüsemann,[†] Oren Yishai,[†] Sophia Belkhelfa,[‡] Hai He,[†] Madeleine Bouzon,[‡] Volker Döring,[‡] and Arren Bar-Even*[,†]

[†]Max Planck Institute of Molecular Plant Physiology, Am Mühlenberg 1, Potsdam-Golm, 14476, Germany
[‡]Génomique Métabolique, Genoscope, Institut François Jacob, CEA, CNRS, Univ Evry, Université Paris-Saclay, Evry, 91057, France

Supporting Information

**ABSTRACT:** Insufficient rate of NADPH regeneration often limits the activity of biosynthetic pathways. Expression of NADPH-regenerating enzymes is commonly used to address this problem and increase cofactor availability. Here, we construct an *Escherichia coli* NADPH-auxotroph strain, which is deleted in all reactions that produce NADPH with the exception of 6-phosphogluconate dehydrogenase. This strain grows on a minimal medium only if gluconate is added as NADPH source. When gluconate is omitted, the strain serves as a "biosensor" for the capability of enzymes to regenerate NADPH *in vivo*. We show that the NADPH-auxotroph strain can be used to quantitatively assess different NADPH-regenerating enzymes and provide essential information on expression levels and concentrations of reduced substrates required to support optimal NADPH production rate. The NADPH-auxotroph strain thus serves as an effective metabolic platform for evaluating NADPH regeneration within the cellular context.

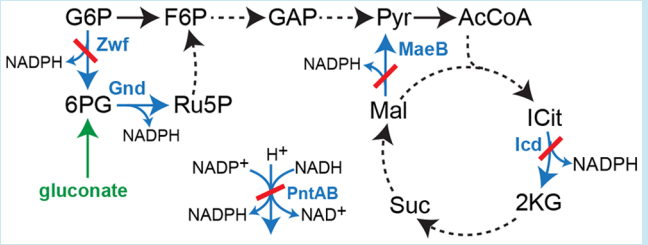


**KEYWORDS:** *NADPH regeneration, auxotroph strain, selection strain, enzyme screening, dihydrolipoamide dehydrogenase, glyceraldehyde 3-phosphate dehydrogenase, formate dehydrogenase, cinnamyl alcohol*



NADPH, the reduced form of nicotinamide adenine dinucleotide phosphate ($NADP^+$), is the main electron donor for anabolic pathways and serves as a primary driving force in the biosynthesis of a wide array of value added chemicals. However, in many cases, the endogenous rate of NADPH regeneration does not suffice to support the production of chemicals, the biosynthesis of which requires high stoichiometric amounts of this cofactor, for example, lysine,[1] valine,[2] arginine,[3] ornithine,[4] chloropropionate,[5] lycopene,[5] and terpenoids.[6] Several strategies are used to overcome this limitation.[7−10] One approach is to divert metabolic flux toward endogenous pathways that produce NADPH, for example, the oxidative pentose phosphate pathway. Alternatively, heterologous overexpression of NADP-dependent oxidoreductase enzymes can enhance cofactor regeneration. This latter strategy is also used in *in vitro* biosynthesis systems, where NADPH is regenerated by the addition of a reduced compound which can donate its electrons to $NADP^+$ via an appropriate enzyme.[11] In some cases, NADH-regenerating enzymes are engineered to accept $NADP^+$, for example, formate dehydrogenase[12] and phosphite dehydrogenase.[13]

Here, we construct an NADPH-auxotrophic *E. coli* strain, deleted in all endogenous NADPH-producing reactions, with the exception of 6-phosphogluconate dehydrogenase. This strain can grow on a minimal medium only if supplemented with gluconate as the sole source of NADPH regeneration. We show that this strain can serve as an efficient "metabolic biosensor" for the ability of different enzymes to regenerate NADPH *in vivo*, providing valuable information on the required expression levels and the optimal concentrations of electron donors. This strain could therefore serve as a useful metabolic platform to compare different strategies of NADPH regeneration, further enabling direct screening of oxidoreductase enzymes for high NADPH production rate.

## RESULTS

**Construction and Characterization of an NADPH Auxotroph Strain.** *E. coli* harbors five enzymes that regenerate NADPH. These are glucose 6-phosphate dehydrogenase (Zwf) and 6-phosphogluconate dehydrogenase (Gnd) of the oxidative pentose phosphate pathway, a malic enzyme (MaeB), isocitrate dehydrogenase (Icd) of the TCA cycle, and a membrane-bound proton-translocating transhydrogenase (PntAB).[14] To create an NADPH-auxotroph strain, we aimed to delete all of these enzymes with the exception of Gnd. As the activity of Gnd depends on the availability of 6-phosphogluconate, disruption of Zwf would deprive the former enzyme from its substrate, rendering it incapable of regenerating NADPH from glucose 6-phosphate (Figure 1). The advantage of this design is that the addition of gluconate serves as a "relaxing substrate": as the conversion of gluconate

Received: July 25, 2018
Published: November 26, 2018




DOI: 10.1021/acssynbio.8b00313
ACS Synth. Biol. 2018, 7, 2742−2749

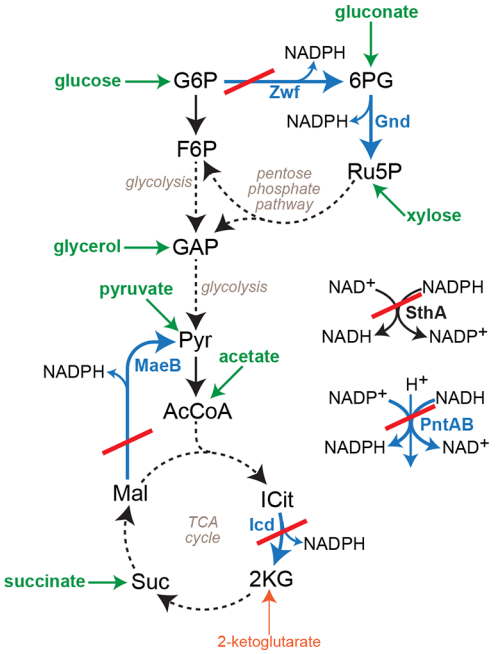


**Figure 1.** Schematic representation of the NADPH auxotrophic *E. coli*. Enzymes producing NADPH are shown in blue arrows. Deleted enzymes are indicated using a red crossing line. Carbon sources are shown in green. Once isocitrate dehydrogenase (Icd) is disrupted, 2-ketoglutarate is added to the medium as a source of glutamate and related amino acids. The membrane-bound transhydrogenase (PntAB) is schematically shown with the proton translocated across the membrane to energize the unfavorable electron transfer. The soluble transhydrogenase (SthA) is disrupted to avoid depletion of the NADPH pool (see main text). Abbreviations: G6P, glucose 6-phosphate; 6PG, 6-phosphogluconate; Ru5P, ribulose 5-phosphate; F6P, fructose 6-phosphate; GAP, glyceraldehyde 3-phosphate; Pyr, pyruvate; AcCoA, acetyl-CoA; ICit, isocitrate; 2KG, 2-ketoglutarate; Suc, succinate; Mal, malate.

to 6-phosphogluconate is independent of the activity of Zwf, this substrate would support NADPH-regeneration by Gnd (Figure 1).

Figure 2 presents the growth phenotypes of intermediate gene deletion strains that were constructed toward an NADPH auxotrophic phenotype. Disruption of Zwf and MaeB (abbreviated by "Z' and 'M" in Figure 2) did not alter growth on any of the carbon sources tested (Figure 2A; concentrations of feedstocks were normalized according to their energies of combustion, see Methods). However, further disruption of PntAB (abbreviated by 'P') severely inhibited growth on gluconate and abolished growth on most other carbon sources, despite the availability of Icd as a NADPH source (Figure 2B). Only growth on acetate remained unperturbed, presumably as acetate oxidation via the TCA cycle produces NADPH at high rate via Icd. We speculated that the growth defect observed with most carbon sources can be explained by the activity of the soluble transhydrogenase (SthA) which depletes the NADPH pool by transferring electrons to $NAD^+$.[14] Indeed, as shown in Figure 2C, upon further disruption of SthA (abbreviated by 'S'), growth on all carbon sources, except of glucose, was restored (the very poor growth on glucose cannot be easily explained but might be related to the vast regulatory effects induced by this carbon source).

Next, we integrated the above gene deletions with the disruption of Icd, a key enzyme of the TCA cycle. As reported before,[15] we found that knockout of the isocitrate dehydrogenase gene reduced growth rate and further required the addition of 2-ketoglutarate—the endogenous product of Icd—as precursor of glutamate and downstream amino acids. When combined with the deletion of *zwf* and *maeB*, disruption of Icd (abbreviated by 'I') resulted in severely impaired growth—considerably worse than that of the Δ*icd* strain alone—with all carbon sources besides the "relaxing" substrate gluconate (Figure 2D). This points to the prime role of Icd for the regeneration of NADPH when Zwf and MaeB are not available. Deletion of *zwf*, *maeB*, *icd*, and *pntAB* completely abolished growth in a minimal medium on all carbon sources (Figure 2E). Yet, further disruption of SthA restored growth on gluconate (Figure 2F), pointing again to the role of SthA in depleting the NADPH pool. This final strain NADPHaux (Δ*zwf* Δ*maeB* Δ*pntAB* Δ*sthA* Δ*icd*) therefore presents the desired growth phenotype, that is, growing only when the "relaxing" substrate gluconate is available.

Next, we tested whether the addition of small amounts of gluconate can rescue the growth of the NADPHaux strain on different carbon sources. As shown in Figure 3, the concentration of added gluconate directly correlates with the final OD reached when cells were grown on multiple carbon sources. We further deleted phosphogluconate dehydratase (Edd) and 2-keto-3-deoxygluconate 6-phosphate aldolase (Eda) of the Entner-Doudoroff pathway, which competes with Gnd on the substrate 6-phosphogluconate. Yet, as demonstrated in Figure 3, the effect of this deletion was relatively small (with several few exceptions). This indicates that under most conditions, in our gene-deletion strain, the majority of 6-phosphogluconate is metabolized via Gnd rather than the Entner−Doudoroff pathway.

**The NADPHaux Strain Enables Direct Selection for NADPH Production by Different Enzymes and Reduced Substrates.** To test whether the NADPHaux strain could be used to evaluate the capability of different enzymes to regenerate NADPH, we used several NADP-dependent oxidoreductases. We started with a dihydrolipoamide dehydrogenase from *E. coli*, a key component of the pyruvate and 2-ketoglutarate dehydrogenase complexes, as well as of the glycine cleavage system, that was engineered to prefer the reduction of $NADP^+$ over $NAD^+$.[16] This engineered enzyme (harboring seven mutations) displays very good kinetics of $NADP^+$, having $k_{cat}$ = 95.2 $s^{-1}$ and $K_M$ = 60 μM, which are considerably better values than those of the average enzyme.[17] Indeed, as shown in Figure 4, when we expressed the enzyme from a medium copy number plasmid (p15A origin of replication) and under the control of a medium strength promoter (variant 10 of *pgi*-promoter[18,19]), we observed stable growth on all tested carbon sources, with the exception of acetate, indicating high production rate of NADPH.

The failure to establish growth on acetate, as well as the poor growth we observe on pyruvate and succinate, can be related to the operation of the PEP−glyoxylate cycle in our strain, in which the TCA cycle is disrupted.[20] Specifically, this cycle, which relies on the glyoxylate shunt, the malic enzyme, and pyruvate dehydrogenase, can replace the TCA cycle and support complete oxidation of carbon feedstocks.[20] Growth on carbon sources that enter "lower" metabolism, that is, acetate, pyruvate, and succinate, are expected to heavily rely on the activity of this alternative cycle for energy production. Excess $NADP^+$ reduction by pyruvate dehydrogenase (carrying the mutated dihydrolipoamide dehydrogenase) could inhibit the


DOI: 10.1021/acssynbio.8b00313
ACS Synth. Biol. 2018, 7, 2742−2749

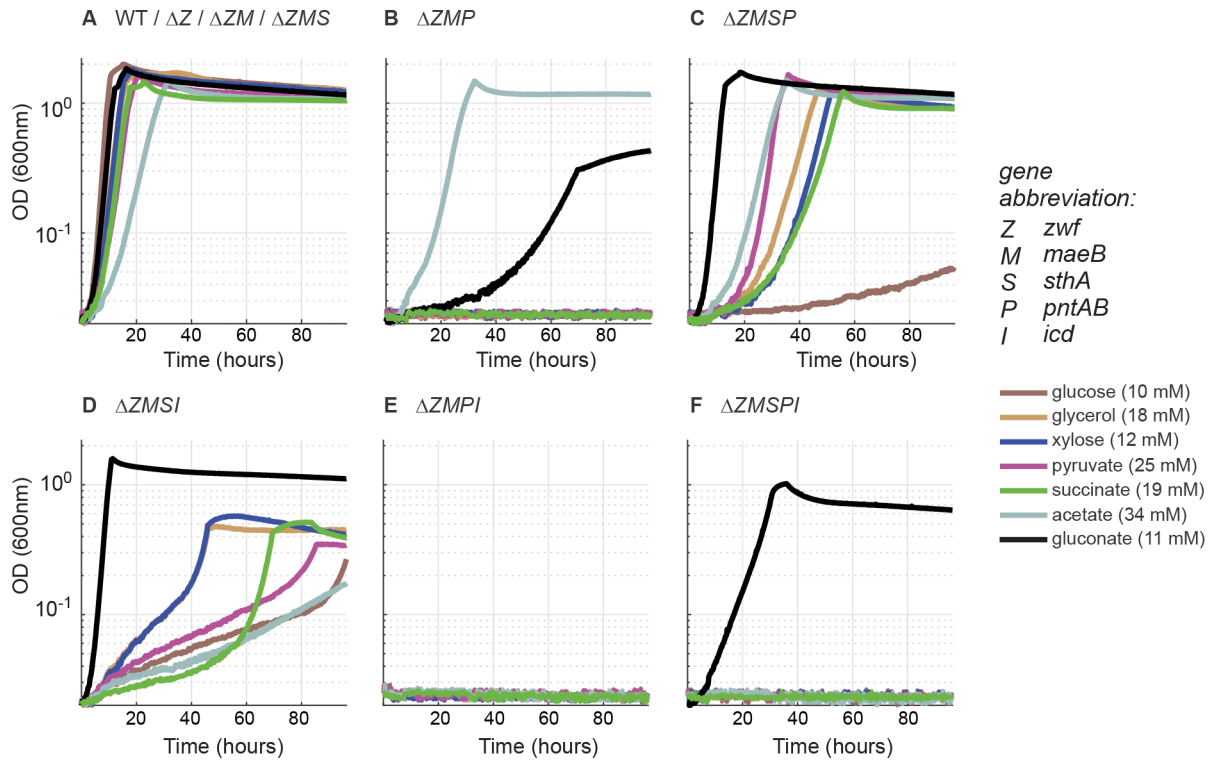


**Figure 2.** Construction of the NADPH auxotroph strain. Growth phenotypes of intermediate gene deletion strains are shown using multiple carbon sources. Concentrations of the carbon sources were normalized to their energy of combustion. All growth experiments were performed in triplicate, which in all cases resulted in identical curves (±5%), indicating that no mutation occurred to enable the observed growth. The growth curves of the WT, ΔZ, ΔZM, and ΔZMS strains on all carbon sources were identical and hence are shown on the same graph.

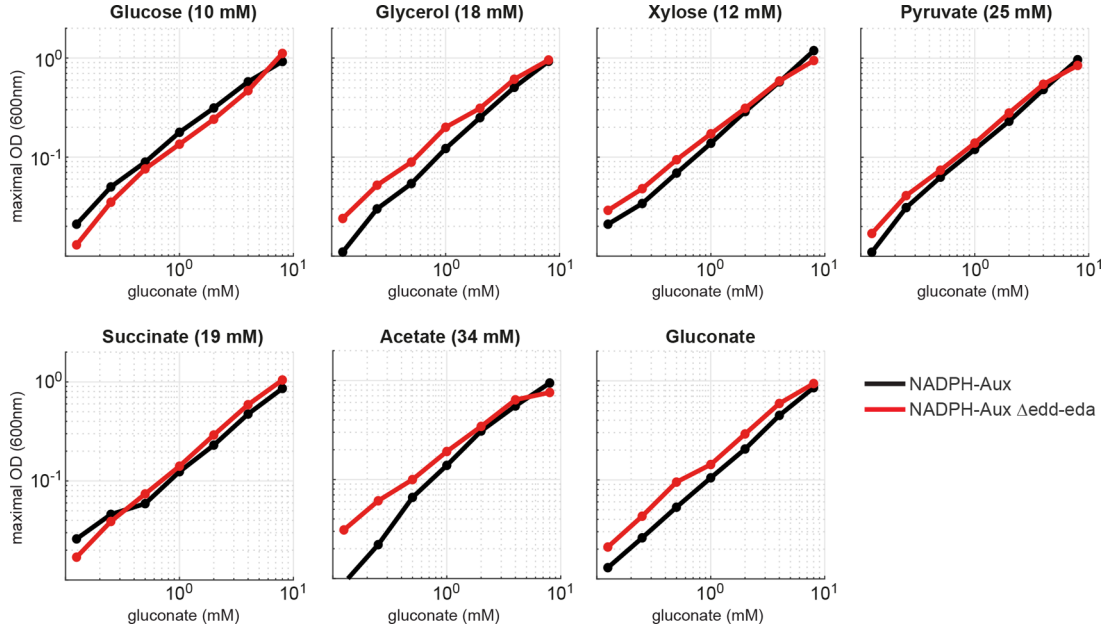


**Figure 3.** Maximal OD of the NADPHaux strain scales with the concentration of gluconate as sole source of NADPH. Different carbon sources present a similar trend. Concentrations of the carbon sources were normalized according to the combustion energy of the compounds, as described in the methods section. To all cultures, 3 mM of 2-ketoglutarate was added. All growth experiments were performed in triplicate, which in all cases resulted in identical curves (±5%), indicating that no mutation occurred to enable the observed growth.

operation of this cycle and hence result in poor or no growth on carbon sources that enter "lower" metabolism.

Next, we tested the NADP-dependent nonphosphorylating glyceraldehyde 3-phosphate dehydrogenase (GapN) of *Streptococcus mutans*.[21] This enzyme irreversibly oxidizes glyceraldehyde 3-phosphate to 3-phosphoglycerate using $NADP^+$ as an electron acceptor. GapN was previously demonstrated to enhance NADPH regeneration,[22] and its kinetic parameters with $NADP^+$ are good: $k_{cat}$ = 60 $s^{-1}$ and $K_M$ = 25 $\mu$M.[23] Yet, overexpression of the enzyme from a medium copy number



DOI: 10.1021/acssynbio.8b00313
ACS Synth. Biol. 2018, 7, 2742−2749

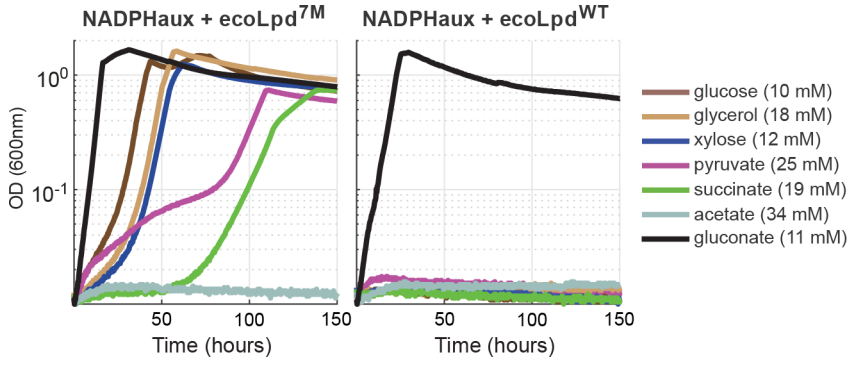


**Figure 4.** Overexpression of engineered dihydrolipoamide dehydrogenase that accepts $NADP^+$ restores growth on all carbon sources except acetate. The engineered enzyme, harboring seven mutations,[16] is marked as $Lpd^{7M}$. Overexpression of nonmutated Lpd, marked as $Lpd^{WT}$, did not rescue growth. Both enzymes were expressed from a medium copy number plasmid under the regulation of a medium strength promoter. In all cases, 3 mM of 2-ketoglutarate was added. All growth experiments were performed in triplicate, which in all cases resulted in identical curves (±5%), indicating that no mutation occurred to enable the observed growth.

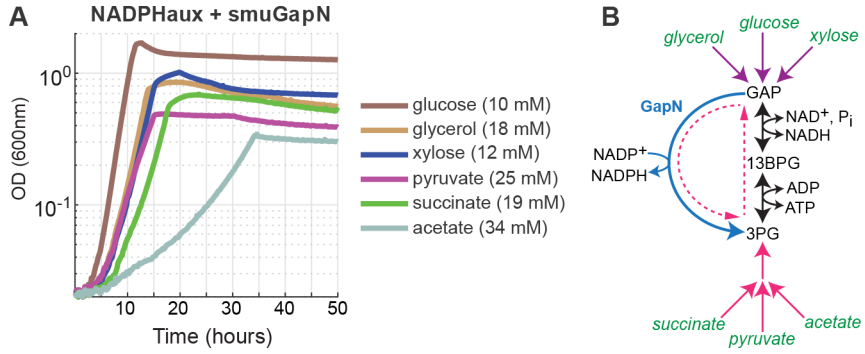


**Figure 5.** Overexpression of NADP-dependent nonphosphorylating glyceraldehyde 3-phosphate dehydrogenase of *Streptococcus mutans* (GapN) rescues the growth of the NADPHaux strain. (A) Growth on different carbon sources is restored upon the expression of GapN from a medium copy number plasmid and under the regulation of a strong promoter. To all cultures, 3 mM of 2-ketoglutarate was added. All growth experiments were performed in triplicate, which in all cases resulted in identical curves (±5%), indicating that no mutation occurred to enable the observed growth. (B) Schematic representation of a cyclic flux when the cell is fed with carbon sources that enter "lower metabolism" (pyruvate, succinate, acetate). This cycle transfers electrons from NADH to NADPH at the expense of ATP hydrolysis.

plasmid and under the control of a medium strength promoter resulted in only poor growth. Only when we replaced the medium strength promoter with a strong promoter (variant 20 of *pgi*-promoter[18,19]), increasing the expression level ~3 fold,[19] did we observe good growth on all carbon sources, as shown in Figure 5A.

Notably, growth on carbon sources that enter "lower" metabolism required a cyclic flux between 3-phosphoglycerate and glyceraldehyde 3-phosphate to produce NADPH, or, more accurately, to transfer electrons from NADH to $NADP^+$. As shown schematically in Figure 5B, this transfer of reducing power comes at the expense of ATP hydrolysis (by the combined activity of 3-phosphoglycerate kinase and glyceraldehyde 3-phosphate dehydrogenase), and thus mimics the activity of PntAB that uses the proton motive force to energize this reaction. This cycle further resembles an endogenous NADPH regeneration cycle, composed of PEP synthetase, PEP carboxylase, oxaloacetate dehydrogenase, and the NADPH-generating malic enzyme (MaeB),[24] the latter being deleted in the NADPHaux strain.

We then tested a previously reported formate dehydrogenase (FDH) from *Mycobacterium vaccae* N10 that was engineered, and demonstrated *in vitro*, to prefer the reduction of $NADP^+$.[25] Yet, the kinetic parameters of the enzyme with $NADP^+$ are quite poor, $k_{cat}$ = 3.1 $s^{-1}$ and $K_M$ = 147 $\mu$M. Indeed, overexpression of the enzyme from a medium copy number plasmid failed to sustain growth upon addition of formate, regardless of the promoter used. Only when we expressed the enzyme from a high copy number plasmid (pMB1 origin of replication; under a medium strength promoter, equivalent to a ~ 6-fold higher expression level compared to a medium copy number plasmid[19]), we could sustain stable formate-dependent growth. As shown in Figure 6, increasing formate concentration up to 30 mM resulted in an increased growth rate, which can be explained by the very high $K_M$ of the enzyme for formate.[25] Concentrations higher than 30 mM did not improve growth, suggesting that the enzyme operates near saturation. (We note that the intracellular formate concentration is not expected to differ substantially from its concentration in the medium as this small molecule can easily diffuse into the cell, which is further assisted by the formate channel focA.[26])

Finally, we tested the ability of *E. coli* to endogenously use different reduced compounds to regenerate NADPH without introducing new enzymes. We tested several alcohols and found one compound that can be natively used to produce NADPH: cinnamyl alcohol. As shown in Figure 7, a concentration as low as 0.25 mM of cinnamyl alcohol sufficed to support growth, albeit at a low rate. We found that 4 mM of cinnamyl alcohol was optimal to support growth, where higher concentrations resulted in a decreased growth rate, probably


DOI: 10.1021/acssynbio.8b00313
ACS Synth. Biol. 2018, 7, 2742−2749

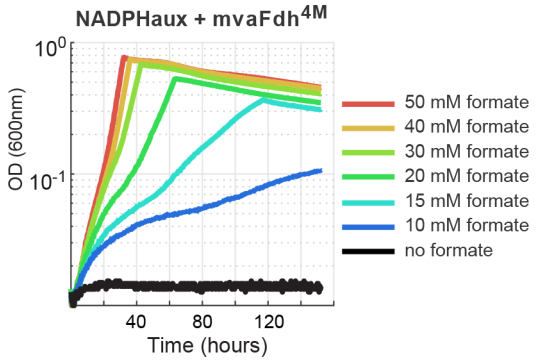


**Figure 6.** Addition of formate rescues the growth of the NADPHaux strain expressing engineered formate dehydrogenase. Engineered formate dehydrogenase from *Mycobacterium vaccae* N10, carrying four mutations ($Fdh^{4M}$), with high specificity toward the reduction of $NADP^+$, was overexpressed from a high copy number plasmid under the regulation of a medium strength promoter. Glycerol (18 mM) served as carbon source and 3 mM of 2-ketoglutarate was added. All growth experiments were performed in triplicate, which in all cases resulted in identical curves (±5%), indicating that no mutation occurred to enable the observed growth.

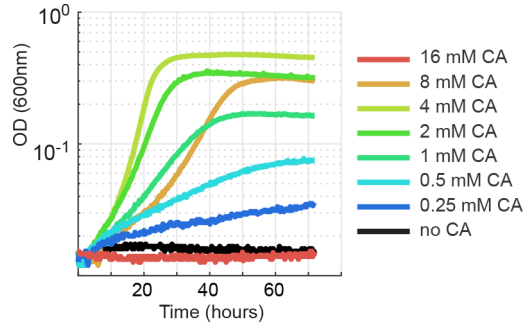


**Figure 7.** Addition of cinnamyl alcohol rescues the growth of the NADPHaux strain. Glycerol (18 mM) served as carbon source and 3 mM of 2-ketoglutarate was added. All growth experiments were performed in triplicate, which in all cases resulted in identical curves (±5%), indicating that no mutation occurred to enable the observed growth.

due to the toxicity of the compound. These results suggest that cinnamyl alcohol is oxidized to cinnamic acid by endogenous, promiscuous alcohol and aldehyde dehydrogenases, of which at least one regenerates NADPH. (Oxidation to cinnamaldehyde without further oxidation to cinnamic acid is unlikely, as the oxidation of an alcohol to aldehyde is unfavorable and would not be efficient at such a low concentration of the alcohol substrate.)

## DISCUSSION

The intermediate deletion strains, constructed *en route* to the NADPHaux strain, present interesting behaviors that indicate how NADPH levels are balanced *in vivo*. Specifically, the growth retardation associated with the strains deleted in *pntAB* but not in *sthA* (Figure 2B,E) suggests that these metabolically counteracting systems are not only expressed when necessary, but rather operate in parallel. Hence, when PntAB is absent (together with Zwf and MaeB) the cell does not deactivate SthA, which leads to a deleterious depletion of the NADPH pool. This finding fits previous reports showing that the regulation of the two transhydrogenases is independent of the actual availability of NADPH and rather corresponds to nutrient levels and growth rate.[27] While it was proposed that *SthA* might be allosterically activated with NADPH and inhibited by $NADP^+$,[14] it seems that this effect does not suffice to prevent the depletion of the NADPH pool by *SthA* (at least in our NADPH-starved strains).

The simultaneous activities of PntAB and SthA suggest the existence of a futile cycle, where NADH is converted to NADPH just to be recycled back to NADH, at the expense of proton relocation that dissipates about a third of the energy of the hydrolysis of one ATP molecule. While this futile cycle might be costly in terms of cellular resources, it could have an important regulatory function, enabling a fast balancing of the levels of NADPH under changing conditions.

Using several examples, we illustrated the applicability of the NADPHaux strain to detect $NADP^+$ reduction activity. Importantly, we demonstrated that the strain can accurately sense the rate of NADPH regeneration, such that enzymes with superior kinetics can be expressed at moderate levels while enzymes characterized by poor kinetics require high expression level to support growth. Our system is therefore useful to quantitatively decipher the suitability of different enzymes to regenerate NADPH and to further suggest appropriate expression levels to efficiently support this activity. Moreover, as we show with the case of formate and cinnamyl alcohol, the NADPHaux strain is useful to quantitatively elucidate the required concentration of an electron donor to support a maximal regeneration rate.

Our findings with regards to NADPH regeneration by formate and FDH is especially interesting in the context of the "formate bioeconomy", that is, using formate, produced via physicochemical means—for example, electrochemical reduction of $CO_2$—as feedstock for microbial growth and bioproduction.[28] Specifically, most formatotrophic organisms transfer electrons from formate to $NAD^+$ to provide reducing power and energy for growth. As some formate assimilation pathways require high NADPH input—for example, reduction of 5,10-methenyltetrahydrofolate within the reductive glycine pathway[29]—the transfer of reducing power from NADH to $NADP^+$, for example, by the activity of PntAB, can dissipate a substantial fraction of cellular energy. Expressing a NADP-dependent formate dehydrogenase, which directly transfers reducing power from formate to $NADP^+$, would therefore provide an energy efficient alternative that could boost biomass and bioproduction yields.

The NADPHaux strain is a simple but effective tool to support enzyme engineering and the successful realization of diverse biosynthetic pathways using a simple growth/no-growth readout. This strain would be especially useful for testing large libraries of enzyme variants: instead of time-consuming screening of each variant for its ability to reduce $NADP^+$ at a sufficient rate, the entire library can be transformed to the NADPHaux strain, and the highly active enzymes isolated from the (fast) growing cells.

## MATERIALS AND METHODS

**Strains and Gene Deletions.** The strains used in this study are listed in Table 1. *E. coli* strain SIJ488,[30] was used as WT for the sequential deletion of genes. SIJ488 genomically carries inducible genes that encode for a recombinase and a flippase, allowing fast turnover for multiple deletions. Most gene deletions were performed by successive rounds of λ-Red recombineering.[30] The gene *icd* was deleted by P1 phage


DOI: 10.1021/acssynbio.8b00313
ACS Synth. Biol. 2018, 7, 2742−2749

**Table 1. Strains and Plasmids Used in This Study**

| name | use/deletion | ref |
|---|---|---|
| DH5$\alpha$ | cloning of overexpression constructs | |
| SIJ488 | WT | 30 |
| JW1122 | icd::kan knockout Keio collection | 32 |
| $\Delta Z$ | $\Delta zwf$ | this study |
| $\Delta ZM$ | $\Delta zwf\ \Delta maeB$ | this study |
| $\Delta ZMP$ | $\Delta zwf\ \Delta maeB\ \Delta pntAB$ | this study |
| $\Delta ZMS$ | $\Delta zwf\ \Delta maeB\ \Delta sthA$ | this study |
| $\Delta ZMPS$ | $\Delta zwf\ \Delta maeB\ \Delta pntAB\ \Delta sthA$ | this study |
| $\Delta ZMPI$ | $\Delta zwf\ \Delta maeB\ \Delta pntAB\ \Delta icd::kan$ | this study |
| $\Delta ZMSI$ | $\Delta zwf\ \Delta maeB\ \Delta sthA\ \Delta icd::kan$ | this study |
| $\Delta ZMPSI$ (NADPHaux) | $\Delta zwf\Delta maeB\ \Delta pntAB\ \Delta sthA\ \Delta icd::kan$ | this study |
| $\Delta ZMPSIEE$ | $\Delta zwf\ \Delta maeB\ \Delta pntAB\ \Delta sthA\ \Delta icd\ \Delta edd\text{-}eda$ | this study |
| pZ-ASM | overexpression plasmid with p15A origin (medium copy number), Streptomycin resistance, constitutive strong promoter (5′-ACCTATTGACAATTAAAGGCTAAAATGCTATAATTCCAC-3′) | 19 |
| pZ-ASS | Overexpression plasmid with p15A origin (medium copy number), Streptomycin resistance, constitutive strong promoter (5′-AATACTTGACATATCACTGTGATTCACATATAATATGCG-3′) | 19 |
| pZ-MSM | Overexpression plasmid with pMB1 origin (high copy number), Streptomycin resistance, constitutive medium strength promoter (5′-ACCTATTGACAATTAAAGGCTAAAATGCTATAATTCCAC-3′) | 19 |
| pZ-ASM-lpd$^{WT}$ | pZ-ASM backbone for overexpression of *E. coli* wildtype *lpd* | this study |
| pZ-ASM-lpd$^{7M}$ | pZ-ASM backbone for overexpression of *E. coli* *lpd*$^{7M}$ (E203 V, M204R, F205 K, D206H, P210R, G185A, G189A) | this study |
| pZ-ASM-gapN | pZ-ASM backbone for overexpression of *gapN* from *S. mutans* | this study |
| pZ-ASS-gapN | pZ-ASS backbone for overexpression of *gapN* from *S. mutans* | this study |
| pZ-ASM-MVfdh$^{4M}$ | pZ-ASM backbone for overexpression of engineered *fdh* from *M. vaccae* (C145S/A198G/D221Q/C255 V) | this study |
| pZ-ASS-MVfdh$^{4M}$ | pZ-ASS backbone for overexpression of engineered *fdh* from *M. vaccae* (C145S/A198G/D221Q/C255 V) | this study |
| pZ-MSM-MVfdh$^{4M}$ | pZ-MSM backbone for overexpression of engineered *fdh* from *M. vaccae* (C145S/A198G/D221Q/C255 V) | this study |

transduction[31] using the *icd* knock out strain from the Keio collection (Table 1) as a donor.[32]

For the recombination, kanamycin resistance cassettes were generated via PCR—"KO" primers with 50 bp homologous arms using the FRT-PGK-gb2-neo-FRT (Km) cassette (Gene Bridges, Germany) as listed in Supplementary Table 1. To prepare cells for gene deletion, fresh cultures were inoculated in LB in the morning and the recombinase genes were induced by the addition of 15 mM L-arabinose at OD ∼ 0.4−0.5. After incubation for 45 min at 37 °C, cells were harvested and washed three times with ice cold 10% glycerol (11 300*g*, 30 s, 2 °C). Approximately 300 ng of Km cassette PCR-product was transformed via electroporation (1 mm cuvette, 1.8 kV, 25 $\mu$F, 200 Ω). After selection on kanamycin, gene deletions were confirmed via PCR using "KO-Ver" primers (Supplementary Table 1). To remove the Km cassette, 50 mM L-rhamnose, which induces flippase gene expression, was added to an exponentially growing 2 mL LB culture at OD 0.5; induction time was ≥3 h at 30 °C. Colonies were screened for kanamycin sensitivity and the removal of antibiotic resistance cassette was confirmed by PCR (using "KO-Ver" primers). For deletion of *icd*, 10 mM gluconate and 5 mM $\alpha$-ketoglutarate were supplied to LB plates as well as to liquid cultures.

**Gene Overexpression.** For overexpression of the dihydrolipoamide dehydrogenase (*lpd*) (including an N-terminal 6x His-Tag) the corresponding gene was amplified from *E. coli* genomic DNA by PCR using primers lpd_A and lpd_D. The PCR product (*lpd*$^{WT}$) was cloned into pNivC vector. To clone the rationally designed *lpd* variants (which are specific to NADP$^+$), the mutations described by Bocanegra et al. were introduced by a fusion PCR of the PCR products generated with primer pairs lpd_A + lpd_B and lpd_C + lpd_D, resulting in the *lpd* variant *lpd*$^{5M}$ (corresponding to Bocanegra's Mutant A: Glu203Val, Met204Arg, Phe205Lys, Asp206His, Pro210Arg). The PCR product was cloned into pNivC vector resulting in pNivC-*lpd*$^{5M}$. To generate pNivC-*lpd*$^{7M}$ (corresponding to Bocanegra's Mutant C Glu203Val, Met204Arg, Phe205Lys, Asp206His, Pro210Arg, Gly185Ala, Gly189Ala) pNivC-*lpd*$^{5M}$ was used as a PCR template, and primers lpd_MutB-F and lpd_MutB-R were used together with pNiv-Amp-F and pNiv-Amp-R, respectively. The PCR products were fused by CPEC cloning[33] to generate pNivC-*lpd*$^{7M}$. The genes were cloned with *EcoR*I and *Pst*I (FastDigest, Thermo Scientific) into the expression vector pZ-ASM (p15A origin, Streptomycin resistance, medium strength promoter), generating pZ-ASM-*lpd*$^{WT}$, and pZ-ASM-*lpd*$^{7M}$.

NADP-dependent nonphosphorylating glyceraldehyde 3-phosphate dehydrogenase from *Streptococcus mutans* (gapN, UniProt: Q59931[21]) and engineered formate dehydrogenase from *Mycobacterium vaccae* (MVa-3M-*fdh*[25]) were synthesized after codon adaptation for *E. coli*.[34] Recognition sites of restriction enzymes required for cloning were removed.[35] Gene synthesis was performed by Baseclear (Leiden, The Netherlands). Each gene was cloned with an N-terminal 6x His-Tag into a pNivC vector downstream of ribosome binding site "C" (AAGTTAAGAGGCAAGA).[35] To generate pNivC-(MVa-4M-*fdh*), primers fdh-Mva-4M-F and fdh-Mva-4M-R were used together with pNiv-Amp-F and pNiv-Amp-R, respectively, on pNivC-(MVa-3M-*fdh*). The PCR products were combined by CPEC cloning.[33] Restriction enzymes *EcoR*I and *Pst*I (FastDigest, Thermo Scientific) were used to transfer the genes into the expression vector pZ-ASM (p15A origin, Streptomycin resistance, medium promoter) or pZ-ASS (p15A origin, Streptomycin resistance, strong promoter) for gapN, resulting in pZ-ASM-gapN and pZ-ASS-gapN. fdh$^{4M}$ was cloned into pZ-ASM, pZ-ASS, and pZ-MSM (pMB1 origin, Streptomycin resistance, medium promoter)[18] resulting in pZ-ASM-fdh$^{4M}$, pZ-ASS-fdh$^{4M}$, and pZ-MSM-fdh$^{4M}$.



DOI: 10.1021/acssynbio.8b00313
*ACS Synth. Biol.* 2018, 7, 2742−2749

**Media and Growth Conditions.** LB medium (1% NaCl, 0.5% yeast extract, 1% tryptone) was used for growth during cloning and to generate gene deletions. When appropriate, antibiotics were used in the following concentrations: kanamycin, 25 $\mu$g/mL; ampicillin, 100 $\mu$g/mL; streptomycin, 100 $\mu$g/mL; and chloramphenicol, 30 $\mu$g/mL. For deletion and maintenance of the *icd* deletion strain, 5 mM 2-ketoglutarate and 10 mM gluconate were added to LB plates. For growth experiments, M9 minimal media (47.8 mM $Na_2HPO_4$, 22 mM $KH_2PO_4$, 8.6 mM NaCl, 18.7 mM $NH_4Cl$, 2 mM $MgSO_4$, 100 $\mu$M $CaCl_2$, 134 $\mu$M EDTA, 31 $\mu$M $FeCl_3{\cdot}6H_2O$, 6.2 $\mu$M $ZnCl_2$, 0.76 $\mu$M $CuCl_2{\cdot}2H_2O$, 0.42 $\mu$M $CoCl_2{\cdot}2H_2O$, 1.62 $\mu$M $H_3BO_3$, and 0.081 $\mu$M $MnCl_2{\cdot}4H_2O$) was used.

Different carbon sources were used as described in the text, in concentrations that were scaled according to their energy of combustion. Specifically, glucose, with an energy of combustion of ~2910 kJ/mol,[36] was set as 10 mM. The concentrations of the other carbon sources were scaled according to the ratio of their combustion energies[36] to that of glucose: glycerol, with ~1650 kJ/mol, was set to 10 × (2910/1650) = 18 mM; pyruvate, with ~1160 kJ/mol, was set to 25 mM; acetate, with ~850 kJ/mol, was set to 34 mM; succinate, with ~1540 kJ/mol, was set to 19 mM; xylose, with ~2440 kJ/mol, was set to 12 mM; gluconate, with ~2660 kJ/mol, was set to 11 mM.

Overnight cultures for growth experiments were incubated in 4 mL of M9 medium containing 11 mM gluconate and 3 mM 2-ketoglutarate. Prior to inoculation, cultures were harvested by centrifugation (3,960*g*, 3 min) and washed three times in M9 medium to clean cells from residual carbon sources. Growth experiments were inoculated to a starting $OD_{600}$ of 0.01 and carried out in 96-well microtiter plates (Nunclon Delta Surface, Thermo Scientific) at 37 °C. Each well contained 150 $\mu$L of culture and, to avoid evaporation, 50 $\mu$L of mineral oil (Sigma-Aldrich). A plate reader (Infinite M200 pro, Tecan) was used for incubation, shaking, and $OD_{600}$ measurements (controlled by Tecan I-control v1.11.1.0). The cultivation program contained three cycles of four shaking phases, 1 min of each: linear shaking, orbital shaking at an amplitude of 3 mm, linear shaking, and orbital shaking at an amplitude of 2 mm. After each round of shaking (~12.5 min), absorbance (OD 600 nm) was measured in each well. Raw data from the plate reader were calibrated to cuvette values according to $OD_{cuvette} = OD_{plate}/0.23$. Growth curves were plotted in MATLAB and represent averages of triplicate measurements; in all cases, variability between triplicate measurements was less than 5%.

## ■ ASSOCIATED CONTENT

### Supporting Information

The Supporting Information is available free of charge on the ACS Publications website at DOI: 10.1021/acssynbio.8b00313.

Oligonucleotide primers used in this work (PDF)

## ■ AUTHOR INFORMATION


### Corresponding Authors

*Tel.: +49 331 567-8910. Email: Lindner@mpimp-golm.mpg.de.

*Tel.: +49 331 567-8910. Email: Bar-Even@mpimp-golm.mpg.de.

### ORCID

Hai He: 0000-0003-1223-2813

Madeleine Bouzon: 0000-0002-9581-6584

Arren Bar-Even: 0000-0002-1039-4328


### Notes

The authors declare no competing financial interest.

## ■ ACKNOWLEDGMENTS

The authors thank Nico Claassens and Charlie Cotton for critical reading of the manuscript. This work was funded by the Max Planck Society. H.H. is funded by the China Scholarship Council. L.G.R. is funded by the Energy Sustainability Grant 429271 of the National Council of Science and Technology and the Mexican Ministry of Energy (CONACYT-SENER).

## ■ REFERENCES


(1) Kabus, A., Georgi, T., Wendisch, V. F., and Bott, M. (2007) Expression of the Escherichia coli pntAB genes encoding a membrane-bound transhydrogenase in Corynebacterium glutamicum improves L-lysine formation. *Appl. Microbiol. Biotechnol. 75*, 47−53.

(2) Blombach, B., Schreiner, M. E., Bartek, T., Oldiges, M., and Eikmanns, B. J. (2008) Corynebacterium glutamicum tailored for high-yield L-valine production. *Appl. Microbiol. Biotechnol. 79*, 471−9.

(3) Park, S. H., Kim, H. U., Kim, T. Y., Park, J. S., Kim, S. S., and Lee, S. Y. (2014) Metabolic engineering of Corynebacterium glutamicum for L-arginine production. *Nat. Commun. 5*, 4618.

(4) Kim, S. Y., Lee, J., and Lee, S. Y. (2015) Metabolic engineering of Corynebacterium glutamicum for the production of L-ornithine. *Biotechnol. Bioeng. 112*, 416−21.

(5) Wang, Y., San, K. Y., and Bennett, G. N. (2013) Improvement of NADPH bioavailability in Escherichia coli through the use of phosphofructokinase deficient strains. *Appl. Microbiol. Biotechnol. 97*, 6883−93.

(6) Ng, C. Y., Farasat, I., Maranas, C. D., and Salis, H. M. (2015) Rational design of a synthetic Entner-Doudoroff pathway for improved and controllable NADPH regeneration. *Metab. Eng. 29*, 86−96.

(7) Spaans, S. K., Weusthuis, R. A., van der Oost, J., and Kengen, S. W. (2015) NADPH-generating systems in bacteria and archaea. *Front. Microbiol. 6*, 742.

(8) Lee, W. H., Kim, M. D., Jin, Y. S., and Seo, J. H. (2013) Engineering of NADPH regenerators in Escherichia coli for enhanced biotransformation. *Appl. Microbiol. Biotechnol. 97*, 2761−72.

(9) Aslan, S., Noor, E., and Bar-Even, A. (2017) Holistic bioengineering: rewiring central metabolism for enhanced bioproduction. *Biochem. J. 474*, 3935−3950.

(10) Zhang, L., King, E., Luo, R., and Li, H. (2018) Development of a High-Throughput, In Vivo Selection Platform for NADPH-Dependent Reactions Based on Redox Balance Principles. *ACS Synth. Biol. 7*, 1715−1721.

(11) van der Donk, W. A., and Zhao, H. (2003) Recent developments in pyridine nucleotide regeneration. *Curr. Opin. Biotechnol. 14*, 421−6.

(12) Tishkov, V. I., and Popov, V. O. (2006) Protein engineering of formate dehydrogenase. *Biomol. Eng. 23*, 89−110.

(13) Johannes, T. W., Woodyer, R. D., and Zhao, H. (2007) Efficient regeneration of NADPH using an engineered phosphite dehydrogenase. *Biotechnol. Bioeng. 96*, 18.

(14) Sauer, U., Canonaco, F., Heri, S., Perrenoud, A., and Fischer, E. (2004) The soluble and membrane-bound transhydrogenases UdhA and PntAB have divergent functions in NADPH metabolism of Escherichia coli. *J. Biol. Chem. 279*, 6613−9.

(15) Kabir, M. M., and Shimizu, K. (2004) Metabolic regulation analysis of icd-gene knockout Escherichia coli based on 2D electrophoresis with MALDI-TOF mass spectrometry and enzyme activity measurements. *Appl. Microbiol. Biotechnol. 65*, 84−96.

(16) Bocanegra, J. A., Scrutton, N. S., and Perham, R. N. (1993) Creation of an NADP-dependent pyruvate dehydrogenase multienzyme complex by protein engineering. *Biochemistry 32*, 2737−40.




DOI: 10.1021/acssynbio.8b00313
*ACS Synth. Biol.* 2018, 7, 2742−2749

(17) Bar-Even, A., Noor, E., Savir, Y., Liebermeister, W., Davidi, D., Tawfik, D. S., and Milo, R. (2011) The moderately efficient enzyme: evolutionary and physicochemical trends shaping enzyme parameters. *Biochemistry 50*, 4402−10.
(18) Braatsch, S., Helmark, S., Kranz, H., Koebmann, B., and Jensen, P. R. (2008) Escherichia coli strains with promoter libraries constructed by Red/ET recombination pave the way for transcriptional fine-tuning. *BioTechniques 45*, 335−7.
(19) Wenk, S., Yishai, O., Lindner, S. N., and Bar-Even, A. (2018) An Engineering Approach for Rewiring Microbial Metabolism. *Methods Enzymol. 608*, 329−367.
(20) Fischer, E., and Sauer, U. (2003) A novel metabolic cycle catalyzes glucose oxidation and anaplerosis in hungry Escherichia coli. *J. Biol. Chem. 278*, 46446−51.
(21) Cobessi, D., Tete-Favier, F., Marchal, S., Azza, S., Branlant, G., and Aubry, A. (1999) Apo and holo crystal structures of an NADP-dependent aldehyde dehydrogenase from Streptococcus mutans. *J. Mol. Biol. 290*, 161−73.
(22) Takeno, S., Murata, R., Kobayashi, R., Mitsuhashi, S., and Ikeda, M. (2010) Engineering of Corynebacterium glutamicum with an NADPH-generating glycolytic pathway for L-lysine production. *Appl. Environ. Microbiol. 76*, 7154−60.
(23) Marchal, S., Rahuel-Clermont, S., and Branlant, G. (2000) Role of glutamate-268 in the catalytic mechanism of nonphosphorylating glyceraldehyde-3-phosphate dehydrogenase from Streptococcus mutans. *Biochemistry 39*, 3327−35.
(24) Sauer, U., and Eikmanns, B. J. (2005) The PEP-pyruvate-oxaloacetate node as the switch point for carbon flux distribution in bacteria. *FEMS Microbiol Rev. 29*, 765−94.
(25) Hoelsch, K., Suhrer, I., Heusel, M., and Weuster-Botz, D. (2013) Engineering of formate dehydrogenase: synergistic effect of mutations affecting cofactor specificity and chemical stability. *Appl. Microbiol. Biotechnol. 97*, 2473−81.
(26) Falke, D., Schulz, K., Doberenz, C., Beyer, L., Lilie, H., Thiemer, B., and Sawers, R. G. (2010) Unexpected oligomeric structure of the FocA formate channel of Escherichia coli: a paradigm for the formate-nitrite transporter family of integral membrane proteins. *FEMS Microbiol. Lett. 303*, 69−75.
(27) Haverkorn van Rijsewijk, B. R., Kochanowski, K., Heinemann, M., and Sauer, U. (2016) Distinct transcriptional regulation of the two Escherichia coli transhydrogenases PntAB and UdhA. *Microbiology 162*, 1672−1679.
(28) Yishai, O., Lindner, S. N., Gonzalez de la Cruz, J., Tenenboim, H., and Bar-Even, A. (2016) The formate bio-economy. *Curr. Opin. Chem. Biol. 35*, 1−9.
(29) Yishai, O., Bouzon, M., Doring, V., and Bar-Even, A. (2018) In Vivo Assimilation of One-Carbon via a Synthetic Reductive Glycine Pathway in Escherichia coli. *ACS Synth. Biol. 7*, 2023.
(30) Jensen, S. I., Lennen, R. M., Herrgard, M. J., and Nielsen, A. T. (2016) Seven gene deletions in seven days: Fast generation of Escherichia coli strains tolerant to acetate and osmotic stress. *Sci. Rep. 5*, 17874.
(31) Thomason, L. C., Costantino, N., and Court, D. L. (2007) E. coli genome manipulation by P1 transduction. *Curr. Protoc Mol. Biol.*, 1.17.1.
(32) Baba, T., Ara, T., Hasegawa, M., Takai, Y., Okumura, Y., Baba, M., Datsenko, K. A., Tomita, M., Wanner, B. L., and Mori, H. (2006) Construction of Escherichia coli K-12 in-frame, single-gene knockout mutants: the Keio collection. *Mol. Syst. Biol. 2*, 2006−2008.
(33) Quan, J., and Tian, J. (2014) Circular polymerase extension cloning. *Methods Mol. Biol. 1116*, 103−17.
(34) Grote, A., Hiller, K., Scheer, M., Munch, R., Nortemann, B., Hempel, D. C., and Jahn, D. (2005) JCat: a novel tool to adapt codon usage of a target gene to its potential expression host. *Nucleic Acids Res. 33*, W526−31.
(35) Zelcbuch, L., Antonovsky, N., Bar-Even, A., Levin-Karp, A., Barenholz, U., Dayagi, M., Liebermeister, W., Flamholz, A., Noor, E., Amram, S., Brandis, A., Bareia, T., Yofe, I., Jubran, H., and Milo, R. (2013) Spanning high-dimensional expression space using ribosome-binding site combinatorics. *Nucleic Acids Res. 41*, No. e98.
(36) Flamholz, A., Noor, E., Bar-Even, A., and Milo, R. (2012) eQuilibrator–the biochemical thermodynamics calculator. *Nucleic Acids Res. 40*, D770−5.


DOI: 10.1021/acssynbio.8b00313
*ACS Synth. Biol.* 2018, 7, 2742−2749

# V. DISCUSSION

In the present study, an evolutionary approach was followed to obtain high methanol tolerant derivatives of two closely related methylotrophic strains, *Methylobacterium extorquens* TK 0001 and AM1. For these strains, methanol serves as sole carbon and energy source, but inhibits growth at concentrations above 1-1.5% (v/v). This limitation challenges the suitability of these organisms as production strains in industrial methanol fermentations.

The GM3 technology of continuous culture was used to perform the stepwise adaptation of cultures of the two strains to grow with up to 10% methanol. Since volatile ingredients of the growth media in a GM3 device are prone to be washed out by the constant air stream flowing through the growing cell suspensions, the methanol concentration in the growth chamber was monitored over time to verify the suitability of the technology for this adaptation. A 10% test medium was kept for four weeks under culture conditions and diluted twice a day. The methanol concentration was found to be stable during this period, just showing some fluctuations around the fixed mark of 10%.

Medium swap culture regimes were employed to select for higher methanol tolerance. This regime, which resembles a chemostat modified to enable the dilution of the culture by two growth media, was found to permit lineages with different genotypes and consequently differing in fitness to prevail in the population (Marlière et al., 2011). For this reason, following a swap adaptation, the GM3 were run under turbidostat mode. During this phase, through selection of fastest growing cells, the populations are genetically homogenized and generally establish a stable generation time. Above 7% methanol (1.7 M), the selection of very high tolerance was performed through incrementing the methanol concentration by 1% until 10% in turbidostat. This adaptation protocol was chosen to avoid prolonged swap periods and to expose the cells to high methanol at a stable concentration.

The evolution of strain TK 0001 to high methanol tolerance, the main objective of this study, took about 1000 generations. At 5%, 7% and 8% methanol, the culture was relaunched with an isolate, a strategy pursued to accelerate the adaptation. Approximately 250 generations accumulated between each of the plateaus. The 8% turbidostat period was characterized by fluctuations in the daily dilution pulses and was prolonged (72 days); the next two steps were ended after about 40 days each.

The growth curves of isolates obtained at different tolerance levels were recorded. It has to be pointed out that both the method and the number of biological replicates were crucial for the determination of valid growth profiles. Evaporation phenomena and oxygenation had to be taken into account for plate reader experiments, notably at high methanol concentrations. In addition, a cell-to-cell phenotypic heterogeneity particularly pronounced has been noticed for *M. extorquens* strains, attributed mainly to strong variations in the timing of the cell division within a population (Bergmiller and Ackermann, 2011; Strovas et al., 2007). For these reasons, a profound determination of growth phenotypes was not performed for all isolates obtained throughout the evolution. However, a growth comparison of isolates representing each tolerance level was done and showed differences. In addition, between isolates of the same tolerance level growth heterogeneity was observed.

Genomic sequencing of six isolates for each methanol tolerance level was performed. This large scale genotypic analysis was conducted to identify mutations responsible for increasing methanol tolerance. As could be deduced from the 1% to 5% medium swap profile, which took only 11 days (about 80 generations) and showed two sharp augmentations in the number of stressing pulses per 24h over this period (Figure 1B), only a few mutations were identified through comparison of the genome sequences between the isolates and the wildtype strain. Strikingly, little genotypic diversion was seen within this group of isolates. Among the three mutated loci, the *metY* gene (missense mutation T34M) specifying O-acetyl-L-homoserine sulfhydrylase has already been described to be related with a methanol resistance phenotype (Leßmeier and Wendisch, 2015).

In addition to the tree point mutations, a 50 kb chromosomal duplication common to all six isolates sequenced was found. Most of the 86 genes contained in this duplicated fragment code for proteins of unknown function. Among the annotated genes, a Ros-like transcriptional regulator is found. This zinc-finger protein belongs, together with the MucR regulator of plant and animal pathogens like *Brucella melitensis* (Mirabella et al., 2013), to a family of functional orthologs (Bouhouche et al., 2000). These regulators were found to modulate the cell envelope and to be involved in the resistance towards oxidative, saline and detergent stresses. They also downregulate the expression of biosynthetic genes of the bacterial flagella (Bahlawane et al., 2008). The multiplication of gene copies on the chromosome of cells adapted in the GM3 has previously been observed and a link between overexpression and the adapted phenotype

established (Döring et al., 2018; Souterre, 2017). Whether this is the case for the Ros regulator cannot easily be determined and would need further testing. No additional mutations shared by all isolates analyzed were found for the adaptations to 7 % in swap regime and the subsequent turbidostat adaptation to 8% methanol. The number of mutations accumulated during the evolution stayed low. This can be attributed to the employed strategy: after each adaptation plateau, the culture was reinitiated with an isolate. Towards the end of the adaptation, however, the number of mutations increased cumulating to eight common mutations for the final six isolates. Also, the 50kB chromosomal duplication persisted throughout the evolution, which is common in long-term evolution (Raeside et al., 2014).

In a parallel evolution in the GM3, *M. extorquens* AM1 was adapted to 10% methanol. A total of 1326 generations were accumulated to reach the final tolerance level. The two medium swap periods were longer than was observed for the TK 0001 strain (Table 32). In consequence, a higher number of mutations were found for the 5% tolerant isolates (including *metY* missense mutations). This trend persisted during the evolution, also reflecting the fact that the adaptation was performed for a single inoculum, contrary to TK 0001 adaptation where at each step of evolution an isolate were selected to be reinoculate. As was the case for TK 0001, the number of common mutations within the isolates of a tolerance-level group increased towards the end of the adaptation. By contrast, no chromosomal duplication was detected.

A.

| | MEM5 | MEM7 | MEM8 | MEM10 |
|---|---|---|---|---|
| Number of generations | 291 | 477 | 734 | 994 |

B.

| | AMM5 | AMM7 | AMM8 | AMM10 |
|---|---|---|---|---|
| Number of generations | 400 | 666 | 826 | 1326 |

**Table 32: Generation time between each step of population for *Methylobacterium extorquens* TK 0001 (MEM) and AM1 (B).**

It is obvious that the number of mutations which accumulated during both strain evolutions is low. The final isolates carried in total between 10 and 14 SNPs or indels at most. While this can be attributed to the clonal re-inoculation in the case of strain TK 0001, the initial cell population evolved all the way until 10% methanol in the case of strain AM1. As a comparison, Hu and coworkers adapted *M. extorquens* AM1 cells to higher butanol tolerance through serial dilutions counting a total of 300 generations (Hu et al., 2016). The adapted isolate sequenced contained around 30 verified mutations.

Several reasons could explain the low number of mutations:

- Tolerance to high methanol does not require a large number of mutations.
- Additional, non-beneficial mutations did not accumulate due to the turbidostat selection periods where only the fittest cells stay in the culture.
- The GM3 devices keep the cell population constantly at exponential growth. It is known that mutation events occur at stationary phase differing from those in exponential phase (Zambrano et al., 1993).

It is also noteworthy that no mutations occurred in the genes coding for proteins involved in the methanol assimilation pathway nor in genes involved in formaldehyde detoxification. This is in accordance with growth phenotypes of the methanol tolerant strain G4105 on formaldehyde and formate, which was not significantly altered with respect to the wildtype strain.

A completely different mutation pattern was found for the six 10% methanol isolates of the AM1 second chamber evolution (paragraph III.2.3). The average number of mutations was multiplied by ten, most probably due to a base pair deletion in the gene *mutS* implicated in error repair. Almost all of the mutations were transitions, as would be expected for impaired MutS activity. A total of 19 mutations were common to at least four of the six isolates sequenced. Several loci already found to carry missense mutations or indels in isolates of the two other evolutions were again affected. The apparent convergences between the mutational profiles obtained in three independent evolutions would need further analysis to unravel the mechanisms of enhanced methanol tolerance.

As was seen before, none of the genes implicated in C1 assimilation or formaldehyde detoxification were mutated. Since the first appearance of the *mutS* mutation in the population is not known, the influence of this mutational event on the overall methanol adaptation remains to be elucidated.

A clear connection between a mutated locus and the tolerance phenotype could be established for gene *metY*. This gene carried non-synonymous changes in all the isolates sequenced. The accumulation of loss of function mutations not affecting cell viability at this locus raises the question of the utility of this gene for the *M. extorquens* strains.

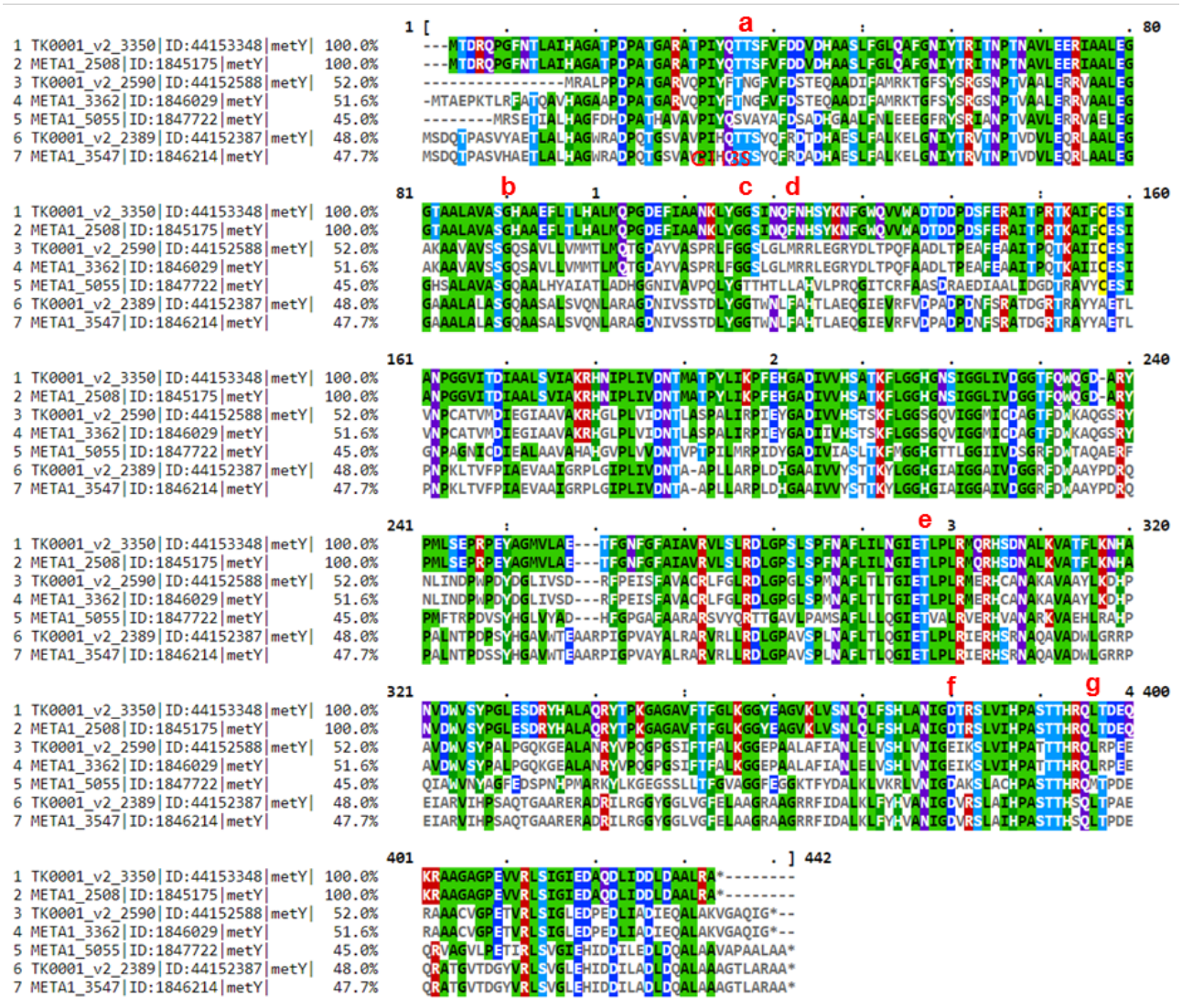


**Figure 46: Sequence comparison between all CDS annoted as *metY* in *Methylobacterium extorquens* TK 0001 (sequence: 1, 3, 6) and AM1 (sequence: 2, 4, 5, 7). Each amino acid mutated during high methanol adaptation is marked by a red letter: a for T34M, b for G87S, c for G113S, d for F119L, e for T290A, f for D373G and g for L389F. The percentage of homology between the CDS 1 and 2 (*metY* containing the mutations, identical sequence) and the other putative *metY* genes is indicated.**

Possibly, a functional O-acetyl-L-homoserine sulfhydrylase widens the methionine precursor reservoir to compounds like methanethiol and dimethyl disulfide which can be used by the enzyme to directly add the terminal S-$CH_3$ group to O-acetyl-L-homoserine to form methionine, as has been shown for MetY from *Corynebacterium glutamicum* (Bolten et al., 2010). Methanol at concentrations toxic for the cells through the MetY side reaction are not likely to be found in the cell's natural habitat.

The methionine biosynthetic pathways of *M. extorquens* have not been studied in detail. As deduced from annotated genes coding for homoserine acetylation, the strains possess panoply of different biosynthesis routes (Figure 35). In this study, the activity of MetY as sulfhydrylase was experimentally shown. In addition, both TK 0001 and AM1 genomes harbor two to three genes also annotated as *metY*. The proteins show around 50% sequence identity with MetY but vary among each other (Figure 46). Is not clear whether these proteins are involved in methionine biosynthesis, being susceptible to add to the methanol toxicity in this case. It is noteworthy that methionine is a target for oxidative stress in the cells (Ezraty et al., 2017). A multiple guaranteed biosynthesis might assure the supply of this crucial amino acid under stress conditions.

As was discussed above, with the exception of *metY*, a direct relation between the few mutations found in the methanol tolerant isolates and the phenotypes of the cells cannot easily be demonstrated. Also, growth profiles on methanol of isolates obtained from the same methanol resistance point were different. These observations pointed to adaptive responses of the cells at the regulatory level of gene expression, as has been found for other stress adaptations. Therefore, a transcriptomic analysis was conducted for the TK 0001 derived strain G4105, which grows stably at 5% methanol, and compared to the wild type. For the short-term response (5 minutes growth on 5% methanol), the most striking differences in expression pattern concerning protein functional families were the following:

- Downregulation of cytochromes and cytochrome oxidases in the TK 0001 wildtype, upregulation in the mutant.
- Downregulation of cell division proteins in the TK 0001 wildtype.
- Stronger downregulation of ribosomal proteins in the TK 0001 wildtype.

- Strong upregulation of certain heat shock and chaperone proteins in the TK 0001 wildtype.

Obviously, the wildtype cells were more perturbed in activities concerning energy production and cell proliferation than the adapted cells. For the long-term expression response (3 hours growth on 5% methanol), the overexpression by the adapted cells of genes involved in $Fe^{3+}$ uptake was noticeable. From these results, it can be concluded that pleiotropic changes in regulation patterns concerning cell proliferation occurred in the cells during adaptation. This becomes also apparent from the expression differences seen after 3 hours of growth in a permissive medium containing 1% methanol. For the adapted cells, the number of overexpressed or repressed genes was more than 3 times higher than for the wildtype cells.
Like what was found for the mutations, the genes directly involved in methanol assimilation were not differentially expressed in a significant amount. However, strain G4105 was found to produce more biomass from 1% methanol than the TK 0001 wild type. A possible production yield difference of a compound directly derived from the central carbon metabolism, D-lactate, was tested by overexpressing the native gene *ldhA*. Adapted cells grown in 1% methanol did produce more D-lactate than the wildtype cells, which is in accordance with the differences in growth phenotype.
The growth of wildtype cells in 5% methanol overexpressing *ldhA* was an unexpected finding which cannot be explained easily. Possibly, the massive inflow of methanol in the cells and its oxidation to formaldehyde and formate deregulates the $NADH/NAD^+$ pool ratio. Reduction of pyruvate to lactate with NADH as cofactor might contribute to regain equilibrium. Alternatively, the enzyme might reduce toxic cellular aldehydes to less toxic alcohol derivatives.

As the second proof of principle, we decided to produce 3-hydroxypropionic acid from malonyl-CoA. That part hasn't been achieved, but promising vectors were built. In fact, an enzymatic screening allowed to select more efficient enzyme to produce this compound. But numerous options can improve the production, the 3-HP production consumed 2 NADPH, as for the NADH/NAD+ balance it could be interesting to find an enzyme to regenerate this metabolite. We worked on this question in *E. coli* strain by building a sensor strain for testing regeneration of NADPH in vivo (Lindner et al., 2018).

Besides the toxicity of the growth substrate methanol, the high oxygen demand of *M. extorquens* strains as strict aerobic bacteria can be an obstacle to efficient upscaling of industrial methanol fermentations. The composition of the gas aerating the cultures growing in GM3 automatons can be modulated. Mixtures of compressed air and nitrogen can be programmed thus fixing the oxygen content at concentrations lower than the 21% present in the atmosphere. This setup makes the GM3 devices ideal tools for the adaptation of microbial strains to growth under oxygen limiting conditions.

*M. extorquens* AM1 cells adapted to growth with low oxygen were selected in 1% methanol permissive medium in turbidostat. It was noticed that the oxygen content of the aeration gas could be lowered to 6.3 % (volume ratio air/nitrogen of 30/70) without a significant increase in generation time. However, the sudden growth acceleration of the culture pointed to a real $O_2$ limitation of growth at this oxygen percentage. An alternative explication would be a sudden gain in the C1 assimilation concomitant with an increase in cell division. However, none of the cultures grown with 1% methanol have ever shown such a growth behavior. Loss of function mutations of gene *metY* (L389F, paragraph III.2.4) were found in sequenced isolates obtained from the culture before the drop-in generation time and cannot be the cause of this selection event.
The same is true for the M270I missense mutation of gene *coxA* coding for subunit 1 of cytochrome c oxidase which appeared late in the evolution (Figure 40). However, this subunit of complex IV of the respiratory chain harbors the heme-copper binuclear center, the active site for oxygen reduction of the protein complex (Wikström et al., 2018). The appearance of a mutated allele of the CoxA peptide in a culture grown under $O_2$ limitation is likely to be linked to this selection pressure. Furthermore, the mutation was fixed quickly in the population.

The cytochrome c oxidases of *Rhodobacter sphaeroidis* and *Paracoccus denitrificans* have been well studied. CoxA of *M. extorquens* AM1 shows 60% identity with the homologous protein of these bacteria. They carry an isoleucine at position 270, showing the M to I change of CoxA* in the adapted cells to be very conservative. Further phenotypic, genetic and biochemical work is needed to elucidate the impact of this mutation in the *Methylobacterium* context.

The present study demonstrates the power of the GM3 technology for microbial strain evolution. Methylotrophic strains growing with 10% methanol (2.4M) have not been described before. The pleiotropic aspect of the adaptation events, notably concerning the gene expression profiles, does not come as a surprise. Methanol procuring all biomass carbon and energy and at the same time being toxic for the cells must necessarily trigger multiple cellular reactions when present in non-optimal concentrations. Further analysis of the cellular machinery would benefit from metabolomics to study cellular pools of central carbon metabolites and redox cofactors. The introduction of gene mutations found in all or multiple isolates in the wildtype cells and test for methanol resistance could verify genotype-phenotype relationships. Likewise, the overexpression of genes which were found upregulated in methanol stressed cells, notably certain members of the heat shock proteins, could enable valid testing of their effects on methanol tolerance.

# SUPPLEMENTARY DATA

**Table S1: Library of inducible or not promoters tested in *Methylobacterium extorquens***

| Promoters | Under control |
|---|---|
| PmxaF | Methanol |
| Plac | IPTG |
| PfumC | constitutif |
| PcoxB | constitutif |
| Ptuf | constitutif |
| Pr | DnaA protein |
| Psyn2 | cumate |
| PalkB | carbone sources |
| Pmmo | cuivre |
| pQ5 | cumate |

A.

| Nanopore | | |
|---|---|---|
| | **Flowcell 1** | **Flowcell 2** |
| Number of Reads | 83 225 | 103 547 |
| Number of bp | 355 398 006 | 450 731 025 |
| Average Size (bp) | 4 270bp | 4 353bp |
| N50 (bp) | 5 986bp | 6 027bp |
| Max Size (bp) | 21 118bp | 35 232bp |
| Coverage | 59X | 75X |
| Total coverage | 134X | |
| Total coverage with reads > 10Kb | 10X | |

B.

| Illumina | |
|---|---|
| | **Run 1** |
| Number of Reads | 3 369 986 |
| Number of bp | 1 017 735 772 |
| Read Size (bp) | 151 bp |
| Coverage | 170X |

C.

| Assembly performed using smartdenovo* (k=17 with reads >5Kbp) | |
|---|---|
| **Assembler** | **smartdenovo** |
| Number of contigs | 1 |
| Cumulative size | 5 687 580bp |
| %GC | 68.23 |

| Polishing with Illumina short reads using Pilon* | |
|---|---|
| | **Final assembly** |
| Number of contigs | 1 |
| Cumulative size | 5 715 512bp |
| %GC | 68.28 |

| Illumina short only assembly using Spades* | |
|---|---|
| | **Final assembly** |
| Number of contigs | 1 326 |
| Cumulative size | 6 564 822bp |
| %GC | 68.30 |

**Figure S1: Summary of Nanopore data (A), Illumina data (B) and Assemblage data (C).**

A.

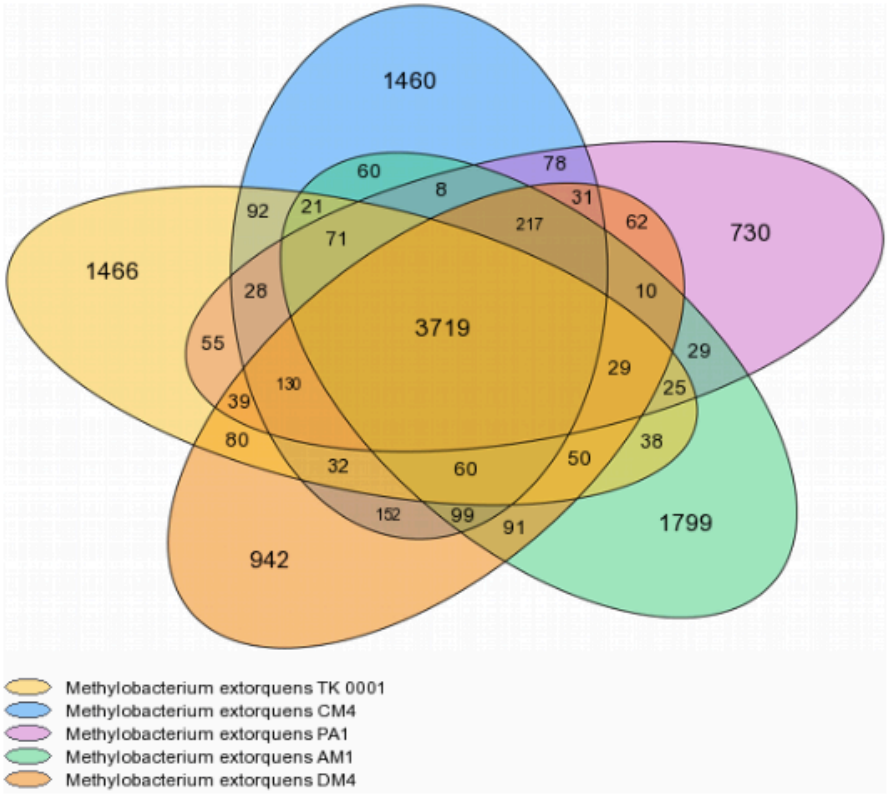


B.

| *Methylobacterium extorquens* strain | Core CDS (%) | Var CDS (%) | Strain specific (%) |
|---|---|---|---|
| AM1 | 57.1 | 42.9 | 27.7 |
| CM4 | 58.7 | 41.3 | 23.3 |
| DM4 | 63.9 | 36.1 | 16.1 |
| PA1 | 70.5 | 29.5 | 13.8 |
| TK 0001 | 62.0 | 38.0 | 24.3 |

**Figure S2: Pan-Core Genome analysis of the *Methylobacterium extorquens* genome: AM1, CM4, DM4, PA1 and TK 0001 from MicroScope platform using 80% amino acid identity on 80% coverage. Venn diagram representing the distribution of the number of Core, variant at specific CDS between each strains (A), and the evaluation in percentage of these values (B).**

**Table S2: DNA sequence for each selected isolate from the evolved population from *M. extorquens* TK 0001 (A) and AM1 (B) and their accession number.**

A.

| Population | Strain number | AC number |
|---|---|---|
| MEM5 | G4102 | ERS2573818 |
| | G4103 | ERS2573819 |
| | G4104 | ERS2573820 |
| | G4105 | ERS2573821 |
| | G4106 | ERS2573822 |
| | G4107 | ERS2573823 |
| MEM7 | G4198 | ERS2781879 |
| | G4199 | ERS2781789 |
| | G200 | ERS2781778 |
| | G4201 | ERS2781794 |
| | G4202 | ERS2781878 |
| | G4203 | ERS2781777 |
| MEM8 | G4363 | ERS2781791 |
| | G4364 | ERS2781790 |
| | G4365 | ERS2781793 |
| | G4366 | ERS2781792 |
| | G4367 | ERS2781776 |
| | G4368 | ERS2781786 |
| MEM10 | G4518 | ERS2573824 |
| | G4519 | ERS2573825 |
| | G4520 | ERS2573826 |
| | G4521 | ERS2573827 |
| | G4522 | ERS2573828 |
| | G4523 | ERS2573829 |

B.

| Population | Strain number | AC number |
|---|---|---|
| AMM5 | G4606 | ERS2781831 |
| | G4607 | ERS2781830 |
| | G4608 | ERS2781829 |
| | G4609 | ERS2773665 |
| | G4610 | ERS2781833 |
| | G4611 | ERS2781832 |
| AMM7 | G4635 | ERS2802203 |
| | G4636 | ERS2802204 |
| | G4637 | ERS2802205 |
| | G4638 | ERS2802206 |
| | G4639 | ERS2802207 |
| | G4640 | ERS2802208 |
| AMM8 | G4597 | ERS2802209 |
| | G4598 | ERS2802210 |
| | G4599 | ERS2802211 |
| | G4600 | ERS2802212 |
| | G4601 | ERS2802213 |
| | G4602 | ERS2802214 |
| AMM10 | G4703 | ERS2802215 |
| | G4704 | ERS2802216 |
| | G4705 | ERS2802217 |
| | G4706 | ERX2857349 |
| | G4707 | ERS2802218 |
| | G4708 | ERS2802219 |

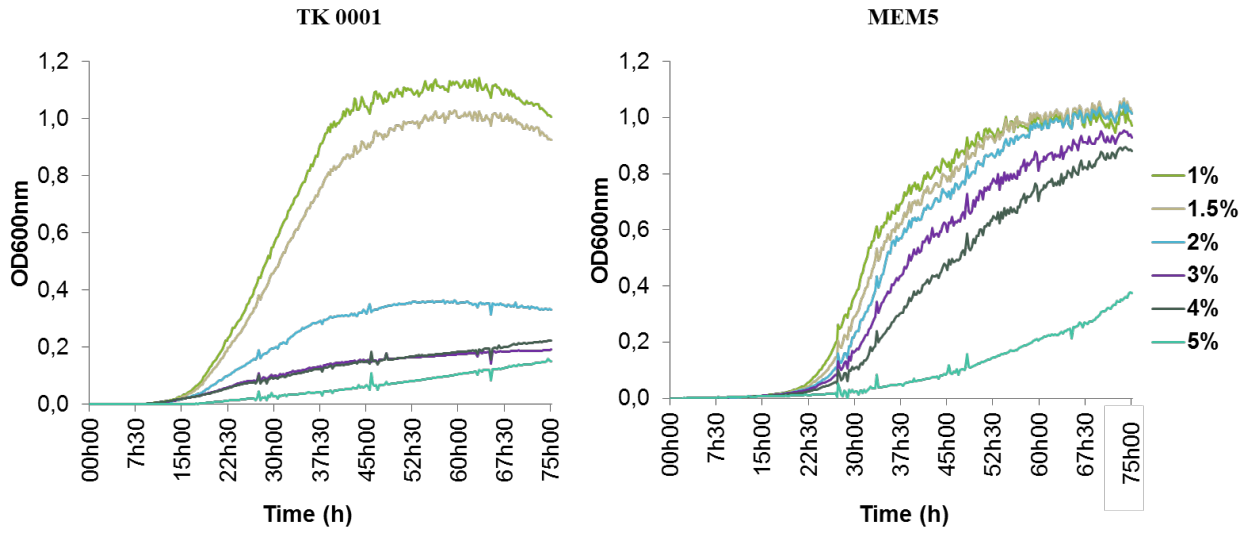


**Figure S3: Growth profile of *M. extorquens* TK 0001 and MEM5 population in smm supplemented with methanol between 1% to 5%.**

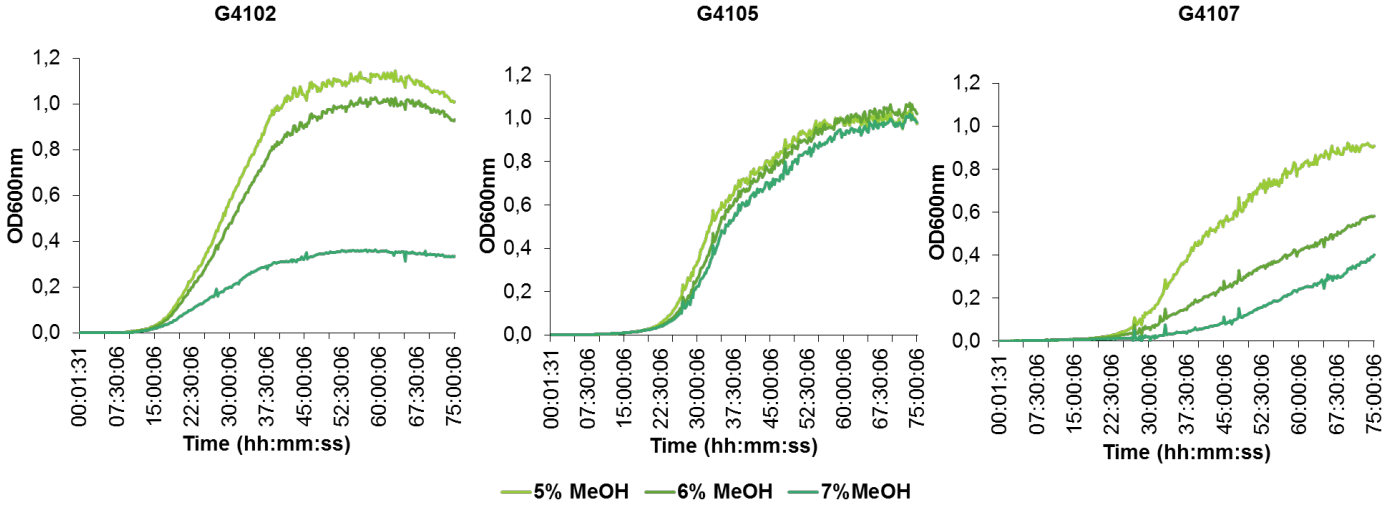


**Figure S4: Growth profile of 3 isolates from MEM5 population in smm supplemented with 5%, 6% or 7% MeOH.**

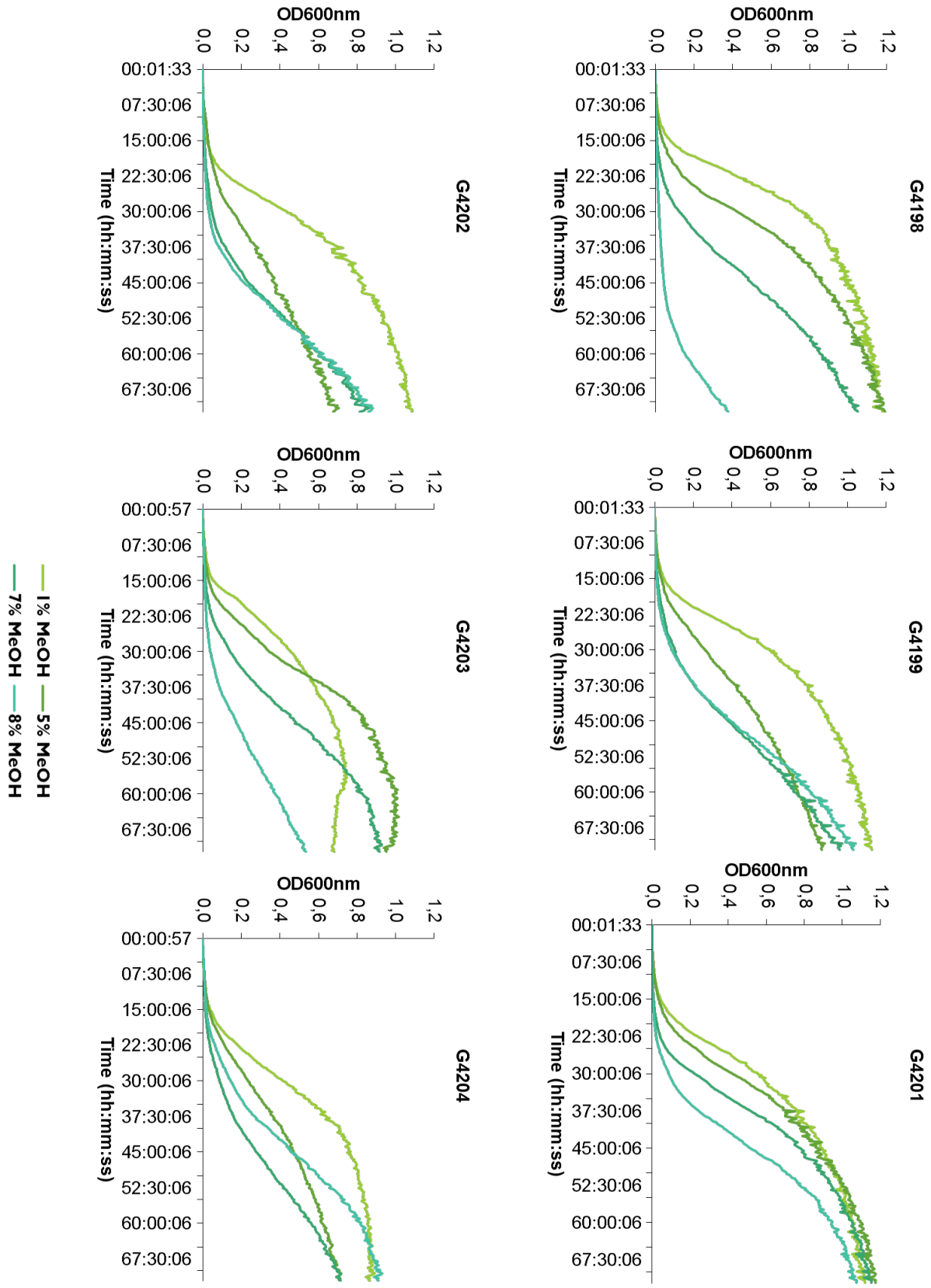


**Figure S5: Growth profile of isolates from MEM7 population in smm supplemented with 1%, 5%, 7% and 8% MeOH.**

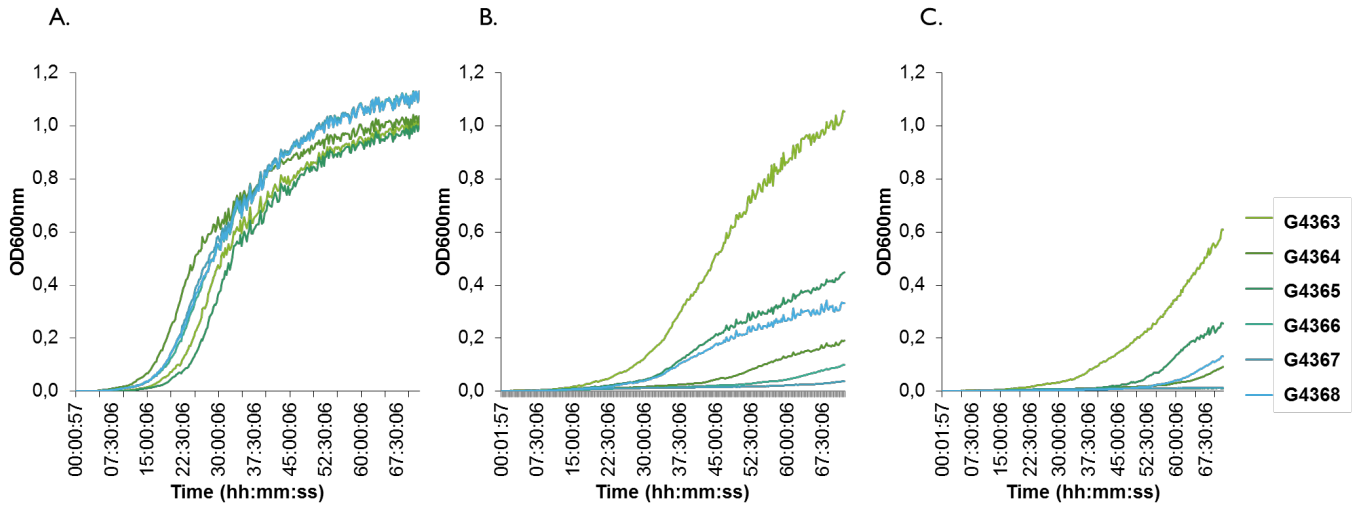


**Figure S6: Growth profile of isolates from MEM8 population in smm supplemented with 1% (A), 8% (B) and 9% (C).**

**Table S3: Mutations identified in the evolved derivatives of *M. extorquens* TK 0001 isolated at each step of progressive adaptation to higher concentrations of methanol, 5 % (A), 7 % (B), 8 % (C) and 10 % (D) (v/v).**

A

| chromosomal position | mutation type | mutation event | mutated gene | amino acid change | intergenic mutation (distance to the flanking gene) | G4103 | G4104 | G4105 | G4106 | G4107 | G4102 |
|---|---|---|---|---|---|---|---|---|---|---|---|
| 1592421 | DEL | C/- | putative membrane protein | | | . | . | . | . | . | . |
| 3075219 | SNP | C/T | metY | T34M | | . | . | . | . | . | . |
| 3450711 | SNP | T/C | ATP-binding region, ATPase-like | T16A | | . | . | . | . | . | . |
| 3821930 | DEL | T/- | dxs | | | . | . | . | . | . | . |
| 5157303 | SNP | A/C | | | conserved exported protein of unknown function/ protein of unknown function (269/130) | . | . | . | . | . | . |
| 5364370 | SNP | G/A | | | putative integral membrane protein/ protein of unknown function (347/122) | | | . | | . | . |
| 5486609 | DEL | G/- | protein of unknown function/protein of unknown function | | | . | . | . | . | . | . |
| 5490464 | SNP | A/C | | | conserved protein of unknown function/Porin (317/130) | . | . | . | . | . | . |
| 5670518 | SNP | T/C | | | conserved protein of unknown function/transposase of ISMdi14, IS110 family (433/61) | . | . | . | . | . | . |

B

| chromosomal position | mutation type | mutation event | mutated gene | amino acid change | intergenic mutation (distance to the flanking gene) | G4198 | G4201 | G4202 | G4203 | G4199 | G4200 |
|---|---|---|---|---|---|---|---|---|---|---|---|
| 1530584 | SNP | C/G | transposase | G121A | | | | | | | . |
| 3075219 | SNP | C/T | metY | T34M | | . | . | . | . | . | . |
| 3280633 | SNP | G/A | | | gapA/conserved protein of unknown function (199/264) | . | . | . | | . | |
| 3450711 | SNP | T/C | ATP-binding region, ATPase-like | T16A | | . | . | . | . | . | . |
| 3821930 | DEL | T/- | dxs | | | . | . | . | . | . | . |
| 3849306 | DEL | G/- | glycosyl transferase | | | | | | . | | |
| 3912422 | SNP | G/T | | | sga/conserved protein of unknown function (561/263) | | | | . | | |
| 4053716 | DEL | G/- | type I secretion membrane fusion protein, HlyD family | | | | | | | | . |
| 4133435 | SNP | T/G | putative glycoside hydrolase/deacetylase | H236P | | | | | | | . |
| 4425495 | SNP | A/G | Putative CelB-like protein | L338P | | . | . | . | | . | |

C

| chromosomal position | mutation type | mutation event | mutated gene | amino acid change | intergenic mutation (distance to the flanking gene) | G4363 | G4364 | G4365 | G4366 | G4367 | G4368 |
|---|---|---|---|---|---|---|---|---|---|---|---|
| 3009825 | SNP | G/C | cckA | V683L | | | | | . | | |
| 3009835 | SNP | G/A | cckA | R686Q | | | | . | | . | . |
| 3075219 | SNP | C/T | metY | T34M | | . | . | . | . | . | . |
| 3280633 | SNP | G/A | | | gapA/conserved protein of unknown function (199/264) | | . | . | . | . | |
| 3450711 | SNP | T/C | ATP-binding region, ATPase-like | T16A | | . | . | . | . | . | . |
| 3496506 | SNP | G/A | rpsL | R94C | | . | . | | | | |
| 3821930 | DEL | T/- | dxs | | | . | . | . | . | . | . |
| 4425495 | SNP | A/G | Putative CelB-like protein | L338P | | | . | . | . | . | . |
| 4453892 | SNP | C/T | conserved exported protein of unknown function | R55C | | . | | | | | |

D

| chromosomal position | mutation type | mutation event | mutated gene | amino acid change | intergenic mutation (distance to the flanking gene) | G4518 | G4519 | G4520 | G4521 | G4522 | G4523 |
|---|---|---|---|---|---|---|---|---|---|---|---|
| 61901 | INS | -/C | Glycosyl transferase family 2 | | | . | | | | | |
| 1044163 | DEL | C/- | | | protein of unknown function/ hrpB | . | . | . | . | . | . |
| 1044164 | DEL | C/- | | | protein of unknown function/ hrpB | . | . | . | . | . | . |
| 1592421 | DEL | C/- | putative membrane protein | | | . | . | . | . | . | . |
| 2811931 | SNP | C/A | | | putative type I secretion system ATPase/pufC (115/283) | . | . | . | . | . | |
| 3075219 | SNP | C/T | metY | T34M | | . | . | . | . | . | . |
| 3280633 | SNP | G/A | | | gapA/conserved protein of unknown function (199/264) | . | . | . | . | . | . |
| 3382459 | SNP | G/A | ybhL | G134D | | | | . | | | |
| 3450711 | SNP | T/C | ATP-binding region, ATPase-like | T16A | | . | . | . | . | . | . |
| 3495847 | SNP | T/C | rpsG | Y154C | | | | | | | . |
| 3496069 | SNP | A/C | rpsG | V80G | | . | . | . | . | . | . |
| 3496506 | SNP | G/A | rpsL | R94C | | . | . | . | . | . | . |
| 3815109 | SNP | C/G | shc | E508D | | | | | | | . |
| 3821930 | DEL | T/- | dxs | | | . | . | . | . | . | . |
| 4425495 | SNP | A/G | Putative CelB-like protein | L338P | | . | . | . | . | . | . |
| 4453892 | SNP | C/T | conserved exported protein of unknown function | R55C | | . | . | . | . | . | . |
| 5486609 | DEL | G/- | | | protein of unknown function/protein of unknown function | . | . | . | . | . | . |

**Table S4: List of the 86 ORF containing in the chromosomal duplication in evolved *M. extorquens* TK 0001 strains.**

| Gene label | Description of the mutated gene/locus |
|---|---|
| TK0001_v2_0506 | conserved protein of unknown function |
| TK0001_v2_0507 | conserved protein of unknown function |
| TK0001_v2_0508 | conserved exported protein of unknown function |
| TK0001_v2_0509 | DNA polymerase V, subunit C |
| TK0001_v2_0510 | Peptidase S24 and S26 domain protein |
| TK0001_v2_0511 | conserved protein of unknown function |
| TK0001_v2_0512 | conserved protein of unknown function |
| TK0001_v2_0513 | conserved protein of unknown function |
| TK0001_v2_0514 | conserved protein of unknown function |
| TK0001_v2_0515 | exported protein of unknown function |
| TK0001_v2_0516 | conserved protein of unknown function |
| TK0001_v2_0517 | conserved protein of unknown function |
| TK0001_v2_0518 | conserved protein of unknown function |
| TK0001_v2_0519 | conserved protein of unknown function |
| TK0001_v2_0520 | conserved exported protein of unknown function |
| TK0001_v2_0521 | conserved protein of unknown function |
| TK0001_v2_0522 | exported protein of unknown function |
| TK0001_v2_0523 | protein of unknown function |
| TK0001_v2_0524 | protein of unknown function |
| TK0001_v2_0525 | conserved exported protein of unknown function |
| TK0001_v2_0526 | protein of unknown function |
| TK0001_v2_0527 | protein of unknown function |
| TK0001_v2_0528 | conserved protein of unknown function |
| TK0001_v2_0529 | protein of unknown function |
| TK0001_v2_0530 | conserved protein of unknown function |
| TK0001_v2_0531 | conserved protein of unknown function |
| TK0001_v2_0532 | protein of unknown function |
| TK0001_v2_0533 | conserved protein of unknown function |
| TK0001_v2_0534 | protein of unknown function |
| TK0001_v2_0535 | conserved protein of unknown function |
| TK0001_v2_0536 | protein of unknown function |
| TK0001_v2_0537 | conserved protein of unknown function |
| TK0001_v2_0538 | conserved protein of unknown function |
| TK0001_v2_0539 | transposase (fragment) |
| TK0001_v2_0540 | transposase |
| TK0001_v2_0541 | protein of unknown function |
| TK0001_v2_0542 | protein of unknown function |
| TK0001_v2_0543 | protein of unknown function |
| TK0001_v2_0544 | conserved protein of unknown function |
| TK0001_v2_0545 | Phage terminase, large subunit, PBSX family |
| TK0001_v2_0546 | conserved protein of unknown function |
| TK0001_v2_0547 | conserved exported protein of unknown function |
| TK0001_v2_0548 | conserved protein of unknown function |
| TK0001_v2_0549 | conserved protein of unknown function |
| TK0001_v2_0550 | Integrase family protein |
| TK0001_v2_0551 | conserved protein of unknown function |
| TK0001_v2_0552 | protein of unknown function |
| TK0001_v2_0553 | conserved protein of unknown function |
| TK0001_v2_0554 | protein of unknown function |
| TK0001_v2_0555 | conserved protein of unknown function |
| TK0001_v2_0556 | protein of unknown function |
| TK0001_v2_0557 | Transcriptional regulatory protein ros |
| TK0001_v2_0558 | protein of unknown function |
| TK0001_v2_0559 | conserved protein of unknown function |
| TK0001_v2_0560 | conserved protein of unknown function |
| TK0001_v2_0561 | conserved protein of unknown function |
| TK0001_v2_0562 | protein of unknown function |
| TK0001_v2_0563 | protein of unknown function |
| TK0001_v2_0564 | conserved protein of unknown function |
| TK0001_v2_0565 | conserved protein of unknown function |
| TK0001_v2_0566 | conserved protein of unknown function |
| TK0001_v2_0567 | conserved protein of unknown function |
| TK0001_v2_0568 | Cyclic nucleotide-binding domain protein |
| TK0001_v2_0569 | conserved protein of unknown function |
| TK0001_v2_0570 | protein of unknown function |
| TK0001_v2_0571 | protein of unknown function |
| TK0001_v2_0572 | conserved protein of unknown function |
| TK0001_v2_0573 | protein of unknown function |
| TK0001_v2_0574 | protein of unknown function |
| TK0001_v2_0575 | conserved protein of unknown function |
| TK0001_v2_0576 | protein of unknown function |
| TK0001_v2_0577 | protein of unknown function |
| TK0001_v2_0578 | protein of unknown function |
| TK0001_v2_0579 | protein of unknown function |
| TK0001_v2_0580 | protein of unknown function |
| TK0001_v2_0581 | conserved protein of unknown function |
| TK0001_v2_0582 | protein of unknown function |
| TK0001_v2_0583 | YqaJ-like viral recombinase |
| TK0001_v2_0584 | conserved protein of unknown function |
| TK0001_v2_0585 | protein of unknown function |
| TK0001_v2_0586 | protein of unknown function |
| TK0001_v2_0587 | conserved protein of unknown function |
| TK0001_v2_0588 | conserved protein of unknown function |
| TK0001_v2_0589 | conserved protein of unknown function |
| TK0001_v2_0590 | conserved protein of unknown function |
| TK0001_v2_0591 | Phage integrase family |

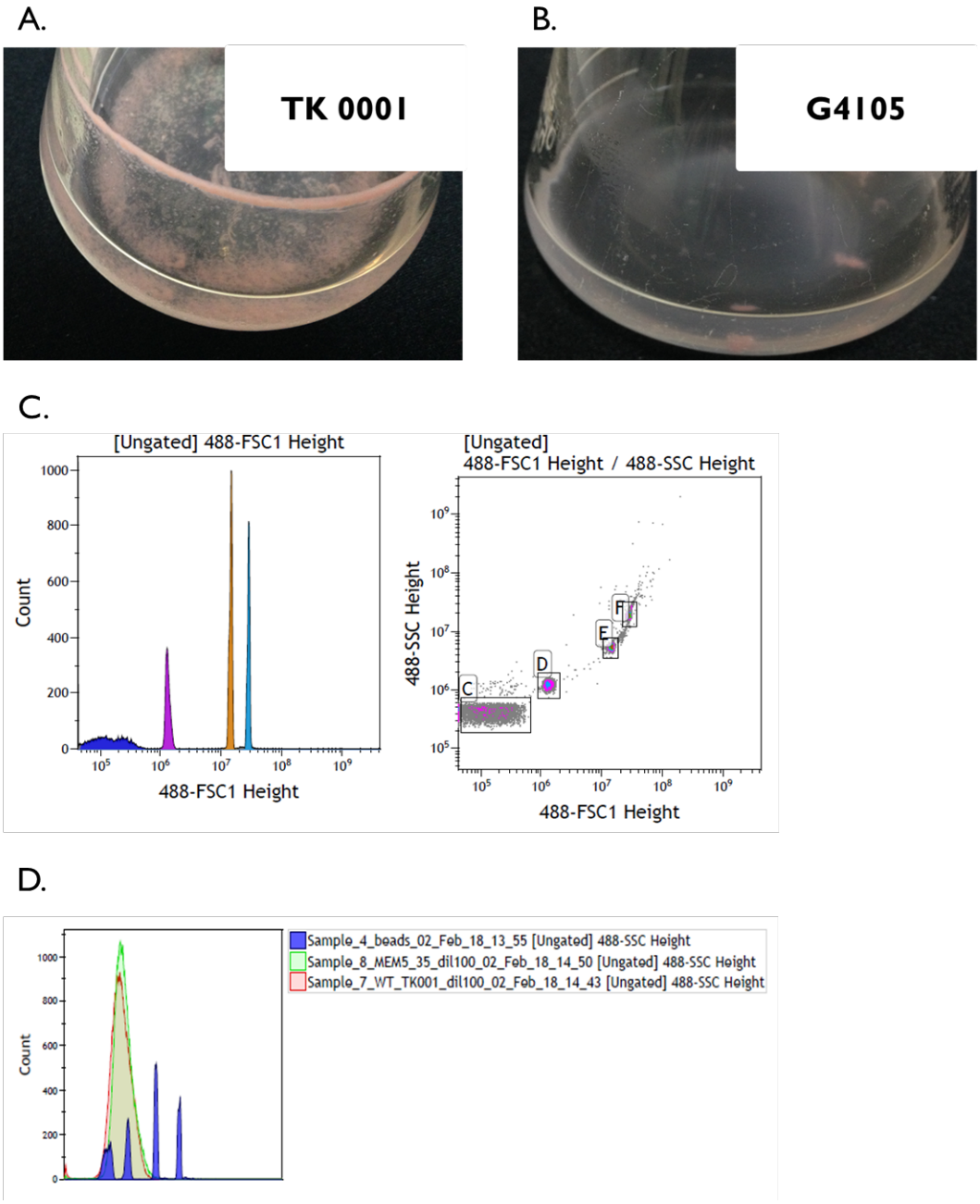


**Figure S7: Phenotypic difference between TK 0001 and the evolved strain G4105. (A) and (B) show the aspect of culture growth and biofilm formation. (C) and (D) shows Facs analysis of size of Methylobacterium extorquens TK 0001 (red pic) and G4105 (green pic). Four beads with different size were passed with the filter 481: 0.22µm (dark blue), 0.45µm (pink), 0.88µm (orange), 1.35µm (light blue) (C). 100 000 cells were analyzed for each sample, the experimentation was done in replicate (D).**

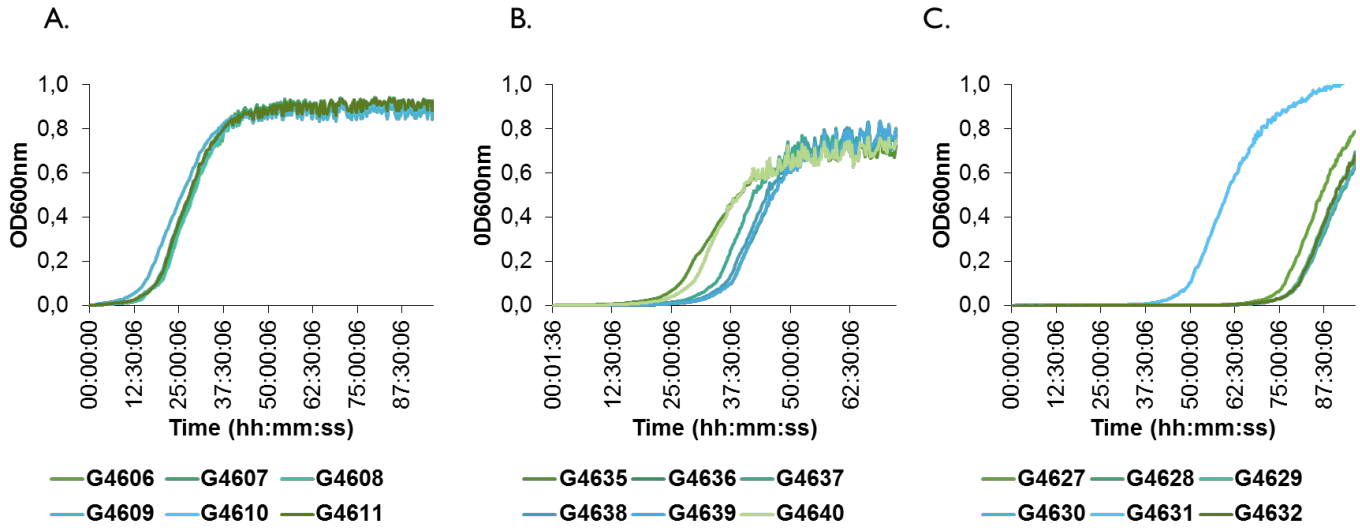


**Figure S8: Growth profile of isolate from AMM5 (A), AMM7 (B), AMM8 (C) population in smm supplemented with 1%.**

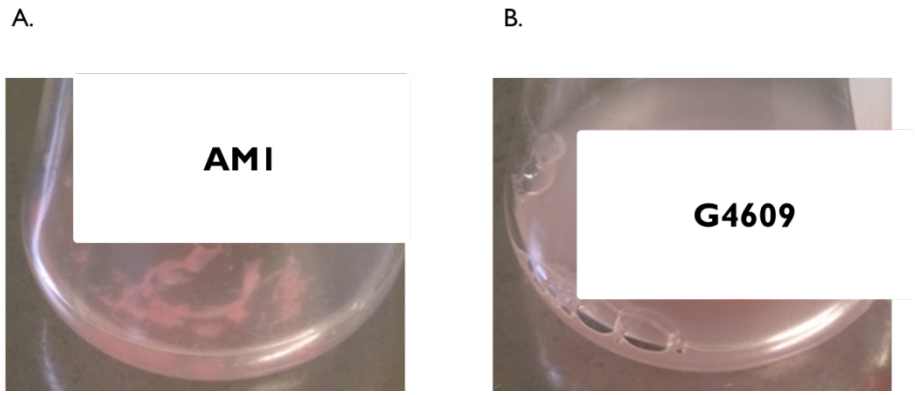


**Figure S9: Growth aspect of cultures of *Methylobacterium extorquens* AM1 and the evolved isolate G4609 (mineral 1% methanol medium, 48 hours growth).**

**Table S5: Mutations identified in the evolved derivatives of *M. extorquens* AM1 isolated at each step of progressive adaptation to higher concentrations of methanol, AMM5 (A), AMM7 (B), AMM8 (C) and AMM10 (D) (v/v).**

A

| chromosomal position | mutation type | mutation event | mutated gene | amino acid change | intergenic mutation (distance to the flanking gene) | G4606 | G4609 | G4610 | G4611 | G4607 | G4608 |
|---|---|---|---|---|---|---|---|---|---|---|---|
| 772127 | SNP | A/C | fragment of response regulator (N-terminal fragment) | Q219P | | . | | . | | | |
| 774230 | SNP | C/T | fragment of response regulator (C-terminal fragment) | R103W | | | | | . | | |
| 1022689 | SNP | G/A | conserved protein of unknown function | R100C | | | | | | . | . |
| 2643058 | SNP | G/A | metY | L389F | | | | | . | . | . |
| 2643105 | SNP | T/C | metY | D373G | | | . | | | | |
| 2643886 | SNP | C/T | metY | G113S | | . | | . | | | |
| 2777457 | SNP | T/G | protein of unknown function | P136P | | . | . | . | . | . | . |
| 2803840 | SNP | T/C | protein of unknown function | G38G | | | | . | . | | . |
| 4120172 | SNP | C/T | protein of unknown function | G314S | | | | | | . | . |
| 5150432 | SNP | T/C | mrp1 | V159A | | . | . | . | . | . | . |
| 5245090 | SNP | C/T | | | mraW/RNAseP (150/317) | . | | . | | | |

B

| chromosomal position | mutation type | mutation event | mutated gene | amino acid change | intergenic mutation (distance to the flanking gene) | G4635 | G4636 | G4637 | G4638 | G4639 | G4640 |
|---|---|---|---|---|---|---|---|---|---|---|---|
| 275566 | SNP | G/A | Glycosyl transferase, group 1 | V199M | | . | . | . | . | . | . |
| 793636 | INS | -/G | aloacid dehalogenase-like hydrolase | | | | . | . | . | . | |
| 843772 | INS | -/A | putative glycosyl transferase | | | . | | | | | |
| 843774 | INS | -/A | putative glycosyl transferase | | | . | | | | | |
| 989097 | SNP | T/C | | | cysE/eshA (123/298) | | | | . | | |
| 2051527 | SNP | T/C | putative Catecholate siderophore receptor fiu precursor | Q150R | | . | | . | . | . | |
| 2235350 | SNP | A/G | rpsL | Y95C | | . | . | . | . | . | . |
| 2643058 | SNP | G/A | metY | L389F | | . | | | | | |
| 2643964 | SNP | C/T | metY | G87S | | . | . | . | . | . | . |
| 2777457 | SNP | T/G | protein of unknown function | P136P | | . | | . | . | . | . |
| 3295041 | SNP | C/G | ftsZ | P380P | | . | . | . | . | . | . |
| 3379040 | SNP | C/T | ilvA | V96M | | . | | | | | |

C

| chromosomal position | mutation type | mutation event | mutated gene | amino acid change | intergenic mutation (distance to the flanking gene) | G4600 | G4601 | G4602 | G4597 | G4598 | G4599 |
|---|---|---|---|---|---|---|---|---|---|---|---|
| 275566 | SNP | G/A | Glycosyl transferase, group 1 | V199M | | . | . | . | . | . | . |
| 793636 | INS | -/G | aloacid dehalogenase-like hydrolase | | | . | . | . | . | . | . |
| 1762460 | SNP | T/C | | | putative aminoglycoside phosphotransferase/plsC (162/270) | | | | | . | |
| 1840287 | SNP | T/G | | | fae/Involved in tetrahydromethanopterin-linked formaldehyde oxidation (48/92) | | . | | . | | . |
| 2235350 | SNP | A/G | rpsL | Y95C | | . | | . | | . | |
| 2544319 | SNP | A/G | clpX | N241S | | | | | | . | |
| 2643964 | SNP | C/T | metY | G87S | | . | . | . | . | . | . |
| 2777457 | SNP | T/G | protein of unknown function | P136P | | . | . | . | . | . | . |
| 2803840 | SNP | T/C | protein of unknown function | G38G | | . | | | | | . |
| 3295041 | SNP | C/G | ftsZ | P380P | | . | . | . | . | . | . |

D

| chromosomal position | mutation type | mutation event | mutated gene | amino acid change | intergenic mutation (distance to the flanking gene) | G4703 | G4704 | G4705 | G4706 | G4706 | G4707 |
|---|---|---|---|---|---|---|---|---|---|---|---|
| 275566 | SNP | G/A | Glycosyl transferase, group 1 | V199M | | . | . | . | . | . | . |
| 793633 | INS | -/G | aloacid dehalogenase-like hydrolase | | | . | . | . | . | . | . |
| 793634 | INS | -/T | aloacid dehalogenase-like hydrolase | | | . | . | . | . | . | . |
| 793636 | INS | -/G | aloacid dehalogenase-like hydrolase | | | . | . | . | . | . | . |
| 793637 | INS | -/G | aloacid dehalogenase-like hydrolase | | | . | . | . | . | . | . |
| 2233641 | SNP | C/G | protein of unknown function | | | | | . | | | |
| 2235350 | SNP | A/G | rpsL | Y95C | | . | . | . | . | . | . |
| 2544178 | SNP | A/C | clpX | N194T | | . | . | . | . | . | . |
| 2643964 | SNP | C/T | metY | G87S | | . | . | . | . | . | . |
| 3061713 | SNP | G/A | pufB | A36T | | | | | . | | |
| 3295041 | SNP | C/G | ftsZ | P380P | | . | . | . | . | . | . |
| 4128915 | SNP | T/C | | | rffG/rfbC (54/80) | | | | | | |
| 4860073 | SNP | T/G | MFS transporter membrane protein | T197P | | | | | | | . |

**O-acetyl-L-homoserine**

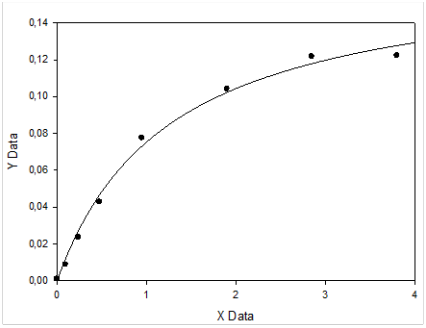


| R | Rsqr | Adj Rsqr | Standard Error of Estimate | | |
|---|---|---|---|---|---|
| 0,9970 | 0,9941 | 0,9931 | | 0,0042 | |
| | **Coefficient** | **Std. Error** | **t** | **P** | **VIF** |
| a | 0,1699 | 0,0087 | 19,4551 | <0,0001 | 7,4963< |
| b | 1,2562 | 0,1653 | 7,5980 | 0,0003 | 7,4963< |

**Sulfide**

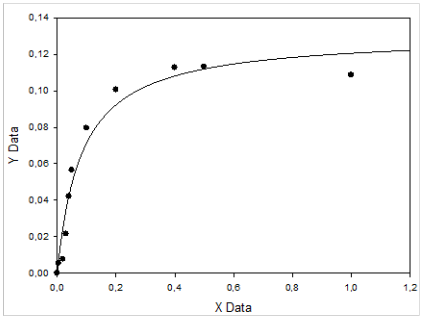


| R | Rsqr | Adj Rsqr | Standard Error of Estimate | | |
|---|---|---|---|---|---|
| 0,9799 | 0,9602 | 0,9557 | | 0,0097 | |
| | **Coefficient** | **Std. Error** | **t** | **P** | **VIF** |
| a | 0,1306 | 0,0084 | 15,4570 | <0,0001 | 2,6175 |
| b | 0,0831 | 0,0178 | 4,6713 | 0,0012 | 2,6175 |

**Methanol**

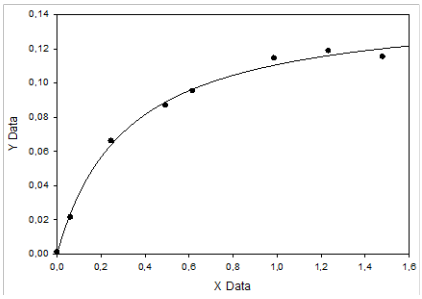


| R | Rsqr | Adj Rsqr | Standard Error of Estimate | | |
|---|---|---|---|---|---|
| 0,9978 | 0,9955 | 0,9948 | | 0,0032 | |
| | **Coefficient** | **Std. Error** | **t** | **P** | **VIF** |
| a | 0,1457 | 0,0048 | 30,2473 | <0,0001 | 6,4428< |
| b | 0,3150 | 0,0344 | 9,1462 | <0,0001 | 6,4428< |

**Figure S10: Kinetic curves of METY *M. extorquens* TK 0001 with the different substrates: O-acetyl-L-homoserine, sulfide and methanol using SigmaPlot.**

**Table S6: RNA sequence and accession number.**

| Strains | AC number | Conditions |
|---|---|---|
| **TK 0001 RNA** | ERS2801532 | sample_CFM_408_TK_0001_1pc_5mn |
| | ERS2801535 | sample_CFM_408_TK_0001_1pc_3h |
| | ERS2801536 | sample_CFM_408_TK_0001_5pc_5mn |
| | ERS2801534 | sample_CFM_408_TK_0001_5pc_3h |
| **G4105 RNA** | ERS2781795 | sample_CFM_408_G4105_1pc_5mn |
| | ERS2773667 | sample_CFM_408_G4105_1pc_3h |
| | ERS2781828 | sample_CFM_408_G4105_5pc_5mn |
| | ERS2801533 | sample_CFM_408_G4105_5pc_3h |

**Table S7: eggNOG class repartition for the CDS from *M. extorquens* TK 0001.**

| Class ID | Description | CDS | % |
|---|---|---|---|
| D | Cell cycle control, cell division, chromosome partitioning | 30 | 0,4870 |
| M | Cell wall/membrane/envelope biogenesis | 279 | 4,5292 |
| N | Cell motility | 76 | 1,2338 |
| O | Posttranslational modification, protein turnover, chaperones | 186 | 3,0195 |
| T | Signal transduction mechanisms | 312 | 5,0649 |
| U | Intracellular trafficking, secretion, and vesicular transport | 56 | 0,9091 |
| V | Defense mechanisms | 62 | 1,0065 |
| W | Extracellular structures | 1 | 0,0162 |
| B | Chromatin structure and dynalmics | 4 | 0,0649 |
| J | Translation, ribosomal structure and biogenesis | 182 | 2,9545 |
| K | Transcription | 251 | 4,0747 |
| L | Replication, recombination and repair | 286 | 4,6429 |
| C | Energy production and conversion | 297 | 4,8214 |
| E | Amino acid transport and metabolism | 278 | 4,5130 |
| F | Nucleotide transport and metabolism | 89 | 1,4448 |
| G | Carbohydrate transport and metabolism | 162 | 2,6299 |
| H | Coenzyme transport and metabolism | 159 | 2,5812 |
| I | Lipid transport and metabolism | 130 | 2,1104 |
| P | Inorganic ion transport and metabolism | 301 | 4,8864 |
| Q | Secondary metabolites biosynthesis, transport and catabolism | 82 | 1,3312 |
| S | Function unknown | 1492 | 24,2208 |

**Table S8: Codon usage table for Methylobacterium extorquens from [https://www.kazusa.or.jp](https://www.kazusa.or.jp).**

***Methylobacterium extorquens*** **[gbbct]: 102 CDS's (34044 codons)**

fields: [triplet] [amino acid] [fraction] [frequency: **per thousand**] ([number])

| | | | | | | | | | | | | | | | |
|---|---|---|---|---|---|---|---|---|---|---|---|---|---|---|---|
| UUU | F | 0.06 | 1.9 | ( 66) | UCU | S | 0.02 | 0.9 | ( 29) | UAU | Y | 0.24 | 4.9 | ( 168) | UGU | C | 0.04 | 0.4 | ( 15) |
| UUC | F | 0.94 | 31.7 | ( 1079) | UCC | S | 0.26 | 12.6 | ( 428) | UAC | Y | 0.76 | 15.8 | ( 538) | UGC | C | 0.96 | 9.7 | ( 331) |
| UUA | L | 0.00 | 0.1 | ( 4) | UCA | S | 0.02 | 0.8 | ( 26) | UAA | * | 0.16 | 0.5 | ( 16) | UGA | * | 0.70 | 2.1 | ( 71) |
| UUG | L | 0.04 | 3.4 | ( 117) | UCG | S | 0.42 | 20.2 | ( 688) | UAG | * | 0.15 | 0.4 | ( 15) | UGG | W | 1.00 | 11.8 | ( 401) |
| CUU | L | 0.04 | 3.6 | ( 123) | CCU | P | 0.03 | 1.4 | ( 47) | CAU | H | 0.26 | 5.8 | ( 198) | CGU | R | 0.06 | 4.3 | ( 145) |
| CUC | L | 0.48 | 42.9 | ( 1462) | CCC | P | 0.34 | 18.4 | ( 626) | CAC | H | 0.74 | 16.3 | ( 556) | CGC | R | 0.64 | 46.3 | ( 1575) |
| CUA | L | 0.01 | 0.6 | ( 21) | CCA | P | 0.01 | 0.8 | ( 27) | CAA | Q | 0.09 | 2.5 | ( 86) | CGA | R | 0.02 | 1.3 | ( 43) |
| CUG | L | 0.43 | 38.9 | ( 1325) | CCG | P | 0.62 | 32.9 | ( 1120) | CAG | Q | 0.91 | 25.5 | ( 868) | CGG | R | 0.26 | 18.9 | ( 645) |
| AUU | I | 0.04 | 2.0 | ( 67) | ACU | T | 0.02 | 0.9 | ( 29) | AAU | N | 0.14 | 3.4 | ( 116) | AGU | S | 0.02 | 0.9 | ( 30) |
| AUC | I | 0.95 | 45.4 | ( 1545) | ACC | T | 0.64 | 33.6 | ( 1143) | AAC | N | 0.86 | 21.2 | ( 721) | AGC | S | 0.27 | 12.8 | ( 437) |
| AUA | I | 0.00 | 0.2 | ( 8) | ACA | T | 0.02 | 0.8 | ( 28) | AAA | K | 0.06 | 2.2 | ( 75) | AGA | R | 0.01 | 0.6 | ( 20) |
| AUG | M | 1.00 | 23.2 | ( 790) | ACG | T | 0.33 | 17.2 | ( 584) | AAG | K | 0.94 | 34.0 | ( 1157) | AGG | R | 0.02 | 1.1 | ( 39) |
| GUU | V | 0.03 | 2.5 | ( 84) | GCU | A | 0.03 | 4.3 | ( 146) | GAU | D | 0.28 | 16.4 | ( 560) | GGU | G | 0.07 | 6.9 | ( 236) |
| GUC | V | 0.50 | 37.3 | ( 1271) | GCC | A | 0.55 | 72.7 | ( 2476) | GAC | D | 0.72 | 43.0 | ( 1464) | GGC | G | 0.76 | 71.4 | ( 2430) |
| GUA | V | 0.01 | 0.9 | ( 30) | GCA | A | 0.03 | 4.0 | ( 137) | GAA | E | 0.21 | 13.3 | ( 452) | GGA | G | 0.04 | 3.3 | ( 113) |
| GUG | V | 0.46 | 34.6 | ( 1177) | GCG | A | 0.39 | 50.8 | ( 1729) | GAG | E | 0.79 | 49.6 | ( 1688) | GGG | G | 0.13 | 11.8 | ( 403) |

Coding GC 68.82% 1st letter GC 68.33% 2nd letter GC 47.58% 3rd letter GC 90.55%

A.

**His-NMCR before codon optimization**

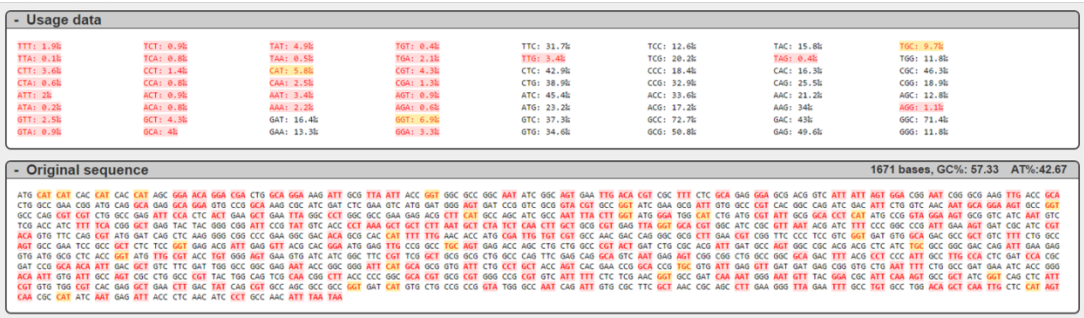


**His-NMCR after codon optimization**

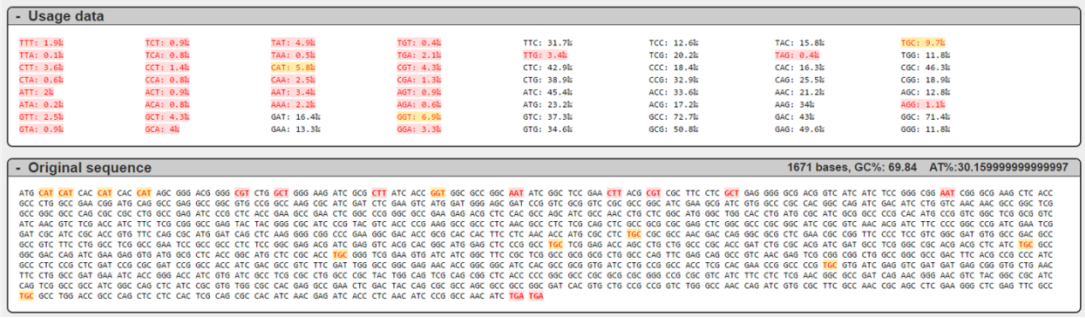


B.

**His-CMCR before codon optimization**

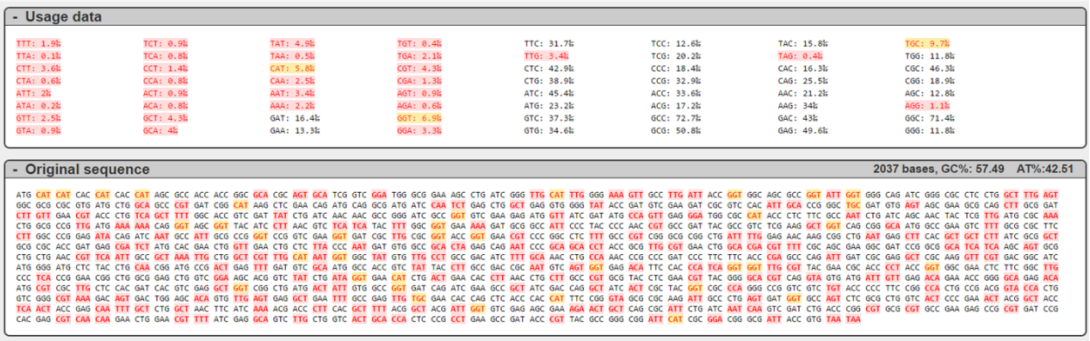


**His CMCR after codon optimization**

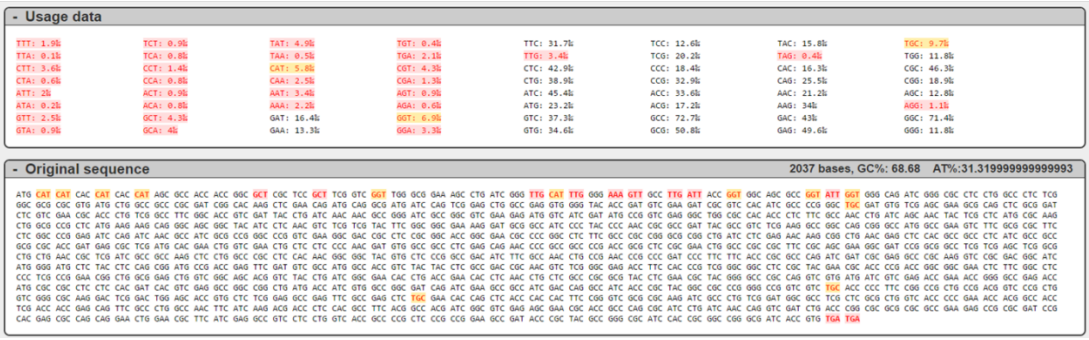


**Figure S11: Codon optimization of N-terminal part of MCR from *Chloroflexus auriantacus* using the codon usage for *M. extorquens* (A). The same method was used to optimize the sequence of C-terminal part of MCR: CMCR (B).**

**Figure S12: Clustering of the 27 candidates.**

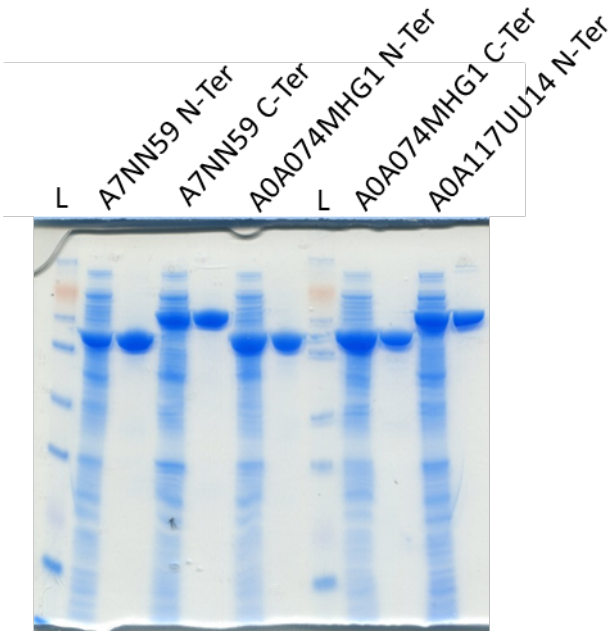


**Figure S13: SDS Gel of the NMCR and CMCR protein.**

# REFERENCES


Abdelaal, A. S., Ageez, A. M., Abd El-Hadi, A. E.-H. A., and Abdallah, N. A. (2015). Genetic improvement of n-butanol tolerance in Escherichia coli by heterologous overexpression of groESL operon from Clostridium acetobutylicum. *3 Biotech* 5, 401–410. doi:10.1007/s13205-014-0235-8.

Abubackar, H. N., Veiga, M. C., and Kennes, C. (2011). Biological conversion of carbon monoxide: rich syngas or waste gases to bioethanol. *Biofuels Bioprod. Biorefining* 5, 93–114. doi:10.1002/bbb.256.

Al-Attar, S., and de Vries, S. (2013). Energy transduction by respiratory metallo-enzymes: From molecular mechanism to cell physiology. *Coord. Chem. Rev.* 257, 64–80. doi:10.1016/j.ccr.2012.05.022.

Andrews, S. C., Robinson, A. K., and Rodríguez-Quiñones, F. (2003). Bacterial iron homeostasis. *FEMS Microbiol. Rev.* 27, 215–237. doi:10.1016/S0168-6445(03)00055-X.

Anicic, B., Trop, P., and Goricanec, D. (2014). Comparison between two methods of methanol production from carbon dioxide. *Energy* 77, 279–289. doi:10.1016/j.energy.2014.09.069.

Anthony, C. (1982). *The biochemistry of methylotrophs*. Academic Press.

Anthony, C. (2011). How half a century of research was required to understand bacterial growth on C1 and C2 compounds; the story of the serine cycle and the ethylmalonyl-CoA pathway. *Sci. Prog.* 94, 109–137. doi:10.3184/003685011X13044430633960.

Atsumi, S., Wu, T.-Y., Machado, I. M. P., Huang, W.-C., Chen, P.-Y., Pellegrini, M., et al. (2010). Evolution, genomic analysis, and reconstruction of isobutanol tolerance in Escherichia coli. *Mol. Syst. Biol.* 6, 449. doi:10.1038/msb.2010.98.

Baharoglu, Z., and Mazel, D. (2014). SOS, the formidable strategy of bacteria against aggressions. *FEMS Microbiol. Rev.* 38, 1126–1145. doi:10.1111/1574-6976.12077.

Bahlawane, C., McIntosh, M., Krol, E., and Becker, A. (2008). Sinorhizobium meliloti regulator MucR couples exopolysaccharide synthesis and motility. *Mol. Plant-Microbe Interact. MPMI* 21, 1498–1509. doi:10.1094/MPMI-21-11-1498.

Barrick, J. E., and Lenski, R. E. (2013). Genome dynamics during experimental evolution. *Nat. Rev. Genet.* 14, 827–839. doi:10.1038/nrg3564.

Barrick, J. E., Yu, D. S., Yoon, S. H., Jeong, H., Oh, T. K., Schneider, D., et al. (2009). Genome evolution and adaptation in a long-term experiment with Escherichia coli. *Nature* 461, 1243–1247. doi:10.1038/nature08480.

Bastard, K., Smith, A. A. T., Vergne-Vaxelaire, C., Perret, A., Zaparucha, A., De Melo-Minardi, R., et al. (2014). Revealing the hidden functional diversity of an enzyme family. *Nat. Chem. Biol.* 10, 42–49. doi:10.1038/nchembio.1387.

Bélanger, L., Figueira, M. ., Bourque, D., Morel, L., Béland, M., Laramée, L., et al. (2004). Production of heterologous protein by *Methylobacterium extorquens* in high cell density fermentation. *FEMS Microbiol. Lett.* 231, 197–204. doi:10.1016/S0378-1097(03)00956-X.

Bennett, R. K., Gonzalez, J. E., Whitaker, W. B., Antoniewicz, M. R., and Papoutsakis, E. T. (2018). Expression of heterologous non-oxidative pentose phosphate pathway from Bacillus methanolicus and phosphoglucose isomerase deletion improves methanol assimilation and metabolite production by a synthetic Escherichia coli methylotroph. *Metab. Eng.* 45, 75–85. doi:10.1016/j.ymben.2017.11.016.

Bergmiller, T., and Ackermann, M. (2011). Pole Age Affects Cell Size and the Timing of Cell Division in Methylobacterium extorquens AM1. *J. Bacteriol.* 193, 5216–5221. doi:10.1128/JB.00329-11.

Bjedov, I. (2003). Stress-Induced Mutagenesis in Bacteria. *Science* 300, 1404–1409. doi:10.1126/science.1082240.

Bogorad, I. W., Chen, C.-T., Theisen, M. K., Wu, T.-Y., Schlenz, A. R., Lam, A. T., et al. (2014). Building carbon–carbon bonds using a biocatalytic methanol condensation cycle. *Proc. Natl. Acad. Sci.* 111, 15928–15933. doi:10.1073/pnas.1413470111.

Bolten, C. J., Schröder, H., Dickschat, J., and Wittmann, C. (2010). Towards methionine overproduction in Corynebacterium glutamicum--methanethiol and dimethyldisulfide as reduced sulfur sources. *J. Microbiol. Biotechnol.* 20, 1196–1203.

Borisov, V. B., Gennis, R. B., Hemp, J., and Verkhovsky, M. I. (2011). The cytochrome bd respiratory oxygen reductases. *Biochim. Biophys. Acta BBA - Bioenerg.* 1807, 1398–1413. doi:10.1016/j.bbabio.2011.06.016.

Borisov, V. B., and Verkhovsky, M. I. (2015). Oxygen as Acceptor. *EcoSal Plus* 6. doi:10.1128/ecosalplus.ESP-0012-2015.

Boudemagh, A.-E., Ali-Khodja, H., Beldjoudi, M. F., Bensouici, K., Kitouni, M., Bulahrouf, A., et al. (2006). Biodegradation of methanol in a batch reactor by a microbial flora isolated from a wastewater treatment plant sludge at Elmenia in Constantine. *Fresinius Environ. Bull.*, 1590–1594.

Bouhouche, N., Syvanen, M., and Kado, C. I. (2000). The origin of prokaryotic C2H2 zinc finger regulators. *Trends Microbiol.* 8, 77–81.

Bourque, D., Ouellette, B., André, G., and Groleau, D. (1992). Production of poly-β-hydroxybutyrate from methanol: characterization of a new isolate of Methylobacterium extorquens. *Appl. Microbiol. Biotechnol.* 37, 7–12. doi:10.1007/BF00174194.

Bourque, D., Pomerleau, Y., and Groleau, D. (1995). High-cell-density production of poly-β-hydroxybutyrate (PHB) from methanol by Methylobacterium extorquens: production of high-molecular-mass PHB. *Appl. Microbiol. Biotechnol.* 44, 367–376. doi:10.1007/BF00169931.

Bradley, A. S., Swanson, P. K., Muller, E. E. L., Bringel, F., Caroll, S. M., Pearson, A., et al. (2017). Hopanoid-free Methylobacterium extorquens DM4 overproduces carotenoids and has widespread growth impairment. *PLOS ONE* 12, e0173323. doi:10.1371/journal.pone.0173323.

Busby, W. F., Ackermann, J. M., and Crespi, C. L. (1999). Effect of methanol, ethanol, dimethyl sulfoxide, and acetonitrile on in vitro activities of cDNA-expressed human cytochromes P-450. *Drug Metab. Dispos. Biol. Fate Chem.* 27, 246–249.

Butterfield, C. N., Li, Z., Andeer, P. F., Spaulding, S., Thomas, B. C., Singh, A., et al. (2016). Proteogenomic analyses indicate bacterial methylotrophy and archaeal heterotrophy are prevalent below the grass root zone. *PeerJ* 4, e2687. doi:10.7717/peerj.2687.

Carroll, S., Chubiz, L., Agashe, D., and Marx, C. (2015). Parallel and Divergent Evolutionary Solutions for the Optimization of an Engineered Central Metabolism in Methylobacterium extorquens AM1. *Microorganisms* 3, 152–174. doi:10.3390/microorganisms3020152.

Cerisy, T., Souterre, T., Torres-Romero, I., Boutard, M., Dubois, I., Patrouix, J., et al. (2017). Evolution of a Biomass-Fermenting Bacterium To Resist Lignin Phenolics. *Appl. Environ. Microbiol.* 83. doi:10.1128/AEM.00289-17.

Chen, N. H., Djoko, K. Y., Veyrier, F. J., and McEwan, A. G. (2016). Formaldehyde Stress Responses in Bacterial Pathogens. *Front. Microbiol.* 7. doi:10.3389/fmicb.2016.00257.

Chistoserdova, L. (2018). Applications of methylotrophs: can single carbon be harnessed for biotechnology? *Curr. Opin. Biotechnol.* 50, 189–194. doi:10.1016/j.copbio.2018.01.012.

Chistoserdova, L., Kalyuzhnaya, M. G., and Lidstrom, M. E. (2009). The Expanding World of Methylotrophic Metabolism. *Annu. Rev. Microbiol.* 63, 477–499. doi:10.1146/annurev.micro.091208.073600.

Cho, K.-S., Hirai, M., and Shoda, M. (1991). Degradation characteristics of hydrogen sulfide, methanethiol, dimethyl sulfide and dimethyl disulfide by Thiobacillus thioparus DW44 isolated from peat biofilter. *J. Ferment. Bioeng.* 71, 384–389. doi:10.1016/0922-338X(91)90248-F.

Choi, Y. J., Bourque, D., Morel, L., Groleau, D., and Miguez, C. B. (2006). Multicopy Integration and Expression of Heterologous Genes in Methylobacterium extorquens ATCC 55366. *Appl. Environ. Microbiol.* 72, 753–759. doi:10.1128/AEM.72.1.753-759.2006.

Choi, Y. J., Gringorten, J. L., Belanger, L., Morel, L., Bourque, D., Masson, L., et al. (2008). Production of an Insecticidal Crystal Protein from Bacillus thuringiensis by the Methylotroph Methylobacterium extorquens. *Appl. Environ. Microbiol.* 74, 5178–5182. doi:10.1128/AEM.00598-08.

Cui, L.-Y., Wang, S.-S., Guan, C.-G., Liang, W.-F., Xue, Z.-L., Zhang, C., et al. (2018). Breeding of Methanol-Tolerant Methylobacterium extorquens AM1 by Atmospheric and Room Temperature Plasma Mutagenesis Combined With Adaptive Laboratory Evolution. *Biotechnol. J.*, 1700679. doi:10.1002/biot.201700679.

Dai, Z., Gu, H., Zhang, S., Xin, F., Zhang, W., Dong, W., et al. (2017). Metabolic construction strategies for direct methanol utilization in Saccharomyces cerevisiae. *Bioresour. Technol.* 245, 1407–1412. doi:10.1016/j.biortech.2017.05.100.

Davidson, V. L., Husain, M., and Neher, J. W. (1986). Electron transfer flavoprotein from Methylophilus methylotrophus: properties, comparison with other electron transfer flavoproteins, and regulation of expression by carbon source. *J. Bacteriol.* 166, 812–817. doi:10.1128/jb.166.3.812-817.1986.

De Bont, J. A. M., Van Dijken, J. P., and Harder, W. (1981). Dimethyl Sulphoxide and Dimethyl Sulphide as a Carbon, Sulphur and Energy Source for Growth of Hyphomicrobium S. *Microbiology* 127, 315–323. doi:10.1099/00221287-127-2-315.

de Fouchécour, F., Sánchez-Castañeda, A.-K., Saulou-Bérion, C., and Spinnler, H. É. (2018). Process engineering for microbial production of 3-hydroxypropionic acid. *Biotechnol. Adv.* 36, 1207–1222. doi:10.1016/j.biotechadv.2018.03.020.

Dhamwichukorn, S., Kleinheinz, G. T., and Bagley, S. T. (2001). Thermophilic biofiltration of methanol and ?-pinene. *J. Ind. Microbiol. Biotechnol.* 26, 127–133. doi:10.1038/sj.jim.7000079.

Döring, V., Darii, E., Yishai, O., Bar-Even, A., and Bouzon, M. (2018). Implementation of a Reductive Route of One-Carbon Assimilation in *Escherichia coli* through Directed Evolution. *ACS Synth. Biol.* 7, 2029–2036. doi:10.1021/acssynbio.8b00167.

Drake, J. W. (1991). A constant rate of spontaneous mutation in DNA-based microbes. *Proc. Natl. Acad. Sci.* 88, 7160–7164. doi:10.1073/pnas.88.16.7160.

Duine, J. A. (1999). Thiols in formaldehyde dissimilation and detoxification. *BioFactors Oxf. Engl.* 10, 201–206.

Dürre, P., and Eikmanns, B. J. (2015). C1-carbon sources for chemical and fuel production by microbial gas fermentation. *Curr. Opin. Biotechnol.* 35, 63–72. doi:10.1016/j.copbio.2015.03.008.

Eberlein, C., Baumgarten, T., Starke, S., and Heipieper, H. J. (2018). Immediate response mechanisms of Gram-negative solvent-tolerant bacteria to cope with environmental stress: cis-trans isomerization of unsaturated fatty acids and outer membrane vesicle

secretion. *Appl. Microbiol. Biotechnol.* 102, 2583–2593. doi:10.1007/s00253-018-8832-9.

Eggeling, L., and Sahm, H. (1981). Enhanced utilization-rate of methanol during growth on a mixed substrate: A continuous culture study with Hansenula polymorpha. *Arch. Microbiol.* 130, 362–365. doi:10.1007/BF00414601.

Ezraty, B., Gennaris, A., Barras, F., and Collet, J.-F. (2017). Oxidative stress, protein damage and repair in bacteria. *Nat. Rev. Microbiol.* 15, 385–396. doi:10.1038/nrmicro.2017.26.

Faria, D., and Bharathi, P. A. L. (2006). Marine and estuarine methylotrophs: their abundance, activity and identity. *Curr. Sci.* 90, 984–989.

Ferry James Gregory, Maranas Costas, and Wood Thomas Keith (2015). Methane-to-acetate pathway for producing liquid biofuels and biorenewables.

Foo, J. L., Jensen, H. M., Dahl, R. H., George, K., Keasling, J. D., Lee, T. S., et al. (2014). Improving Microbial Biogasoline Production in *Escherichia coli* Using Tolerance Engineering. *mBio* 5. doi:10.1128/mBio.01932-14.

Foster, P. L. (2007). Stress-Induced Mutagenesis in Bacteria. *Crit. Rev. Biochem. Mol. Biol.* 42, 373–397. doi:10.1080/10409230701648494.

Fu, X. (2014). Chaperone function and mechanism of small heat-shock proteins. *Acta Biochim. Biophys. Sin.* 46, 347–356. doi:10.1093/abbs/gmt152.

G A Armstrong, A Schmidt, G Sandmann, and J E Hearst (1990). Genetic and biochemical characterization of carotenoid biosynthesis mutants of Rhodobacter capsulatus. 265.

Gak Evgeniy Rodionovich, Rorshkova Natalya Vasilievna, and Tokmakova Irina l Vovna A method for producing pyrroloquinoline quinone using a bacterium of the genus Methylobacterium or Hyphomicrobium.

García, V., Godoy, P., Daniels, C., Hurtado, A., Ramos, J.-L., and Segura, A. (2009). Functional analysis of new transporters involved in stress tolerance in Pseudomonas putida DOT-T1E: New transporters in solvent tolerance. *Environ. Microbiol. Rep.* 2, 389–395. doi:10.1111/j.1758-2229.2009.00093.x.

Garg, S., Wu, H., Clomburg, J. M., and Bennett, G. N. (2018). Bioconversion of methane to C-4 carboxylic acids using carbon flux through acetyl-CoA in engineered Methylomicrobium buryatense 5GB1C. *Metab. Eng.* 48, 175–183. doi:10.1016/j.ymben.2018.06.001.

Ghasemzadeh, K., Sadati Tilebon, S. M., Nasirinezhad, M., and Basile, A. (2018). “Economic Assessment of Methanol Production,” in *Methanol* (Elsevier), 613–632. doi:10.1016/B978-0-444-63903-5.00023-6.

Goeppert, A., Czaun, M., Jones, J.-P., Surya Prakash, G. K., and Olah, G. A. (2014). Recycling of carbon dioxide to methanol and derived products – closing the loop. *Chem Soc Rev* 43, 7995–8048. doi:10.1039/C4CS00122B.

Gommers, P. J. F., van Schie, B. J., van Dijken, J. P., and Kuenen, J. G. (1988). Biochemical limits to microbial growth yields: An analysis of mixed substrate utilization. *Biotechnol. Bioeng.* 32, 86–94. doi:10.1002/bit.260320112.

Gontard, N., Sonesson, U., Birkved, M., Majone, M., Bolzonella, D., Celli, A., et al. (2018). A research challenge vision regarding management of agricultural waste in a circular bio-based economy. *Crit. Rev. Environ. Sci. Technol.* 48, 614–654. doi:10.1080/10643389.2018.1471957.

Gonzalez, J. E., Bennett, R. K., Papoutsakis, E. T., and Antoniewicz, M. R. (2018). Methanol assimilation in Escherichia coli is improved by co-utilization of threonine and deletion of leucine-responsive regulatory protein. *Metab. Eng.* 45, 67–74. doi:10.1016/j.ymben.2017.11.015.

Groleau, D., Bourque, D., and Pomerieau, Y. Methylobacterium extorquwns microorganism useful for the preparation of poly-β-hydroxybutyric acid polymers.

Gunji, Y., and Yasueda, H. (2006). Enhancement of l-lysine production in methylotroph Methylophilus methylotrophus by introducing a mutant LysE exporter. *J. Biotechnol.* 127, 1–13. doi:10.1016/j.jbiotec.2006.06.003.

Gutiérrez, J., Bourque, D., Criado, R., Choi, Y. J., Cintas, L. M., Hernández, P. E., et al. (2005). Heterologous extracellular production of enterocin P from *Enterococcus faecium* P13 in the methylotrophic bacterium *Methylobacterium extorquens*. *FEMS Microbiol. Lett.* 248, 125–131. doi:10.1016/j.femsle.2005.05.029.

Haft, R. J. F., Keating, D. H., Schwaegler, T., Schwalbach, M. S., Vinokur, J., Tremaine, M., et al. (2014). Correcting direct effects of ethanol on translation and transcription machinery confers ethanol tolerance in bacteria. *Proc. Natl. Acad. Sci.* 111, E2576–E2585. doi:10.1073/pnas.1401853111.

Haslbeck, M., Weinkauf, S., and Buchner, J. (2018). Small heat shock proteins: Simplicity meets complexity. *J. Biol. Chem.*, jbc.REV118.002809. doi:10.1074/jbc.REV118.002809.

He, S., Zhou, X., Shi, C., and Shi, X. (2016). Ethanol adaptation induces direct protection and cross-protection against freezing stress in *Salmonella enterica* serovar Enteritidis. *J. Appl. Microbiol.* 120, 697–704. doi:10.1111/jam.13042.

Heck, d'Henry A., Casanova, M., and Starr, T. B. (1990). Formaldehyde Toxicity—New Understanding. *Crit. Rev. Toxicol.* 20, 397–426. doi:10.3109/10408449009029329.

Heipieper, H. J., Meinhardt, F., and Segura, A. (2003). The *cis–trans* isomerase of unsaturated fatty acids in *Pseudomonas* and *Vibrio* : biochemistry, molecular biology and

physiological function of a unique stress adaptive mechanism. *FEMS Microbiol. Lett.* 229, 1–7. doi:10.1016/S0378-1097(03)00792-4.

Henard, C. A., Smith, H., Dowe, N., Kalyuzhnaya, M. G., Pienkos, P. T., and Guarnieri, M. T. (2016). Bioconversion of methane to lactate by an obligate methanotrophic bacterium. *Sci. Rep.* 6. doi:10.1038/srep21585.

Hermann, M., Fayolle, F., Marchal, R., Podvin, L., Sebald, M., and Vandecasteele, J. P. (1985). Isolation and characterization of butanol-resistant mutants of Clostridium acetobutylicum. *Appl. Environ. Microbiol.* 50, 1238–1243.

Heuson, E., Petit, J.-L., Debard, A., Job, A., Charmantray, F., de Berardinis, V., et al. (2016). Continuous colorimetric screening assays for the detection of specific l- or d-α-amino acid transaminases in enzyme libraries. *Appl. Microbiol. Biotechnol.* 100, 397–408. doi:10.1007/s00253-015-6988-0.

Höfer, P., Vermette, P., and Groleau, D. (2011). Production and characterization of polyhydroxyalkanoates by recombinant Methylobacterium extorquens: Combining desirable thermal properties with functionality. *Biochem. Eng. J.* 54, 26–33. doi:10.1016/j.bej.2011.01.003.

Holo, H. (1989). Chloroflexus aurantiacus secretes 3-hydroxypropionate, a possible intermediate in the assimilation of CO2 and acetate. *Arch. Microbiol.* 151, 252–256. doi:10.1007/BF00413138.

Horst, J. P., Wu, T. H., and Marinus, M. G. (1999). Escherichia coli mutator genes. *Trends Microbiol.* 7, 29–36.

Hu, B., and Lidstrom, M. E. (2014). Metabolic engineering of Methylobacterium extorquens AM1 for 1-butanol production. *Biotechnol. Biofuels* 7. doi:10.1186/s13068-014-0156-0.

Hu, B., Yang, Y.-M., Beck, D. A. C., Wang, Q.-W., Chen, W.-J., Yang, J., et al. (2016). Comprehensive molecular characterization of Methylobacterium extorquens AM1 adapted for 1-butanol tolerance. *Biotechnol. Biofuels* 9. doi:10.1186/s13068-016-0497-y.

Huerta-Cepas, J., Szklarczyk, D., Heller, D., Hernández-Plaza, A., Forslund, S. K., Cook, H., et al. (2018). eggNOG 5.0: a hierarchical, functionally and phylogenetically annotated orthology resource based on 5090 organisms and 2502 viruses. *Nucleic Acids Res.* doi:10.1093/nar/gky1085.

Huffer, S., Clark, M. E., Ning, J. C., Blanch, H. W., and Clark, D. S. (2011). Role of Alcohols in Growth, Lipid Composition, and Membrane Fluidity of Yeasts, Bacteria, and Archaea. *Appl. Environ. Microbiol.* 77, 6400–6408. doi:10.1128/AEM.00694-11.

Hügler, M., Menendez, C., Schägger, H., and Fuchs, G. (2002). Malonyl-coenzyme A reductase from Chloroflexus aurantiacus, a key enzyme of the 3-hydroxypropionate cycle for autotrophic CO(2) fixation. *J. Bacteriol.* 184, 2404–2410.

Hwang, H., Yeon, Y. J., Lee, S., Choe, H., Jang, M. G., Cho, D. H., et al. (2015). Electro-biocatalytic production of formate from carbon dioxide using an oxygen-stable whole cell biocatalyst. *Bioresour. Technol.* 185, 35–39. doi:10.1016/j.biortech.2015.02.086.

Hwang, S., Shao, Q., Williams, H., Hilty, C., and Gao, Y. Q. (2011). Methanol Strengthens Hydrogen Bonds and Weakens Hydrophobic Interactions in Proteins – A Combined Molecular Dynamics and NMR study. *J. Phys. Chem. B* 115, 6653–6660. doi:10.1021/jp111448a.

Isar, J., and Rangaswamy, V. (2012). Improved n-butanol production by solvent tolerant Clostridium beijerinckii. *Biomass Bioenergy* 37, 9–15. doi:10.1016/j.biombioe.2011.12.046.

Ivanova, E. G., Doronina, N. V., and Trotsenko, Y. A. (2001). Aerobic Methylobacteria Are Capable of Synthesizing Auxins. *Microbiology* 70, 392–397. doi:10.1023/A:1010469708107.

Ivanova, E. G., Fedorov, D. N., Doronina, N. V., and Trotsenko, Y. A. (2006). Production of vitamin B12 in aerobic methylotrophic bacteria. *Microbiology* 75, 494–496. doi:10.1134/S0026261706040217.

Jakobsen, Ø. M., Benichou, A., Flickinger, M. C., Valla, S., Ellingsen, T. E., and Brautaset, T. (2006). Upregulated transcription of plasmid and chromosomal ribulose monophosphate pathway genes is critical for methanol assimilation rate and methanol tolerance in the methylotrophic bacterium Bacillus methanolicus. *J. Bacteriol.* 188, 3063–3072. doi:10.1128/JB.188.8.3063-3072.2006.

Jena, N. R. (2012). DNA damage by reactive species: Mechanisms, mutation and repair. *J. Biosci.* 37, 503–517.

Jiang, H., Chen, Y., Jiang, P., Zhang, C., Smith, T. J., Murrell, J. C., et al. (2010). Methanotrophs: Multifunctional bacteria with promising applications in environmental bioengineering. *Biochem. Eng. J.* 49, 277–288. doi:10.1016/j.bej.2010.01.003.

Joo, H.-J., Ahn, S.-H., Lee, H.-R., Jung, S.-W., Choi, C.-W., Kim, M.-S., et al. (2012). The Effect of Methanol on the Structural Parameters of Neuronal Membrane Lipid Bilayers. *Korean J. Physiol. Pharmacol.* 16, 255. doi:10.4196/kjpp.2012.16.4.255.

Joon-H, C., Jung H, K., Daniel, M., and Lebeault, J. M. (1989). Optimization of Growth Medium and Poly- β -hydroxybutyric Acid Production from Methanol in Methylobacterium organophilum. *Microbiol. Biotechnol. Lett. KoreaScience* 17, 392–396.

Kabelitz, N., Santos, P. M., and Heipieper, H. J. (2003). Effect of aliphatic alcohols on growth and degree of saturation of membrane lipids in *Acinetobacter calcoaceticus*. *FEMS Microbiol. Lett.* 220, 223–227. doi:10.1016/S0378-1097(03)00103-4.

Kamatari, Y. O., Konno, T., Kataoka, M., and Akasaka, K. (1996). The Methanol-induced Globular and Expanded Denatured States of Cytochromec: A Study by CD Fluorescence, NMR and Small-angle X-ray Scattering. *J. Mol. Biol.* 259, 512–523. doi:10.1006/jmbi.1996.0336.

Kaszycki, P., and Kołoczek, H. (2000). Formaldehyde and methanol biodegradation with the methylotrophic yeast Hansenula polymorpha in a model wastewater system. *Microbiol. Res.* 154, 289–296. doi:10.1016/S0944-5013(00)80002-6.

Kell, D. B., Swainston, N., Pir, P., and Oliver, S. G. (2015). Membrane transporter engineering in industrial biotechnology and whole cell biocatalysis. *Trends Biotechnol.* 33, 237–246. doi:10.1016/j.tibtech.2015.02.001.

Khosravi-Darani, K., Mokhtari, Z.-B., Amai, T., and Tanaka, K. (2013). Erratum to: Microbial production of poly(hydroxybutyrate) from C1 carbon sources. *Appl. Microbiol. Biotechnol.* 97, 5657–5657. doi:10.1007/s00253-013-4807-z.

Kildegaard, K. R., Hallström, B. M., Blicher, T. H., Sonnenschein, N., Jensen, N. B., Sherstyk, S., et al. (2014). Evolution reveals a glutathione-dependent mechanism of 3-hydroxypropionic acid tolerance. *Metab. Eng.* 26, 57–66. doi:10.1016/j.ymben.2014.09.004.

Kildegaard, K. R., Jensen, N. B., Schneider, K., Czarnotta, E., Özdemir, E., Klein, T., et al. (2016). Engineering and systems-level analysis of Saccharomyces cerevisiae for production of 3-hydroxypropionic acid via malonyl-CoA reductase-dependent pathway. *Microb. Cell Factories* 15. doi:10.1186/s12934-016-0451-5.

Kim Yong Hwan, Jang Jeong Ho, and Choi Eun-Gyu (2017). Shewanella Oneidensis microorganism for synthesizing formic acid, and method for synthesizing formic acid by using same.

Kircher, M. (2012). The transition to a bio-economy: national perspectives. *Biofuels Bioprod. Biorefining* 6, 240–245. doi:10.1002/bbb.1341.

Komaba Shinichi, Kubota Kei, and Hosaka Tomooki (2018). Electrolyte solution for potassium ion batteries, potassium ion battery, electrolyte solution for potassium ion capacitors, and potassium ion capacitor.

Korotkova, N., Chistoserdova, L., Kuksa, V., and Lidstrom, M. E. (2002a). Glyoxylate Regeneration Pathway in the Methylotroph Methylobacterium extorquens AM1. *J. Bacteriol.* 184, 1750–1758. doi:10.1128/JB.184.6.1750-1758.2002.

Korotkova, N., Chistoserdova, L., and Lidstrom, M. E. (2002b). Poly- -Hydroxybutyrate Biosynthesis in the Facultative Methylotroph Methylobacterium extorquens AM1: Identification and Mutation of gap11, gap20, and phaR. *J. Bacteriol.* 184, 6174–6181. doi:10.1128/JB.184.22.6174-6181.2002.

Kumar, V., Ashok, S., and Park, S. (2013). Recent advances in biological production of 3-hydroxypropionic acid. *Biotechnol. Adv.* 31, 945–961. doi:10.1016/j.biotechadv.2013.02.008.

Kunkel, T. A., and Erie, D. A. (2005). DNA MISMATCH REPAIR. *Annu. Rev. Biochem.* 74, 681–710. doi:10.1146/annurev.biochem.74.082803.133243.

Kurashova Viktor Mikhailovich, and Sakhno tamara Vladimirovna (2002). Microbiological method for producing petroleum hydrocarbons from solid fossil fuels, oil tars and products of biological decomposition of organic substrates and an agent for carying out said method.

Lan, E. I., Chuang, D. S., Shen, C. R., Lee, A. M., Ro, S. Y., and Liao, J. C. (2015). Metabolic engineering of cyanobacteria for photosynthetic 3-hydroxypropionic acid production from CO2 using Synechococcus elongatus PCC 7942. *Metab. Eng.* 31, 163–170. doi:10.1016/j.ymben.2015.08.002.

Large, P. (1972). *Demethylation of trimethylamine N-oxide by Pseudomonas aminovorans*.

Lee, H., Popodi, E., Tang, H., and Foster, P. L. (2012). Rate and molecular spectrum of spontaneous mutations in the bacterium Escherichia coli as determined by whole-genome sequencing. *Proc. Natl. Acad. Sci.* 109, E2774–E2783. doi:10.1073/pnas.1210309109.

Leopold Eugen (2018). Method and device for producing urea.

Leßmeier, L., and Wendisch, V. F. (2015). Identification of two mutations increasing the methanol tolerance of Corynebacterium glutamicum. *BMC Microbiol.* 15. doi:10.1186/s12866-015-0558-6.

Li, H., Opgenorth, P. H., Wernick, D. G., Rogers, S., Wu, T.-Y., Higashide, W., et al. (2012). Integrated Electromicrobial Conversion of CO2 to Higher Alcohols. *Science* 335, 1596–1596. doi:10.1126/science.1217643.

Lidstrom, M. E., and Marx, C. J. (2001). Development of improved versatile broad-host-range vectors for use in methylotrophs and other Gram-negative bacteria. *Microbiology* 147, 2065–2075. doi:10.1099/00221287-147-8-2065.

Liesivuori, J., and Savolainen, and H. (1991). Methanol and Formic Acid Toxicity: Biochemical Mechanisms. *Pharmacol. Toxicol.* 69, 157–163. doi:10.1111/j.1600-0773.1991.tb01290.x.

Limberg, M. H., Schulte, J., Aryani, T., Mahr, R., Baumgart, M., Bott, M., et al. (2017). Metabolic profile of 1,5-diaminopentane producing *Corynebacterium glutamicum* under scale-down conditions: Blueprint for robustness to bioreactor inhomogeneities: Blueprint for Robustness. *Biotechnol. Bioeng.* 114, 560–575. doi:10.1002/bit.26184.

Lindner, S. N., Ramirez, L. C., Krusemann, J. L., Yishai, O., Belkhelfa, S., He, H., Bouzon, M., Doring, V., and Bar-Even, A. (2018). NADPH-Auxotrophic *E. coli*: A Sensor Strain for Testing *in Vivo* Regeneration of NADPH. *ACS Synthetic Biology* 7, 2742-2749. doi:10.1021/acssynbio.8b00313

Lipman, T. (2011). An Overview of Hydrogen Production and Storage Systems with Renewable Hydrogen Case Studies.

Lisa Anne, Laffend Vasantha, Nagarajan Charles, Edwin Nakamura, and Lisa Anne LaffendVasantha NagarajanCharles Edwin Nakamura (1995). Bioconversion of a fermentable carbon source to 1,3-propanediol by a single microorganism.

Liu, C., Ding, Y., Xian, M., Liu, M., Liu, H., Ma, Q., et al. (2017). Malonyl-CoA pathway: a promising route for 3-hydroxypropionate biosynthesis. *Crit. Rev. Biotechnol.* 37, 933–941. doi:10.1080/07388551.2016.1272093.

Liu, C., Ding, Y., Zhang, R., Liu, H., Xian, M., and Zhao, G. (2016). Functional balance between enzymes in malonyl-CoA pathway for 3-hydroxypropionate biosynthesis. *Metab. Eng.* 34, 104–111. doi:10.1016/j.ymben.2016.01.001.

Liu, C., Wang, Q., Xian, M., Ding, Y., and Zhao, G. (2013). Dissection of Malonyl-Coenzyme A Reductase of Chloroflexus aurantiacus Results in Enzyme Activity Improvement. *PLoS ONE* 8, e75554. doi:10.1371/journal.pone.0075554.

Lyubovsky, M. (2017). Shifting the paradigm: Synthetic liquid fuels offer vehicle for monetizing wind and solar energy. *J. Energy Secur.*

Ma, M., and Liu, Z. L. (2010). Mechanisms of ethanol tolerance in Saccharomyces cerevisiae. *Appl. Microbiol. Biotechnol.* 87, 829–845. doi:10.1007/s00253-010-2594-3.

Mai, H. T. N., Lee, K. M., and Choi, S. S. (2016). Enhanced oxalic acid production from corncob by a methanol-resistant strain of Aspergillus niger using semi solid-sate fermentation. *Process Biochem.* 51, 9–15. doi:10.1016/j.procbio.2015.11.005.

Maki, H., and Sekiguchi, M. (1992). MutT protein specifically hydrolyses a potent mutagenic substrate for DNA synthesis. *Nature* 355, 273–275. doi:10.1038/355273a0.

Maleszka, R., Skelly, P. J., and Clark-Walker, G. D. (1991). Rolling circle replication of DNA in yeast mitochondria. *EMBO J.* 10, 3923–3929. doi:10.1002/j.1460-2075.1991.tb04962.x.

Marlière, P., Patrouix, J., Döring, V., Herdewijn, P., Tricot, S., Cruveiller, S., et al. (2011). Chemical Evolution of a Bacterium's Genome. *Angew. Chem. Int. Ed.* 50, 7109–7114. doi:10.1002/anie.201100535.

Mars, R. A. T., Mendonça, K., Denham, E. L., and van Dijl, J. M. (2015). The reduction in small ribosomal subunit abundance in ethanol-stressed cells of Bacillus subtilis is mediated by a SigB-dependent antisense RNA. *Biochim. Biophys. Acta BBA - Mol. Cell Res.* 1853, 2553–2559. doi:10.1016/j.bbamcr.2015.06.009.

Marx, C. J. (2004). Development of an insertional expression vector system for Methylobacterium extorquens AM1 and generation of null mutants lacking mtdA and/or fch. *Microbiology* 150, 9–19. doi:10.1099/mic.0.26587-0.

Marx, C. J., Bringel, F., Chistoserdova, L., Moulin, L., Farhan Ul Haque, M., Fleischman, D. E., et al. (2012). Complete genome sequences of six strains of the genus Methylobacterium. *J. Bacteriol.* 194, 4746–4748. doi:10.1128/JB.01009-12.

Marx, C. J., and Lidstrom, M. E. (2002). Broad-Host-Range *cre-lox* System for Antibiotic Marker Recycling in Gram-Negative Bacteria. *BioTechniques* 33, 1062–1067. doi:10.2144/02335rr01.

Marx, C. J., Van Dien, S. J., and Lidstrom, M. E. (2005). Flux Analysis Uncovers Key Role of Functional Redundancy in Formaldehyde Metabolism. *PLoS Biol.* 3, e16. doi:10.1371/journal.pbio.0030016.

McEvoy, E., Wright, P. C., and Bustard, M. T. (2004). The effect of high concentration isopropanol on the growth of a solvent-tolerant strain of Chlorella vulgaris. *Enzyme Microb. Technol.* 35, 140–146. doi:10.1016/j.enzmictec.2004.01.012.

Meena, K. K., Kumar, M., Mishra, S., Ojha, S. K., Wakchaure, G. C., and Sarkar, B. (2015). Phylogenetic Study of Methanol Oxidizers from Chilika-Lake Sediments Using Genomic and Metagenomic Approaches. *Indian J. Microbiol.* 55, 151–162. doi:10.1007/s12088-015-0510-3.

Methanol, Process Economics Program Report 43C (2000). IHS Markit Available at: https://ihsmarkit.com/products/chemical-technology-pep-methanol-2000.html.

Michener, J. K., Camargo Neves, A. A., Vuilleumier, S., Bringel, F., and Marx, C. J. (2014). Effective use of a horizontally-transferred pathway for dichloromethane catabolism requires post–transfer refinement. *eLife* 3. doi:10.7554/eLife.04279.

Miguez, C. B., Figueira, Figueira, M. M., Laramee, L., and Murrell, C. J. (2003). Methylotrophic bacterium for the production of recombinant proteins and other produts.

Miller, J. H. (1996). SPONTANEOUS MUTATORS IN BACTERIA: Insights into Pathways of Mutagenesis and Repair. *Annu. Rev. Microbiol.* 50, 625–643. doi:10.1146/annurev.micro.50.1.625.

Mirabella, A., Terwagne, M., Zygmunt, M. S., Cloeckaert, A., De Bolle, X., and Letesson, J. J. (2013). Brucella melitensis MucR, an Orthologue of Sinorhizobium meliloti MucR, Is Involved in Resistance to Oxidative, Detergent, and Saline Stresses and Cell Envelope Modifications. *J. Bacteriol.* 195, 453–465. doi:10.1128/JB.01336-12.

Mogk, A., Mayer, M. P., and Deuerling, E. (2002). Mechanisms of Protein Folding: Molecular Chaperones and Their Application in Biotechnology. *ChemBioChem* 3, 807–814. doi:10.1002/1439-7633(20020902)3:9<807::AID-CBIC807>3.0.CO;2-A.

Mokhtari-Hosseini, Z. B., Vasheghani Farahani, E., Shojaosadati, S. A., Karimzadeh, R., and Khosravi Darani, K. (2009). Media Selection for Poly(hydroxybutyrate) Production from Methanol by Methylobacterium Extorquens DSMZ 1340. *Iran. J. Chem. Chem. Eng. IJCCE* 28, 45–52.

Montes Martin, Loughman Thomas Ciaram, Rouma Chantal, and Cherif-Cheikh Roland (2018). Process for the preparation of pharmaceutical compositions for the sustained release of somatostatin analogs.

Mørland, J., and Bessesen, A. (1977). Inhibition of protein synthesis by ethanol in isolated rat liver parenchymal cells. *Biochim. Biophys. Acta* 474, 312–320.

Mothes, G., Ackermann, J.-U., and Babel, W. (1998). Regulation of poly(β-hydroxybutyrate) synthesis in Methylobacterium rhodesianum MB 126 growing on methanol or fructose. *Arch. Microbiol.* 169, 360–363. doi:10.1007/s002030050583.

Muffler, K., and Ulber, R. (2008). Use of Renewable Raw Materials in the Chemical Industry – Beyond Sugar and Starch. *Chem. Eng. Technol.* 31, 638–646. doi:10.1002/ceat.200800066.

Mukhopadhyay, A. (2015). Tolerance engineering in bacteria for the production of advanced biofuels and chemicals. *Trends Microbiol.* 23, 498–508. doi:10.1016/j.tim.2015.04.008.

Mutzel, R., and Marlière, P. (2001). Method and device for selecting accelerated proliferation of living cells in suspension.

Mutzel, R., Marlière, P., and Mazel, D. (2004). Method for obtaining new life forms.

Novick, A., and Szilard, L. (1950). Experiments with the Chemostat on spontaneous mutations of bacteria. *Proc. Natl. Acad. Sci. U. S. A.* 36, 708–719.

Ochsner, A. M., Sonntag, F., Buchhaupt, M., Schrader, J., and Vorholt, J. A. (2015). Methylobacterium extorquens: methylotrophy and biotechnological applications. *Appl. Microbiol. Biotechnol.* 99, 517–534. doi:10.1007/s00253-014-6240-3.

Oh, Y.-K., Hwang, K.-R., Kim, C., Kim, J. R., and Lee, J.-S. (2018). Recent developments and key barriers to advanced biofuels: A short review. *Bioresour. Technol.* 257, 320–333. doi:10.1016/j.biortech.2018.02.089.

Okochi, M., Kanie, K., Kurimoto, M., Yohda, M., and Honda, H. (2008). Overexpression of prefoldin from the hyperthermophilic archaeum Pyrococcus horikoshii OT3 endowed Escherichia coli with organic solvent tolerance. *Appl. Microbiol. Biotechnol.* 79, 443–449. doi:10.1007/s00253-008-1450-1.

Ono Yukiko, Yasueda Hisashi, Kawahara Yoshio, and Sugimoto Shinichi (2001). Methods for producing L-amino acids.

Orita, I., Nishikawa, K., Nakamura, S., and Fukui, T. (2014). Biosynthesis of polyhydroxyalkanoate copolymers from methanol by Methylobacterium extorquens AM1 and the engineered strains under cobalt-deficient conditions. *Appl. Microbiol. Biotechnol.* 98, 3715–3725. doi:10.1007/s00253-013-5490-9.

Orita, I., Sakamoto, N., Kato, N., Yurimoto, H., and Sakai, Y. (2007). Bifunctional enzyme fusion of 3-hexulose-6-phosphate synthase and 6-phospho-3-hexuloisomerase. *Appl. Microbiol. Biotechnol.* 76, 439–445. doi:10.1007/s00253-007-1023-8.

Osawa, F., Fujii, T., Nishida, T., Tada, N., Ohnishi, T., Kobayashi, O., et al. (2009). Efficient production of L-lactic acid by Crabtree-negative yeast *Candida boidinii*. *Yeast* 26, 485–496. doi:10.1002/yea.1702.

Ostafin, M., Haber, J., Doronina, N. V., Sokolov, A. P., and Trotsenko, Y. A. (1999). Methylobacterium extorquens strain P14, a new methylotrophic bacteria producing poly-beta-hydroxybutyrate (PHB). *Acta Microbiol. Pol.* 48, 39–51.

Ostling, C. E., and Lindgren, S. E. (1993). Inhibition of enterobacteria and Listeria growth by lactic, acetic and formic acids. *J. Appl. Bacteriol.* 75, 18–24.

Oyama, Y., Sakai, H., Arata, T., Okano, Y., Akaike, N., Sakai, K., et al. Cytotoxic e¡ects of methanol, formaldehyde, and formate on dissociated rat thymocytes: A possibility of aspartame toxicity. 8.

Pérez-Fortes, M., Schöneberger, J. C., Boulamanti, A., and Tzimas, E. (2016). Methanol synthesis using captured CO 2 as raw material: Techno-economic and environmental assessment. *Appl. Energy* 161, 718–732. doi:10.1016/j.apenergy.2015.07.067.

Perham, M., Liao, J., and Wittung-Stafshede, P. (2006). Differential Effects of Alcohols on Conformational Switchovers in α-Helical and β-Sheet Protein Models †. *Biochemistry* 45, 7740–7749. doi:10.1021/bi060464v.

Peyraud, R., Schneider, K., Kiefer, P., Massou, S., Vorholt, J. A., and Portais, J.-C. (2011). Genome-scale reconstruction and system level investigation of the metabolic network of Methylobacterium extorquens AM1. *BMC Syst. Biol.* 5, 189. doi:10.1186/1752-0509-5-189.

Pfeifenschneider, J., Brautaset, T., and Wendisch, V. F. (2017). Methanol as carbon substrate in the bio-economy: Metabolic engineering of aerobic methylotrophic bacteria for production of value-added chemicals: Methanol as carbon substrate in the bio-economy. *Biofuels Bioprod. Biorefining* 11, 719–731. doi:10.1002/bbb.1773.

Pfeifer, G. P., You, Y.-H., and Besaratinia, A. (2005). Mutations induced by ultraviolet light. *Mutat. Res. Mol. Mech. Mutagen.* 571, 19–31. doi:10.1016/j.mrfmmm.2004.06.057.

Pollich, M., and Klug, G. (1995). Identification and sequence analysis of genes involved in late steps in cobalamin (vitamin B12) synthesis in Rhodobacter capsulatus. *J. Bacteriol.* 177, 4481–4487. doi:10.1128/jb.177.15.4481-4487.1995.

Price, J. V., Chen, L., Whitaker, W. B., Papoutsakis, E., and Chen, W. (2016). Scaffoldless engineered enzyme assembly for enhanced methanol utilization. *Proc. Natl. Acad. Sci.* 113, 12691–12696. doi:10.1073/pnas.1601797113.

Raeside, C., Gaffe, J., Deatherage, D. E., Tenaillon, O., Briska, A. M., Ptashkin, R. N., et al. (2014). Large Chromosomal Rearrangements during a Long-Term Evolution Experiment with Escherichia coli. *mBio* 5. doi:10.1128/mBio.01377-14.

Rau, M. H., Calero, P., Lennen, R. M., Long, K. S., and Nielsen, A. T. (2016). Genome-wide Escherichia coli stress response and improved tolerance towards industrially relevant chemicals. *Microb. Cell Factories* 15. doi:10.1186/s12934-016-0577-5.

Reyes, L. H., Abdelaal, A. S., and Kao, K. C. (2013). Genetic Determinants for *n* -Butanol Tolerance in Evolved Escherichia coli Mutants: Cross Adaptation and Antagonistic Pleiotropy between *n* -Butanol and Other Stressors. *Appl. Environ. Microbiol.* 79, 5313–5320. doi:10.1128/AEM.01703-13.

Reyes, L. H., Almario, M. P., and Kao, K. C. (2011). Genomic Library Screens for Genes Involved in n-Butanol Tolerance in Escherichia coli. *PLoS ONE* 6, e17678. doi:10.1371/journal.pone.0017678.

Rohde, M.-T., Tischer, S., Harms, H., and Rohwerder, T. (2017). Production of 2-Hydroxyisobutyric Acid from Methanol by Methylobacterium extorquens AM1 Expressing ( *R* )-3-Hydroxybutyryl Coenzyme A-Isomerizing Enzymes. *Appl. Environ. Microbiol.* 83, e02622-16. doi:10.1128/AEM.02622-16.

Roy, H. (2009). Tuning the properties of the bacterial membrane with aminoacylated phosphatidylglycerol. *IUBMB Life* 61, 940–953. doi:10.1002/iub.240.

Ruffing, A. M., and Trahan, C. A. (2014). Biofuel toxicity and mechanisms of biofuel tolerance in three model cyanobacteria. *Algal Res.* 5, 121–132. doi:10.1016/j.algal.2014.07.006.

Rutherford, B. J., Dahl, R. H., Price, R. E., Szmidt, H. L., Benke, P. I., Mukhopadhyay, A., et al. (2010). Functional Genomic Study of Exogenous n-Butanol Stress in Escherichia coli. *Appl. Environ. Microbiol.* 76, 1935–1945. doi:10.1128/AEM.02323-09.

Salis, H. M. (2011). "The Ribosome Binding Site Calculator," in *Methods in Enzymology* (Elsevier), 19–42. doi:10.1016/B978-0-12-385120-8.00002-4.

Schada von Borzyskowski, L., Remus-Emsermann, M., Weishaupt, R., Vorholt, J. A., and Erb, T. J. (2015). A Set of Versatile Brick Vectors and Promoters for the Assembly, Expression, and Integration of Synthetic Operons in *Methylobacterium extorquens* AM1 and Other Alphaproteobacteria. *ACS Synth. Biol.* 4, 430–443. doi:10.1021/sb500221v.

Schotte, P., Dewerte, I., De Groeve, M., De Keyser, S., De Brabandere, V., and Stanssens, P. (2016). Pichia pastoris MutS strains are prone to misincorporation of O-methyl-l-homoserine at methionine residues when methanol is used as the sole carbon source. *Microb. Cell Factories* 15. doi:10.1186/s12934-016-0499-2.

Schrader, J., Schilling, M., Holtmann, D., Sell, D., Filho, M. V., Marx, A., et al. (2009). Methanol-based industrial biotechnology: current status and future perspectives of methylotrophic bacteria. *Trends Biotechnol.* 27, 107–115. doi:10.1016/j.tibtech.2008.10.009.

Schuler Dirk, and Kolinko Isabel (2015). Production of magnetic nanoparticles in recombinant host cell.

SHUNSAKU UEDA, SEIJI MATSUMOTO, AYA TAKAGI, and TSUNEO YAMANE (1992). Synthesis of Poly(3-Hydroxybutyrate-Co-3-Hydroxyvalerate) from Methanol and n-Amyl Alcohol by the Methylotrophic Bacteria Paracoccus denitrtificans and Methylobacterium extorquens.

Silva-Rocha, R., Martínez-García, E., Calles, B., Chavarría, M., Arce-Rodríguez, A., de Las Heras, A., et al. (2013). The Standard European Vector Architecture (SEVA): a coherent platform for the analysis and deployment of complex prokaryotic phenotypes. *Nucleic Acids Res.* 41, D666-675. doi:10.1093/nar/gks1119.

Singh, P., and Geuzebroek, F. (2018). Opportunities for $CO_2$ Utilization Other Than EOR. in *Abu Dhabi International Petroleum Exhibition & Conference* (Abu Dhabi, UAE: Society of Petroleum Engineers). doi:10.2118/193077-MS.

Sixma, T. K. (2001). DNA mismatch repair: MutS structures bound to mismatches. *Curr. Opin. Struct. Biol.* 11, 47–52.

Skrzydlewska, E., Elas, M., Farbiszewski, R., and Roszkowska, A. (2000). Effect of methanol intoxication on free-radical induced protein oxidation. *J. Appl. Toxicol. JAT* 20, 239–243.

So, A. G., and Davie, E. W. (1964). The Effects of Organic Solvents on Protein Biosynthesis and Their Influence on the Amino Acid Code *. *Biochemistry* 3, 1165–1169. doi:10.1021/bi00896a027.

Song, C. W., Kim, J. W., Cho, I. J., and Lee, S. Y. (2016). Metabolic Engineering of *Escherichia coli* for the Production of 3-Hydroxypropionic Acid and Malonic Acid through β-Alanine Route. *ACS Synth. Biol.* 5, 1256–1263. doi:10.1021/acssynbio.6b00007.

Sonntag, F., Buchhaupt, M., and Schrader, J. (2014). Thioesterases for ethylmalonyl–CoA pathway derived dicarboxylic acid production in Methylobacterium extorquens AM1. *Appl. Microbiol. Biotechnol.* 98, 4533–4544. doi:10.1007/s00253-013-5456-y.

Sonntag, F., Kroner, C., Lubuta, P., Peyraud, R., Horst, A., Buchhaupt, M., et al. (2015). Engineering Methylobacterium extorquens for de novo synthesis of the sesquiterpenoid α-humulene from methanol. *Metab. Eng.* 32, 82–94. doi:10.1016/j.ymben.2015.09.004.

Souterre, T. (2017). Optimization of enzymes via directed evolution in vivo.

Stephanopoulos, G., Alper, H., and Moxley, J. (2004). Exploiting biological complexity for strain improvement through systems biology. *Nat. Biotechnol.* 22, 1261–1267. doi:10.1038/nbt1016.

Strovas, T. J., Dragavon, J. M., Hankins, T. J., Callis, J. B., Burgess, L. W., and Lidstrom, M. E. (2006). Measurement of Respiration Rates of Methylobacterium extorquens AM1 Cultures by Use of a Phosphorescence-Based Sensor. *Appl. Environ. Microbiol.* 72, 1692–1695. doi:10.1128/AEM.72.2.1692-1695.2006.

Strovas, T. J., Sauter, L. M., Guo, X., and Lidstrom, M. E. (2007). Cell-to-Cell Heterogeneity in Growth Rate and Gene Expression in Methylobacterium extorquens AM1. *J. Bacteriol.* 189, 7127–7133. doi:10.1128/JB.00746-07.

Stuani, L. (2014). Nouveaux aspects du métabolisme d'acinetobacter baylyi ADP1 : une approche métabolomique.

Swings, T., Van den Bergh, B., Wuyts, S., Oeyen, E., Voordeckers, K., Verstrepen, K. J., et al. (2017). Adaptive tuning of mutation rates allows fast response to lethal stress in Escherichia coli. *eLife* 6. doi:10.7554/eLife.22939.

Taidi, B., Anderson, A. J., Dawes, E. A., and Byrom, D. (1994). Effect of carbon source and concentration on the molecular mass of poly(3-hydroxybutyrate) produced by Methylobacterium extorquens and Alcaligenes eutrophus. *Appl. Microbiol. Biotechnol.* 40, 786–790. doi:10.1007/BF00173975.

Takeshi, N., Junko, T., Nobuo, K., Yasuyoshi, S., Daisuke, M., Hitoshi, et al. (1999). Synergistic effect of the combination of phytases on hydrolysis of phytic acid.

Tenaillon, O., Barrick, J. E., Ribeck, N., Deatherage, D. E., Blanchard, J. L., Dasgupta, A., et al. (2016). Tempo and mode of genome evolution in a 50,000-generation experiment. *Nature* 536, 165–170. doi:10.1038/nature18959.

Thulasi, K., Jayakumar, A., Balakrishna Pillai, A., Gopalakrishnapillai Sankaramangalam, V. K., and Kumarapillai, H. (2018). Efficient methanol-degrading aerobic bacteria isolated from a wetland ecosystem. *Arch. Microbiol.* doi:10.1007/s00203-018-1509-z.

Tian, S.-Q., Zhao, R.-Y., and Chen, Z.-C. (2018). Review of the pretreatment and bioconversion of lignocellulosic biomass from wheat straw materials. *Renew. Sustain. Energy Rev.* 91, 483–489. doi:10.1016/j.rser.2018.03.113.

Tolonen, A. C., Zuroff, T. R., Ramya, M., Boutard, M., Cerisy, T., and Curtis, W. R. (2015). Physiology, Genomics, and Pathway Engineering of an Ethanol-Tolerant Strain of Clostridium phytofermentans. *Appl. Environ. Microbiol.* 81, 5440–5448. doi:10.1128/AEM.00619-15.

Tran, T. H., Krishnamoorthy, K., Begley, T. P., and Ealick, S. E. (2011). A novel mechanism of sulfur transfer catalyzed by *O* -acetylhomoserine sulfhydrylase in the methionine-biosynthetic pathway of *Wolinella succinogenes*. *Acta Crystallogr. D Biol. Crystallogr.* 67, 831–838. doi:10.1107/S0907444911028010.

Traxler, M. F., Summers, S. M., Nguyen, H.-T., Zacharia, V. M., Hightower, G. A., Smith, J. T., et al. (2008). The global, ppGpp-mediated stringent response to amino acid starvation in Escherichia coli. *Mol. Microbiol.* 68, 1128–1148. doi:10.1111/j.1365-2958.2008.06229.x.

Tremblay, P.-L., Höglund, D., Koza, A., Bonde, I., and Zhang, T. (2015). Adaptation of the autotrophic acetogen Sporomusa ovata to methanol accelerates the conversion of CO2 to organic products. *Sci. Rep.* 5. doi:10.1038/srep16168.

Tseng, H.-C., and Prather, K. L. J. (2012). Controlled biosynthesis of odd-chain fuels and chemicals via engineered modular metabolic pathways. *Proc. Natl. Acad. Sci.* 109, 17925–17930. doi:10.1073/pnas.1209002109.

Valentin, H., and Steinb�chel, A. (1993). Cloning and characterization of the Methylobacterium extorquens polyhydroxyalkanoic-acid-synthase structural gene. *Appl. Microbiol. Biotechnol.* 39. doi:10.1007/BF00192084.

Vallenet, D., Calteau, A., Cruveiller, S., Gachet, M., Lajus, A., Josso, A., et al. (2017). MicroScope in 2017: an expanding and evolving integrated resource for community expertise of microbial genomes. *Nucleic Acids Res.* 45, D517–D528. doi:10.1093/nar/gkw1101.

Van Dien, S. J., and Lidstrom, M. E. (2002). Stoichiometric model for evaluating the metabolic capabilities of the facultative methylotrophMethylobacterium extorquens AM1, with application to reconstruction of C3 and C4 metabolism. *Biotechnol. Bioeng.* 78, 296–312. doi:10.1002/bit.10200.

Vorholt, J. (2002). Cofactor-dependent pathways of formaldehyde oxidation in methylotrophic bacteria. *Arch. Microbiol.* 178, 239–249. doi:10.1007/s00203-002-0450-2.

Vuilleumier, S., Chistoserdova, L., Lee, M.-C., Bringel, F., Lajus, A., Zhou, Y., et al. (2009a). Methylobacterium Genome Sequences: A Reference Blueprint to Investigate Microbial Metabolism of C1 Compounds from Natural and Industrial Sources. *PLoS ONE* 4, e5584. doi:10.1371/journal.pone.0005584.

Vuilleumier, S., Chistoserdova, L., Lee, M.-C., Bringel, F., Lajus, A., Zhou, Y., et al. (2009b). Methylobacterium Genome Sequences: A Reference Blueprint to Investigate Microbial Metabolism of C1 Compounds from Natural and Industrial Sources. *PLoS ONE* 4, e5584. doi:10.1371/journal.pone.0005584.

Wang, X., Yu, Z., Tang, J., Yi, D., and Chen, S. (2018). Efficient production of (R)-(−)-2-hydroxy-4-phenylbutyric acid by recombinant Pichia pastoris expressing engineered d-lactate dehydrogenase from Lactobacillus plantarum with a single-site mutation. *Bioprocess Biosyst. Eng.* doi:10.1007/s00449-018-1965-5.

Wang, Y., Shi, M., Niu, X., Zhang, X., Gao, L., Chen, L., et al. (2014). Metabolomic basis of laboratory evolution of butanol tolerance in photosynthetic Synechocystis sp. PCC 6803. *Microb. Cell Factories* 13. doi:10.1186/s12934-014-0151-y.

Wang, Y., Sun, T., Gao, X., Shi, M., Wu, L., Chen, L., et al. (2016). Biosynthesis of platform chemical 3-hydroxypropionic acid (3-HP) directly from CO 2 in cyanobacterium Synechocystis sp. PCC 6803. *Metab. Eng.* 34, 60–70. doi:10.1016/j.ymben.2015.10.008.

Wessels, H. J. C. T., de Almeida, N. M., Kartal, B., and Keltjens, J. T. (2016). "Bacterial Electron Transfer Chains Primed by Proteomics," in *Advances in Microbial Physiology* (Elsevier), 219–352. doi:10.1016/bs.ampbs.2016.02.006.

Whitaker, W. B., Jones, J. A., Bennett, R. K., Gonzalez, J. E., Vernacchio, V. R., Collins, S. M., et al. (2017). Engineering the biological conversion of methanol to specialty chemicals in Escherichia coli. *Metab. Eng.* 39, 49–59. doi:10.1016/j.ymben.2016.10.015.

Whitaker, W. B., Sandoval, N. R., Bennett, R. K., Fast, A. G., and Papoutsakis, E. T. (2015). Synthetic methylotrophy: engineering the production of biofuels and chemicals based on the biology of aerobic methanol utilization. *Curr. Opin. Biotechnol.* 33, 165–175. doi:10.1016/j.copbio.2015.01.007.

Wikström, M., Krab, K., and Sharma, V. (2018). Oxygen Activation and Energy Conservation by Cytochrome *c* Oxidase. *Chem. Rev.* 118, 2469–2490. doi:10.1021/acs.chemrev.7b00664.

Wilkins, M. R., Widmer, W. W., and Grohmann, K. (2007). Simultaneous saccharification and fermentation of citrus peel waste by Saccharomyces cerevisiae to produce ethanol. *Process Biochem.* 42, 1614–1619. doi:10.1016/j.procbio.2007.09.006.

Witthoff, S., Schmitz, K., Niedenführ, S., Nöh, K., Noack, S., Bott, M., et al. (2015). Metabolic Engineering of Corynebacterium glutamicum for Methanol Metabolism. *Appl. Environ. Microbiol.* 81, 2215–2225. doi:10.1128/AEM.03110-14.

Wu, T.-Y., Chen, C.-T., Liu, J. T.-J., Bogorad, I. W., Damoiseaux, R., and Liao, J. C. (2016). Characterization and evolution of an activator-independent methanol dehydrogenase from Cupriavidus necator N-1. *Appl. Microbiol. Biotechnol.* 100, 4969–4983. doi:10.1007/s00253-016-7320-3.

Yang, Y.-M., Chen, W.-J., Yang, J., Zhou, Y.-M., Hu, B., Zhang, M., et al. (2017). Production of 3-hydroxypropionic acid in engineered Methylobacterium extorquens AM1 and its reassimilation through a reductive route. *Microb. Cell Factories* 16. doi:10.1186/s12934-017-0798-2.

Yishai, O., Bouzon, M., Döring, V., and Bar-Even, A. (2018). *In Vivo* Assimilation of One-Carbon *via* a Synthetic Reductive Glycine Pathway in *Escherichia coli*. *ACS Synth. Biol.* 7, 2023–2028. doi:10.1021/acssynbio.8b00131.

Yomano, L. P., York, S. W., and Ingram, L. O. (1998). Isolation and characterization of ethanol-tolerant mutants of Escherichia coli KO11 for fuel ethanol production. *J. Ind. Microbiol. Biotechnol.* 20, 132–138. doi:10.1038/sj.jim.2900496.

Yurimoto, H., Kato, N., and Sakai, Y. (2009). Genomic organization and biochemistry of the ribulose monophosphate pathway and its application in biotechnology. *Appl. Microbiol. Biotechnol.* 84, 407–416. doi:10.1007/s00253-009-2120-7.

Zambrano, M. M., Siegele, D. A., Almirón, M., Tormo, A., and Kolter, R. (1993). Microbial competition: Escherichia coli mutants that take over stationary phase cultures. *Science* 259, 1757–1760.

Zeng, A.-P. (2019). New bioproduction systems for chemicals and fuels: Needs and new development. *Biotechnol. Adv.* doi:10.1016/j.biotechadv.2019.01.003.

Zhang, W., Zhang, T., Wu, S., Wu, M., Xin, F., Dong, W., et al. (2017). Guidance for engineering of synthetic methylotrophy based on methanol metabolism in methylotrophy. *RSC Adv.* 7, 4083–4091. doi:10.1039/C6RA27038G.

Zhou, X., Lü, S., Xu, Y., Mo, Y., and Yu, S. (2015). Improving the performance of cell biocatalysis and the productivity of xylonic acid using a compressed oxygen supply. *Biochem. Eng. J.* 93, 196–199. doi:10.1016/j.bej.2014.10.014.

Zhou, X., Zhou, X., and Xu, Y. (2017). Improvement of fermentation performance of Gluconobacter oxydans by combination of enhanced oxygen mass transfer in compressed-oxygen-supplied sealed system and cell-recycle technique. *Bioresour. Technol.* 244, 1137–1141. doi:10.1016/j.biortech.2017.08.107.

Zhu, W.-L., Cui, J.-Y., Cui, L.-Y., Liang, W.-F., Yang, S., Zhang, C., et al. (2016). Bioconversion of methanol to value-added mevalonate by engineered Methylobacterium extorquens AM1 containing an optimized mevalonate pathway. *Appl. Microbiol. Biotechnol.* 100, 2171–2182. doi:10.1007/s00253-015-7078-z.

Zingaro, K. A., and Terry Papoutsakis, E. (2013). GroESL overexpression imparts Escherichia coli tolerance to i-, n-, and 2-butanol, 1,2,4-butanetriol and ethanol with complex and unpredictable patterns. *Metab. Eng.* 15, 196–205. doi:10.1016/j.ymben.2012.07.009.

Zúñiga, C., Morales, M., Le Borgne, S., and Revah, S. (2011). Production of poly-β-hydroxybutyrate (PHB) by Methylobacterium organophilum isolated from a methanotrophic consortium in a two-phase partition bioreactor. *J. Hazard. Mater.* 190, 876–882. doi:10.1016/j.jhazmat.2011.04.011.

# RESUME

## La transition des énergies fossiles aux énergies renouvelables - un défi mondial

En 2015, les énergies fossiles représentent plus de 80% de la consommation totale d'énergie dans le monde (statistiques de l'Agence d'information sur l'énergie, 2014). Cette dépendance a un impact économique mais aussi écologique. Les combustibles fossiles tels que le pétrole, le charbon et le gaz naturel libèrent du carbone, stocké pendant des millions d'années dans la croûte terrestre, sous forme de $CO_2$ lorsqu'il est utilisé pour le chauffage domestique, le transport ou les processus industriels. Le $CO_2$, gaz à effet de serre, est en grande partie directement responsable du réchauffement climatique enregistré depuis le début de la révolution industrielle. Dans ce contexte, la Commission européenne a présenté une nouvelle version de la directive sur la promotion des sources d'énergie renouvelables (SER), dans le cadre du paquet plus large «Énergie propre pour tous les Européens». L'objectif principal de la refonte de la directive sur les énergies renouvelables est de porter la part des énergies renouvelables dans le bouquet énergétique de l'Union européenne (UE) à 27% d'ici 2030 (Conseil européen d'octobre 2014), afin de garantir que l'UE devienne le leader mondial des énergies renouvelables. l'énergie (RED II, 2016).

## Réduction des composés monocarbonés comme vecteurs d'énergie

Dans le présent travail, nous nous sommes concentrés sur l'utilisation de méthanol comme matière première de fermentation. La production mondiale de méthanol est en croissance constante, avec un volume total de 49 millions de tonnes métriques produites en 2010, 75 millions de tonnes métriques en 2015 et environ 95 millions de tonnes métriques en 2021 (IHS Markit, 2017). Cette augmentation de la capacité de production annuelle continuera à entraîner une baisse de son prix, ce qui rendra son utilisation encore plus attrayante.

Le méthanol a une grande variété d'applications en tant que précurseur de nombreux produits industriels tels que le formaldéhyde, l'acide acétique ou le diméthyléther, etc. (Figure 1). Ces dérivés sont pour la plupart des produits chimiques essentiels (Komaba Shinichi et al., 2018; Leopold Eugen, 2018; Montes Martin et al., 2018). En outre, environ 200 000 tonnes de

méthanol sont utilisées comme matière première chimique. Le méthanol est une substance biodégradable et à combustion propre (Boudemagh et al., 2006; Dhamwichukorn et al., 2001; Kaszycki et Kołoczek, 2000).

En outre, le méthanol peut être produit à un prix concurrentiel à partir de dioxyde de carbone et d'hydrogène en tant que donneur d'énergie (Ghasemzadeh et al., 2018; Methanol, Process Economics Program Report 43C, 2000). L'hydrogène est à son tour obtenu à l'aide de sources d'énergie renouvelables telles que l'énergie éolienne et solaire (Anicic et al., 2014; Pérez-Fortes et al., 2016).

## La bioproduction en tant que procédé de production prometteur

Aujourd'hui, la majorité des processus de fermentation à grande échelle utilisent des glucides comme source de carbone et d'énergie pour les micro-organismes producteurs. Les hydrates de carbone proviennent de cultures cultivées sur des terres arables, ce qui entraîne une concurrence avec le secteur des aliments pour animaux et des denrées alimentaires (Muffler et Ulber, 2008). Il est impératif de préserver les réserves alimentaires et de se préparer lorsque la population mondiale atteindra 8,3 milliards de personnes pour 2030 (Organisation de coopération et de développement économiques (OCDE), La bioéconomie à l'horizon 2030 - élaborer un programme politique, Éditions OCDE 13 (2009); (Kircher, 2012).

L'utilisation de matières premières dérivées de sources non alimentaires telles que la ligno-cellulose est une alternative développée ces dernières années (Tian et al., 2018; Zeng, 2019). Cependant, des difficultés techniques empêchent toujours une exploitation efficace (Ochsner et al., 2015). Une autre possibilité pour éviter la concurrence avec le secteur de l'alimentation consiste à utiliser des microorganismes photoautotrophes tels que les cyanobactéries et les microalgues qui convertissent le $CO_2$ atmosphérique en composés carbonés complexes en utilisant la lumière du soleil comme source d'énergie (projet Vasco2, projet Jupiter 1000). Les difficultés liées au captage du $CO_2$, aux besoins importants en surface et aux séparations coûteuses des produits chimiques produits à partir de cultures à faible densité doivent être surmontées pour rendre cette approche économiquement viable (Singh et Geuzebroek, 2018).

Une biotechnologie basée sur la fermentation du méthanol synthétisé à partir de CO2 et de H2 produits à l'aide d'énergies renouvelables pourrait limiter la dépendance aux hydrates de carbone en biotechnologie industrielle (Pfeifenschneider et al., 2017; Schrader et al., 2009) et permettre la mise en place d'un cycle de production fermé. éviter les sources d'énergie et de carbone fossiles (Goeppert et al., 2014; Hwang et al., 2015) (Figure 2).

## Méthylotrophie naturelle

Une variété de microorganismes méthylotrophes se trouvent dans presque tous les types d'habitats naturels (Butterfield et al., 2016; Chistoserdova et al., 2009; Faria et Bharathi, 2006; Meena et al., 2015; Thulasi et al., 2018). Les méthylotrophes font partie de différentes branches de l'arbre de vie, telles que la levure, les archées et les bactéries (Chistoserdova et al., 2009). Certains dépendent entièrement de composés à un seul carbone (C1) (méthylotrophes obligatoires), tandis que d'autres peuvent également se développer sur des sources multicarbonées (méthylotrophes facultatifs). Les substrats C1 utilisés peuvent varier d'une souche à l'autre ; le méthanol est le composé commun assimilé, d'autres bactéries ont la capacité d'utiliser le méthane ($CH_4$), le formiate (HCOOH), le dioxyde de carbone ($CO_2$), le monoxyde de carbone (CO), le méthane sulfonate, l'amino méthane, le chlorométhane, etc. (Chistoserdova, 2018; Dürre et Eikmanns, 2015) (Figure 3).

## Les organismes méthylotrophes naturels en tant que souches de plate-forme biotechnologique

Comme indiqué ci-dessus, des composés C1 réduits tels que le méthanol peuvent être produits à partir de $CO_2$ et d'énergie renouvelable. Le méthanol est peu coûteux, soluble et facile à manipuler. Il est plus réduit que les sucres couramment utilisés, nécessaires aux besoins nutritionnels d'une population mondiale croissante. En outre, la majorité des souches microbiennes connues ne se développent pas sur le méthanol en tant que source unique de carbone et d'énergie. Les fermentations industrielles sont donc moins menacées par les contaminations que pour les glucides. Les organismes méthylotrophes peuvent servir de châssis métabolique dans lequel des voies hétérologues peuvent être introduites pour produire des produits chimiques destinés à des plateformes à des fins industrielles (Jiang et al., 2010; Ochsner et al., 2015) (tableau 2). Depuis les années 1960, les bactéries méthylotrophes sont

utilisées industriellement pour la production d'acides aminés, de protéines, de plastiques biodégradables, etc. (Zhu et al., 2016).

## *Methylobacterium extorquens* en tant qu'organisme de plate-forme biotechnologique

*M. extorquens* AM1 en tant que souche de référence est la souche du cycle de la sérine la plus étudiée (Ochsner et al., 2015). L'ensemble du génome de cette souche, comprenant un chromosome de (6,8 Mo) et quatre plasmides a été séquencé (Marx et al., 2012; Vuilleumier et al., 2009a). Les progrès dans la compréhension de la physiologie et de la génétique de cette souche, les modèles métaboliques établis (Marx et al., 2005; Peyraud et al., 2011) et le développement d'outils de biologie moléculaire ont permis la réalisation de projets d'ingénierie. Plusieurs systèmes de vecteurs sont maintenant disponibles pour *M. extorquens* AM1. Ils comprennent des plasmides pour l'expression de protéines en utilisant un panel de promoteurs inductibles, comme par exemple le promoteur PmxaF de l'opéron méthanol déshydrogénase (tableau S1). L'expression à partir de plasmides réplicatifs est possible, ainsi qu'à partir du chromosome par le biais de systèmes intégratifs (site katA, attTn7-site ref). Des protocoles de mutagenèse, d'insertion aléatoire de cassettes et de recombinaison homologue ont été établis (Choi et al., 2006; Marx, 2004; Marx et Lidstrom, 2002; Schada von Borzyskowski et al., 2015). Ainsi, des tentatives ont été faites pour optimiser l'assimilation du méthanol en inserant les étapes essentielles à la conversion du formaldéhyde (Carroll et al., 2015) mais aussi à d'autres composés C1 utilisés comme substrats (Michener et al., 2014; Zhu et al., 2016 ).

*M. extorquens* AM1 a trouvé des applications en tant qu'organisme de châssis pour les bioproductions (tableau 3). Sa capacité à croître sur des sources de carbone complexes telles que le succinate simplifie la mise en œuvre de voies d'assimilation modifiées de C1 et laisse apparaître un large éventail d'intermédiaires métaboliques susceptibles de devenir le point de départ de nouvelles voies de synthèse (Eggeling et Sahm, 1981; Gommers et al., 1988). ). De plus, les thioesters constituant la voie de régénération du glyoxylate dans l'éthylmalonyl-CoA sont utilisés comme précurseurs de la production de produits chimiques fins ou en vrac (Korotkova et al., 2002, Yang et al., 2018). Enfin, les métabolites secondaires tels que les caroténoïdes produits par AM1 présentent un intérêt industriel, ainsi que le polymère naturel polyhydroxybutyrate (PHB) (Schrader et al., 2009).

Une souche industrielle est caractérisée doit valider une liste de caractéristiques. Les points clés suivants en font partie :

• Stabilité génétique
• Production efficace de produit
• Besoins nutritionnels simples
• Source de carbone et d'énergie bon marché
• Facilement génétiquement modifié
• Sécurité
• Facilement récolté de moyen
• Facilement cassable si produit intracellulaire
• Produits limités en milieu de fermentation.

Sur la base de ces caractéristiques, qui seront discutées dans ce rapport, une des approches alternatives consiste à créer des souches industrielles consiste à améliorer le phénotype de la souche naturelle de manière ciblée. En général, les améliorations des souches visent à augmenter la production et à réduire les coûts. Dans cette étude, deux aspects limitants des souches méthylotrophes naturelles sont ciblés : la toxicité du méthanol et le besoin en oxygène.

## Toxicité des solvants pour les souches productrices de biocarburants et leur adaptation à une tolérance plus élevée

La nature toxique des solvants pour bactéries est un obstacle majeur à la production de produits chimiques économiquement viables ou pouvant être utilisés comme sources de carbone.

De nombreux rapports décrivent les effets inhibiteurs sur la prolifération cellulaire de l'éthanol de biocarburant en vrac (Ruffing et Trahan, 2014), mais également du n-butanol et de l'isobutanol, des composés qui ont acquis un intérêt comme biocarburants potentiels en raison de leurs propriétés physicochimiques favorables (Tseng et Prather , 2012). Habituellement, ces agents stressants du solvant ont des effets pléiotropes sur l'intégrité chimique des composants cellulaires et perturbent les mécanismes intracellulaires vitaux de diverses manières (Stephanopoulos et al., 2004). Outre les approches de conception rationnelle, où les transporteurs de membrane détoxifiants (García et al., 2009; Kell et al., 2015) ou les chaperons

sont surexprimés pour réduire la charge toxique des agents stressants du solvant (Okochi et 2008), stratégies orientées sur l'évolution des souches sont suivies pour sélectionner la tolérance améliorée.

Le méthanol, bien que son utilisation actuelle en tant que substitut de carburant dans certaines applications, n'a pas le potentiel pour devenir un biocarburant comme c'est le cas pour l'éthanol ou éventuellement le n-butanol. En conséquence, les effets du méthanol en tant que solvant sur la prolifération cellulaire n'ont pas été étudiés en détail.

Des rapports traitant de son activité sur les composants cellulaires, notamment les protéines et les bicouches lipidiques ont été publiés. Ils montrent que le méthanol peut modifier la structure des protéines en stabilisant des intermédiaires globulaires non natifs et en renforçant les conformations secondaires des hélices alpha et des feuillets bêta (Hwang et al., 2011; Kamatari et al., 1996; Perham et al., 1996). ., 2006). Il augmente la concentration de radicaux libres d'oxygène qui induisent à leur tour une oxydation des protéines (Skrzydlewska et al., 2000). Il peut perturber les activités enzymatiques ou même la synthèse des protéines (Busby et al., 1999). Une modification de la fluidité des bicouches lipidiques induite par le méthanol a également été observée, avec des conséquences possibles sur la conformation spatiale des protéines membranaires (Joo et al., 2012).

## Évolution dirigée de souches microbiennes / Propagation à long terme de populations cellulaires

Les suspensions de souches microbiennes cultivées dans des conditions définies pendant de longues périodes permettent d'étudier l'accumulation et la fixation de mutations dans des populations cellulaires. Il ouvre également la voie à la sélection de descendants ayant acquis de nouveaux phénotypes qui pourraient présenter un intérêt scientifique et / ou des objets d'applications industrielles. On distingue deux types d'expériences sur l'évolution des populations de cellules : le transfert de cellules en série et la culture continue (Barrick et Lenski, 2013).

La formation à long terme de suspensions cellulaires est entravée par la formation de biofilms à la surface du vaisseau interne. Dans une population en croissance sous un régime de dilution,

des mutants capables de coller à la surface du vaisseau apparaissent et sont sélectionnés. En formant des biofilms, ces «mutants collants» échappent à la sélection imposée à la culture par des impulsions de dilution sans acquérir le phénotype amélioré recherché.
Pour contourner cet obstacle, le dispositif autonettoyant GM3 automatisant les opérations de culture continue a été développé (Figure 7) (Mutzel et al., 2004; Mutzel et Marlière, 2001).

## Objectifs de ce projet

Une large gamme de voies de biosynthèse a été mise en œuvre dans les souches méthylotrophes naturelles du genre *Methylobacterium* permettant la production de divers produits chimiques de base à partir de méthanol, une matière première renouvelable suscitant l'intérêt pour les processus biotechnologiques. En revanche, moins d'efforts ont été déployés pour doter ces souches de propriétés améliorées en tant que châssis de production. Dans ce contexte, les questions suivantes ont été posées :

Les souches de *M. extorquens* peuvent-elles évoluer vers une croissance stable à des concentrations élevées en méthanol ? Le méthanol en tant que solvant alcoolique et précurseur des intermédiaires d'oxydation formaldéhyde et formiate est toxique pour les cellules. Cette toxicité limite les rendements de production en fermentation.

Quels seraient les processus cellulaires en cours lors d'une telle adaptation au méthanol ? Des analyses phénotypiques, génomiques, transcriptomiques et biochimiques devaient être menées pour identifier les gènes mutés et les réseaux de régulation modifiés, ainsi que pour tester les variants enzymatiques en vue d'une nouvelle activité.

La mise en œuvre d'une voie de synthèse dans une cellule tolérante au méthanol permettrait-elle la production d'un composé industriel avec un rendement plus élevé que la même voie mise en œuvre dans la souche de type sauvage ?

Les souches de *M. extorquens* peuvent-elles évoluer vers une croissance efficace sous des concentrations limitant l'oxygène ? Ces cellules aérobies obligatoires ont une forte demande en oxygène, ce qui rend difficile la montée en puissance des processus de fermentation et diminue le rendement en produit grâce à la capture d'électrons de haute énergie par la chaîne respiratoire.

## Résultats

Parmi les souches de *M. extorquens* déposées dans des collections de souches publiques mais non étudiées en détail, nous avons identifié la souche TK 0001, isolée du sol en Pologne et disponible au DSMZ (DSM n ° 1337), et procédé à une caractérisation physiologique et génomique. La figure 16 montre la croissance de cette souche sur des plaques de milieu minéral et dans des cultures liquides additionnées de 1% (v / v) de méthanol. Les cellules forment des colonies et des filaments de couleur rose typiques du genre Methylobacterium.

Le rendement de croissance après 48 heures de croissance de la souche TK 0001 avec du méthanol était linéaire pour un ensemble de concentrations testées. Par extrapolation, un rendement de 2,8 x 10-5 $mg.mL^{-1}.mM^{-1}$ a été calculé (1% de MeOH équivalent à 0,24 M) (Figure 19A). La linéarité a également été trouvée pour la détermination du rendement de croissance avec le succinate et par extrapolation, un rendement de 6,0 x 10-5 $mg.mL^{-1}.mM^{-1}$ de succinate a été calculé (Figure 19B). En termes de molarité, croissance sur succinate; qui contient quatre molécules de carbone; donne lieu à une production de biomasse supérieure à celle du méthanol. Alors que le succinate contient quatre atomes de carbone et le méthanol, un seul, l'écart de rendement n'est pas très élevé. Cependant, le rendement de la biomasse par le carbone est plus élevé avec le méthanol que le succinate, le méthanol est plus réduit et a donc un contenu énergétique plus élevé que le succinate.

Une enquête sur la résistance à divers antibiotiques couramment utilisés pour les manipulations génétiques a été réalisée pour la souche TK 0001. Une première évaluation a été réalisée à l'aide de filtres sur un milieu solide contenant du méthanol minéral afin d'obtenir une réponse qualitative (cf. II.1.2). TK 0001 s'est révélé résistant à l'ampicilline et au thiamphénicol, mais sensible à la tétracycline, à la kanamycine, à la rifampicine, au chloramphénicol et à la streptomycine après 72 heures d'incubation (tableau 20).

Les plasmides pourraient être introduits dans les cellules de *M. extorquens* TK 0001 par électroporation. Les cellules transformées ont été sélectionnées sur des plaques contenant la concentration appropriée d'antibiotique. Une autre méthode, basée sur le transfert par conjugaison de plasmides de *E. coli* à des cellules TK 0001, a également été utilisée avec succès.

Des plasmides navette contenant les origines de réplication des deux souches et un module de mobilisation oriT ont été utilisés, ainsi qu'une souche auxiliaire portant le plasmide pRK2073 (Bradley et al., 2017, don de F. Bringel, Université de Strassburg).

Les souches du genre *Methylobacterium* diffèrent par leur organisation génomique. Certains, comme la souche de référence AM1, hébergent des plasmides, tandis que d'autres ne contiennent que de l'ADN chromosomique. Aucun plasmide n'a été trouvé dans la souche TK 0001 de *M. extorquens*, en utilisant des méthodes électrophorétiques. Pour cela, nous avons examiné la migration d'un bouchon d'agarose contenant l'ADN total (comme décrit par Maleszka et al., 1991).
L'ADN chromosomique de TK 0001 a été extrait et séquencé au Genoscope à l'aide des technologies Illumina et Nanopore, pour atteindre une couverture de 134 fois (Figures S1A et B). Un seul contig a été obtenu à partir de l'assemblage final de 5,71 Mo avec une teneur en G / C de 68,2% (Belkhelfa et al., 2018) (Figure S1C). L'annotation fonctionnelle automatique a été réalisée à l'aide de la plate-forme du microscope (Vallenet et al., 2017) (Figure 20). Parmi les 6 251 objets génomiques identifiés, 6 160 étaient des séquences codantes (CDS), 17 ARN divers, 59 ARNt et 15 ARNr (5 5S, 5 16S et 5 23S).

En résumé, *M. extorquens* TK 0001 peut se développer dans un milieu minimal additionné de méthanol, est génétiquement manipulable et présente une taille de génome réduite en ce qui concerne AM1. Ces résultats prometteurs nous ont amenés à faire évoluer cette souche en parallèle avec la souche modèle AM1.

***Methylobacterium extorquens* TK 0001 évolution :**
Le méthanol sert de source unique de carbone et d'énergie pour les bactéries méthylotrophes telles que *Methylobacterium extorquens*. En tant que solvant alcoolique, il interagit avec les composants cellulaires en modifiant leur structure et leur stabilité chimique de manière dépendante de la concentration. Sa conversion métabolique en composé cytotoxique, le formaldéhyde, constitue également une menace chimique pour les cellules. Les tests de croissance sur un lecteur de plaques ont montré un maximum de croissance avec 1% de méthanol pour les souches TK 0001 et AM1 de *M. extorquens*. À 2% de méthanol, la croissance a été considérablement inhibée (figure 21). Pour utiliser ces souches en tant que châssis de production dans des processus biotechnologiques, une plus grande tolérance au méthanol et une

production de biomasse présenteraient un intérêt. Nous avons utilisé la technologie GM3 de culture continue automatisée pour faire évoluer les souches TK 0001 (Figure 22) et AM1 (Figure 27) en augmentant les concentrations de méthanol jusqu'à 10%.

Nous avons étudié le phénotype de croissance des souches dérivées de TK 0001 résistantes au méthanol. Une première observation faite pour les cellules adaptées était une croissance plus homogène en culture liquide caractérisée par l'absence de filaments (Figure S7AB). Ce phénotype est devenu évident à un stade précoce de l'évolution mais était également apparent à des stades ultérieurs. Néanmoins, la taille de la souche évoluée G4105 de la première population MEM5 à étapes développées est similaire à celle du type sauvage (figure S7CD).

Le temps de doublement pendant la croissance exponentielle a été déterminé pour les souches G4105 (adaptation au méthanol à 5%) et G4521 (adaptation au méthanol à 10%) dans des erlenmeyers à des concentrations de méthanol permissives et comparées à la souche de type sauvage. La figure 23A montre une réduction significative du temps de doublement à 0,25% de méthanol pour les deux souches adaptées par rapport au type sauvage. L'accélération de la croissance était beaucoup moins prononcée à 1% de méthanol. Inversement, la détermination du rendement maximal de la biomasse a révélé un gain considérable pour les souches adaptées à 1% de méthanol, mais seulement un faible effet à 0,25% (Figure 23B). Aucune différence significative ni en termes de taux de croissance ni de rendement n'a été observée pour les deux souches adaptées testées.

Nous avons en outre examiné si les phénotypes de croissance des cellules résistantes diffèrent à des concentrations élevées en méthanol en utilisant un lecteur de plaques. Ces résultats montrent que la population cellulaire a continué d'évoluer jusqu'à atteindre une croissance de 10% de méthanol dans le turbidostat (Figure 24E).

Pour identifier les mutations spécifiques survenues lors de l’adaptation des populations cellulaires à la croissance sur du méthanol élevé, un séquençage génomique a été réalisé pour les six isolats obtenus à partir de cultures adaptées à 5% (culture MEM5), 7% (culture MEM7), 8%. (culture MEM8) et 10% (culture MEM10) de méthanol, respectivement, et comparés au génome de type sauvage. Le tableau S3 résume les mutations dans chaque ensemble de six isolats. Les polymorphismes mononucléotidiques (SNP) et les délétions / insertions courtes ont

affecté les gènes et les régions intergéniques. De plus, une duplication chromosomique a été trouvée dans tous les isolats séquencés, contenant 86 cadres de lecture ouverts (ORF) (Tableau S4).

Le séquençage n'a révélé qu'un petit nombre de mutations chromosomiques, qui ont augmenté au cours de l'adaptation. Les mutations en point d'arbre étaient partagées entre tous les isolats séquencés. L'une était la mutation ponctuelle du gène *metY* codant pour l'O-acétyl-L-homosérine sulfhydrylase affectait un locus déjà impliqué dans la résistance au méthanol (Leßmeier et Wendisch, 2015; Schotte et al., 2016).

Les propriétés biophysiques des membranes biologiques sont importantes pour les réponses adaptatives des bactéries aux facteurs de stress externes. Mais aucune différence significative n'a été observée entre le WT et les cellules évoluées, ce qui indique que la composition membranaire est stable tout au long de l'évolution à des concentrations élevées en méthanol (figure 26).

***Methylobacterium extorquens* AM1 évolution :**

Dans une expérience parallèle, la souche de référence AMI de *M. extorquens* a évolué pour se développer sur du méthanol à 10% dans l'automate GM3. Les régimes de culture, la sélection des isolats et le séquençage ont été effectués comme pour la souche TK 0001 (Figure S8). Les cellules AM1, cependant, ont évolué vers des résistances élevées au méthanol à partir d'une seul inoculation de la souche de type sauvage. Tous les isolats développés de AM1 ont été répertoriés dans le tableau S2B. La figure 27A montre l'évolution de la population de cellules AM1 jusqu'à la croissance sur 10% de méthanol.

Le temps de doublement pendant la croissance exponentielle a été déterminé pour les souches AM1 de type sauvage et G4605 (adaptation au méthanol à 5%) dans des flacons d'Erlenmeyer à des concentrations de méthanol permissives et comparé à la souche de type sauvage. La souche développée à 5% de MeOH G4609 produit plus de biomasse que AM1 à la même concentration de formiate.

Cinq gènes ont été affectés dans tous les isolats obtenus à partir de la culture de résistance finale à 10%, y compris le gène *rpsL* codant pour la protéine ribosomale S12. Ce locus a également

été affecté dans les cellules TK 0001 adaptées à un taux très élevé de méthanol, impliquant toutefois un résidu différent (Tableau S3 et S5). En ce qui concerne l'adaptation TK 0001, le seul gène muté dans tous les isolats AM1 séquencés était le code *metY* pour la O-acétyl-L-homosérine sulfhydrylase, ce qui montre que ce locus est un point chaud de résistance au méthanol. Bien qu'une seule mutation (T34M) ait été trouvée dans tous les isolats résistants au méthanol TK 0001, quatre allèles différents de *metY* ont été identifiés dans les isolats AM1, qui étaient répartis de manière différentielle (tableau 29A).

Comme pour les isolats TK 0001, aucune différence significative n'a été observée entre l'AM1 WT et les cellules évoluées, ce qui montre qu'une composition membranaire stable a été préservée pendant l'adaptation.

Les appareils GM3 sont conçus pour permettre des adaptations de contrainte en double. En outre, les cultures AM1 ont été adaptées en parallèle à une teneur élevée en méthanol. Comme le montre la figure 33, l'adaptation de la « seconde chambre » s'est déroulée essentiellement par périodes de permutation de milieu et de turbidostat, de la même manière que la première culture en chambre décrite précédemment. L'analyse mutationnelle a été limitée à six isolats finaux en croissance avec 10% de méthanol. Comme le montre le tableau 27, le nombre de SNP détectés s'élevait à environ 100 par isolat en moyenne, environ 10 fois plus que les isolats finaux de la culture en chambre 1. Ce résultat peut être attribué à un phénotype de mutateur probable des cellules qui portaient toutes une insertion de paire de bases dans le gène *mutS*.

**Le rôle de metY au cours de l'évolution :**

Tous les isolats intermédiaires et finaux obtenus à partir des adaptations à haute teneur en méthanol des souches TK 0001 et AM1 de *M. extorquens* portaient une mutation faux-sens dans le gène *metY*, codant pour la O-acétyl-L-homosérine sulfhydrylase. Cette enzyme catalyse la synthèse de l'homocystéine, précurseur de la méthionine, à partir de la O-acétyl-L-homosérine et de l'hydrogène sulfuré (Yamagata, 1989), mais peut également produire de la méthionine directement à partir de la O-acétyl-L-homosérine et du méthanethiol (Bolten et autres). ., 2010). Le gène metY s'est révélé impliqué dans la toxicité du méthanol pour *Corynebacterium glutamicum* (Leßmeier et Wendisch, 2015). Chez *Pichia pastoris*, il a été démontré que MetY était lié à la production de l'analogue toxique de la méthionine, la méthoxine (O-méthyl-L-homosérine), qui se produit lors de la croissance à haute concentration en méthanol. La

méthoxine peut remplacer la méthionine lors de la synthèse protéique ribosomale, ce qui entraîne l'accumulation de peptides dysfonctionnels (Schotte et al., 2016).

Tous les gènes *metY* séquencés à partir des isolats TK 0001 codés pour le variant MetY T34M. En revanche, les isolats AM1 hébergeaient quatre allèles différents de la *metY*: G113S, D373G, L389F et G87S (tableau 29). En comparant la séquence avec MetY de *Wolinella succinogenes* (identité de 35% avec l'enzyme de *M. extorquens* sur une couverture de requête de 93%, figure 34), pour laquelle une structure cristalline a été obtenue, les résidus mutants pourraient être localisés dans la protéine (Tran et al. ., 2011). Ainsi, les résidus T34 et L389 font partie de la boucle N-terminale désordonnée impliquée dans l'interface monomère-monomère de la protéine dimère. Les résidus G87 et G113 semblent jouer un rôle dans le site actif, G87 formant probablement une liaison hydrogène avec le cofacteur pyridoxal-phosphate de l'enzyme.

Nous avons exprimé le gène de type sauvage *metY* et les cinq mutants dans E. coli et avons purifié les protéines à l'aide de méthodes standard. Les paramètres cinétiques déterminés pour l'enzyme MetY de type sauvage sont présentés dans le tableau 29B (figure S10). Le méthanol s'est en effet avéré être un substrat pour l'enzyme, corroborant les découvertes antérieures (voir ci-dessus). Le KM pour le méthanol était environ 400 fois plus élevé que le KM pour le sulfure. Cependant, le kcat pour le méthanol n'étant que trois fois moins que le kcat pour le sulfure, la synthèse de méthoxine entre probablement en compétition avec la synthèse d'homocystéine. Inversement, les cinq variants MetY mutants énumérés dans le tableau 10A se sont révélés inactifs. La O-acétyl-L-homosérine n'a pas réagi de manière mesurable avec le sulfure ou avec le méthanol lors des tests in vitro. Ainsi, en supprimant l'activité des enzymes, les mutations ont également supprimé la réaction secondaire toxique avec le méthanol.

Pour examiner plus en détail le rôle possible du locus metY dans la toxicité du méthanol, nous avons exprimé le gène de type sauvage metY du plasmide pTE102 (Addgene, Figure 13) dans les souches G4105 et G4521 tolérantes au méthanol (Figure 36). Comme prévu, à des concentrations plus élevées (1% et 5% (v / v) de méthanol), les cellules exprimant metY ont augmenté plus lentement, avec un gain de temps de doublement de 28% avec 5% de méthanol. De même, la production de biomasse de cellules G4105_pTE102 metY a été réduite d'environ 26% à cette concentration élevée en méthanol par rapport aux cellules témoins. Les mêmes observations sont faites pour G4521_pT102 metY comparées aux cellules contenant un

plasmide vide. Ces résultats confirment l'implication de la O-acétyl-L-homosérine sulfhydrylase dans la toxicité du méthanol.

Outre les mutations chromosomiques, l'évolution des microorganismes pour résister aux stresseurs des solvants provoque généralement des altérations de l'expression génique suggérant des mécanismes adaptatifs au niveau de la transcription (Reyes et al., 2013). Nous avons effectué une analyse du transcriptome pour étudier de manière systématique la réponse de l'expression génique de la souche G4105 de M. *extorquens* TK 0001 à une exposition à une concentration élevée de méthanol et à la comparaison avec la réponse de la souche de type sauvage ancestrale (tableau S6). Nous avons mesuré les variations d'expression génique provoquées par une exposition à court terme (5 minutes) de cultures en phase médiane développées à 1% de méthanol à une concentration de méthanol (5%) et la modulation de l'expression génique dans des cellules exposées % ou 5% de méthanol à long terme (après 3 heures de culture).

## Production de lactate

Les cellules de *M. extorquens* TK 0001 adaptées à une concentration élevée de méthanol produisent plus de biomasse à partir de méthanol que les cellules de type sauvage (Figure 23). Cette découverte suggère qu'un composé synthétisé par les cellules adaptées via une voie dérivant du métabolisme central pourrait être obtenu avec un rendement supérieur à celui synthétisé par les cellules de type sauvage. Pour vérifier cette hypothèse, la production en une étape de D-lactate à partir de pyruvate, catalysée par la D-lactate déshydrogénase en utilisant $NADH_2$ en tant que donneur d'électrons, a été choisie comme système de test. Le pyruvate est un métabolite du métabolisme central du carbone. La taille des pools de pyruvate et de $NADH_2$, tous deux finalement produits à partir de méthanol, est susceptible d'indiquer un flux de carbone accru dans les cellules. La quantification du lactate a été réalisée par analyse LC-HRMS, en fonction de la zone EIC dans ses métabolomes et d'une courbe d'étalonnage. À partir de cultures indépendantes de 2,5 ml normalisées à une $DO_{600nm}$ = 1, nous avons pu estimer la quantité de lactate produite dans les différentes souches. Les résultats sont présentés à la figure 40. La quantité de lactate n'était pas différente entre les échantillons TK 0001 plasmide vide et pTE102 ldhA et G4105 plasmide vide (groupe a) G4605 mais était significativement plus élevée dans l'échantillon G4105 pTE102 ldhA ($p < 0,001$ entre l'échantillon G4105 pTE102 ldhA et

plasmide vide; p <0,001 entre G4105 pTE102 ldhA et TK 0001 avec le même plasmide et p = 0,01 entre l'échantillon G4105 pTE102 ldhA et TK 0001 pTE102 ldhA).

**Titre :** Adaptation génétique des bactéries methylotrophes à la production industrielle des composés chimiques

**Mots clés :** Methylotrophe, adaptation, génétique, bioproduction, lactate

**Résumé :** Ce projet a pour objectif l'amélioration de souches châssis méthylotrophes capables de convertir le méthanol fourni comme source de carbone et d'énergie en biomasse et, à terme, en composés chimiques dans les conditions de production industrielle. Le méthanol est une alternative aux glucides en tant que matière première pour les fermentations industrielles, car son utilisation n'entre pas en concurrence avec les denrées alimentaires et il peut être produit par réduction chimique du $CO_2$.

Une condition préalable à la production efficace à grande échelle de composés d'intérêt est la stabilité de la souche méthylotrophe productrice dans des concentrations élevées de méthanol. À cette fin, deux souches méthylotrophes apparentées, *Methylobacterium extorquens* AM1 et TK 0001, qui croient de façon optimale avec 1% de méthanol, ont été adaptées en culture continue à la prolifération en présence de concentrations de méthanol allant jusqu'à 10%. Ces adaptations ont été réalisées à l'aide des automates de culture GM3, qui permettent de maintenir des populations de microorganismes en croissance à long terme dans des conditions contrôlées.

Les courbes de croissance enregistrées pour des isolats issus de populations évoluées ont montré une prolifération accrue en présence de 5 % de méthanol en comparaison avec les cellules non évoluées. Les isolats croissent de façon comparable mais non identique, ce qui suggère une hétérogénéité des cellules adaptées dans une même population.

Le séquençage génomique de clones isolés à différentes étapes de l'évolution en concentration croissante de méthanol a révélé des profils mutationnels variés. En revanche, le gène *metY* codant pour la O-acétyl-L-homosérine sulfhydrylase est muté dans tous les isolats. L'enzyme codée catalyse une réaction secondaire en présence de méthanol produisant la méthoxine, analogue de la méthionine, connue pour sa toxicité par son incorporation dans les protéines. Les résultats des tests enzymatiques réalisés sur les protéines MetY mutées montrent une perte de fonction presque complète avec le méthanol ainsi qu'avec les substrats naturels, suggérant la participation de MetY dans la toxicité du méthanol.

Une analyse transcriptomique a été entreprise afin d'étudier l'expression génique de la souche évoluée G4105 de *M. extorquens* TK 0001 en réponse à une exposition brève ou prolongée à une concentration élevée de méthanol en comparaison avec la réponse de la souche sauvage. Les gènes impliqués dans la division cellulaire, la structure des ribosomes et des flagelles, la stabilité des protéines et l'absorption du fer montrent une différence d'expression entre les deux souches.

Les variantes de *M. extorquens* TK 0001 adaptées à une concentration élevée de méthanol produisent plus de biomasse à partir de méthanol que les cellules de type sauvage. On peut supposer qu'un composé synthétisé via une voie dérivant du métabolisme central par des cellules adaptées pourrait être produit à partir de méthanol avec un rendement supérieur à celui atteint par des cellules de type sauvage. La production de D-lactate a été testée dans les souches sauvage et évoluée sur-exprimant la lactate déshydrogénase endogène. Les cellules évoluées produisent plus de lactate que la souche contrôle, confirmant ainsi l'intérêt de cette adaptation au méthanol.

**Title:** Genetic adaptation of methylotrophic bacteria for industrial production of chemical compounds

**Keywords:** Methylotroph, adaptation, genetic, bioproduction, lactate

**Abstract:** The objective of this project was the development of enhanced methylotrophic chassis strains capable of converting methanol as carbon and energy source into biomass and ultimately into commodity chemicals under industrial conditions. Methanol is an alternative to carbohydrates as feedstock in industrial biotechnology as its use does not interfere with food supply and its production can start from $CO_2$.

A prerequisite for an efficient and large scale industrial fermentation is stable growth of the methylotrophic producer strain on high methanol concentrations. For this purpose, two closely related methylotrophic strains, *Methylobacterium extorquens* AM1 and TK 0001, which both have a growth optimum at about 1% methanol, were adapted in continuous culture to proliferate stably in the presence of methanol of up to 10% (v/v). The adaptations were conducted using GM3 devices enabling automated long term cultivation of microorganisms.

Growth curves recorded for isolates obtained from evolved populations showed enhanced proliferation in the presence of methanol at 5% as compared with wild type cells. The isolates showed comparable albeit not identical growth pointing to heterogeneity among the adapted cells in the population.

Genomic sequencing of isolated clones at different steps of the adaptation revealed differences in their mutation profiles. The gene *metY* coding for O-acetyl-L-homoserine sulfhydrylase was found to be mutated in all isolates. This enzyme undergoes a side reaction with methanol leading to the production of the methionine analogue methoxine known to be toxic through incorporation into proteins.

Enzymatic tests conducted with these mutants showed an almost complete loss of activity even with their natural substrates, validating the involvement of MetY in methanol toxicity.
Transcriptomic analysis was performed to study the gene expression response of an evolved derivative of *M. extorquens* TK 0001 to short and long term exposure to high methanol and compared with the response of the ancestor strain. Genes implicated in cell division, ribosomal and flagellar structures, protein stability and iron uptake showed differences in expression patterns between the strains.

The *M. extorquens* TK 0001 cells adapted to high methanol produced more biomass from methanol than the wildtype cells. This suggests that a compound synthesized through a pathway branching from the central metabolism would be produced in higher yield from methanol by the adapted cells compared to the wildtype cells. The production of D-lactate was tested for wildtype and evolved cells both overexpressing native lactate dehydrogenase. The evolved cells produced more lactate than the control cells, confirming the interest of this methanol adaptation.